STATISTICAL TREATMENT OF SPECTRA FROM THE (n,γ) REACTION

STATISTICAL TREATMENT OF SPECTRA FROM THE (n,γ) REACTION

by

ANTHONY H. COLENBRANDER, B. Eng.

A Thesis

Submitted to the Faculty of Graduate Studies

in Partial Fulfilment of the Requirements

for the Degree

Doctor of Philosophy

McMaster University

July 1972

DOCTOR OF PHILOSOPHY
(Physics)

McMASTER UNIVERSITY
Hamilton, Ontario

TITLE: Statistical Treatment of Spectra from the (n,γ) Reaction

AUTHOR: Anthony H. Colenbrander, B.Eng. (McMaster University)

SUPERVISOR: Professor T. J. Kennett

NUMBER OF PAGES: vi, 128

SCOPE AND CONTENTS:

Some general results applicable to complicated spectra are derived. These involve the mathematical simplification of a system response, as well as an investigation of some statistical properties of data. The technique is applicable to all spectra with distributed features. This work involves a study of the gamma radiation spectra following thermal neutron capture in 15 nuclides in the mass range $28 \leq A \leq 204$. Invoking a statistical model of the nucleus allows a determination of nuclear temperature and level spacing from the spectra. On the basis of the model and the spectral multiplicity we assign absolute intensities to spectroscopic data. The results are found to agree with previously reported values based upon other data and methods.

ACKNOWLEDGEMENTS

The completion of this work represents a milestone in my career. A prime factor in its attainment has been the camaraderie pervading my research environment. I can but attempt to adequately acknowledge some of the people involved.

Dr. T. J. Kennett, my research director, deserves special thanks. His perspicacity and perspiration have provided me with a foundation in scientific methods.

Dr. J. A. Cameron and Dr. G. L. Keech, members of my supervisory committee, have helped to keep me oriented in the right direction.

Mr. and Mrs. J. W. Colenbrander, my parents, have a faith which has done much to make this work possible.

Mr. J. B. McDougall, as well as many other members of the reactor staff, has been most generous in his cooperation.

Many people involved with the McMaster University Computing Centre have provided fast and cheerful service.

Dr. L. W. Nichol and Mr. R. Robertson were kind enough to instruct and assist me in the art of detector fabrication.

Mr. A. J. Dilay and Dr. G. R. Norman have provided friendly guidance throughout my time at the Nuclear Research Building.

The artistry and perfection of Mrs. H. Kennelly at the typewriter has been much appreciated.

The financial assistance of the National Research Council of Canada and the Province of Ontario is gratefully acknowledged.

TABLE OF CONTENTS

LIST OF ILLUSTRATIONS

LIST OF TABLES

CHAPTER 1

INTRODUCTION

Since the goal of scientific investigation is to extract information from experimental results, it is appropriate that this work deal with both a method of extraction and the information itself. The result of any measurement can be regarded as a random variable sampled from the applicable distribution, and therefore any quantitative information that is sought is a value of a parameter of a distribution. It is shown that new and relevant information can be extracted from observed spectral fluctuations through the application of descriptive statistical methods.

The present study concerns itself with gamma radiation spectra. The term spectrum, which has come to denote many different phenomena, is here used to describe the experimental results. In this case the spectrum represents a definite relationship between the intensity of gamma radiation and the energy of the gamma radiation. A simple way of presenting such results is by means of a graph.

The observed spectra result from the absorption of neutrons of low kinetic energy by assemblages of nuclei. Each interaction releases a large amount of internal energy, which is usually emitted by the produced nucleus as gamma radiation. Characteristic

of the radiation sources under study is their discrete nature. This is a consequence of the fact that the internal energy of a particular kind of nucleus can assume only certain discrete values, and the radiations represent transitions between such allowable energy levels. Therefore a large number of distinct gamma rays, distributed in energy in a discontinuous manner, are expected to be present.

An examination of a spectrum of the radiation emitted by a nuclide of low mass shows this to be true. Such data contain distinct maxima in some energy regions. These peaks have been found to be the manifestation of nearly monoenergetic gamma rays. In the case of the Ge(Li) pair spectrometer used in this study, the shape of the peaks can be approximated to Gaussian distributions. When a peak is known to represent a monoenergetic gamma ray, the inverse of its width in appropriate units is termed the resolving power of the experimental system. The total spectral distribution resulting from a monoenergetic gamma ray is known as as the system response. We shall consider a spectrum to consist of the linear superposition of many such response functions, arising from an equal number of gamma rays of appropriate energy and intensity.

The development of the Ge(Li) spectrometer has yielded an order of magnitude improvement in resolving power over previously applicable techniques (1). This allows greater precision and accuracy in the energy determinations of known gamma radiations,

as well as the observation of lower intensity gamma rays previously masked by other peaks nearby. In complicated spectra the ratio of the average spacing between peaks and their average width becomes small, and a point is reached at which discrete features can no longer be recognized. The spectrum contains apparently random fluctuations from which no information has as yet been extracted. A system with a higher resolving power would, of course, enable the observation of discrete peaks in such an energy region of the spectrum.

Technical difficulties associated with increasing the system resolving power led us to investigate other possible methods of extracting information from spectra. From a statistical viewpoint we treat a spectrum as an ensemble of peaks, randomly distributed in energy and intensity. A mathematical relationship is found between the observed spectral fluctuations and parameters describing the distributions of these variables. Assumptions concerning the forms of the distributions are made and justified. Estimates of gamma ray intensity and spacing are obtained directly from spectral data.

The precision of the information obtainable is directly related to the resolving power of the system and the total number of events contained in the observed spectrum. Data were collected using the best available high resolution detector associated with a sophisticated electronic system. Therefore tabulations of the observed gamma radiations are also presented. Discrete gamma

ray energies were obtained graphically because of difficulties associated with computational approaches (2).

Information obtained via the analysis of the observed spectral fluctuations can be related to the nuclear temperature, a parameter in a statistical description of the nucleus. Determinations of nuclear energy level density can also be made. The present application of the statistical method of extracting information from spectra is, to date, unique.

The measurement of nuclear parameters is a contribution of this work. It should be emphasized, however, that the applicability of the statistical technique is not limited to the analysis of gamma radiation spectra. Many other kinds of data may be treated. Seismic signals, or the output of a device which measures density in a droplet containing blood cells, are examples totally unrelated to the present study. A criterion of the experimental results is that they be, or may be treated as, distributed variables. The form of the distributions is then used to obtain estimates of some parameters describing the data. It is expected that the technique will be applied to obtain new information from experimental results and to reduce the tedium of some data reduction methods.

CHAPTER 2

GENERAL CONSIDERATIONS

In this chapter we first define the nature of the complex spectra to which the analysis has been applied. Some areas of nuclear physics involved, and some general observations that were made, are indicated. This is followed by the discussion of some theoretical ramifications. We conclude with a short survey of related work.

NATURE OF THE COMPLEX SPECTRA UNDER STUDY

A nuclear reaction is said to occur when a projectile, i, is incident on a target, T, and the products, P and f, are formed[3]. This is written

$$T + i \rightarrow f + P$$

or

$$T(i,f)P$$

where T and P are nucleons or groups of nucleons. Each can have a kinetic and internal excitation energy. The i and f can be nucleons, groups of nucleons, or electromagnetic radiation. A nuclear reaction involves all forces known to exist in nature[4]. Knowledge of the strong interaction can be increased by applying theories concerning gravitational, weak, and electromagnetic interaction to the study of nuclear reactions.

We have chosen to study complex gamma radiation spectra of odd-odd nuclides following the capture of a thermal neutron by a nucleus:

$$A_Z^N(n,\gamma)A_Z^{N+1} .$$

This reaction can be considered to take place in two steps[5]; the absorption of the neutron, and the emission of gamma radiation.

The McMaster University nuclear reactor is of the pool type, and uses enriched ^{235}U as fuel. Thermal neutrons are neutrons in thermal equilibrium with the moderator at ordinary temperatures. This implies a Maxwellian energy distribution with a mean energy of 1/40 eV. At a nominal operating power of 2 megawatts, the thermal neutron flux in the region of the reactor core is about 10^{13} n/cm^2 sec. Higher energy (resonant and fission) neutrons are also present. However this flux is lower - $\sim 10^{12}$ n/cm^{2}sec. This, combined with the fact that the probability of neutron induced reactions other than (n,γ) is small, is the reason that the (n,γ) interaction predominates.

When a neutron is absorbed by a nucleus the excitation energy of the system is equal to the binding energy of the neutron plus its kinetic energy. This binding energy, or neutron separation energy, is referred to as the Q value of the (n,γ) reaction, and is usually of the order of 6-8

MeV. In the case of thermal capture the kinetic energy of the neutron can therefore be neglected. The system de-excites via the emission of one or more gamma radiation quanta. Many decay modes are possible. Their relative probability is described by Fermi's golden rule of time dependent perturbation theory:

$$\Gamma(i,f) = \frac{2\pi}{\hbar} \, |\langle f|O|i\rangle|^2 \rho_f. \qquad (2.1)$$

Here i and f represent the initial and final states of the system, known to be discrete. The symbol ρ_f represents the density of final states available to the system. An electromagnetic operator, O, provides the representation for the interaction between the initial and final states.

The function $\Gamma(i,f)$ is a partial width. Through the Heisenberg uncertainty principle, it is proportional to the transition probability and therefore the intensity of the transition. The radiation spectrum represents the intensities and energies of all the transitions for all possible decay modes. Its complexity increases with the number of available states of the system, which happens in the following instances:

1. As A, the nucleon number, increases
2. Away from the well known 'magic numbers' of the shell model of the nucleus[6]
3. For odd-neutron odd-proton systems, where two unpaired nucleons exist.

An observed spectrum reflects not only the true spectrum but also certain properties of the data acquisition system. We limit our discussion to the observation of gamma radiation spectra.

A 'true' spectrum consists of a distribution of n gamma rays of energy γ_i in m channels of mean energy E_j. It may be represented by a column vector T:

$$T = \begin{pmatrix} t_1 \\ t_2 \\ \cdot \\ \cdot \\ \cdot \\ \cdot \\ t_m \end{pmatrix} \quad \text{where } t_j = \sum_{i=1}^{n} A_i \int_{\substack{\text{channel} \\ E_j}} \delta(E_j - \gamma_i)\, dE_j \qquad (2.2)$$

A_i is the intensity of γ_i and δ is the Dirac delta function[7].

Similarly the observed spectrum may be represented by a column vector, S. These vectors are related by the response, now represented by a square m×m matrix R, such that

$$S = RT \ . \qquad (2.3)$$

If the inverse of R exists, the true spectrum can be found,[8] viz.

$$T = R^{-1}S \ .$$

Limitations of this method include the difficulty of determining and inverting R, and statistical fluctuations that are magnified to large errors[2]. In Chapter 5 we indicate how these difficulties can be circumvented.

The observation of a gamma ray of energy E' depends

on the probability of its interaction with the detector. We used a Ge(Li) detection device, and therefore, the interactions of radiation with germanium is of interest. These interactions are normally described as cross sections of various types. The photoelectric, Compton effect, and pair production cross sections are well known[9]. Each of these contributes a component to the response $R(E,E')$, which depends on the energy, and the type of spectrometer used.

It is possible to simplify R experimentally by associating the Ge detector with a pair detection device. Such a configuration is known as a pair spectrometer[10].

NUCLEAR MODELS AND LEVEL DENSITY

A model is a conceptual artifact introduced strictly as an aid to understanding complex behaviour. It need have no physical significance whatsoever, and its limitations should always be remembered. Models are only useful insofar as they correspond to reality - they may be questioned, restricted, or invalidated by experiment[9].

Nuclear reactions are generally characterized by one of two extreme models - the statistical model or Compound Nucleus, or the Direct Reaction model[4]. Which description best applies depends on many factors. There are processes, viz. the evidence for doorway states, that do not fall into either category, but somewhere in between. The time taken

for the interaction is a critical parameter. Since this is long ($\sim 10^{-16}$ sec) for the (n,γ) reaction, it is generally accepted that the interaction is adequately described by the statistical model. For a detailed description of these models the reader is referred to Ericson's excellent review article[11]. Suffice it to state here that the statistical description applies to equilibrium systems, which means that no phase relations exist between formation and decay modes of the system. Decay modes depend only on the parameters describing the equilibrium system.

We call the system formed by the absorption of a thermal neutron by a nuclide a compound nucleus[4]. The description of the compound nucleus with respect to level density is of interest, since, through equation (2.1), this information governs its decay modes. A thermodynamic approach dating back to 1937[12] forms the foundation for all level density theory to date. Depending on the assumptions made most theories fall into one of two generally recognized classes - Bethe's free Fermion gas model, and a constant nuclear temperature model first suggested by Bohr[13].

Bethe[12] considers the nucleus as a system of independent Fermions, ignoring residual interactions. The observed rapid increase in level density with excitation energy leads to the deduction that the levels represent the excitation of many nucleons, instead of just one nucleon. That the energies

of many single particle Fermion states can be added is assumed. The problem of calculating the density of levels then becomes combinatorial, familiar in statistical mechanics. This results in a level density of the form

$$\rho(E) = C\exp(\sqrt{E}). \tag{2.4}$$

A more detailed calculation yields the result[14],

$$\rho(E) = \frac{\sqrt{\pi}}{12} \frac{\exp(2\sqrt{aE})}{A^{1/4}\ E^{5/4}}, \tag{2.5}$$

where E is the excitation energy of the nucleus, and a is a parameter related to the spacing of the single Fermion states. This formalism has been extended by Bloch[15], Cameron[16], and Newton[17] who include shell model effects by assuming a shell model potential with no residual interactions.

The second, referred to as the constant temperature approach, refined by Ericson[18], considers a nucleon pairing interaction. This is suggested by the energy gap between the ground and first excited states of even-even nuclides. Existence of correlations between nucleon pairs implies a second order phase transition. Again using thermodynamical arguments, the nuclear temperature is expected to remain constant during this phase transition[19]. The theory indicates that the results should be valid to an excitation energy of 15-18 MeV, well beyond the range of energy con-

sidered here[20]. A simple Taylor expansion of the entropy function leads to a level density of the form

$$\rho(E) = \rho_o \exp(E/T). \qquad (2.6)$$

According to the detailed compilation of Gilbert and Cameron[14], nature tends to favour Ericson's constant temperature model.

We now introduce the dependence of level density on spin and parity. These quantities are of interest since they relate to the nature of the transitions between nuclear states. The foregoing results did not depend on them, a consequence of the thermodynamical nature of the derivations.

The result

$$\rho(E,J,\pi) = \frac{(2J+1)\rho(E)}{4\sqrt{2\pi}\ \sigma^3} \exp(-J(J+1)/(2\sigma^2)) \qquad (2.7)$$

which incorporates spin and parity with the above indicated level densities, is due to Bethe[12].

Positive and negative parity levels are assumed to exist in equal number. This is seen to be reasonable by considering the combination of many single particle states. The spin dependence is also statistically derived. The distribution of j values of the single particle wave functions is assumed to obey a simple Fermi gas prediction. The Central Limit theorem[21] is then invoked to obtain the distribution of J. The dispersion parameter is also known as the spin cut-off factor, σ[22], which is related to nuclear well information.

We now return to the concept of complex spectra. The nuclear density models that have been introduced predict the existence of distributions of states which are described by distributions of wave functions. These wave functions may be used to derive more explicit forms of the transition probabilities associated with radiation[23]. The well known Weisskopf estimates for partial radiation widths[24] were calculated assuming single particle states, and the appropriate electromagnetic operator. We use the Moszkowski estimates[25], which are in fact very similar in value and form, but more recent:

$$\begin{aligned} \Gamma(E1) &= 1.0 \times 10^{14}\ A^{2/3}\ E^{3}\ \mathrm{sec}^{-1} \\ \Gamma(E2) &= 7.4 \times 10^{7}\ A^{4/3}\ E^{5}\ \mathrm{sec}^{-1} \\ \Gamma(M1) &= 2.9 \times 10^{13}\ E^{3}\ \mathrm{sec}^{-1} \\ \Gamma(M2) &= 8.4 \times 10^{7}\ A^{2/3}\ E^{5}\ \mathrm{sec}^{-1}\ . \end{aligned} \tag{2.8}$$

When E is expressed in MeV, A is the mass of the nuclide under consideration, the coefficients are defined in such a manner as to yield the transition probability in transitions per second.

The nature of the radiation possible between states of the nucleus depends on selection rules related to the values of the angular momentum (spin) and parity of the states involved. The description of the nuclear states by means of nuclear wave functions also accounts for the fluctuations in the partial widths. This was described by

Porter and Thomas[26], who indicated that the distribution of partial widths could be expected to follow a chi-squared distribution of one degree of freedom.

RELATED WORK

In conclusion, much of the foregoing theory has been developed as a result of the study of radiation following the (n,γ) reaction. Some predictions of workers such as Blatt and Weisskopf[3] and Porter and Thomas[26] were undoubtedly based on the magnetic pair spectrometer work of Kinsey and Bartholomew[27]. As technology advanced, precision improved and increasingly finer structure became resolvable. Multi-parameter measurements allowed the identification of prominent gamma cascades.

Recent years have seen the accumulation of huge quantities of ever more precise spectroscopic gamma radiation data. Bartholomew et al.[28] have contributed greatly to the work by increasing the availability of the results via their excellent compilations. The work of Rasmussen[29] is particularly impressive because of the large number of pair spectrometer results which he tabulated. Although numerous other investigators are active in this field[30, 31], and some results have been improved upon over those obtained by Rasmussen, no one has attempted to cover such a large mass range in such great detail. However the automated method of data reduction which he used did not preclude the inclusion

of some spurious data, nor obviate the possibility of omission of some results. The compilations of Gilbert and Cameron[14] of existing data in order to fit it to available level density theory, associated with an excellent review article, represents the most comprehensive level density information available to date. Baba[32] has recently calculated the level spacings of many nuclides. A review of theoretical approaches to level density has been provided by Ericson[11]. Further work relevant to this effort includes the theses of L. B. Hughes[33] and D. D. Slavinskas[8]. Hughes obtained the spectra of 10 odd-odd nuclides, and determined the nuclear temperatures as functions of mass number. Slavinskas presented a mathematical approach to data reduction through the inversion of calculable response functions.

Work less relevant than the above to this work, yet related to it in some way, has been done by the following:

Muelhause[34] was the first to measure multiplicites of gamma ray spectra, in 1949. He used a coincidence detection system, and deduced the multiplicity from the counting rates of 30 nuclides.

Draper and Springer[35] derived spectral multiplicities as a function of neutron capture in various resonances. A neutron time-of-flight apparatus and a comparison with a reported multiplicity was involved.

Johnson and Hintz[36] studied fluctuations in proton and alpha spectra. Values of nuclear temperature and the variance of the level spacing distribution are obtained.

Many workers, including Yost[37], Berqvist and Starfelt[38], Paulsen[22], Sarantites[39], Hillman and Grover[40], Sperber[41], Troubetzkoy[42], Huizenga and Vandenbosch[43], and Vonach[44] have conducted investigations of various aspects of the statistical model of the nucleus by means of theoretical calculations. The calculations of von Egidy[45], who obtains gamma ray spectra and distributions of spectral quantities, are in some respects similar to those presented in this work.

The quality of the data continues to improve. The analysis presented here accounts for all features of the spectrum, resolved or not. This allows for new tests of existing theories. Data is compared to the constant temperature level density model, and nuclear temperatures are reported. Spectral shapes are compared with predictions of a statistical model, and multiplicities are estimated.

CHAPTER 3

EXPERIMENT

The gamma radiation spectra of 17 nuclides following the thermal neutron capture were obtained. Calibration of the detection system was via the $^{14}N(n,\gamma)^{15}N$ reaction. The gamma radiation data used was that reported in Marion's[46] compilation, and is reproduced in Appendix 4. This appendix is also a data bank containing some of the present observations in both graphical and tabular forms. We refer to these results throughout the remainder of this work.

A chronological summary of the experiments is given in Table 3.1. This list does not include numerous background and calibration runs. The complexity of the spectrum is indicated. Simple refers to spectra such as N with fewer than 10 observable transitions, whereas complex refers to spectra such as Rh where below ∿5 MeV most features are unresolved.

A pool type reactor provides great flexibility for experiments requiring high neutron fluxes, since experimental configurations near the core can be changed almost at will. Only activities and heat produced in samples and equipment, the displacement of water as a moderator, and a means of observing the reaction - i.e. via beam tubes - need be considered in experimental design.

TABLE 3.1

Summary of experiments

SPECTRUM	RUN TIME (hours)	COMPLEXITY	COMMENTS
^{76}As	280	Complex	3 runs, different backgrounds, different systems of sample changing methods
^{204}Tl	139	Intermediate	Anomalous spectrum - well spaced high energy peaks - not much intensity <4 MeV
^{56}Mn	70	Intermediate	
^{41}Ar	14	Simple	
^{104}Rh	106	Complex	
^{60}Co	55	Intermediate	
^{134}Cs	88	Complex	
^{198}Au	138	Complex	
^{28}Al	282	Intermediate	Stabilized on spectral peaks
^{64}Cu	290	Intermediate	Separated isotope
^{116}In	134	Complex	Separated isotope - introduction or rabbit tube
^{46}Sc	65	Intermediate	Data used to confirm spectral properties
^{110}Ag	76	Complex	Separated isotope
^{186}Re	83	Complex	Separated isotope
^{13}C	3.1	Simple	
^{29}Si	3.5	Simple	
^{15}N	12.4	Simple	
	76 Days		

Gamma radiation spectra following the capture of thermal neutrons may be studied in various ways, depending on target placement[47]. A neutron beam may be extracted from the reactor. The target is placed in the beam and the detector is placed adjacent to it. This method offers flexibility and few hazards, but obtains low count rates and low signal/noise ratios. Coincidence measurements between various gamma radiation quanta of a decay mode are possible. However the simplification of the response of a detector via mechanisms such as pair production is normally impractical, since such a technique is most effective when the radiation field surrounding the primary detector is low. This is difficult to accomplish using the external target configuration since much shielding material is required at the gamma ray energies involved.

An experimental configuration having complementary characteristics to the external target scheme was used. It is illustrated in Fig. 3.1. Placing the sample in a high neutron flux area near the reactor core allows the extraction of a relatively intense, well collimated gamma radiation beam. In an effort to reduce neutron damage to the detector by neutrons scattered from the target, and to reduce the number of low energy photons, the detector was shielded by 18" of borated wax, 24" of wax, and 1/8" of lead. With such shielding and with the available neutron flux and detector,

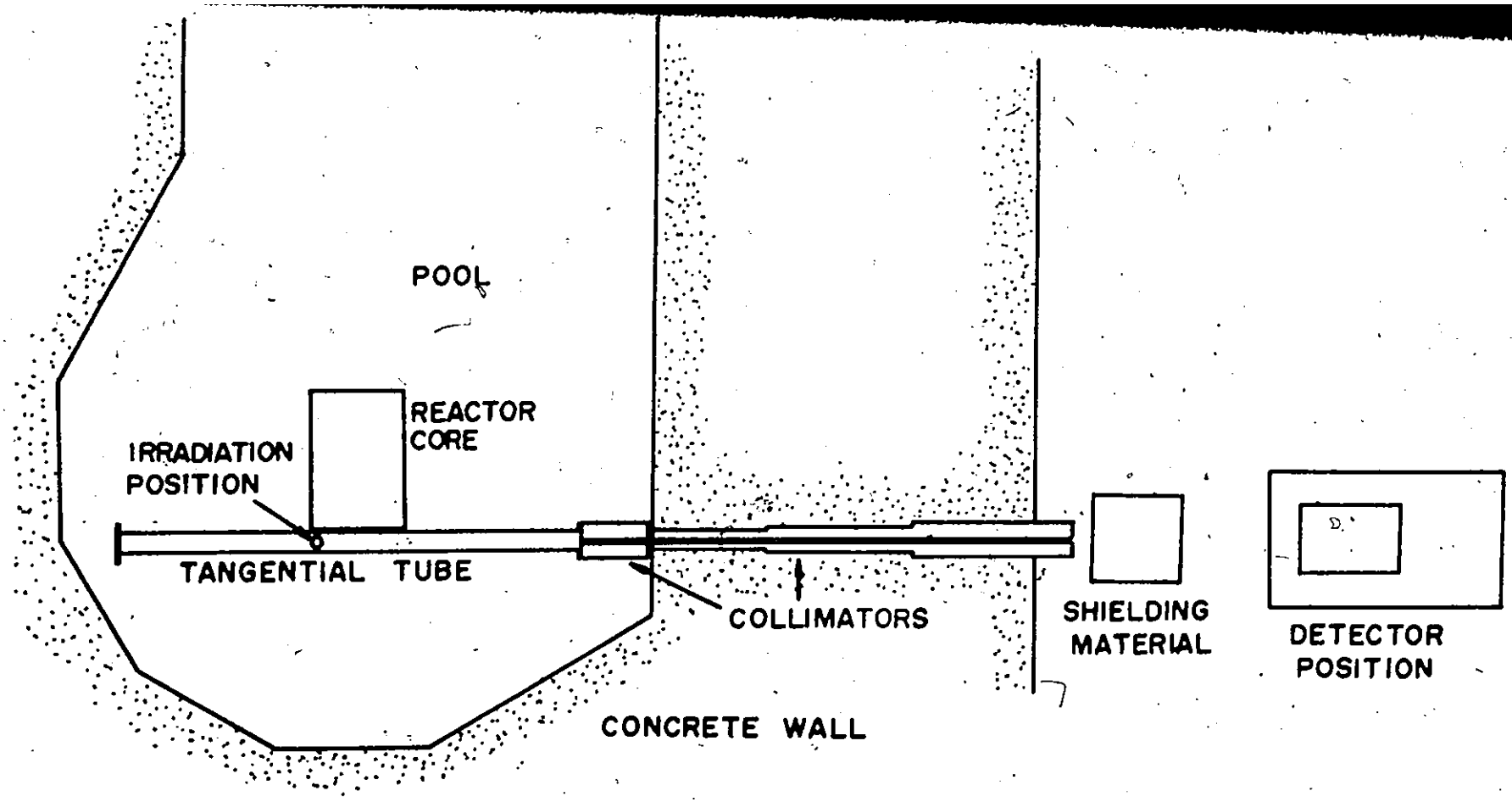

FIG 3·1 – TANGENTIAL TUBE IRRADIATION FACILITY

a sample size of approximately 50 mmb. (milli-mole-barns) was found to be suitable. In the case of powder samples with high thermal neutron cross sections, such as ^{185}Re, an effort was made to reduce the amount of self-shielding[5] by mixing it with some reactor grade graphite powder. This was also done with samples which were in short supply or small in volume, such as ^{109}Ag or ^{63}Cu, in order to ensure that they were visible to the detector.

Physically, the facility consists of a 3" aluminum tube supported on two fixed stands. There are collimators in the pool and the wall which define a 1 cm. diameter beam external to the reactor. The sample of interest was placed, in a reactor grade graphite container when necessary, at the end of the reactor core remote from the detection apparatus. In order to observe radiation originating in the core that is Compton scattered from the sample it must be scattered through an angle greater than 90 degrees. Radiation of this type could therefore not have an energy greater than 511 keV[48]. For normal runs the tube was evacuated to a pressure of 10^{-3} torr, in order to reduce contribution to the spectrum caused by the presence of air. A constant background was present during all experiments. This was determined from runs with the tube empty, and was attributed largely to capture in the aluminum of the tube and the reactor structure, and the hydrogen of the water. Figure 3.2 shows a background spectrum as well as the ^{28}Al spectrum for com-

SYSTEM BACKGROUND & ^{26}AL SPECTRUM FIG 3-2

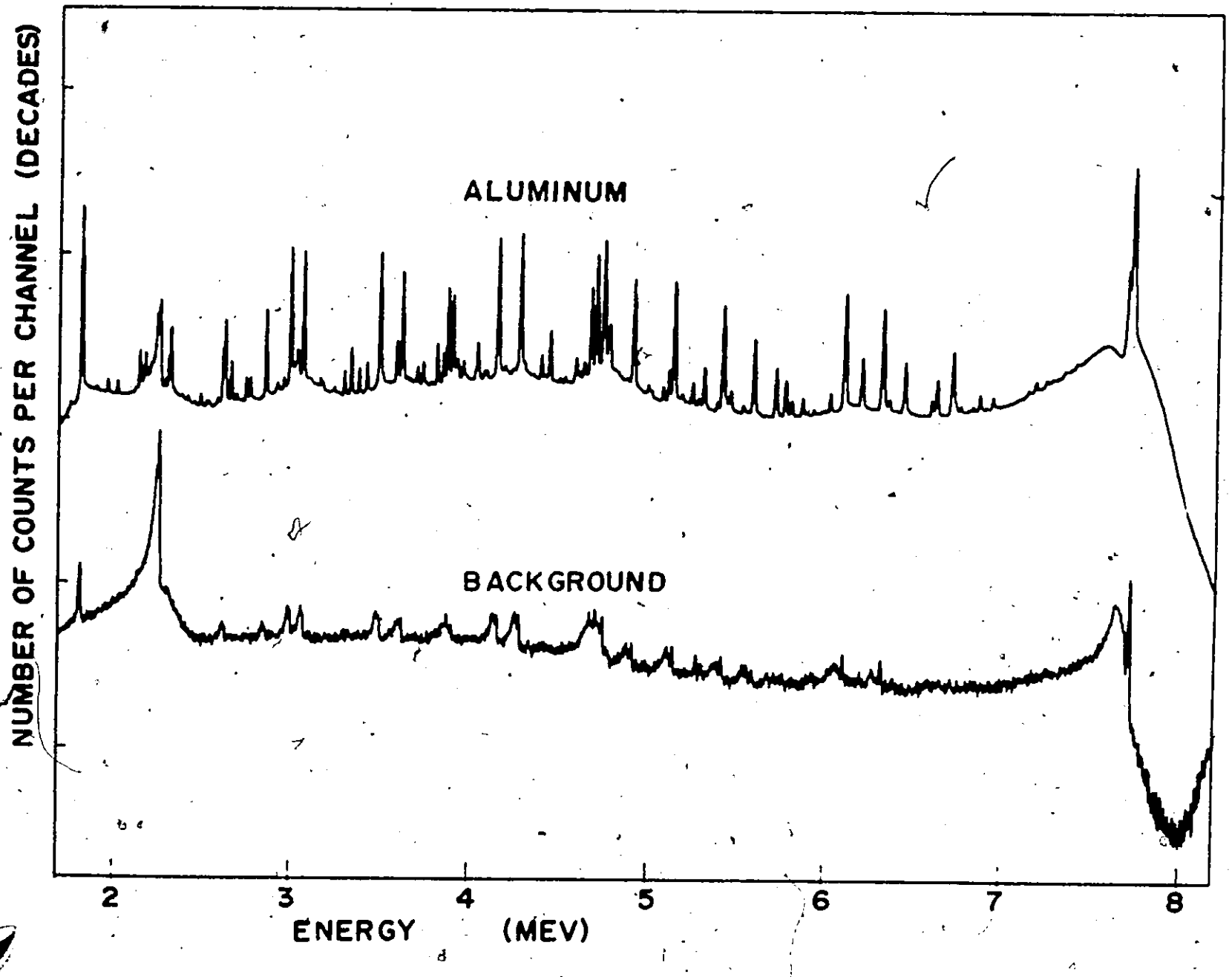

parison.

Materials used in the construction of in pool type experiments must not react with the pool water nor deteriorate in areas of high neutron flux. Radio isotopes produced by the nuclear reactions should be minimal or have suitably short half lives so that health hazards are minimized. An aluminum alloy, 65 st, is suitable. Activities produced are 2.3 min ^{28}Al, and some Fe and Mn which are added to the aluminum in order to allow it to be machined. This grade of aluminum is used for all parts in high neutron flux areas. Gaskets in high neutron flux areas are made of lead, the only significant activity produced being ^{209}Pb, a 3.3 minute pure β^- emitter. In areas outside of the neutron flux plastics (PVC), rubber, and stainless steel may be used, which are also non corrosive, cheaper, and more easily worked than aluminum.

Several improvements were made to the facility in order to effect more rapid, convenient, and safe sample changes. Two methods are described, and pertinent details are illustrated in Figures 3.3A and 3.3B.

The first method involves removal of the tangential tube from the reactor pool by means of long stainless steel cables attached to the tube ends. Another tube with a sample already placed in it replaces the first in order to effect a sample change. The graphite sample container is

SAMPLE POSITIONING

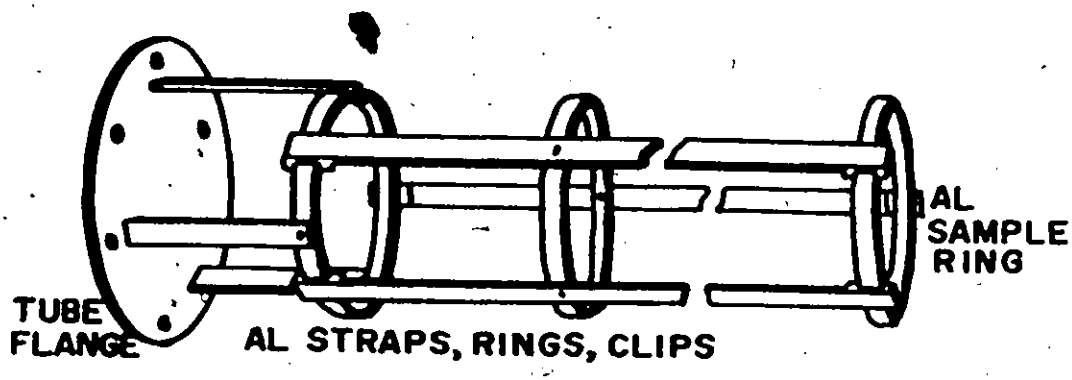

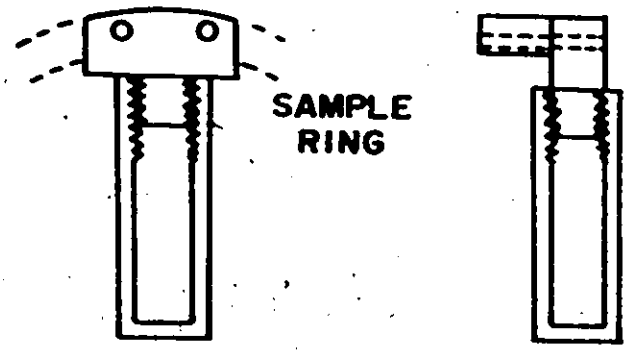

GRAPHITE SAMPLE CONTAINER

FIG 3·3A - METHOD I

SAMPLE POSITIONING

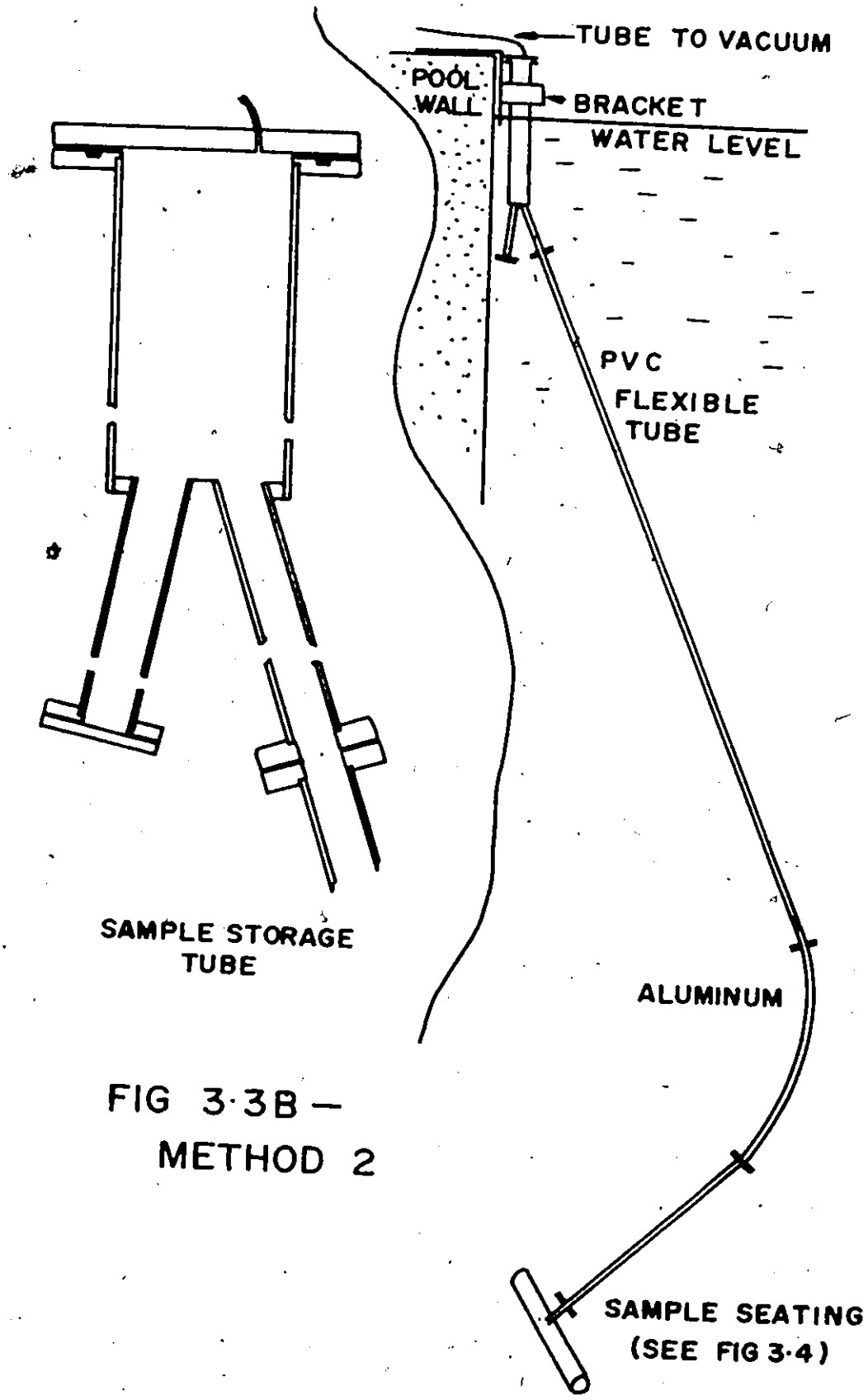

FIG 3·3B — METHOD 2

fastened to an aluminum ring which is used to centre the sample in the tangential tube. This ring is clipped to a strap arrangement which is fastened to the end flange of the tube. The clips allow for a minimum of handling of the sample, and reduces the storage requirements of irradiated samples considerably over previous methods.

After a short cooling period in the reactor pool, samples are usually still quite radioactive. To allow for a longer cooling time, three such tubes are in operation. Since the reactor core must be moved for a sample change, this procedure involves approximately one hour of 'reactor down' time.

In order to further simplify sample handling and reduce health hazards as well as reactor down time, a second method of changing samples was devised (Fig. 3.3B). The sample is lowered to the irradiation position via a 1" I.D. 'rabbit' tube connected to the tangential tube. Fig. 3.4 shows the sample holder and indicates the seating method used to position the samples.

Sample changes are effected by flooding the whole system with N_2 gas to atmospheric pressure. The upper flange is removed and the sample is withdrawn by means of a nylon cord attached to it. Normally it can be stored immediately in the storage side of the upper chamber, since sufficient shielding is provided for the safe handling of most activities

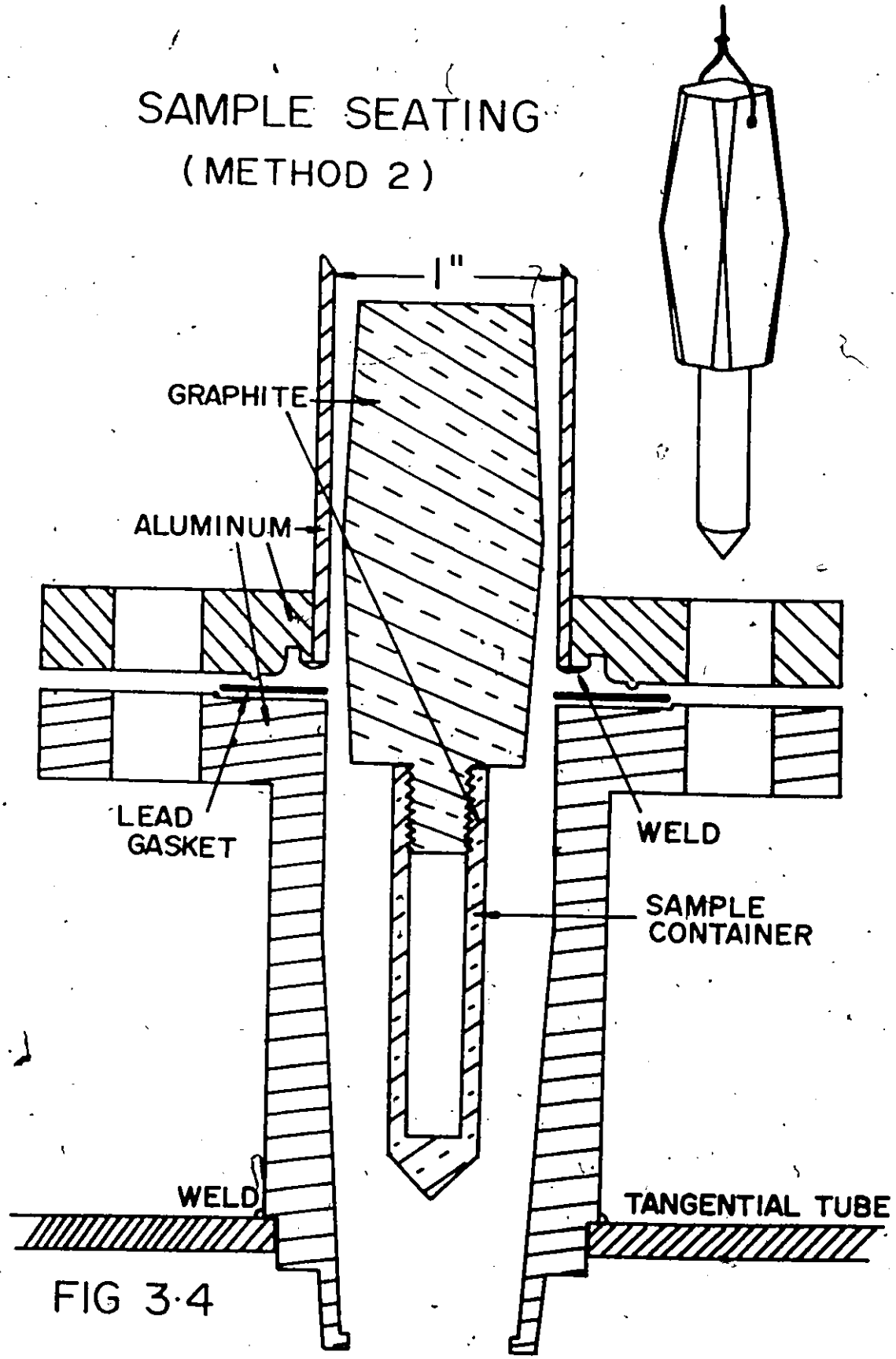
SAMPLE SEATING
(METHOD 2)
1"
GRAPHITE
ALUMINUM
LEAD
GASKET
WELD
SAMPLE
CONTAINER
WELD
TANGENTIAL TUBE

FIG 3·4

encountered. Another sample is then lowered to the irradiation position. After a suitable cooling period in the storage side, a specially designed lead gasket is placed on top of the flange of the upper chamber. The sample can be removed remotely from the storage chamber to the shielded container for disposal. Samples can be changed in approximately 10 minutes. The configuration of the materials adjacent to the core is not changed significantly by a target change. Therefore a shutdown of the reactor is not necessary during such a procedure.

The measurements were made using a pair spectrometer[10]. Such an instrument consists of several detectors, amplifiers, and associated electronic circuits. A detected photon is accepted for analysis only if its interaction with a high resolution main detector is via pair production. A schematic of the system is shown in Fig. 3.5.

A germanium semiconductor diode manufactured in this laboratory[49] served as the main radiation detector. Its active volume was estimated to be 18 cc. Cooled to liquid nitrogen temperatures, it was mounted in a cryostat of special design. This enabled it to be surrounded by a NaI annular detector 15.2 cm. long with an outside diameter of 23 cm. Since annihilation photons are correlated at 180°, the annulus was optically split into quadrants, each with its own photomultiplier. Logic circuitry was used to enable the system only when a pair production event was detected.

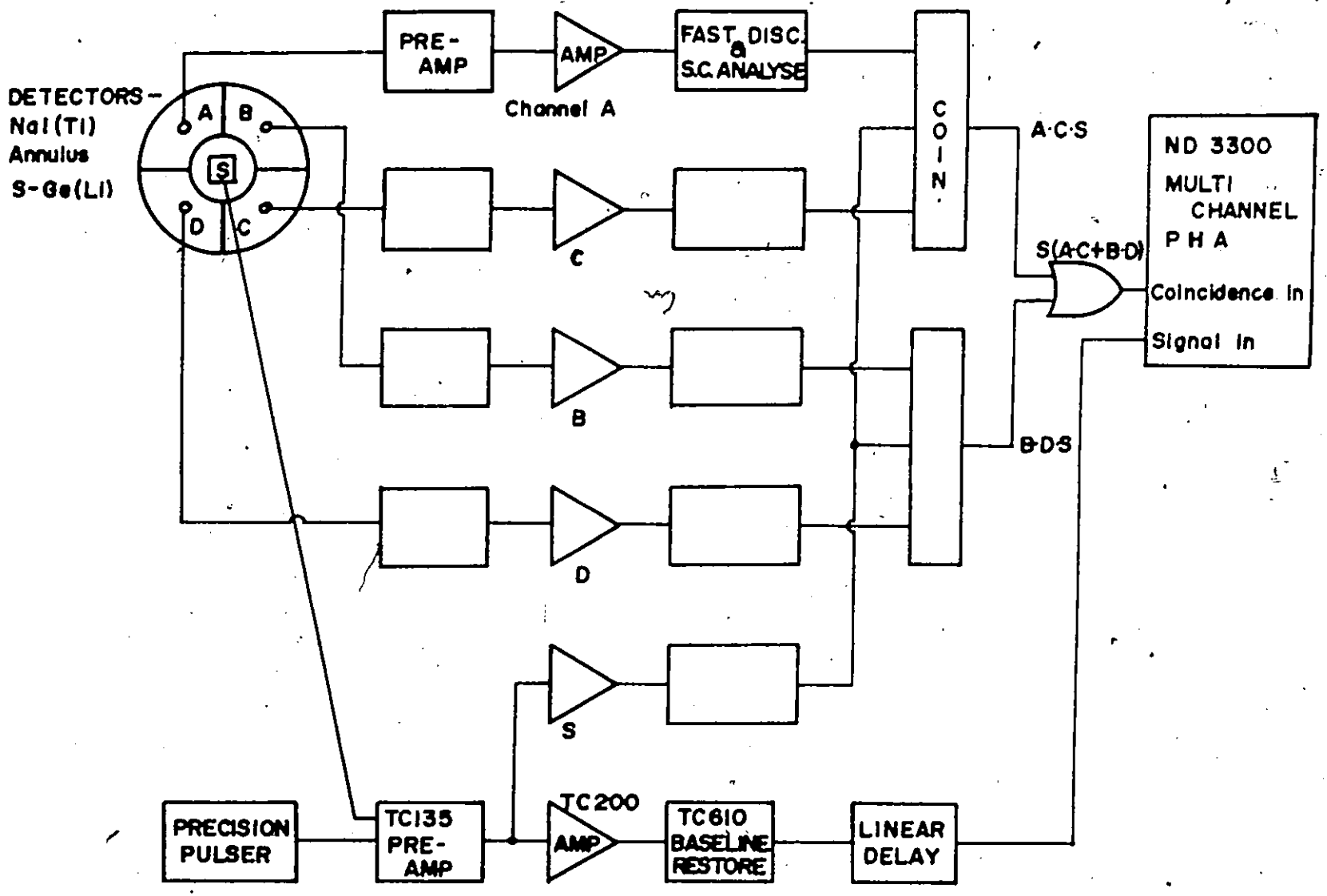

FIG 3·5 – PAIR SPECTROMETER SCHEMATIC

This involves the detection of an event in the central detector, and the simultaneous detection (within the resolution time of the system of ∿ 80 nsec.) of a pair of 511 keV annihilation photons in opposite quadrants of the annulus.

A Tennelec TC135 charge sensitive preamplifier was used in conjunction with a Tennelec TC200 main amplifier in order to shape the pulses from the Ge(Li) detector. This signal was presented to a 4K ramp ADC of high linearity of a Nuclear Data 3300 pulse height analyzer with 16K of memory. Output was via CRT display, typewriter, plotter, or CDC-compatible magnetic tape.

System stability with respect to gain changes and zero shifts is of great importance in the present instance, where experimental runs of long duration were undertaken. It has been observed[50] that such changes can cause 2-4 keV shifts in the positions of spectral features. Difficult to trace, causes of instabilities that have been pointed out include changes in temperature, humidity, line voltage, and the electronics. A precision pulser with the facility to provide peaks at the high and low ends of the spectrum was used in an effort to overcome this problem[51]. This signal was injected into the TC135 preamplifier at the second stage of preamplification. A Nuclear Data series 3300 digital spectrum stabilizer associated with the ADC therefore provided stability from this preamplifier stage to the converter.

Instabilities prior to this stage were reduced by maintaining the preamplifier and the detector connector in a controlled atmosphere of dry nitrogen gas. Stability of this system was high, since no resolution deterioration could be detected when data accumulated for days were compared to those accumulated over one hour.

With a target of typical size, 50 mmb., the spectrometer rate was ∿ 180 events/sec. The rate in the central detector ~~was,~~ however, much higher, since most events have no detectable 511 keV annihilation photons associated with them. Scattering and other processes, as well as a measured greater abundance of low energy photons, contributed further to this rate. Under these conditions the use of a Tennelec TC610 baseline restorer contributed a noticeable improvement in system resolution. Optimum system resolution of ∿ 8 keV at 4 MeV or ∿ 11 keV at 8 MeV was obtained at a detector bias voltage of 2200 v, using monopolar pulses. For the total duration of the experiments, no significant deterioration in the detection system was observed.

Figure 3.6 presents a portion of the gamma ray spectrum following the capture of thermal neutrons in rhodium. The pulser peaks are evident, as are the deuteron and aluminum ground state transitions, the most prominent features of the tube background. An example of a complex spectrum, we see that although the resolution of the system is high, the

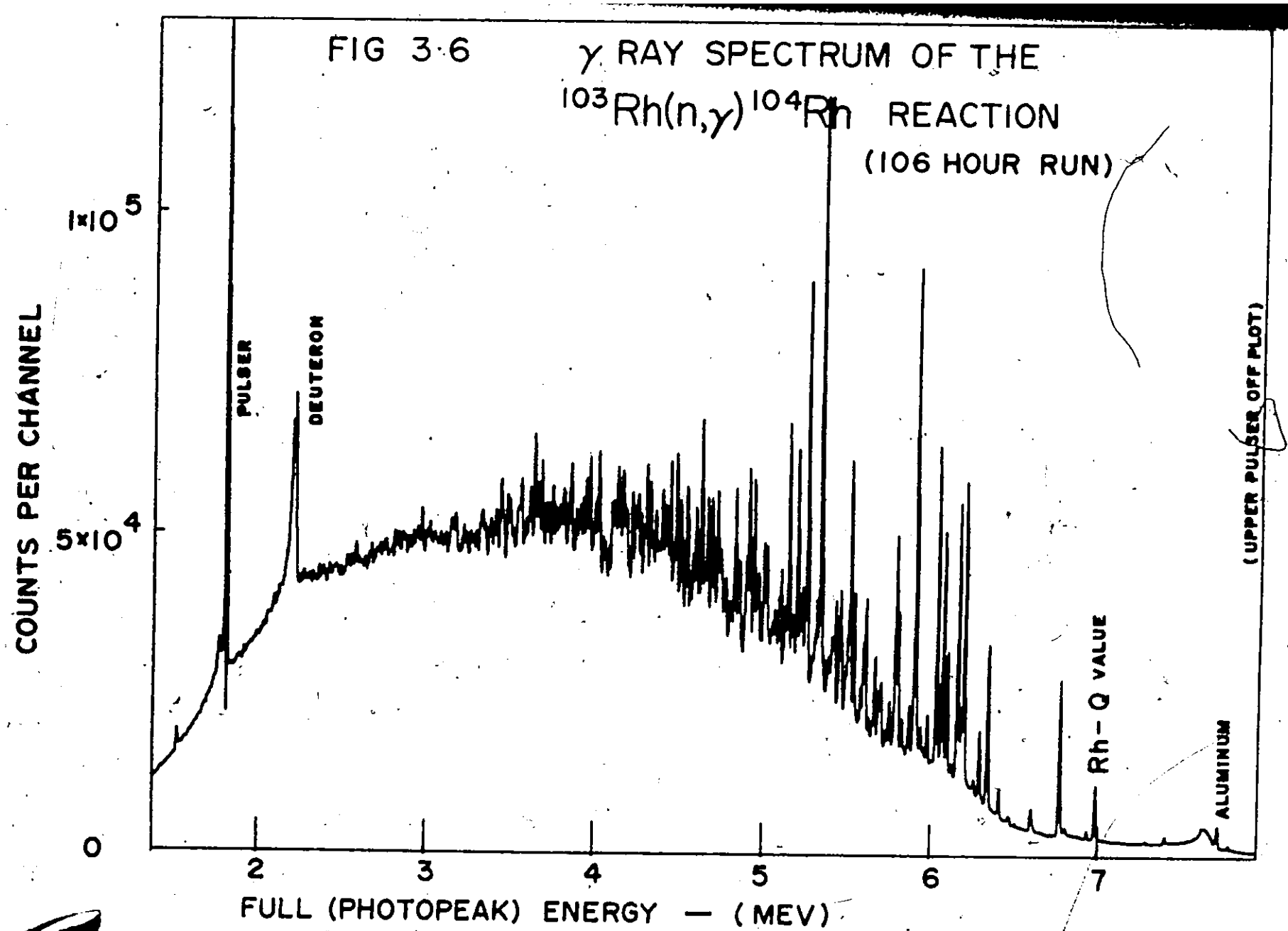
FIG 3·6
γ RAY SPECTRUM OF THE
$^{103}Rh(n,\gamma)^{104}Rh$ REACTION
(106 HOUR RUN)
COUNTS PER CHANNEL
1×10^5
5×10^4
0
PULSER
DEUTERON
Rh-Q VALUE
ALUMINUM
(UPPER PULSER OFF PLOT)
2
3
4
5
6
7
FULL (PHOTOPEAK) ENERGY — (MEV)

line density in the region from 2-4 MeV is so high that few individual peaks can be resolved. A conventional approach to the analysis of such a spectrum yields a loss in observed features due to the overlapping of peaks (resolution effects) and their low intensity (threshhold effects). However, it is to be noted that although individual peaks are not discernable, the observed fluctuations are not of the statistical or $\sqrt{n}$ type[8]. This is apparent from the number of counts per data channel of the spectrum. Where non-statistical fluctuations are observed, they may be attributed to the superpositioning of several or many peaks.

Another typical spectrum, that following the capture of thermal neutrons in ^{14}N, is reproduced in Fig. 3.7. Although some of the foregoing comments with respect to rhodium apply here also, we note that the fluctuations here are statistical. The paucity of transitions is real, since the product nucleus has few energy levels between which gamma ray transitions can occur[52]. In such an instance, an experiment of longer duration will serve only to reduce statistical fluctuations. We hypothesize all features of the system response (other than the Gaussian shaped second escape peak) to be slowly varying functions of energy. These additional features are evident as wide distributions both at a higher energy and at a lower energy than the peak. Therefore no additional information would be gained by a longer experiment,

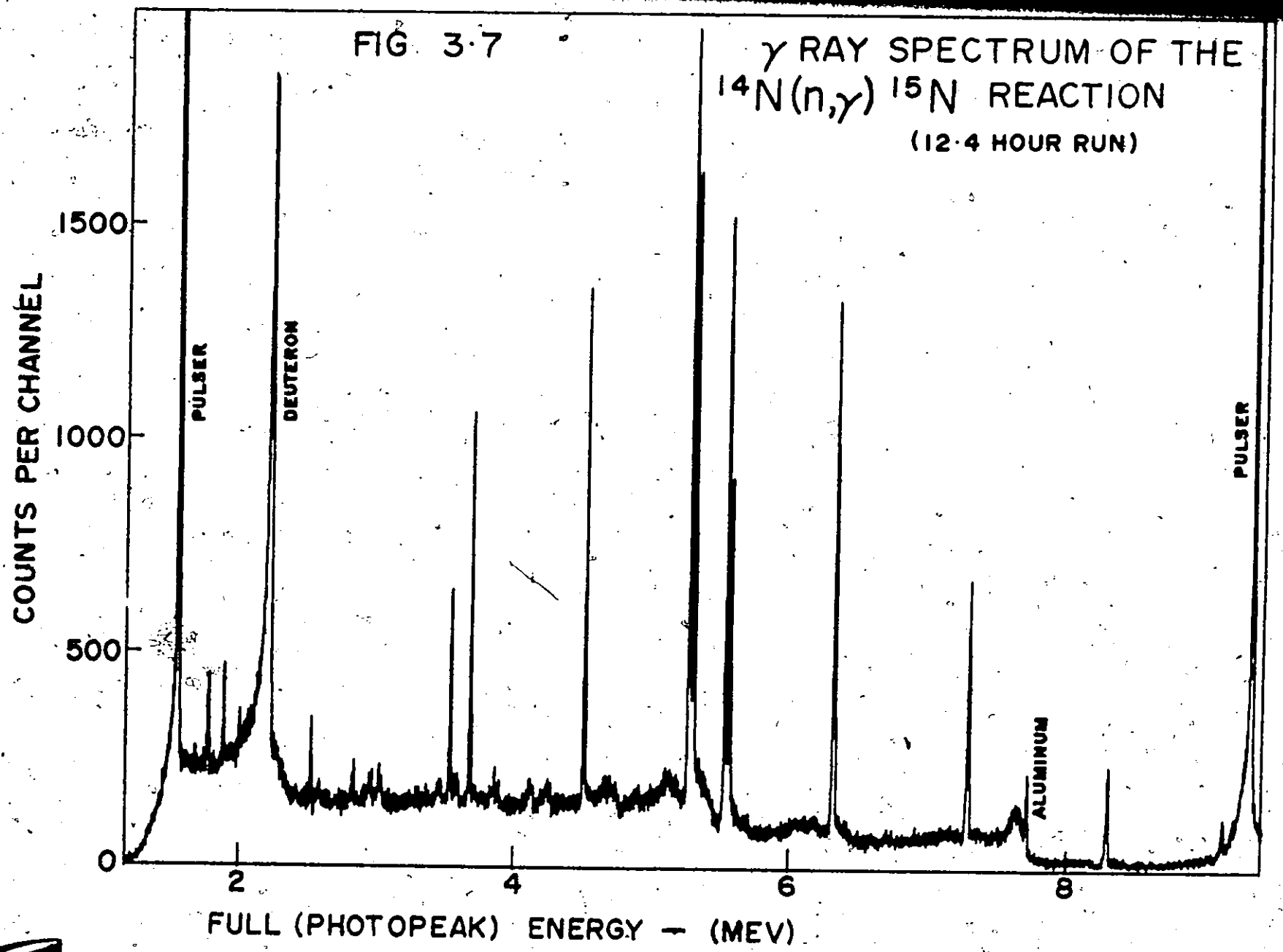
FIG. 3·7
γ RAY SPECTRUM OF THE
$^{14}N(n,\gamma)\,^{15}N$ REACTION
(12·4 HOUR RUN)
COUNTS PER CHANNEL
1500
1000
500
0
PULSER
DEUTERON
ALUMINUM
PULSER
2
4
6
8
FULL (PHOTOPEAK) ENERGY — (MEV)

other than greater statistical accuracy. The method of obtaining the response function from this spectrum as well as from the spectra of ^{29}Si and ^{41}Ar is described in Chapter 5.

Its successful use by other workers[53] led us to use the nitrogen data for the gamma ray transitions compiled by Marion[46] as a calibration for the system. This confirmed that the non-linearity of the ADC was small indeed - the energy-channel relationship was fitted most satisfactorily by a quadratic, which was, typically,

$$E(CH) = 1.1846 + 2.0157\times \frac{CH}{1000} + .07405\times\left(\frac{CH}{1000}\right)^2$$

where E is in MeV when CH is expressed as the channel number of the experiment. Slight gain changes resulting from rate effects were taken into account by monitoring the Al and D ground state transitions, and the coefficients were adjusted accordingly. It has been shown[53] that the total error introduced by this transformation is normally distributed with a $\sigma \sim .2$ keV.

The relative efficiency of the spectrometer was also found using Marion's[46] data. This has been plotted in Fig. 3.8. Also shown is the pair production cross section for germanium. At the outset these curves might be expected to be identical in form. However, several considerations dictate that this should not be so:

SYSTEM EFFICIENCY

FIG 3·8

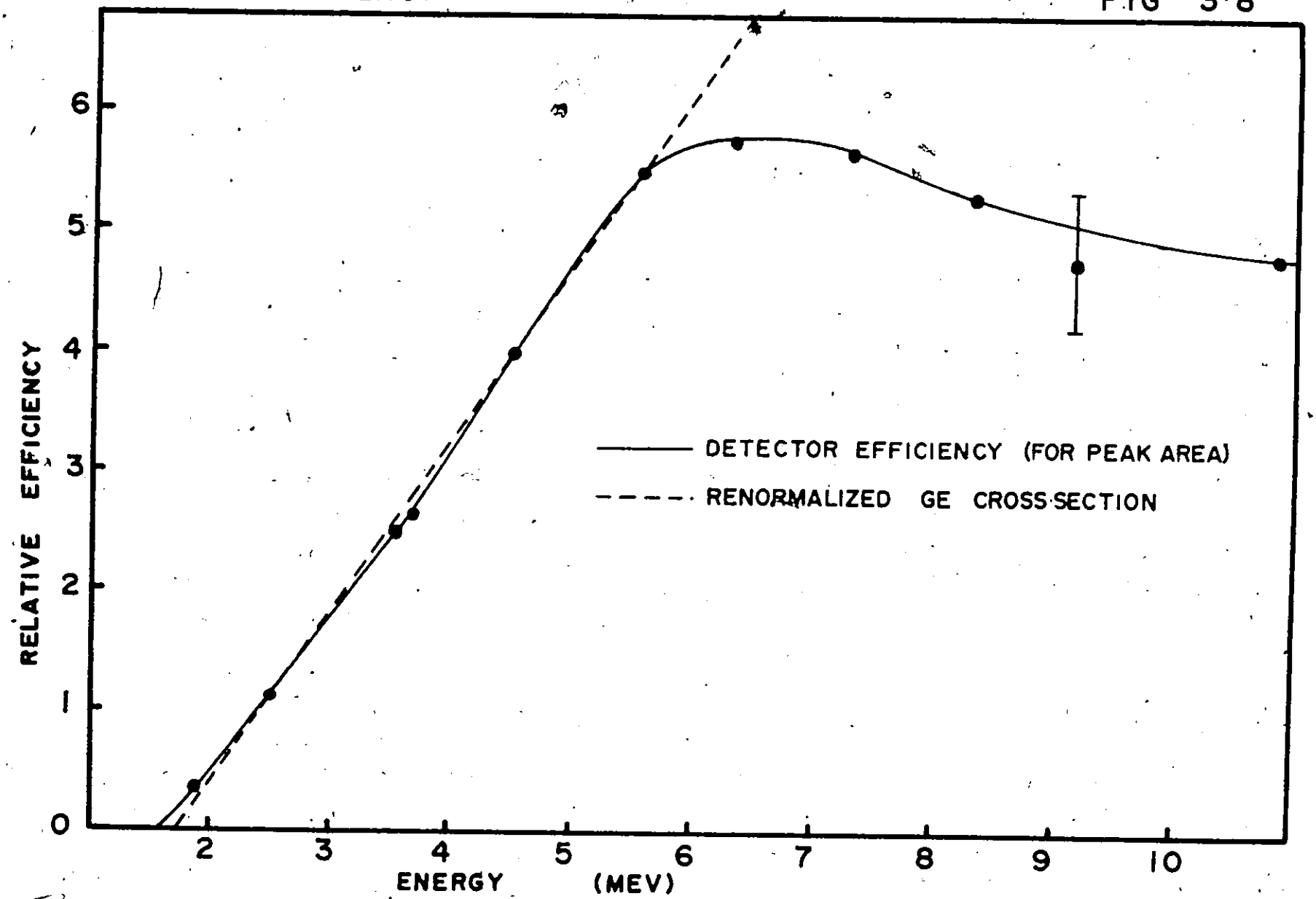

1. The hardening of the gamma beam by the interpositioning of shielding materials between the target and detector.
2. The finite size of the detector, and other characteristics such as its inactive volume.
3. Considerations such as random addition and the escape of Bremsstrahlung photons, which are discussed in Chapter 5.

The relative efficiency curve was also empirically fitted to a quadratic, however in this case three regions were considered:

$$\mathrm{Eff}(E) = \begin{cases} .1E^2 + .7E - 1.2 & 2 < E \leq 5 \\ -.4E^2 + 5.3E - 11.7 & 5 < E \leq 7 \\ .05E^2 - 1.15E + 11.4 & 7 < E \leq 11 \end{cases}$$

This function describes the system efficiency for the peak area, as opposed to peak height. The energy E is expressed in MeV.

The resolution of the system is just that of the Ge(Li) central detector. Resolution limitations are placed by such considerations as surface leakage currents and fluctuations in the number of electron-hole pairs[54] created by a gamma ray of energy E. The latter involves the Fano factor[55] which is given by

$$F = \frac{\sigma^2}{n}$$

where n is the number of electron-hole pairs produced, and

σ^2 is the variance in this yield. If ε is the energy required to create an electron-hole pair, then for a gamma ray of energy E

$$n = \frac{E}{\varepsilon} .$$

Using the full width at half the maximum of the peak as a criterion, the energy resolution is then given by:

$$FWHM = 2.35 \quad \sigma = 2.35 \sqrt{\varepsilon E/\varepsilon}$$

For most Ge(Li) counters the Fano factor varies between .05 and .1[56], and ε = 2.8 eV for germanium. Therefore on the basis of statistical effects only, the best possible resolution obtainable by a Ge(Li) detector is ∿ 2.4 keV at 4 MeV, and ∿ 3.5 keV at 8 MeV. Factors other than statistical contributed to resolution defects in the counter used in this study. These include surface leakage currents, poor charge collection and fluctuations in the baseline that were not compensated for by the baseline restorer. An adequate representation of the system resolution was found to be

$$W(E) = 3.95 + .934E$$

as shown in Fig. 3.9. W is the FWHM of the peak in keV when E is expressed in MeV.

These relationships were used in the following statistical analysis as well as in the tabulations of Appendix 4.

SYSTEM RESOLUTION FIG 3·9

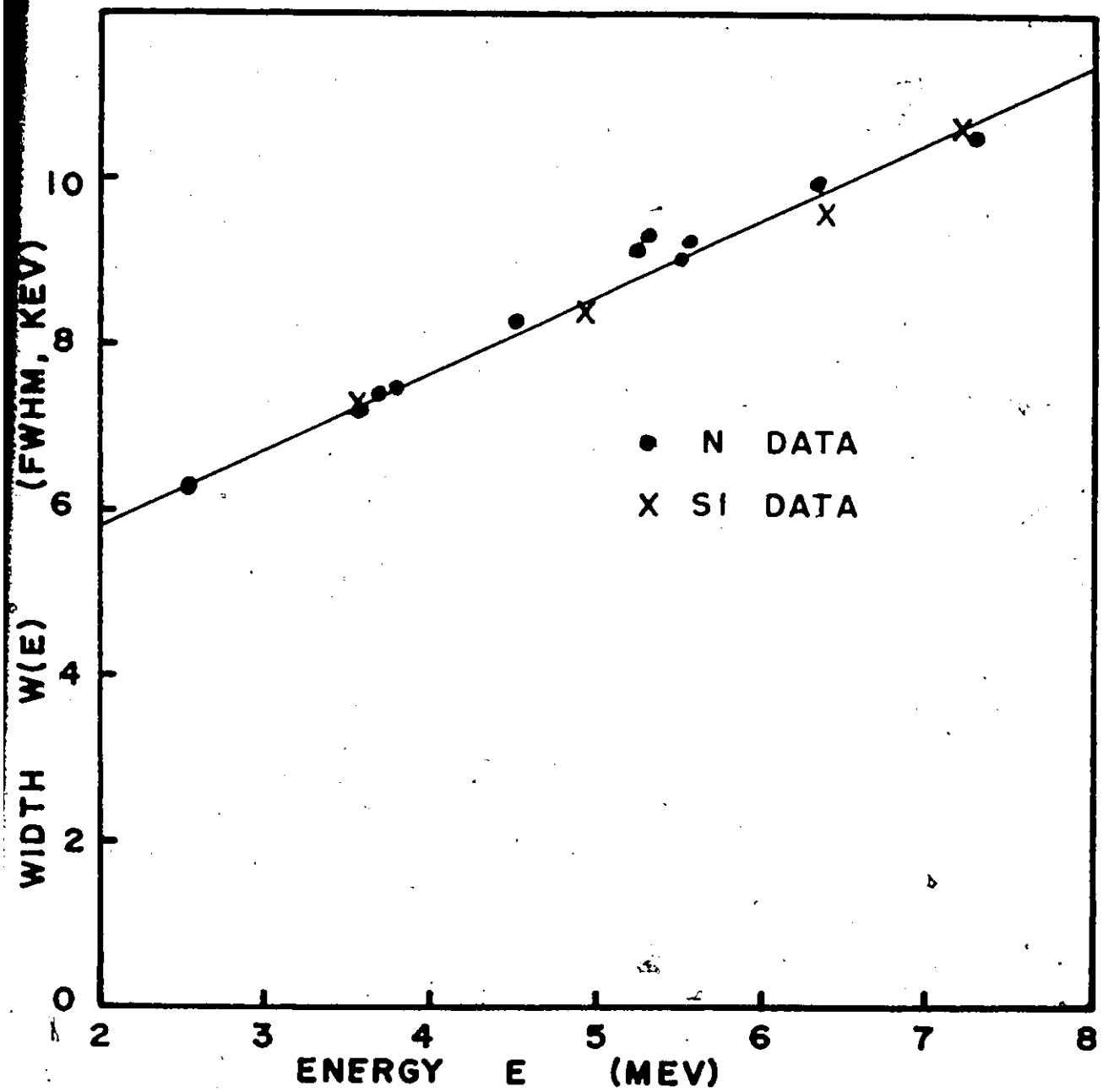

CHAPTER 4

A SIMPLE STATISTICAL MODEL OF THE NUCLEUS

In order to evaluate the utility of the information we plan to extract from the spectra under study we introduce a simple statistical model of the nucleus. Its basic components are a nuclear level density distribution and an estimate of gamma ray transition probabilities. Under certain assumptions results may be analytically obtained. When this is impossible we resort to a computational technique which allows the inclusion of existing level density information. This method also allows for a variation of the forms of the basic components of the model. A summary of some additional information which may be obtained from this description is given in Appendix 3.

ANALYTICALLY OBTAINABLE RESULTS

Some aspects of the statistical model are mathematically very easily formulated. We consider Ericson's constant nuclear temperature model[11] for the level density, namely

$$\rho(E) = \rho_o \exp(E/T) \qquad (2.6)$$

Below some arbitrary energy Q (the neutron separation energy or 'Q' value for the (n,γ) reaction), there are M discrete nuclear levels:

$$M = \int_0^Q \rho(E)dE = \rho_0 T(\exp(Q/T)-1) \quad . \qquad (4.1)$$

From a combinatorial approach the total number of possible transitions N between levels is given by

$$N = M(M-1)/2 \quad . \qquad (4.2)$$

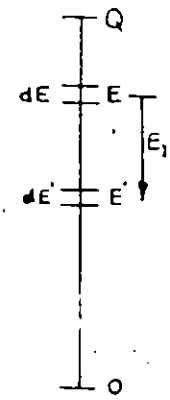

That the continuous level density is consistent with this can be seen by performing

$$\int_0^Q [\int_0^E \rho(E')dE']\rho(E)dE \quad .$$

This integral represents all transitions between levels at E and E', and yields, using equation (4.1), a value of $M^2/2$ which is in agreement with equation (4.2).

The derivation of a relationship between the energy and density of transitions using the statistical model is no more complex. If $E_\gamma = E - E'$, the gamma ray transition energy, we write $n(E_\gamma)$, the number of transitions per unit energy as

$$n(E_\gamma) = \int_{E_\gamma}^Q \rho(E)\rho(E-E_\gamma)dE$$

$$= \int_{E_\gamma}^Q \rho(2E/T)\exp(-E_\gamma/T)dE$$

$$= \frac{\rho_o^2 T}{2} \exp(-E_\gamma/T)\{\exp(2Q/T)-\exp(2E_\gamma/T)\}$$

Therefore

$$n(E_\gamma) = \rho_o^2 T \exp(Q/T)\sinh((Q-E_\gamma)/T). \qquad (4.3)$$

The correctness of this result is confirmed by performing

$$N = \int_0^Q n(E_\gamma) = M^2/2,$$

again in agreement with equation (4.2)

Through equation (4.3) the statistical model therefore predicts a relationship between the transition density and the nuclear temperature.

COMPUTER CALCULABLE RESULTS

A continuation of the analytical calculation shows that such an approach to the calculation of spectral shapes involves a multiple integral over a number of variables equal to the number of levels below Q. This is because the intensity of a transition depends on the population of the initial state, which depends on the populations of all the states above it.

Fortunately the advent of large scale, high speed computers allows us to calculate spectra to as great an accuracy as desired. Several workers[37,38,42] have achieved varying degrees of success in performing such calculations. We have chosen to digitize the energy level density into

bins of arbitrary and equal energy width. Figure 4-1 indicates the result of calculations for different bin sizes. A greater accuracy requires smaller bins and therefore more computational effort. We define a level density D(E,S,P) and a population T(E,S,P) for each bin. Bins are labelled by E, a number proportional to energy, S, a spin and P, a parity index. The form of D is given by the level density theory assumed and can be modified when the levels are known. An estimate for transition probability is then introduced, $\Gamma(\Delta E,\Delta S,\Delta P)$, as well as X(E,S,P), a factor proportional to the intensity leaving a bin, similar to a branching ratio. T and X are introduced in order to reduce the computational effort required to calculate the actual spectrum. The spectral intensity S of energy E_γ is then just

$$S(E_\gamma) = \sum_{\substack{\text{energy} \\ \text{such that} \\ E_i - E_f = E_\gamma}} \; \sum_{\substack{\text{spin} \\ \text{parity}}} \{D_i \cdot D_f \cdot T_i \cdot X_i \cdot \Gamma(E_\gamma, \Delta S, \Delta P)\}. \quad (4.4)$$

The subscripts i and f in the above equation are used to label the initial and final energy bins. Appendix 3 indicates some other distributions which may be calculated using the above formalism.

Calculated Spectrum

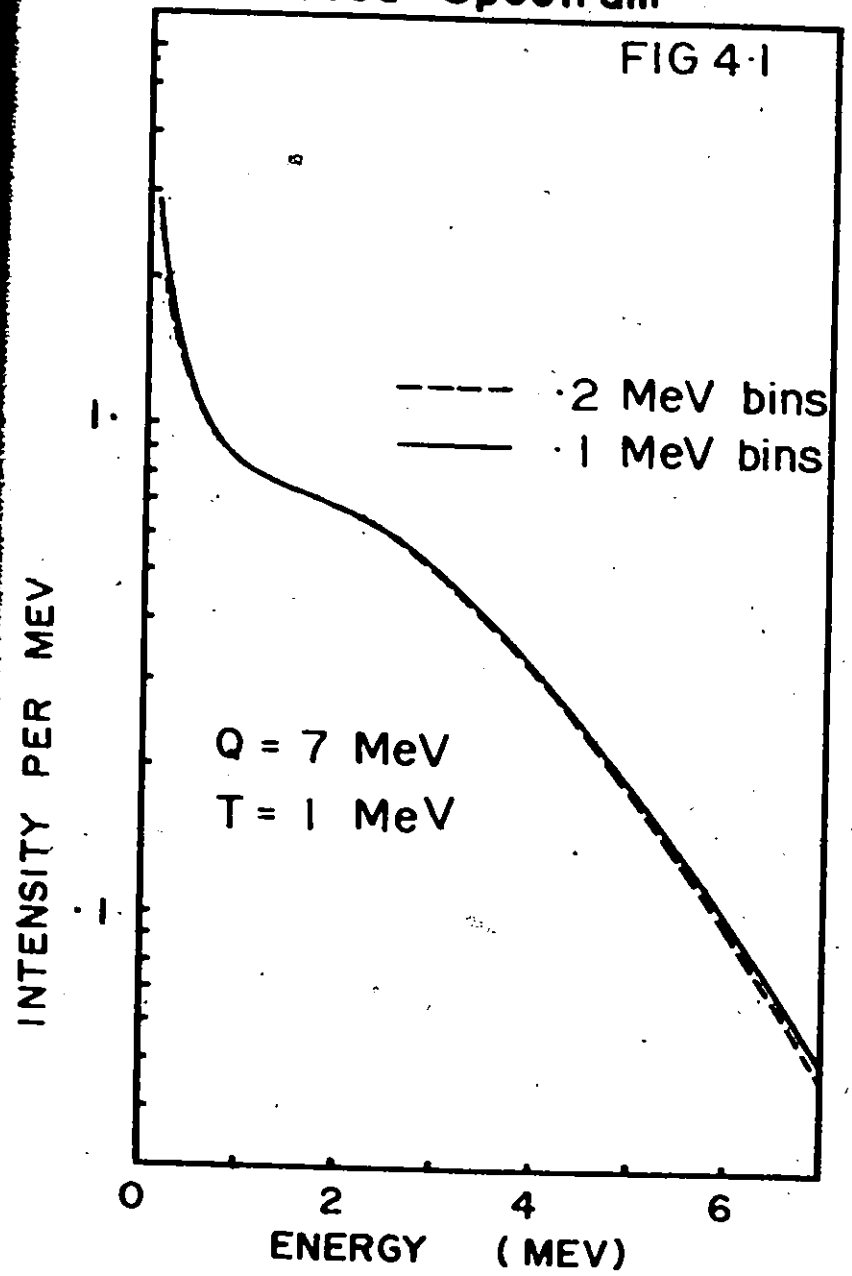

CHAPTER 5

TREATMENT OF DATA

Complex spectra are discussed in the light of a conventional method of analysis, in order to motivate a statistical approach to their reduction. The data obtained from the gamma spectrometer are simplified by a consideration of the system response.

RESOLUTION LOSSES

All the spectra obtained were analysed conventionally. The tabulations of the energy and amplitude of spectral features appear in Appendix 4.

In general a detection system may be classed as to whether it is paralyzable or non-paralyzable[57]. If σ is the time required to analyse an event, or the 'dead time' of the system, then a non-paralyzable system can accept no events while it is 'busy'. However in the paralyzable case, although events occuring while the system is busy are not detected, they extend the length of the dead time. An ADC behaves as a member of the former class, whereas a Geiger Müller tube is paralyzable.

We now consider the experimenter as a detection system for the peaks and their amplitudes in complex spectra. What is usually considered to be a time domain is now energy. We select the ^{46}Sc results and focus our attention on the

energy range 2260-6750 keV, because the apparent transition density is constant in this region. Since we are interested in investigating the relationship between the apparent loss in number of peaks and the resolution of the system, one of these variables must be studied as a function of the other.

As a starting point we tabulated the number of transitions observed in this energy region, and found the energy resolution of the system. For the purposes of a model, averages over the region of interest were considered. The resolution of the observed spectrum was then degraded by means of convolving a Gaussian function with it. It may be shown[21] that the convolved data is equivalent to the data that would be observed by a system with poorer resolution. The number of transitions observed and the average energy resolution in this region were also obtained for several of these convolved spectra.

Now for the paralyzable model, it can be shown[57] that

$$n_o = ne^{-k\sigma n}$$

where n_o is the observed peak density

n is the true peak density

σ is the resolution (FWHM).

This approach yields a value of $k = 0.621$, which is physically realistic. Fig. 5.1 shows the number of transitions observed as a function of the system resolution. If we use

EFFECT OF RESOLUTION ON OBSERVATION

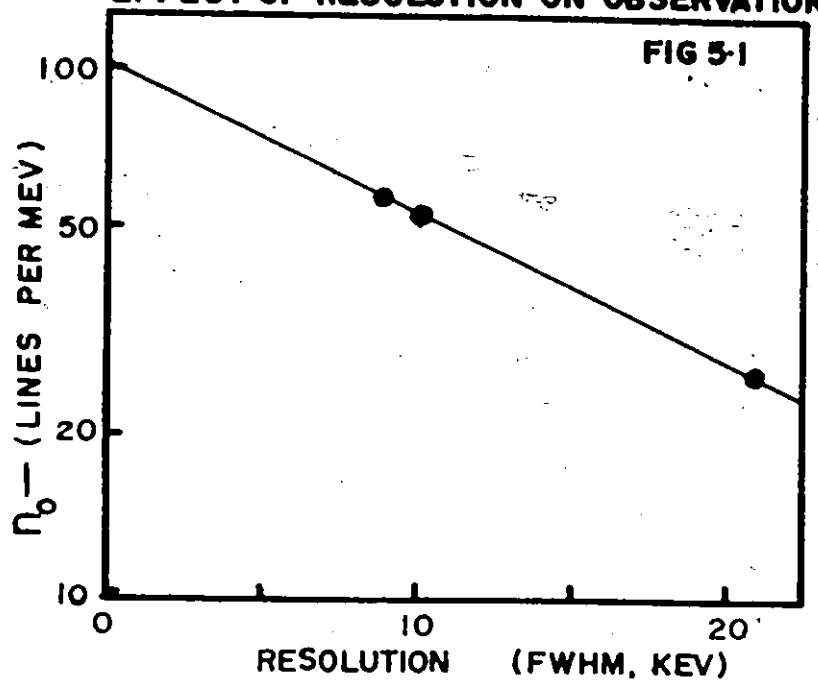

EFFECT OF LOSSES ON OBSERVATION

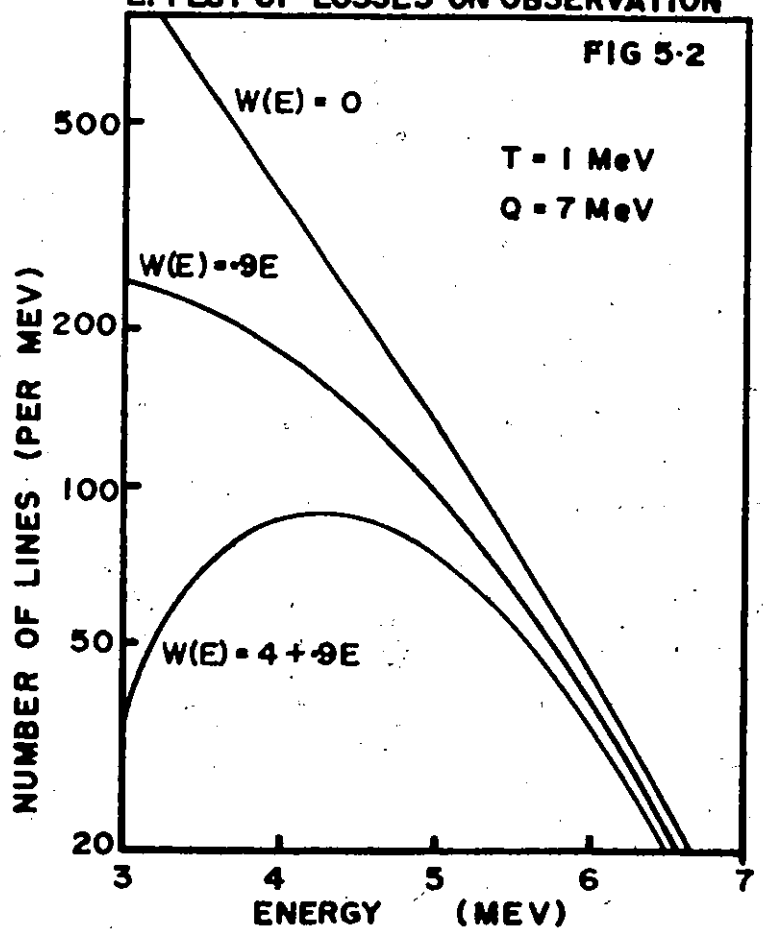

this result to extrapolate to $\sigma = 0$, we obtain the result $n = 103$ transitions/MeV. The number actually observed was 57 transitions/MeV. Therefore it appears that even for spectra of moderate complexity, such as scandium, only a fraction of the number of components actually present are observed.

In Fig. 5.2 the functions of Chapter 4 are used to plot the transition density. The result for a nuclide with $Q = 7$ MeV, a nuclear temperature of 1 MeV, and a $\rho_o = 200$ is presented. A typical curve, the actual data, and the ultimate curve obtainable with present statistically limited detectors are shown. If one considers the non-paralyzable model it is found that k increases with increasing losses. Although this model may have some physical reality, the data do not support it.

In the following section we describe the detector response function.

RESPONSE SIMPLIFICATION

As was seen in Chapter 3, the use of a pair spectrometer simplifies the response function R(E,E') from a complex one by discriminating against all but the pair production events. Ideally, R(E,E') is simplified to the second escape peak - a delta function observed at an energy E' - 1022 keV. Realistically, defects and noise in the detector and electronics degrade the delta function to a Gaussian peak of finite width. Furthermore, previously negligible contributions to the response function now become observable.

TYPICAL HIGH ENERGY GE (LI) DETECTOR RESPONSE

FIG 5·3

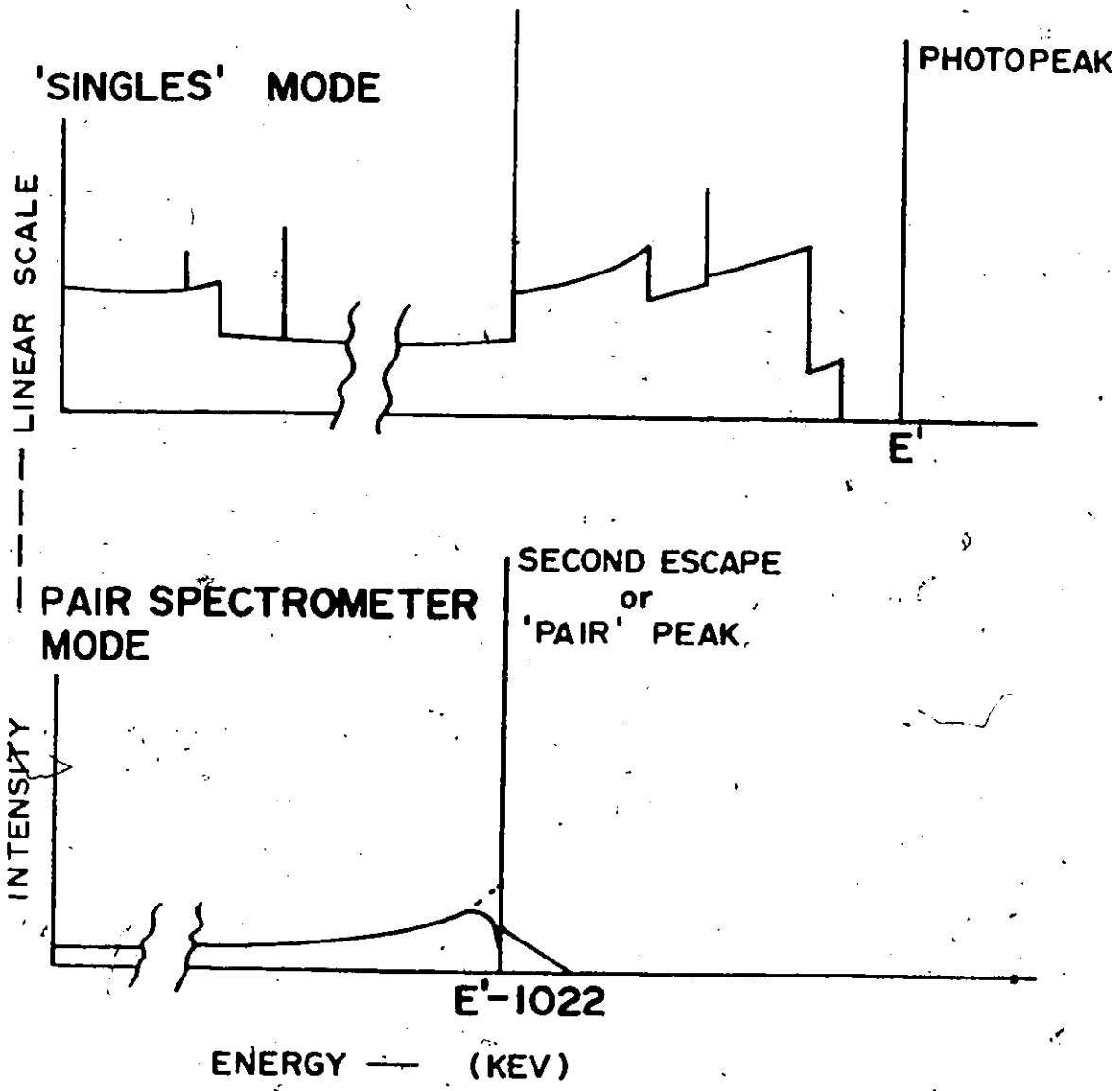

Figure 5.3 shows a comparison between the response of a pair spectrometer and that of the same detector used without the restrictions imposed by the pair spectrometer circuits. It should be noted that throughout this work we adopt the practice of shifting the energy scale by assigning the full energy or 'photopeak' energy to the second escape peak. Where significant, the appropriate energy correction for the recoil of the nucleus is made. We now proceed to account for some of the observed features in the pair spectrometer response.

Bremsstrahlung[58] or braking radiation, is electromagnetic radiation which is created by accelerating charges. In pair production the electron-positron pair has a kinetic energy which is transformed by collision to an electric charge consisting of electrons and 'holes'. This state is reached in a time which is very short compared to the time required for charge collection. The negative acceleration of charges which is required to attain this state is accompanied with the production of bremsstrahlung. It is the escape of one or more bremsstrahlung photons from the detector which accounts for the feature of the response shown in Fig. 5.4. It can also be shown that the escape of an electron from the active volume of the central detector before all of its energy has been dissipated may account for a flat distribution below the energy of the second escape peak.

BREMSSTRAHLUNG

FIG 5·4

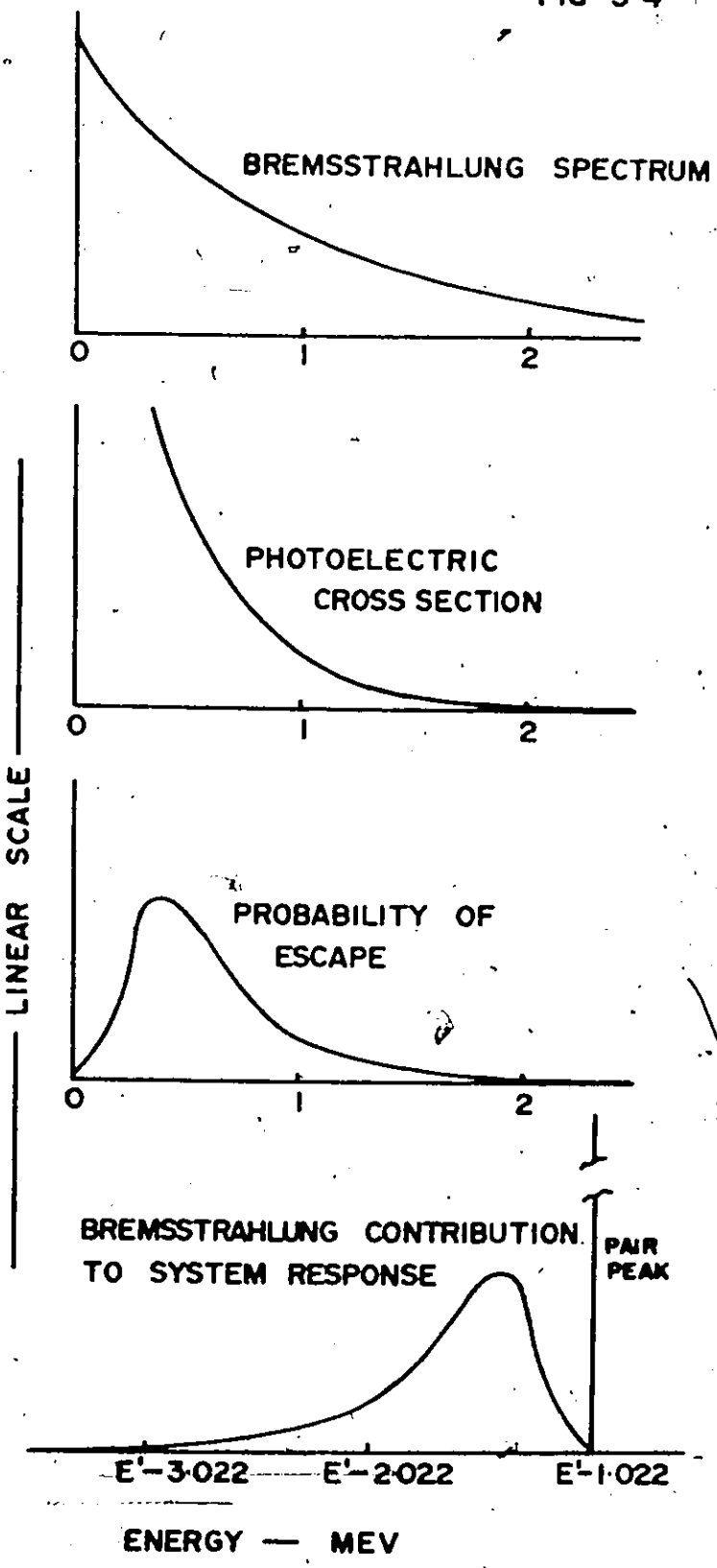

The remaining features of the observed response are ramifications of conditions which may, under ideal circumstances, be controlled. Finite temporal resolution normally results in a chance or singles component to the spectrum. This was not observed, and therefore the effect was negligible. The random addition of low energy events in the data acquisition system, avoidable by reducing the count rate, is manifest. When two events occur in an interval short compared to the decay time of the pulses which represent then in the data acquisition system, the amplitude of the second pulse may appear greater than it is. This is a result of the addition of the low frequency components of the first to the amplitude of the second. Sophisticated circuits in the amplifier system such as a baseline restore circuit do not entirely compensate for this effect. Random addition is experimentally indistinguishable from some other effects. The detection of non-511 keV events by the NaI scintillator is an example. Conditions were such that events less than 511 keV in energy would in fact trigger the coincidence circuits. Such an event might result from the Compton scattering of an annihilation photon within the Ge detector, or it might be a bremsstrahlung photon. In any case all these effects, labelled as random adding, displace events to a higher energy in the spectrum.

The response of the system thus has three natural components. Each of these may be represented by a response

matrix such that their matrix product is equal to the total response matrix. Equation (2.3) may therefore be written as:

$$S = R_{ra} R_b R_g T.$$

The action of R_g on T, the observed spectrum, represents the degradation of the resolution to a Gaussian. The action of R_b represents the contribution of the bremsstrahlung and the electron escape to the response. The action of R_{ra} represents random adding effects.

Of these three matrices R_{ra} and R_b can be adequately represented by functions involving nine parameters and two variables. The functions were found entirely empirically, and the parameters were optimized using a non-linear least squares computer fitting technique. Since convergence was slow and difficult, not all the parameters were allowed to vary at the same time. Figure 5.5 illustrates a typical idealized shape for the response at channel x to a gamma ray of intensity I. It also indicates the sequence of the calculation. The relation between energy and the channels of the experiment has been indicated in Chapter 3.

The effect of random addition is to displace events from a channel i to some channel j, where j > i. The R_{ra} is therefore an upper triangular matrix. In Appendix 1 the exact equivalence between multiplication by the inverse of a triangular matrix and a convolution approach requiring much less computational effort is detailed.

RESPONSE CALCULATION

FIG 5·5

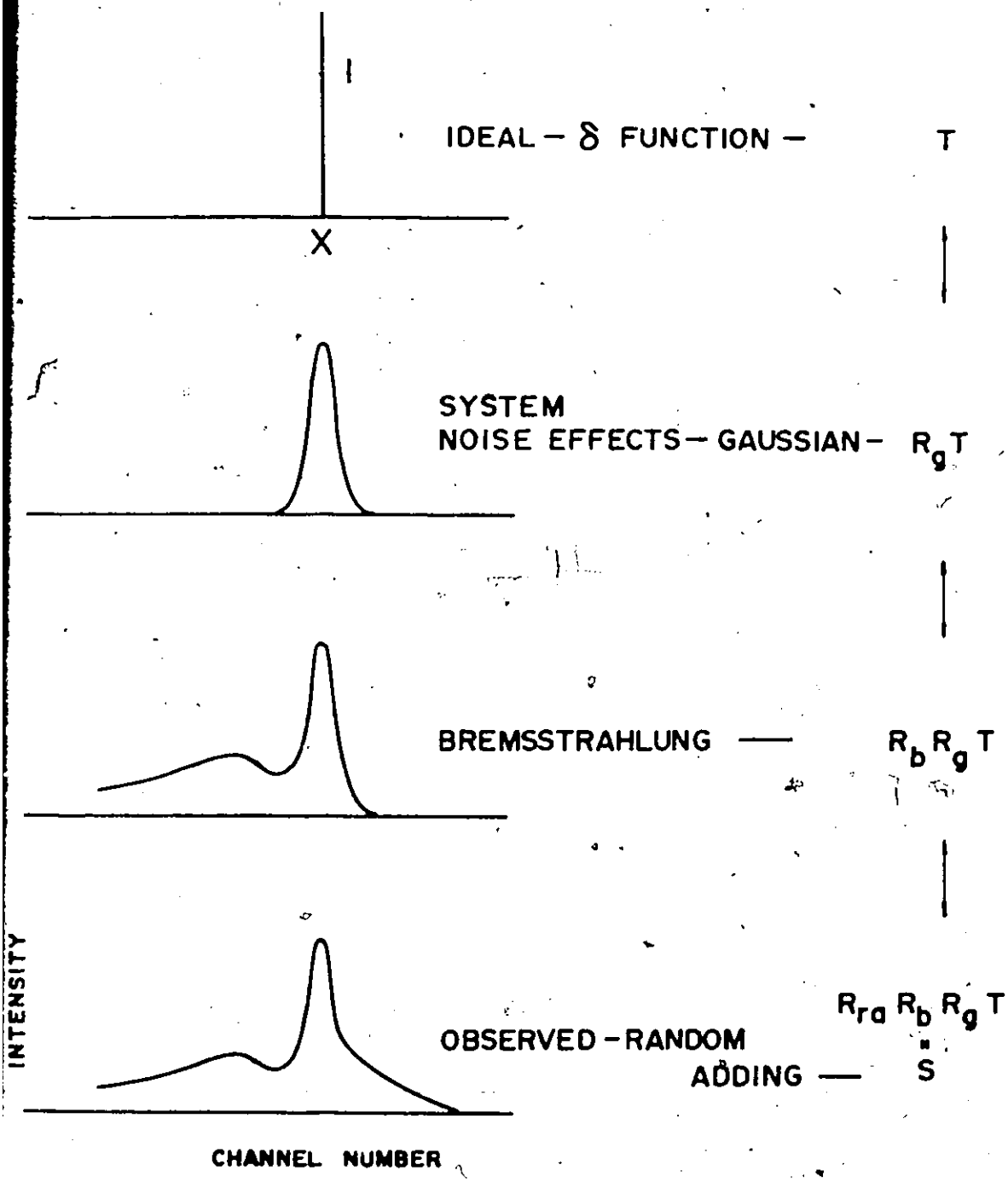

In a like manner the effect of bremsstrahlung and electron escape is to displace events from channel i to channel j where j<i. Therefore R_b may be represented by a lower triangular matrix. The multiplication of the spectrum by the inverse of R_g was not carried out. This is because of an amplification of statistical errors that is associated with this operation[2]. We therefore simplify the spectrum to the extent that it consists of a distribution of Gaussian peaks:

$$\text{simplified spectrum} = R_b^{-1} R_{ra}^{-1} S = R_g T.$$

We define the efficiency of the system to be the efficiency for the detection of double escape events. The peak is considered before any response corrections are made. Note that each response correction can be made to either eliminate events not in the peak from the spectrum, or include these events in the peak. For both the bremsstrahlung and random addition corrections, the former was done.

Random adding and bremsstrahlung contributions to the response can be considered as long range correlations, whereas the Gaussian peak and statistical fluctuations are short range. Since the response simplifications involved only the long range correlations, it was found that the above operations could be carried out using 10 channel (20.15 keV) increments.

In practice, the technique allows a determination of the low frequency components of the spectrum consisting of the bremsstrahlung and random adding events. The spectrum containing solely Gaussian 'pair' peaks is obtained by subtraction of these components from the observed spectrum.

CHAPTER 6

STATISTICAL DESCRIPTION OF PEAKS

An application of the calculation indicated in Chapter 5 reduces the complexity of the system response to a single Gaussian peak. Short range correlations between neighbouring data channels, such as the shape of these Gaussian peaks and statistical fluctuations, are not significantly affected. In the present chapter we develop a technique to account for all features, whether resolved or not, in the simplified spectrum. The notions of a peak density and average peak amplitude are considered.

GENERAL

As a starting point, some statistical properties of spectra were investigated. We focussed our attention on the distribution of spacings between gamma rays and the distribution of amplitudes of these transitions. We considered spectra of intermediate complexity, where it was assumed most peaks could be resolved. Amplitude distributions of these spectra were also plotted. In order to correct for any gradual variation across the spectrum, each value of the parameter was divided by a local average of that parameter, taken over seven neighbouring values. Results for scandium, which were

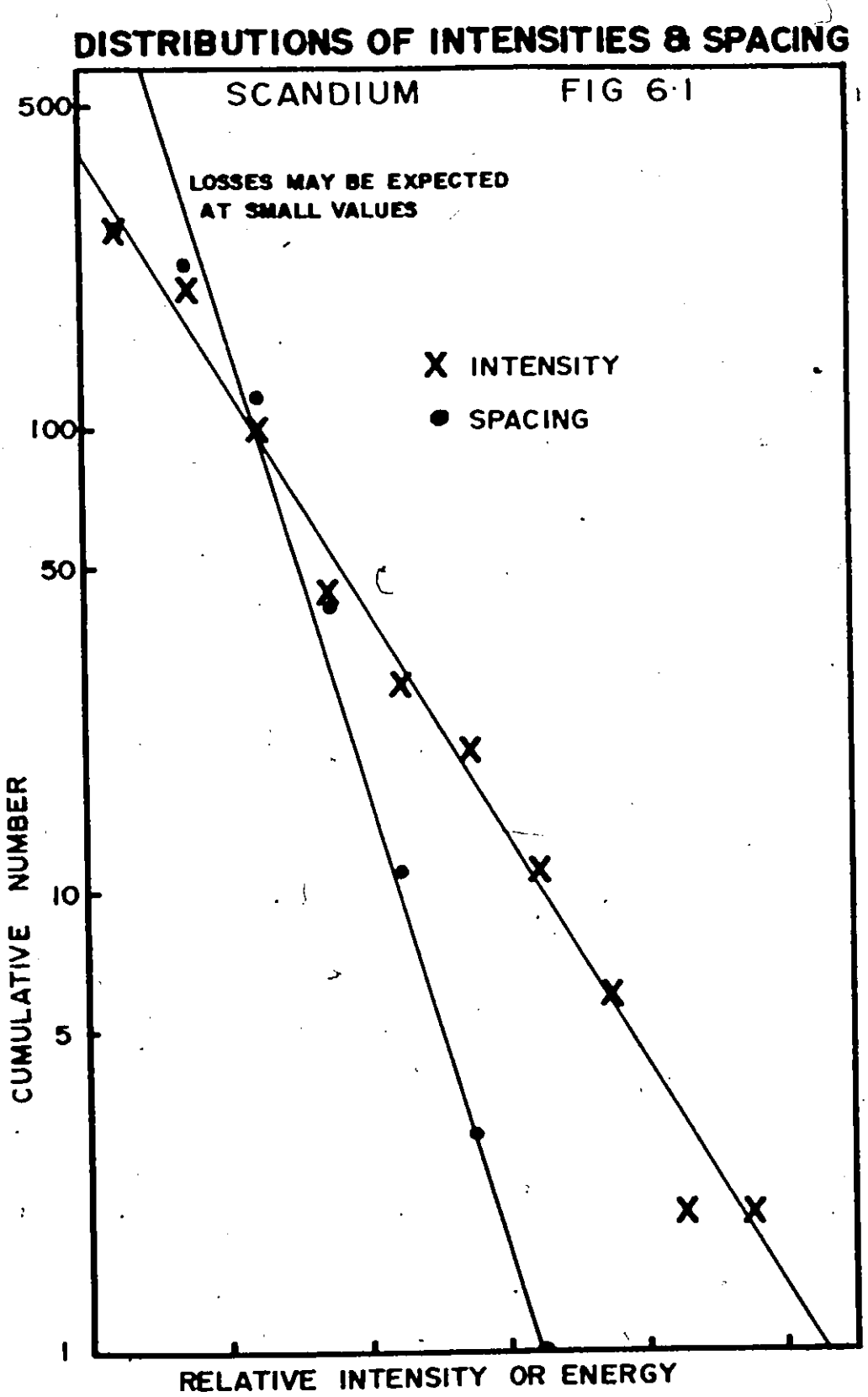
DISTRIBUTIONS OF INTENSITIES & SPACING
SCANDIUM
FIG 6·1
LOSSES MAY BE EXPECTED
AT SMALL VALUES
X INTENSITY
● SPACING
500
100
50
10
5
1
CUMULATIVE NUMBER
RELATIVE INTENSITY OR ENERGY

typical, are indicated in Fig. 6.1 and may be seen to be exponential for both the spacing and amplitude distributions. The integrals of the distributions are presented. We assume that this result is general, and would be obtained also from spectra of greater complexity if spectrometers of appropriate resolution and efficiency were available.

In such spectra the peaks are no longer all resolved. The mechanisms by which they are lost may be identified as overlapping or resolution and insufficient intensity or statistical. However it is noted that in regions where no features can be resolved, short range correlations exist leading to a variance which is greater than what would be predicted from statistical considerations alone.

The exponential distribution of spacings between gamma transitions indicates that the number of spectral components, m, that fall within a given interval of the spectrum follows a Poisson distribution[59].

$$P(m) = \frac{N^m}{m!} e^{-N} \quad . \tag{6.1}$$

Here N is the average number of components in the interval. Furthermore since the amplitudes of the components are also exponentially distributed we write the distribution of the total intensity I arising from m components as

$$P_m(I) = \frac{I}{I_o}\left(\frac{I}{I_o}\right)^{m-1} \frac{e^{-I/I_o}}{(m-1)!} \quad (\text{for } m \geq 1)$$

$$P_o(I) = \delta(I) \tag{6.2}$$

where $\delta(I)$ is the Dirac delta function[7]. This follows immediately from a convolution of m exponential probability distributions. In the above I_o represents the average intensity of a spectral component.

We combine these results to give

$$P_{mN}(I) = \frac{1}{I_o} \left(\frac{I}{I_o}\right)^{m-1} \frac{N^m}{(m-1)!\,m!} \exp\left(- N - \frac{I}{I_o}\right)$$

$$(\text{for } m \geq 1) \qquad (6.3)$$

which is the probability of observing a total intensity I in a given interval from m spectral components, as a function of average peak density N. Since I can arise from many values of m even when N and I_o are fixed, we must sum over the m's.

In order to properly consider m = 0 and I = 0, we have two regions, and denote $x = I/I_o$:

(1) $x = 0$

From equations (6.1) and (6.2) we have for the total probability

$$P_N(C) = e^{-N}\left(1 + \frac{N}{I_o}\right)$$

which arises from m = 0 and m = 1. We get no contribution from m > 1 since by equation (6.2) the probability of zero intensity with more than one component is zero.

(2) $x > 0$

We have contributions due to $m \geq 1$:

$$P_N(x) = \frac{1}{I_o}[N\exp(-x-N) + \frac{xN^2}{2!}\exp(-x-N) + \frac{x^2N^3}{2!3!}\exp(-x-N) + \ldots]$$

$$= \frac{N}{I_o}\exp(-N-x)\ [1 + \frac{xN}{2!} + \frac{x^2N^2}{2!3!} + \ldots + \frac{x^nN^n}{n!(n+1)!} + \ldots] .$$

To examine some of these distributions it is convenient to scale the independent axis. Since $x = I/I_o$ we can replace x by $x = \alpha N$. Then we have

$$P_N(\alpha) = \frac{N}{I_o}\exp(-N(1+\alpha))[1 + \frac{\alpha N^2}{2!} + \frac{\alpha^2N^4}{2!3!} + \ldots + \frac{\alpha^nN^{2n}}{n!(n+1)!} + \ldots] \quad (6.4)$$

Figure 6.2 shows this result as a surface. The distribution describes the intensity expected in an interval when N features are expected to be present there. The value of $\alpha = I/NI_o$ is the ratio of the actual total intensity to the mean total intensity. As expected, the most probable value of this ratio tends to 1 as N increases. For small N, the density tends to resemble an exponential function, a reflection of the exponential distribution of the intensity of individual features. For large N, the density function appears to approach a Gaussian distribution, which may be regarded as a consequence of the convolution of a large number of exponential distributions. (The plotting program for Figure 6.2 was developed[60] at the McMaster University Computing Centre).

TRANSITION DENSITY

We now proceed to determine whether a relationship between discrete and statistical spectral properties can be found. More explicitly, we seek a relationship between the

FIG 6·2

PROBABILITY DENSITY

$P_N(\alpha)$

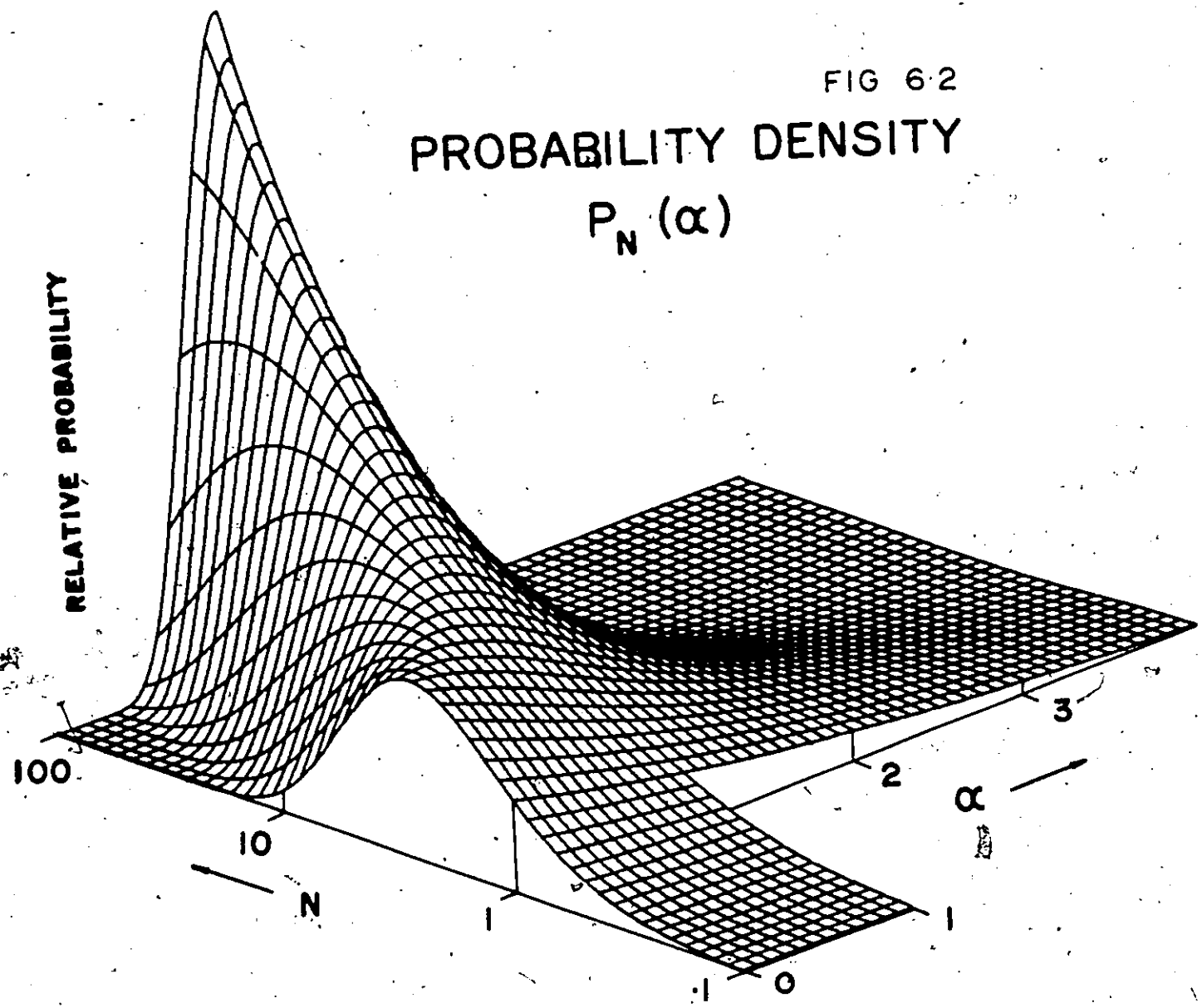

peak density or average intensity of a peak and some statistically determinable quantities, such as the variance of the spectrum.

Let us consider a spectrum, digitized by the ADC. Each interval or channel is small compared to the width of the Gaussian peak of the system response. It contains a number representing the number of events detected following a reaction. This number is proportional to the time of the experiment, the number of photons of the appropriate energy, and the efficiency of the detection system. It is easy to correct for the relative efficiency, as was indicated in Chapter 3. The time of the experiment is also relative, and of no interest provided it is long enough. That is to say the probability density function of the number of events in an isolated channel is Poisson, $P(N_c)$, where N_c is the average number of counts, or expectation value of the number of counts, in the channel. Therefore the standard deviation in the number of counts is $\sqrt{N_c}$, so that the relative error can be made as small as desired by making N_c large enough. This is accomplished by choosing the length of time of the experiment appropriate to the counting statistics desired.

At this point we emphasize the distinction between the statistical variance of the spectrum, which can be made as small as desired, and the variance of the spectrum. The former has been described. The latter refers to the distri-

bution of the means, N_c, of many intervals or channels.

We shall treat each channel of the spectrum as an interval in which an intensity I is measured. From the spectrum it is simple to calculate various quantities such as the average intensity per channel, the variance per channel, and the higher order moments. These same quantities may also be calculated as expectation values using the probability density function introduced in the previous section. Initially, we assume an ideal or delta function response of the detection system. This implies that if a spectral component falls in an interval, all of the intensity associated with it falls in that interval, and is evenly distributed within it. We next consider a realistic Gaussian response function. Then only a part of the intensity associated with the components whose centroids fall within the interval contributes to the intensity in the interval. Moreover, all intervals near the interval of interest contribute an amount to its intensity. For convenience, we use the notation for the expectation value[59]:

$$\langle f(I)\rangle = \sum_m \int_I f(I) P_{mN}(I)\, dI \ . \qquad (6.5)$$

In Appendix 2 we derive some results involving this expectation formula, including the moments of I:

$$\langle 1\rangle = 1$$

$$\langle I\rangle = NI_o$$

$$\langle I^2\rangle = N(N+2)I_o^{\ 2}$$

where, again, N is the average number of features per interval,

and I_o is their average intensity. Then, for an ideal or delta function response, we have

$$\langle \text{mean} \rangle = \langle I \rangle = NI_o \tag{6.6}$$

$$\begin{aligned} \langle \text{variance} \rangle &= \langle (I-\langle I \rangle)^2 \rangle \\ &= \langle (I^2-2I\langle I \rangle+\langle I \rangle^2) \rangle \\ &= \langle I^2 \rangle - \langle I \rangle^2 \\ &= 2NI_o^2 \quad . \end{aligned} \tag{6.7}$$

In the case of a Gaussian response we must consider contributions to the intensity in the interval of interest from components whose centroids fall outside of this interval, as well as components whose centroids fall within it. This may be accomplished by considering a normalized Gaussian function:

$$G(x) = \frac{1}{\sqrt{2\pi}\ \sigma} \exp(-x^2/2\sigma^2) \ . \tag{6.8}$$

This Gaussian is digitized into intervals or channels of the same width, say Δ, where $\sigma >> \Delta$:

$$G_i = \int_{x_i-\Delta/2}^{x_i+\Delta/2} G(x)dx \ . \tag{6.9}$$

Here $x_i = i\Delta$ and $-\infty < i < \infty$.

Let us label the interval of interest with the index $j=0$. Then intervals of all j, $-\infty<j<\infty$, will contribute to the total intensity in the $j=0$ interval. Now the expectation values of

of the quantities calculated is independent of the interval under consideration, since they are described by the same probability density function. Therefore in the case of a Gaussian function we have

$$\begin{aligned} \langle \text{mean} \rangle_g &= \sum_n G_n \langle I \rangle \\ &= \langle I \rangle \sum_n G_n \\ &= N I_o \end{aligned}$$

We now list some further useful relationships involving the digitized Gaussian function

$$\sum_n G_n = 1 \qquad \text{(normalization)}$$

$$\sum_n G_n^2 = \int_{-\infty}^{\infty} G^2(x)\,dx$$

$$= \frac{1}{2\sqrt{\pi}\,\sigma} \qquad (6.10)$$

$$\sum_{n \neq p}\sum G_n G_p = \sum_n \sum_p G_n G_p - \sum_n G_n^2$$

$$= 1 - \frac{1}{2\sqrt{\pi}\,\sigma} \; .$$

Let us now evaluate the expectation value of the variance.

$$\begin{aligned} \langle \text{variance} \rangle_g &= \langle (\sum_n G_n I - \langle I \rangle)^2 \rangle \\ &= \langle ((\Sigma G_n I)^2 - 2(\sum_n G_n I)\langle I \rangle + \langle I \rangle^2) \rangle \\ &= \langle (\Sigma G_n I)^2 \rangle - \langle I \rangle^2 \; . \end{aligned}$$

In the evaluation of the first term, involving the square of a series, care must be taken to distinguish between $\langle I^2 \rangle$ and $\langle I \rangle^2$. For clarification we include a subscript on the I

$$\langle (\sum_n G_n I_n)^2 \rangle$$

$$= \langle (\sum_n \sum_p G_n I_n G_p I_p) \rangle$$

$$= \langle (\sum_n G_n^2 I_n^2 + \sum_{n \neq p} \sum G_n G_p I_n I_p) \rangle$$

$$= \langle I^2 \rangle \frac{1}{2\sqrt{\pi}\,\sigma} + \langle I \rangle^2 (1 - \frac{1}{2\sqrt{\pi}\,\sigma}) \ .$$

Therefore

$$\langle \text{variance} \rangle_g = \frac{\langle I^2 \rangle}{2\sqrt{\pi}\,\sigma} + \langle I \rangle^2 (1 - \frac{1}{2\sqrt{\pi}\,\sigma}) - \langle I \rangle^2$$

$$= \frac{N(N+2) I_o^2}{2\sqrt{\pi}\,\sigma} - \frac{N^2 I_o^2}{2\sqrt{\pi}\,\sigma}$$

$$= \frac{N I_o^2}{\sqrt{\pi}\,\sigma} \ . \qquad (6.11)$$

We can now evaluate N, the transition density, in the case of both a delta function and a Gaussian response. We write $\langle \text{variance} \rangle$ as V and $\langle \text{mean} \rangle$ as M.

The delta function response $\quad N = \frac{2M^2}{V}$

$$(6.12)$$

The Gaussian response $\quad N = \frac{M^2}{\sqrt{\pi}\,\sigma V} \ .$

This is the desired result, since the peak density is expressed in terms of statistically calculable quantities. It is in-

dependent of the observation of any discrete spectral features.

We now consider the effect of relaxing the requirement that $\sigma >> \Delta$. This means that the second moment of the Gaussian ΣG_n^2 is no longer given by equation (6.10). If we define

$$\eta = \frac{V}{2NI_o^2}$$

from the foregoing we have

σ	η
delta function	1
large	$\frac{.282}{\sigma}$

We calculate, for width σ expressed in terms of interval units

σ	η	$\frac{1}{2\sqrt{\pi}\,\sigma}$
.5	.516	.56
1.0	.271	.282

We see that for $\sigma = \Delta$ the approximation is reasonable, and improves as σ increases. In this work $\sigma \sim 2\Delta \rightarrow 3\Delta$ where Δ was taken to be the width of one channel of the spectrum.

For a response function width less than the interval length, the delta function description of the spectrum applies. This may be exploited in order to obtain a measure of the width of the spectral features. The variance is computed in two ways, labelled 1 and 2. Method one corresponds to a long interval compared to the width - the features are considered as delta functions. Method two corresponds to a short interval

compared to the width - the features are considered as Gaussian distributions. Since the theory indicates that N, the density must be independent of the method, we have

$$N = \frac{2M_1^2}{V_1} = \frac{M_2^2}{\sqrt{\pi}\ \sigma V_2} .$$

Now $M_1 = M_2$. Therefore

$$\sigma = \frac{V_1}{2\sqrt{\pi}\ V_2}$$

may be used to obtain the width of spectral features, here considered as Gaussians.

Care must be taken that the units are correct. If we call the basic interval a channel, we note the dimensions of the foregoing quantities.

[N] - peaks/interval

[I_o] - counts/peak

[σ] - interval/units

[M] - counts/interval

[V_1] - counts^2/interval-peak

[V_2] - counts^2/interval^2-peak

It may be seen that these units are consistent.

As mentioned earlier, in order to obtain the variance of the spectrum there is always a statistical variance which must be subtracted from the total variance which is calculated. In all cases under study the statistical variance was at most two orders of magnitude less than the spectral variance.

ERROR CONSIDERATIONS

We use the propagation of error result from statistical theory to determine the error in N[21]:

$$\sigma_N^2 = \left(\frac{\partial N}{\partial M}\right)^2 \sigma_M^2 + 2\left(\frac{\partial N}{\partial M}\right)\left(\frac{\partial N}{\partial V}\right)\sigma_{MV}^2 + \left(\frac{\partial N}{\partial V}\right)^2 \sigma_V^2 \quad . \qquad (6.13)$$

Since, in the case of the delta function response,

$$N = \frac{2M^2}{V}$$

Therefore

$$\frac{\partial N}{\partial M} = \frac{4M}{V} = \frac{2}{I_o}$$

$$\frac{\partial N}{\partial V} = -\frac{2M^2}{V^2} = -\frac{1}{2I_o^2} \quad .$$

The required variances are calculated in Appendix 2.

$$\sigma_M^2 = 2NI_o^2$$

$$\sigma_{MV}^2 = 6NI_o^3$$

$$\sigma_V^2 = (8N^2 + 13N)I_o^4 \quad .$$

Therefore

$$\sigma_N^2 = \frac{4}{I_o^2}(2NI_o^2) - \frac{1}{I_o^3}(6NI_o^3) + \frac{1}{4I_o^4}(8N^2+13N)I_o^4$$

$$= 2N^2 + \frac{21}{4}N \quad .$$

The relative error is therefore given by

$$\frac{\sigma_N}{N} = \sqrt{2 + \frac{21}{4N}} \qquad (6.14)$$

So for a large number of peaks in a single interval, we have

$$\frac{\sigma_N}{N} \sim \sqrt{2}.$$

This is the error associated with the calculation of the level density assuming a delta function system response. An examination of the result of the previous section indicates that the effect of the introduction of the finite Gaussian response is to reduce the variance, V. For convenience let us define a factor, k, in the result for the transition density.

$$N = \frac{kM^2}{V} \quad . \tag{6.15}$$

If this is to represent the result obtained using the delta function response, $k = 2$; if it represents exponentially distributed Gaussians of width σ, $k = 1/\sqrt{\pi}\,\sigma$. Since the variance of the spectrum is in effect damped, we expect a similar reduction in the relative error in the transition density in going from the delta function to the Gaussian response. This can be made more plausible by a consideration of how the damping of the variance arises - it results from an averaging of the intensity contributions from several neighbouring intervals. Since the amount of effort required in considering the Gaussian response has been found to be disproportionate to the results obtainable, we continue to limit our error discussion to the delta function response. It may be regarded as the 'worst possible' limit.

The determination of N from the spectrum can be made

more precise by considering a number of adjacent intervals of the spectrum. If N and I_c are not expected to change in L such intervals, we can determine the average values of these quantities over this record length. From elementary statistics we therefore have a relative error in the mean of L such intervals of

$$\frac{\sigma_N}{N\sqrt{L}} \quad . \tag{6.16}$$

This result may also be derived by considering sums over the number of intervals, L, in the previous derivation for a single interval. We now tabulate typical relative errors for record lengths consisting of 1 and 100 intervals.

	N	.01	.1	1	10	100	∞
one interval:	$\frac{\sigma_N}{N}$	24	7.4	2.7	1.54	1.43	1.41
L=100:	$\frac{\sigma_N}{N\sqrt{L}}$	2.4	.74	.27	.154	.143	.141

In this work it was found expedient to consider a record length consisting of 100 intervals. For all but the simplest spectra under study, this assured that the record length contained at least one peak. An estimate of the peak density per channel and the average intensity per peak was obtained for each record. Since the number of peaks were also summed over the whole spectrum, and the errors involved in each determination are independent, we may assume that the relative

error introduced into the sum based on the statistical distribution of spectral features is also given approximately by result (6.16). Then L is the total number of intervals considered, which depends on the interval length and the energy range over which the calculation applies.

In the calculation of N from the spectral data there are other factors which must be examined. The M^2 and V statistics in equation (6.12) are calculated by a consideration of L intervals of data. Since L is finite in this work, there exists the possibility of a biasing of the result due to the distributions of these quantities.

A Monte Carlo investigation was therefore conducted. This confirmed the existence of a bias. As expected, although N varied from .05 to 3.0, the bias remained constant, depending only upon the record length. Table 6.1 shows the result of the analysis. The bias factor, B(L), is defined such that

$$N_\infty = N_L \, B(L)$$

where N_∞ is the true value of N which would be obtained for an infinite record length. A total record of 1000 channels was used and four runs were done for each value of N and each value of L. The value of σ ranged from 2 to 6 interval units. The case of distributed delta functions was also considered. An examination of the variance of the results led to estimate of the error in the bias factor of 10%.

Table 6.1

Bias Factor

L	Bias Factor (Monte Carlo)	$B(L) = 1 + \frac{4}{\frac{.4}{\sigma} L-2}$
25	2.23	2.33
50	1.50	1.50
100	1.23	1.22
250	1.085	1.083
1000	1.04	1.04

An attempt to justify the bias factor observed is now made. The distribution in the mean intensity, M, is given by equation (6.4). For large values of N (see Fig. 6.2) we may consider this distribution to be normal. In such a case the distribution of M^2 may be approximated by a χ^2 distribution. Similarly the distribution of V may be assumed to be close to a χ^2 distribution.

In principle, when the distributions of M^2 and V are known, the distribution in the ratio may be found. In this case the calculation must take into account the correlation which undoubtedly exists between M^2 and V. Since in addition precise knowledge of these density functions is unavailable, the value of the result of such an effort is difficult to assess. However, an illustration of the effect of the distributive nature of the variables is given.

Let us consider the distribution in V for a constant value of M^2. In this case we have, for a delta function system response,

$$N_\infty = \langle \frac{2M^2}{V} \rangle = 2M^2 \langle \frac{1}{V} \rangle .$$

However, the value of V which we calculate from the data is $\langle V \rangle$. Therefore

$$N_L = \frac{2M^2}{\langle V \rangle}$$

and

$$B(L) = \langle \frac{1}{V} \rangle \langle V \rangle .$$

If we assume V to be distributed as a χ^2 distribution with f degrees of freedom, we have[59]

$$P(V)\,d(\frac{V}{2}) = \frac{1}{\Gamma(\frac{f}{2})} (\frac{V}{2})^{\frac{f}{2}-1} e^{-\frac{V}{2}} d(\frac{V}{2}) .$$

Therefore

$$B(L) = \int \frac{1}{V} P(V)\,d(\frac{V}{2}) \times \int VP(V)\,d(\frac{V}{2})$$

$$= \frac{1}{2\Gamma(\frac{f}{2})} \int (\frac{V}{2})^{\frac{f}{2}-2} e^{-\frac{V}{2}} d(\frac{V}{2}) \times \frac{2}{\Gamma(\frac{f}{2})} \int (\frac{V}{2})^{\frac{f}{2}} e^{-\frac{V}{2}} d(\frac{V}{2})$$

$$= \frac{\Gamma(\frac{f}{2}-1)}{\Gamma(\frac{f}{2})} \times \frac{\Gamma(\frac{f}{2}+1)}{\Gamma(\frac{f}{2})}$$

$$= 1 + \frac{2}{f-2} .$$

This result may be taken to represent the bias factor obtained because of the distribution in V. As noted previously, many other considerations should be applied to the calculation of the bias factor.

Let us associate f with the number of records, L. Then taking

$$B(L) = 1 + \frac{4}{L-2},$$

obtains a reasonable empirical fit to the results of the Monte Carlo calculation where the delta function system response was assumed.

We now choose to apply this result to the case of a distribution of Gaussian functions by postulating the existence of another damping factor similar to the k introduced for the variance (equation (6.15)). We assume that the transition to this case may be neglected if most of the intensity associated with the Gaussian function may be assumed to fall within the interval of interest. This could happen if the interval length, Δ, is made large compared to σ, for then we have seen that the delta function analysis applies. For a fixed record length we must therefore postulate a reduction in the effective value of L. A reasonable value to assume for this new value of L is

$$L_g = \frac{\beta}{\sigma} L.$$

The value of the damping factor, β, was empirically

found to be .4. On the basis of the foregoing discussion, a first order calculation obtains a value of .32 for β. In view of the number of assumptions made, these values are consistent. The values of the fit to the Monte Carlo calculation are also presented in Table 6.1.

CHAPTER 7

RESULTS

A simplification of the response of the gamma ray spectrometer to a Gaussian function facilitates a statistical description of the spectrum in terms of a peak density and average peak amplitude. The peak density is related to the nuclear temperature. A knowledge of the Q value of the reaction then leads to a value for the multiplicity of the spectrum. Combined with the total relative intensity, the multiplicity allows us to calculate the absolute intensity of special features. We conclude with a comparison of s-wave level density data with values of level density obtained in this work.

NUCLEAR TEMPERATURE

Ericson's constant temperature model of the nucleus[11] expresses the density of states as

$$\rho(E) = \rho_o \exp(E/T) \qquad (2.6)$$

where T is called the nuclear temperature. An interpretation of this parameter is attempted here.

In classical thermodynamics temperature is related

to the average kinetic energy per particle. The well known result

$$\langle K.E./particle \rangle = 3/2\ kT$$

is obtained by integrating the energy distribution

$$dn = B\sqrt{2E}\ \exp(-E/kT)\,dE \qquad (7.1)$$

derived by Maxwell[61]. The imposition of quantum mechanical constraints on the system led to the derivation of an energy distribution of the form

$$dn = C\ \exp(-E/kT)\,dE \qquad (7.2)$$

due to Boltzmann. Equations (7.1) and (7.2) describe the distribution in energy of particles of an assemblage, such as molecules of a gas, or nucleons of a nucleus. The B, C, k, and T are constants, with k, the Maxwell-Boltzmann constant, defined in such a way that T is the thermodynamic temperature in degrees Kelvin.

The reason for the label nuclear temperature becomes clear by a comparison of equations (2.6) and (7.2). Equation (7.2) represents an energy density in the same way that (2.6) represents a level density - the roles of T are analogous. The analogy breaks down, however, when we try to relate nuclear temperature to an average kinetic energy per nucleon. Nuclear temperature is no more than a measure of the rate of increase of level density with energy ; the thermodynamic temperature of a nucleus is given by equation (7.2). Nuclear

temperature need not be a constant, as can be seen by comparing Bethe's[12] level density description (equation (2.4)) with equation (7.2).

That the transition density and the rate of change in transition density with photon energy are related to the nuclear temperature was indicated in Chapter 4:

$$n(E_\gamma) = \rho_o^2 T \exp(Q/T)\sinh((Q-E)/T). \qquad (4.3)$$

By integrating this result from some energy E to the Q value, we obtain the result

$$N(E) = \rho_o^2 T^2 \exp(Q/T)\{\cosh((Q-E)/T)-1\}, \qquad (7.3)$$

the cumulative number of transitions between energy E and the Q value. Fig. 7.1 shows this result as a family of curves for a range of values of T usually encountered. Note that it is the integral that is presented, in order to facilitate the comparison of this result with actual data. The ordinate of the plot is the number of transitions with an energy between Q and the energy represented by the abscissa. The energy is given with respect to Q. The plotted curves are independent of Q and ρ_o, since these appear as multiplicative factors, and have been omitted for convenience of normalization. In the case of real data, the slope of the cumulative number of transition curve depends only on T, and its intercept with the E=0 axis is $\frac{\rho_o^2 T^2}{2} \exp(\frac{2}{T})$. A consideration of this

FIG 7·1

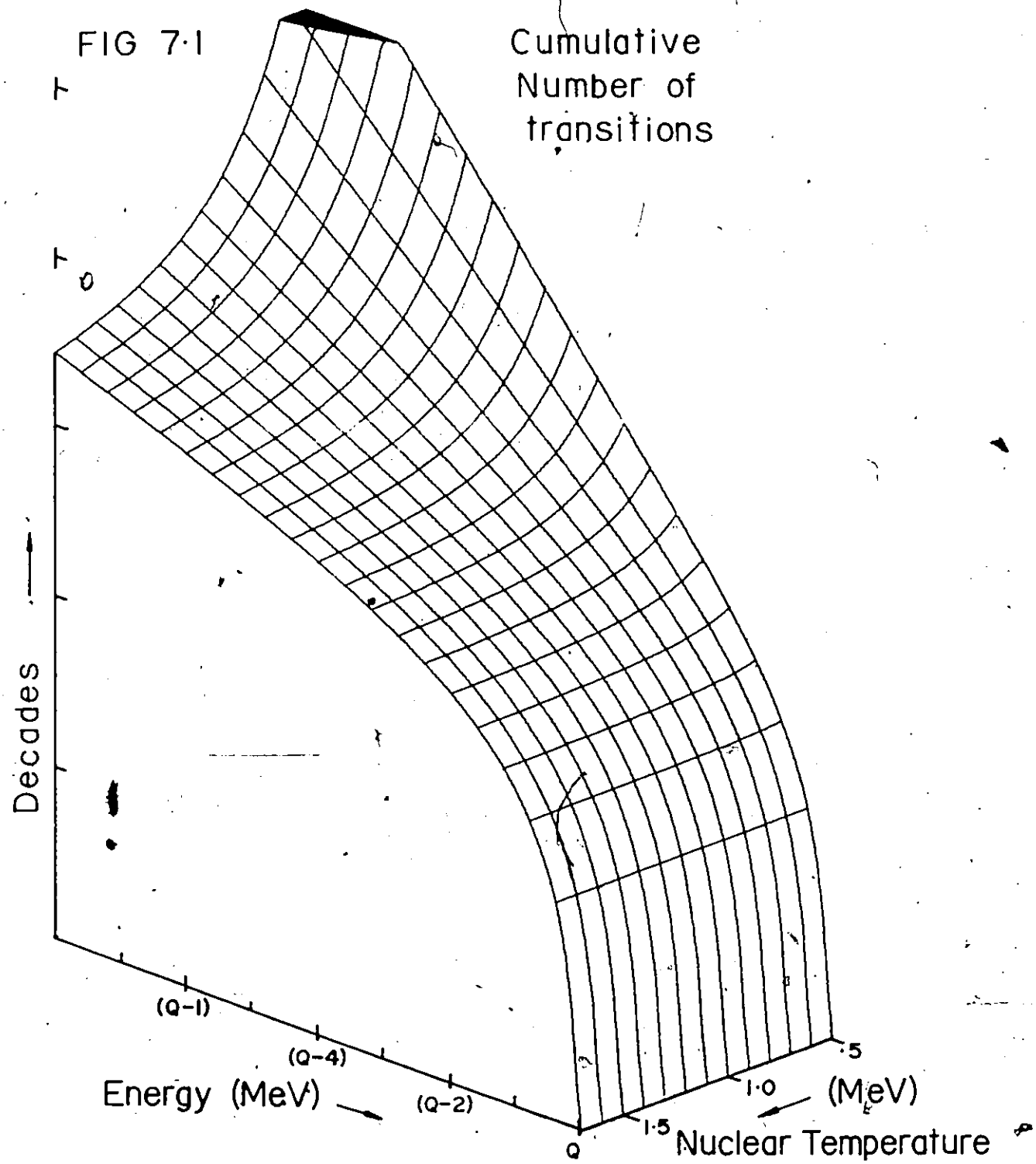
Cumulative
Number of
transitions
Decades
(Q-1)
(Q-4)
(Q-2)
Q
Energy (MeV)
·5
1·0
1·5
(MeV)
Nuclear Temperature

cumulative number of transition curve of a nuclide therefore allows a determination of the parameters T and ρ_o of Ericson's model for the nuclear level density.

Figures 7.2A and B show a comparison of the cumulative number of transition curves for several of the nuclides under study. The upper plots, labeled A, represent the results of the statistical calculation. The 'losses' formalism introduced in Chapter 5 is used to obtain the lower of the two curves in A. These may be compared directly with the respective figures B, which indicate the result of conventional observations. A complete set of the data is given in Appendix 4.

A least squares fit of our data to an exponential function yielded values of nuclear temperature and zero level spacing, ρ_o. The range of the fit was $2.4 \leq E \leq (Q-1)$ MeV. The lower limit was determined by the efficiency of the detection system and the presence of the deuteron transition. The upper limit was (Q-1) MeV since above this energy equation (7.3) begins to deviate significantly from an exponential form. The values of the nuclear temperatures obtained using this method are summarized in Table 7.1. Also shown are the results of some other workers.

The errors in our determination are difficult to assess, because the sources of error are so numerous. These include the background radiation contributed by the facility, the calculation of the response function, and the assumption of

CUMULATIVE NUMBER OF TRANSITIONS

FIG 7·2

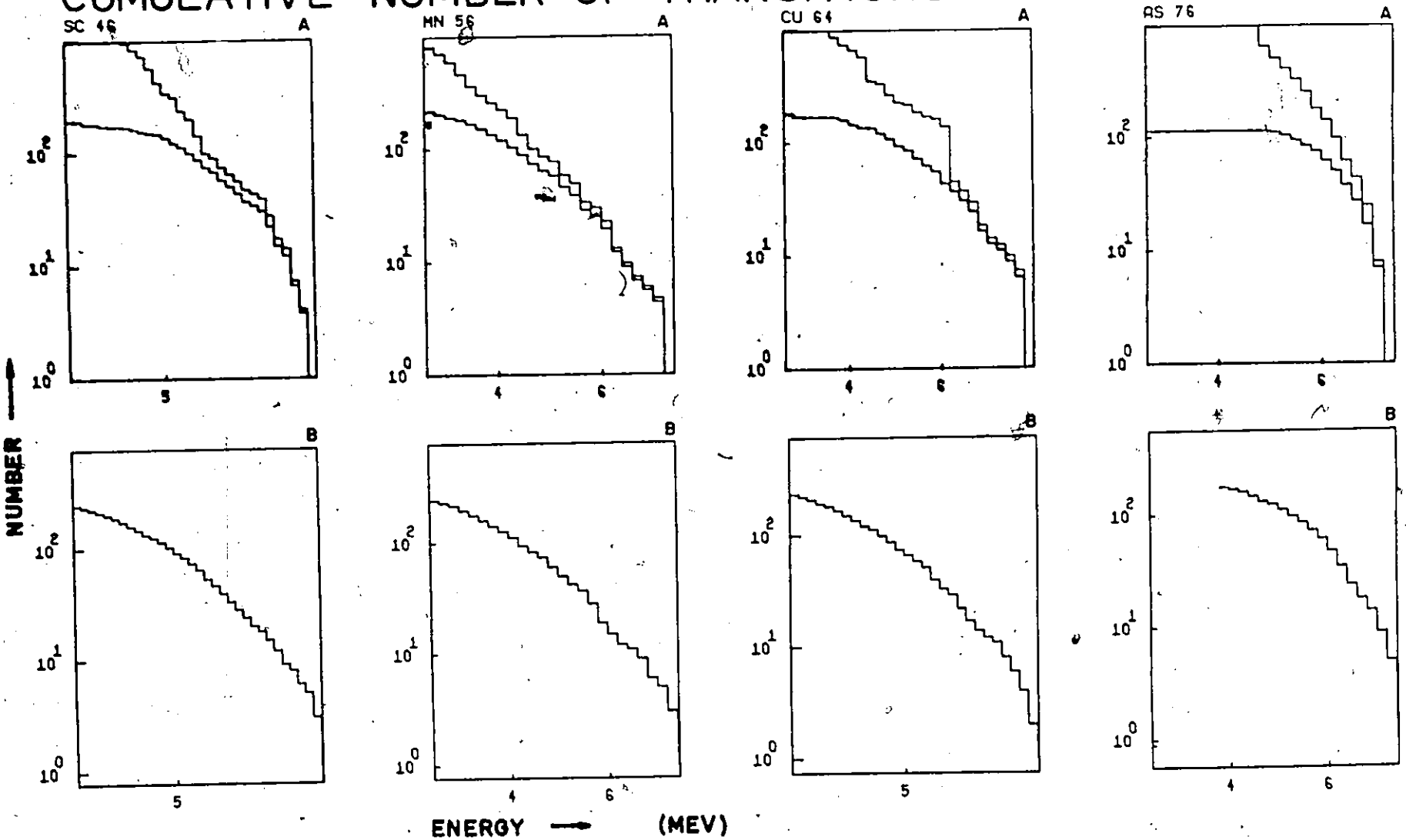

Table 7-1

Nuclear Temperature, 'Q' value, and Multiplicity

Spectrum	T (MeV) present work	T (MeV) L.B.H. (33)	T (MeV) G.& C. (14)	Q (MeV) present	ν (number/cascade) present calculated
^{28}Al	4.5	1.5	1.5	7.7253	2.92
^{46}Sc	1.12	-	1.35	8.7647	3.94
^{56}Mn	.96	1.6	1.06	7.2703	3.80
^{60}Co	.86	1.4	1.14	7.4920	4.03
^{64}Cu	.98	1.0	.995	7.9152	3.94
^{76}As	.55	-	-	7.3277	4.98
^{104}Rh	.53	.74	.60	6.9983	4.93
^{110}Ag	.43	-	-	6.8066	5.48
^{116}In	.40	-	-	6.5608	5.65
^{134}Cs	.51	-	.53	5.8904	4.98
^{186}Re	.36	-	-	6.1796	6.04
^{198}Au	.52	.62	.53	6.5109	4.74
^{204}Tl	.44	.75	-	6.6557	5.31

the statistical model of the compound nucleus. The results of three independent experiments using ^{76}As as a target, and several partial runs compared to the total run using a ^{104}Rh source, indicate that 10% in the nuclear temperature, and a factor of two in the level spacing, is a reasonable estimate of the errors involved.

The choice of the constant temperature model is arbitrary. It was contingent only on the requirement that the model provide reasonable agreement with observation. That such agreement exists has been indicated. Significant deviation between results obtained from the data and analytical curves obtained from the model would indicate a deficiency in the latter. The comparison should then be applied to a different model.

MULTIPLICITIES

The term multiplicity describes the average number of transitions in a gamma ray cascade when a nucleus de-excites. Since an excited compound nucleus has many decay modes available to it, this number can have a considerable range of values, but is usually reported to be of the order of 3-5 for most nuclides[43]. The multiplicity may be considered to provide a constraint to theories. It is given by

$$\nu = \int_0^Q S(E)dE \qquad (7.4)$$

which is the integral of the spectrum, S(E), when suitable

normalization is adopted.

When non-gamma decay modes are available, the multiplicity can be less than one. Such is in fact the case for boron. De Juren and Rosenwasser[62] reported a value for the multiplicity of ^{10}B of .935. Draper and Springer[35] reported the multiplicities of spectra following neutron capture in several resonances of several targets.

In theoretical analyses the multiplicity is sometimes considered a free parameter. This is not so in our calculation, where it is a consequence of the model. Calculated values of multiplicity are in agreement with those of other workers[34,35]. Figure 7.3 summarizes the relationship between values of multiplicity, Q, and T.

These results assume the level density to be adequately described by equation (2.6)[11] and uses Moszkowski's estimates[25] for the transition probabilities. We can therefore estimate the multiplicity solely on the basis of a knowledge of T and Q. Values of ν for some of the nuclides under study are also given in Table 7.1.

In this calculation the spin and parity distributions of all states were assumed to be those indicated by Bethe (equation (2.7)). This is equivalent to assuming no specific knowledge of any state, including capture or ground. However, in most cases, at least some of this information is available[63]. In fact, multiplicity is of interest since it can be related

CALCULATED GAMMA RAY MULTIPLICITY FIG 7·3

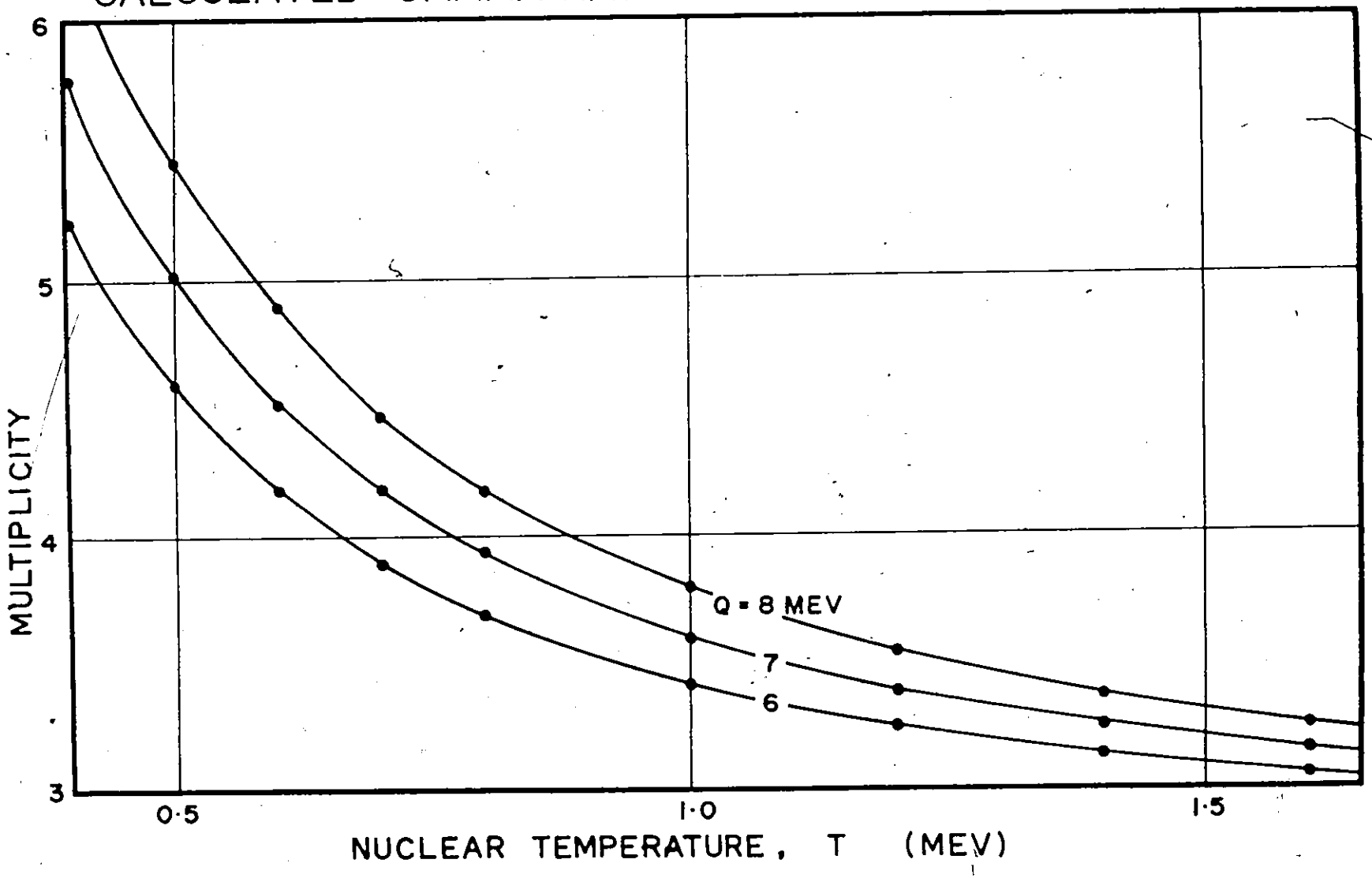

to the difference in spin and parity between states of the compound nucleus. For example, the greater the difference in spin between the capture and ground states of a nuclide, the greater the average number of gamma rays per cascade. A preliminary investigation has been conducted as to the feasibility of using this result to identify or restrict the value of the spin and parity of compound nuclear states.

The computer code described in Chapter 4 and in Appendix 3 was used to calculate the multiplicity of a spectrum as a function of spin and parity of the capture state of a reaction. An example to which the analysis was applied was the reaction

$$^{51}V(p,\gamma)^{52}Cr \ .$$

The product nucleus, ^{52}Cr is an even-even nucleus which exhibits the well known vibrational level scheme[4]. Resonances above the proton separation energy are widely spaced, so that capture may be attributed to a definite compound nuclear state. It is hoped that the ratios of intensities of the transitions between the low lying vibrational states will yield further information about the character of the capture states. All known level energies, spins and parities[64] were included in the calculation. The results of the calculation for ^{52}Cr are shown in Fig. 7.4. An investigation at the McMaster University tandem accelerator indicated that the restriction of the spin values of resonances is feasible by this method.

CALCULATED ^{52}CR MULTIPLICITY

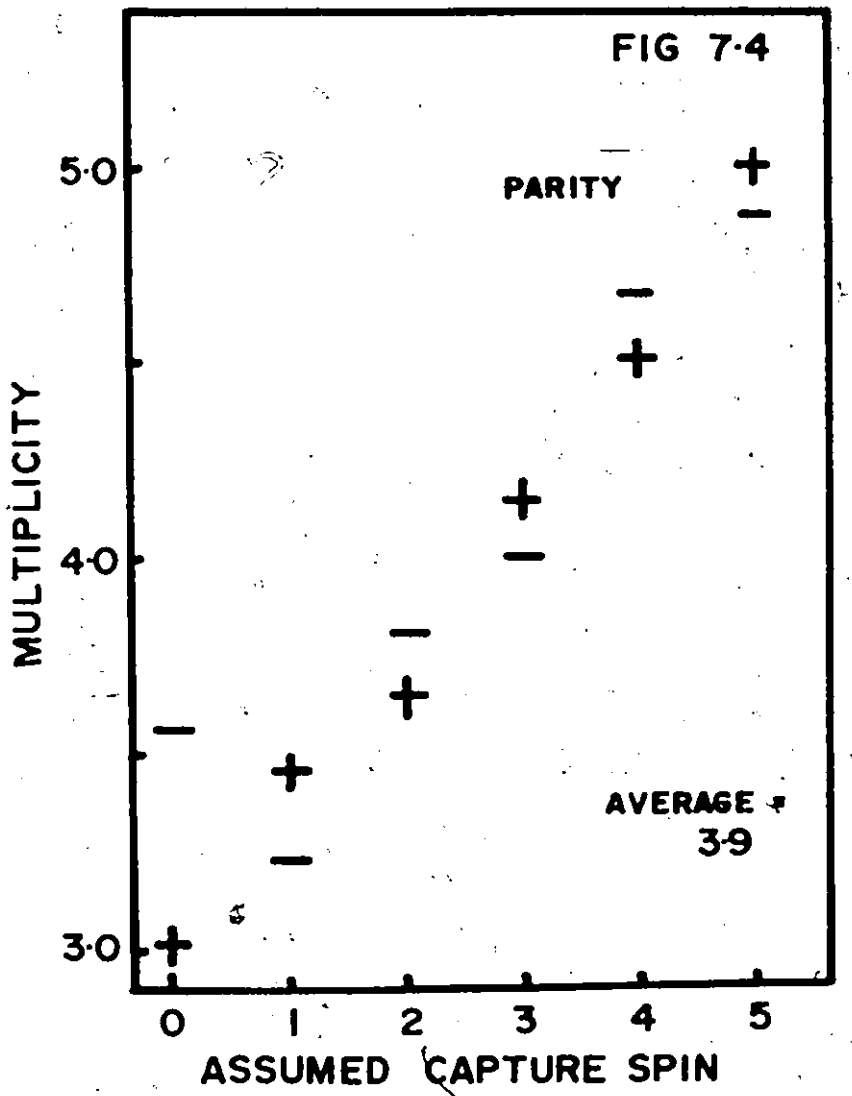

ABSOLUTE INTENSITY

As was noted in Chapter 3, the relative efficiency of the system was obtained from a consideration of the ^{15}N spectrum. Experimentally, no effort was made to obtain the absolute intensities of the radiative transitions. Present uncertainties in the knowledge of the absolute neutron flux, the neutron cross sections of the nuclides under study, the geometry of the experiment, and the relative efficiency of the system at gamma radiation energies less than 2 MeV dictate that the results of any such determination be unreliable. At best the absolute intensity determination is an extremely difficult problem. The compilation of (n,γ) results by Bartholomew et al.[28] indicates that discrepancies of factors of two between the results of different workers are quite common.

It was therefore decided to present values of the absolute intensities that might be expected, based on the assumption of the statistical model. Let us examine some possibilities. Consider S(E) to be a probability density function, Then, using equation (7.4), we have

$$\bar{E} = \frac{\int_0^Q E\ S(E)dE}{\int_0^Q S(E)dE} = \frac{Q}{\nu},$$

so that

$$\int_0^Q E\ S(E)dE = Q. \qquad (7.5)$$

We now write

$$S(E) = kS'(E) ,$$

where S is the absolute intensity, S' is the relative intensity as calculated via the relative system efficiency, and k is a constant to be determined.

We therefore have

$$k \int_0^Q S'(E)dE = \nu$$

$$k \int_0^Q ES'(E)dE = Q. \qquad (7.6)$$

The integrals in (7.6) may be partially determined, since from our calculation we obtain S' for $E \geq 2.4$ MeV. We choose to extrapolate S'(E) to zero energy by assuming its form to be determined by the statistical model as discussed in Chapter 4. Values of k obtained in this way were used to calculate most of the intensities presented in Appendix 4.

It is of interest to compare the present discrete data with those of Rasmussen[29]. As a figure of merit we have chosen to calculate the fraction of gamma rays observed in the spectrum:

$$F = \frac{\sum_i E_i I_i}{Q} .$$

The sum is taken over all gamma rays of energy E_i and intensity I_i above 2.4 MeV in energy. Note that a high energy gamma ray contributes more to this sum than a low energy gamma ray of the same intensity. The same fraction, F_R, was computed for

Table 7.2

Intensity Comparison

Spectrum	F	F_R (29)	R	R_R (29)
Al	.55	.49	1.80	1.60
Sc	.57	.64	1.82	1.56
Mn	.92	.79	1.39	1.32
Co	.64	.64	1.42	1.39
Cu	.99	.85	1.28	1.18
As	.21	.23	1.29	1.33
Rh	.12	.16	1.40	1.43
Ag	.13	.18	1.43	1.50
In	.08	.08	1.50	1.46
Cs	.10	.17	1.35	1.35
Re	.07	-	1.19	-
Au	.36	.40	1.25	1.22
Tl	.37	.31	1.26	1.26

Rasmussen's data, over the same energy range. The results are presented in Table 7.2. Differences in F and F_R may be attributed to different detectors and therefore 'resolution losses', as well as the absolute nature of the measurement. This is further discussed in Chapter 8. In order to remove the effect of the absolute nature of the intensities we have also calculated the ratio

$$R = Q \frac{\Sigma I_i}{\Sigma I_i E_i} \qquad (7.7)$$

where the sums, I_i and E_i are as above in equation (7.6). The ratio R is independent of the normalization and therefore reflects other differences. It may be expected to be correlated with ν, since equation (7.7) reduces to (7.5) if all intensity is included in the sum. Results of this calculation are also presented in Table 7.2. When compared on this basis, the present data agree well with the work of Rasmussen.

ENERGY LEVEL SPACINGS

We offer a comparison between the s-wave state density[14] and the level density derived from the gross gamma ray spectrum. At the outset one might expect these quantities to be related. The errors from both determinations are quite large and are not easily assessed. For simplicity we shall assume both to have factor of 2 errors. The data used are given in Table 7.3.

Because of the wide dynamic range and the uncertainty

Table 7.3

Level Density

Spectrum	ρ_γ (levels/MeV) present	ρ_s G.& C. (14)
Al	12.5	25
Sc	330	440
Mn	165	500
Co	400	400
Cu	350	1000
As	5000	11500
Rh	6000	28500
Ag	17000	45000
In	17000	154000
Cs	9000	54000
Re	50000	250000
Au	8000	62000
Tl	150	500

COMPARISON OF LEVEL DENSITIES AT NEUTRON BINDING ENERGY

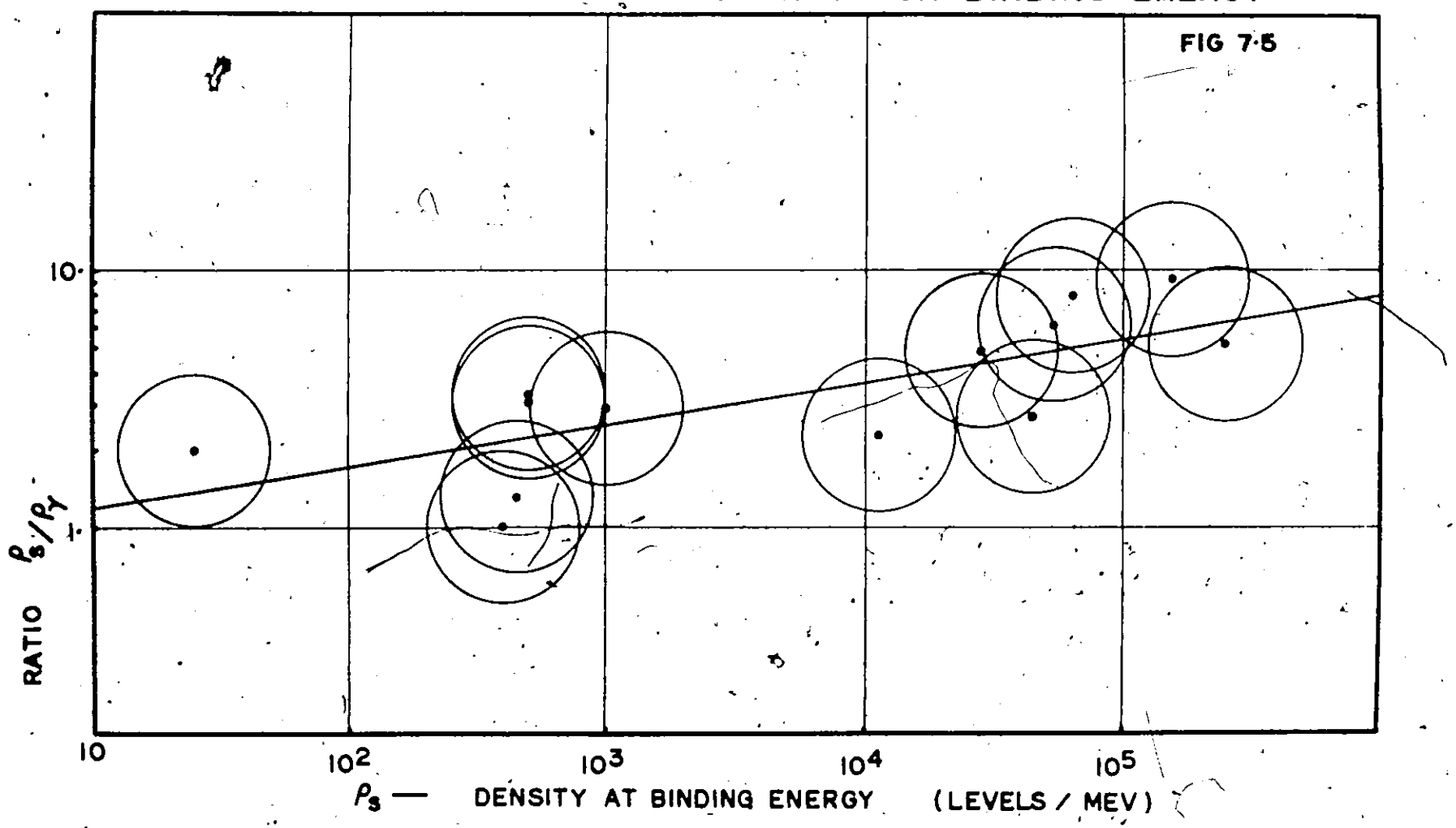

of the functional arrangement that may exist we chose to fit

$$\log(\text{Ratio}) = a \log \rho_s + G .$$

The s-wave determination of the density is indicated by ρ_s. The ratio is that of the s-wave level density to the level density ρ_γ at E = Q, as determined in this work. The data are shown in Fig. 7.5

The result found is

$$\rho_\gamma = 1.09^{+.5}_{-.35}\ \rho_s^{\ 0.84\pm.05}$$

A priori one might have expected that these quantities would be directly proportional in the manner

$$\rho_\gamma = f(J)\rho_s^{\ x}$$

where f(J) takes into account the weighting associated with the levels populated via the two processes. Normally one would expect that f(J) would be in the range 1→3. The power x is expected to be unity. The results obtained are remarkably close to these expectations. This is even more remarkable when one considers that the density ranges over four orders of magnitude.

CHAPTER 8

CONCLUSIONS AND DISCUSSION

A new technique of extracting information from complex spectra has been introduced. We have attempted to demonstrate that the number of features in an energy interval of a spectrum may be determined without losses. A statistical study has yielded a spectral description in terms of a peak density and an average amplitude. Conditions limiting the natures of the spectra that may be studied are not particularly restrictive. The system response must be either local, or its reduction to such a response must be possible. Features must be distributed in their position.

The response function of the pair spectrometer used to obtain the data has been empirically determined. A suitable mathematical description of this response allowed its simplification to a single Gaussian peak. Such a response satisfies the conditions for the foregoing technique. The complex gamma ray spectra of 17 nuclides following the capture of thermal neutrons have also been conventionally analysed. Spectroscopic data is tabulated in Appendix 4.

The statistical analysis is independent of whether features are resolved or not. In a study of the gamma radiation

spectrum following neutron capture in rhodium, for example, peak densities of 10000 features per MeV have been encountered. Distributions in parameters of the response features, such as peak width or amplitude, do not invalidate the technique, although these distributions must be known locally in the spectrum. The statistical description of several complex spectra has been obtained, and is presented here. A comparison with a constant temperature model of the compound nucleus obtains agreement with previous level density data determined using different methods.

The most practical form of statistical description of the spectrum has been found to be the 'cumulative number of transitions'. This is a function of the gamma ray energy which represents the total number of peaks observed above that energy, independent of intensity. A simple statistical model for the nuclear level density allows the calculation of some parameters from this description. The nuclear temperature and level spacing of the constant temperature model are reported. The present analysis indicates that spectra varying greatly in complexity may all be satisfactorily described by Ericson's[11] constant temperature model of the nucleus.

In addition the model allows a calculation of the spectral shape when a suitable estimate for the gamma ray transition probability is made. The nuclear temperature

determined here, as well as known energy data, was utilized in a calculation of the multiplicity of the spectra. This estimate of the multiplicity was used in conjunction with a relative system efficiency to determine the absolute intensities of the gamma ray transitions.

The transition density analysis is quite independent of system efficiency. Only the resolution of the detector is of importance, and this is the major source of error in the results here. The intensity analysis, however, depends also on a knowledge of the relative efficiency. On this basis, and on the basis of the assumption of a statistical model, errors in the intensities may be relatively large. We note however that the comparison included in Chapter 7 of the results obtained for copper, silver, and indium, may not be realistic since separated isotopes were used in this work.

The discrete data presented in Appendix 4 does not list several weak lines which were attributable to aluminum, iron, nitrogen and chlorine contaminants present in the sample or system. The argon spectrum shows several manganese lines - this is a result of the spectrum being taken following the failure of the manganese sample. No effort has been made to eliminate from the listings gamma transitions following inelastic scattering, except where it was obvious, such as for carbon. In the case of nitrogen, silicon, and argon, the calculation reducing the response to a Gaussian clearly indicates that

the response function determined here is reasonable. An examination of the results of the thallium spectrum calculation reveals that the anomalous bump[65] is most likely entirely due to observable transitions.

To suggest refinements in the method of the experiment is not really relevant at this point, since the technique was designed to overcome some experimental shortcomings. General suggestions with regard to the calculational technique are equally irrelevant, since it is implicitly claimed to be optimal. However to those who may consider a study similar to the present one, the following is proferred:

(a) The determination of the response function might have been more accurate had the runs of simple spectra, from which it was obtained, been longer.

(b) No deterioration of peak resolution was observed for the duration of the experiment. Such deterioration would have been important only insofar as it might indicate a change in the long range components of the response function. For more accurate results the spectrometer response should be monitored regularly by means of a standard spectrum.

(c) The background in the facility was relatively high, and has been considerably reduced. An internal collimator has been installed, and an aluminum window has been eliminated

from the gamma beam. This means that the matrix inversion technique would represent a smaller perturbation to the raw data since random addition is reduced.

This work may be expanded with a greater emphasis on the intensity analysis. Distributions of spectral features, here obtained from the spectra themselves, could be investigated with the aid of a simple cascade model of the nucleus based on the model presented here. This approach will allow a test of gamma ray transition probability theory in complex spectra. Such work would be useful, since as the complexity of spectra under study increases, the effect of spectral fluctuations becomes less important.

It is hoped that the collective technique of describing spectra and the matrix inversion response simplification may lend itself to other areas of study. These could include the reduction of proton or X-ray spectra of nuclear physics. Investigators in other disciplines such as chemistry may find other applications for the present analysis. The statistical description of spectral features such as gamma ray transitions presents an alternate approach to the conventional tabulations of data. It is useful in describing unresolved peaks, and yields a crude upper limit to the number of peaks that an experimenter can hope to observe with an ideal spectrometer with infinite resolving power at an infinite cost, available in the year infinity.

APPENDIX 1

MATRIX MULTIPLICATION

In this section we prove that the convolution of a spectrum represented by a vector with a suitable function can be exactly equivalent to its multiplication by the inverse of a response matrix. The response matrix must be triangular, either upper or lower. The proof offered here is for a lower triangular matrix. An upper triangular matrix may be dealt with in a similar manner. The form of the convolution function is indicated.

The concept of elementary matrices is well known to mathematicians[66]. It provides a powerful and elegant method for certain matrix proofs, such as the following.

ELEMENTARY MATRICES

We define an elementary matrix, $E_{ij}(c)$, which is a matrix identical to the unit (diagonal) matrix except that the element in row i and column j is replaced by c. For example,

$$E_{21}(-a_{21}) = \begin{pmatrix} 1 & 0 & 0 & \cdot \\ -a_{21} & 1 & 0 & \cdot \\ 0 & 0 & 1 & \cdot \\ \cdot & \cdot & \cdot & \cdot \\ \cdot & \cdot & \cdot & \cdot \\ \cdot & \cdot & \cdot & \cdot \end{pmatrix} \qquad \text{(A1.1)}$$

is a particular elementary matrix.

Premultiplication of any matrix A by $E_{ij}(c)$ shows that the effect of $E_{ij}(c)$ corresponds to a simple row operation, i.e. row i is replaced by itself plus the product of c and row j. This is indicated as

$$r_i \to r_i + cr_j .$$

If we call the matrix formed by the action of $E_{ij}(c)$ on A a new matrix A_1, the matrices A and A_1 are said to be row equivalent. This is written

$$A \underset{r_i \to r_i + cr_j}{\sim} A_1 .$$

Since the inverse row operation is just

$$r_i \to r_i - cr_j$$

we see that

$$E_{ij}(-c)A_1 = A.$$

Operating on this equation with $E_{ij}(c)$ we have

$$E_{ij}(c)E_{ij}(-c)A_1 = E_{ij}(c)A = A_1.$$

Therefore

$$E_{ij}(c)E_{ij}(-c) = I.$$

We have therefore found the inverse of the elementary matrix:

$$(E_{ij}(c))^{-1} = E_{ij}(-c) . \qquad \text{(A1.2)}$$

TRIANGULAR MATRIX WITH UNIT DIAGONAL

Consider a triangular matrix, A, of the form

$$A = \begin{bmatrix} 1 & & & & \\ a_{21} & 1 & & 0 & \\ a_{31} & a_{32} & 1 & & \\ a_{41} & a_{42} & \cdot & 1 & \\ \cdot & \cdot & \cdot & & 1 \\ \cdot & \cdot & \cdot & a_{n,n-1} & \end{bmatrix} \qquad (A1.3)$$

It is well known that simple elementary row operations will reduce this to the unit matrix, I. In terms of the elementary matrices, this is written

$$\underline{E_{n,n-1}(-a_{n,n-1})}\,\underline{E_{n,n-2}(-a_{n,n-2})E_{n-1,n-2}(-a_{n-1,n-2})}\,\underline{E_{n,n-3}(\ldots\ldots\times}$$

$$\underline{\ldots E_{31}(-a_{31})E_{21}(-a_{21})}A = I. \qquad (A1.4)$$

The underlined groups of operations may be considered to correspond to matrices of a simple form which are related to the form of the convolution function.

We write

$$A_j = \prod_{i=j+1,n} E_{ij}(a_{ij}).$$

If, for j=n, $A_n = I$, then

$$A_j^{-1} = \prod_{i=j+1,n} E_{ij}(-a_{ij}) .$$

(The elementary matrices referring to different rows of one

column commute, since the order in which elements in a column are made zero is irrelevant.)

Equation (A1.4) can now be written as

$$A_n^{-1} A_{n-1}^{-1} A_{n-2}^{-1} \ldots A_1^{-1} A = I.$$

Therefore

$$A^{-1} = A_n^{-1} A_{n-1}^{-1} A_{n-2}^{-1} \ldots A_1^{-1}$$

where explicitly

$$A_j^{-1} = \begin{pmatrix} 1 & & & & & & \\ & 1 & & & & 0 & \\ \cdot & & 1 & & & & \\ \vdots & & & & & & \\ \cdot & & -a_{j+1,j} & & & & \\ & & -a_{j+2,j} & & & 1 & \\ 0 & & \cdot & & 0 & \cdot & 1 \\ \cdot & & -a_{n,j} & & & & \end{pmatrix} \qquad \text{(A1.5)}$$

It may be seen that a matrix multiplication by a series of matrices of this form is equivalent to convolving the spectrum with a function indicated by equation (A1.5).

GENERAL TRIANGULAR MATRIX

Consider A to be of the form

$$A = \begin{pmatrix} a_{11} & & 0 \\ a_{21} & a_{12} & \\ a_{31} & a_{32} & a_{33} \\ \cdot & \cdot & \\ \cdot & \cdot & \end{pmatrix} \qquad \text{(A1.6)}$$

The proof follows as in the previous section. Each elementary matrix argument is now divided by the diagonal element of that column. In addition it can be seen that a factor a_{ij} must be taken out of the matrix each time a column j is made zero by elementary row operations. (See equation (A1.4)). This is so that the right hand side of equation (A1.4) becomes a unit, not a diagonal matrix.

We then have, in analogy with equation (A1.5),

$$A_j^{-1} = \frac{1}{a_{jj}} \begin{pmatrix} 1 & & & & & 0 \\ & 1 & & & & \\ & & 1 & & & \\ & & -a_{j+1,j}/a_{jj} & & & \\ & 0 & -a_{j+2,j}/a_{jj} & & & \\ & & \cdot & & & \\ & & \cdot & & & \\ & & \cdot & \cdot & 1 & 0 \\ 0 & & -a_{n,j}/a_{jj} & \cdot & 0 & 1 \end{pmatrix} \qquad \text{(A1.7)}$$

Since this is the inverse, the factor a_{ij} appears as $1/a_{jj}$.

Taking out $1/a_{jj}$ as a common factor gives

$$A_j^{-1} = \frac{1}{a_{jj}^2} \begin{pmatrix} 1 & & & & & 0 \\ & 1 & & & 0 & \\ & & a_{jj} & & & \\ & 0 & -a_{j+1,j} & & & \\ & & -a_{j+2,j} & & 1 & \\ & & & 0 & & \\ 0 & & -a_{n,j} & & & 1 \end{pmatrix} \qquad \text{(A1.8)}$$

The convenience and simplicity of this method is a consequence of the similarity between this matrix, which represents one step of a convolution, and the total response matrix, represented by equation (A1.6). Note that the matrices A_j^{-1} do not commute. Therefore the order of summation involved in the convolution is critical, and is opposite in the case of an upper triangular matrix.

We again consider the equation

$$S = RT \tag{2.3}$$

where S and T are the vectors representing the observed and true spectra respectively, and R is the response function, here represented by a matrix. The matrix inversion and multiplication is then indicated as

$$T = R^{-1}S$$

while the convolution can be indicated as

$$t_i = \sum_j q_{ij} \cdot s_j$$

where t_i and s_i are elements of the vector and q_{ij} are elements of the convolution function, the values of which are obtained directly from R, as suggested by equation (A1.8).

In Chapter 5 it was suggested that the response correction can be made either to include events not in the peak into the peak, or to eliminate events not in the peak from the spectrum. The former is equivalent to a normalization condition. A constant number of events in the spectra S

and T is equivalent to the requirement that the sum of any column of the response matrix be one. This may be seen to be equivalent to the requirement that the sum of the convolution function at any point be one. If such is not the case, events may be eliminated from the spectrum.

We have attempted to show the equivalence between the inversion and multiplication of a vector by a triangular matrix, and the convolution of this vector by a function indicated by equation (A1.8). This is motivated by the fact that the computational effort required for the latter is very much less. The effort is proportional to the number of elements which must be summed, which depends on the range or extent of the response of the system under consideration.

APPENDIX 2
STATISTICAL DERIVATIONS

In Chapter 6 we present the probability density function:

$$P_{mN} = \frac{1}{I_o} \left(\frac{I}{I_o}\right)^{m-1} \frac{N^m}{(m-1)!\,m!} \exp\left(-N - \frac{I}{I_o}\right). \qquad (6.3)$$

This result expresses the probability of an intensity I being present in an interval of the spectrum. The number of components actually present, their average intensity, and the average number expected in the interval are given by m, I_o, and N.

We now calculate some results which are used in Chapter 6, using the formula for the expectation:

$$\langle f(I)\rangle = \sum_m \int_I f(I) P_{mN}(I)\,dI \ . \qquad (6.5)$$

The form of $P_{mN}(I)$ indicates that this expression may be evaluated by first considering the integral over I, and then the sum over m.

We write

$$P_m(I) = \frac{1}{I_o} \left(\frac{I}{I_o}\right)^{m-1} \frac{1}{(m-1)!} e^{-I/I_o}$$

and again make the substitution $x = I/I_o$. Therefore we have, for the moments of $P_m(I)$:

$$\int_0^\infty P_m(I)\,dI = \int_0^\infty \frac{x^{m-1} e^{-x}}{(m-1)!}\,dx = 1$$

$$\int_0^\infty I\, P_m(I)dI = I_o \int_0^\infty \frac{x^m e^{-x}}{(m-1)!}\, dx = I_o m \int_0^\infty \frac{x^m e^{-x}}{m!}\, dx = I_o m$$

$$\int_0^\infty I^2 P_m(I)dI = I_o^{\,2} \int_0^\infty x^{m+1} \frac{e^{-x}}{(m-1)!}\, dx = I_o^{\,2} m(m+1) \int_0^\infty \frac{x^{m+1} e^{-x}}{(m+1)!}$$

$$= I_o^{\,2} m(m+1) \ .$$

Similarly it follows that

$$\int I^3 P_m(I)dI = I_o^{\,3} m(m+1)(m+2)$$

and

$$\int I^4 P_m(I)dI = I_o^{\,4} m(m+1)(m+2)(m+3) \ .$$

We now consider the sum over m, for which we need

$$P(m) = \frac{N^m e^{-N}}{m!} \ . \qquad (6.1)$$

This represents the probability of having m components in an interval, when the average number is N.

We compute the sums:

$$\sum_{m=0}^{\infty} P(m) = \Sigma \frac{N^m e^{-N}}{m!} = e^{-N} \Sigma \frac{N^m}{m!} = e^{-N} e^{N} = 1$$

$$\Sigma\, mP(m) = \Sigma m N^m \frac{e^{-N}}{m!} = N \frac{\Sigma N^{m-1}}{(m-1)!} e^{-N} = N$$

$$\Sigma m^2 p(m) = \Sigma m^2 N^m \frac{e^{-N}}{m!} = \Sigma\{m(m-1)\frac{N^m e^{-N}}{m!} + mN^m \frac{e^{-N}}{m!}\}$$

$$= N^2 \qquad + N$$

$$\Sigma m^3 p(m) = \Sigma m^3 N^m \frac{e^{-N}}{m!} = \Sigma\{m(m-1)(m-2)N^m \frac{e^{-N}}{m!} + (3m^2-2m)N^m \frac{e^{-N}}{m!}\}$$

$$= N^3 \qquad + 3(N^2+N)-2N$$

$$= N^3 + 3N^2 + N$$

$$\Sigma m^4 p(m) = \Sigma m^4 N^m \frac{e^{-N}}{m!} = \Sigma\{m(m-1)(m-2)(m-3)N^m \frac{e^{-N}}{m!} + (6m^3-11m^2+6m)\frac{N^m e^{-N}}{m!}\}$$

$$= N^4 + 6(N^3+3N^2+N) - 11(N^2+N) + 6N$$

$$= N^4 + 6N^3 + 7N^2 + N .$$

Now combining the above results we obtain

$$\langle 1\rangle = 1$$

$$\langle I\rangle = I_o \Sigma m p(m) = I_o N$$

$$\langle I^2\rangle = I_o^2 \Sigma\, m(m+1)p(m) = I_o^2(N^2+N+N) = I_o^2(N^2+2N)$$

$$\langle I^3\rangle = I_o^3 \Sigma(m(m+1)(m+2)p(m)) = I_o^3 \Sigma(m^3+3M^2+2m)p(m) = I_o^3(N^3+6N^2+6N)$$

$$\langle I^4\rangle = I_o^4 \Sigma(m(m+1)(m+2)(m+3)p(m)) = I_o^4 \Sigma(m^4+6m^3+11m^2+6m)p(m)$$

$$= I_o^4(N^4 + 12N^3 + 36N^2 + 13N)$$

We use these results in the following calculation, where $M = NI_o$ and $V = 2NI_o^2$.

$$\sigma_V^2 = \langle ((I-M)^2-V)^2 \rangle$$

$$= \langle (I^2 - 2MI + M^2 - V)^2 \rangle \quad \text{(where we write } M^2 - V = B\text{)}$$

$$= \langle I^4 + 4M^2I^2 + B^2 - 4MI^3 + 2BI^2 - 4MBI \rangle$$

$$= \langle I^4 \rangle - 4M\langle I^3 \rangle + (4M^2+2B)\langle I^2 \rangle - 4MB\langle I \rangle + B^2$$

$$= \{N^4+12N^3+36N^2+13N-4N^4-24N^3-24N^2+6N^4+8N^3-8N^2-4N^4+8N^3 + N^4-4N^3+4N^2\} I_o^4$$

$$= (8N^2+13N) I_o^4$$

$$\sigma_{MV}^2 = \langle ((I-M)^2-V)(I-M) \rangle$$

$$= \langle (I^2-2MI+M^2-V)(I-M) \rangle$$

$$= \langle (I^3-2MI^2+M^2I-VI-MI^2+2M^2I-M^3+MV) \rangle$$

$$= \langle I^3 \rangle - 3M\langle I^2 \rangle + (3M^2-V)\langle I \rangle - M^3 + MV \rangle$$

$$= \{N^3+6N^2+6N-3N^3-6N^2+3N^3-2N^2-N^3+2N^2\} I_o^3$$

$$= 6NI_o^3$$

Naturally, as shown in Chapter 6 (equation (6.7)),

$$\sigma_M^2 = 2NI_o^2 .$$

These results are used in the error analysis of Chapter 6.

APPENDIX 3

SPECTRAL CALCULATIONS

We summarize some of the results that were obtained during the development of the scheme adopted in Chapter 4.

Any spectral calculation requires the knowledge of energy levels and transition probabilities. We recognize two different methods of solving the problem. A continuous level density is assumed, with an option of inserting information about discrete levels where this is known. Alternatively a Monte Carlo technique may be used to construct a set of discrete levels. Note that any form of level density may be used in the calculations described here. We adopt the level density and transition probability of equations (2.6) and (2.8).

DISCRETE LEVELS

A consideration of random matrices led Wigner[67] to surmise the form of the distribution of spacings between two nuclear levels of the same spin J. It is of the form

$$P(D) = \frac{\pi}{2\bar{D}^2} \exp\left(-\frac{\pi D^2}{4\bar{D}^2}\right).$$

Here D is the spacing, and $\bar{D}$ is the average spacing. Although theoretically not entirely correct[68] this distribution agrees well with observation[69].

At any energy, a nucleus has a distribution of spins (equation (2.7)). This is equivalent to the superposition of several mono-spin descriptions. The result is to randomize the level distribution.

We therefore construct a level scheme of a hypothetical nucleus by sampling level spacings from an exponential distribution. Each level is then assigned a spin and a parity by sampling from the appropriate distributions. As in Chapter 4, starting from the capture state we calculate the intensity from successive levels to all levels below them. At this point we have the option of introducing the fluctuations reported by Porter and Thomas[26]. This may be done by multiplying the calculated intensity of a transition by a factor sampled from a χ^2 distribution. In our work we approximate this distribution by an exponential distribution.

This technique allows a study of effects of the spacing distribution and Porter-Thomas fluctuations on intensity. It also indicates the effects of fluctuations in levels of the spectral shape. Populations of various states as a function of spin and parity of capture and ground states may be calculated.

The actual fluctuations in level density and transition probability limit the usefulness of this method in predicting shapes of spectra of real nuclides with few energy levels. For large numbers of levels, the effects of the samplings were found to average out. Since this was the case

for most of the complex spectra under study, the continuous scheme presented in Chapter 4 was adopted. The discrete scheme served to confirm the exponential natures of the gamma ray spacing distribution and of the gamma ray intensity and distribution.

CONTINUOUS SCHEME

For a large number of levels (greater than about 100) the computational effort required for the discrete calculation becomes prohibitive. The method described in Chapter 4 was therefore introduced. The calculation of spectral shape is there described. Other functions of potential interest may also be calculated using this formulation. This description allows the inclusion of spin-parity considerations, as well as known level information in the calculation of transition density functions.

The transition density may be calculated by considering

$$n(E_\gamma) = \sum_{\substack{\text{energy} \\ \text{such that} \\ E_i - E_f = E_\gamma}} \sum_{\substack{\text{spin} \\ \text{parity}}} D_i \, D_f \; .$$

The average intensity per gamma ray is then just

$$I_o(E_\gamma) = \frac{S(E_\gamma)}{n(E_\gamma)}$$

where $S(E_\gamma)$ is given by equation (4.4).

A primary gamma ray transition is one which connects the capture state with any state in the compound nucleus. A secondary gamma ray connects any level population produced by a primary gamma ray to a level of lower energy. A cascade is a number of discrete transitions connecting the capture state of a compound nucleus to its ground state.

Spectra of primary, secondary, tertiary, etc. gamma rays may be simply obtained. This is done by including a subscript in the population, T which keeps a record of the number of transitions required to contribute each portion of the population of the set of levels in a particular bin. Such a decomposition of a spectrum into components is shown in Fig. A3.1. These curves may be used as an aid to constructing decay schemes. The possibility of high energy secondary gamma transitions is indicated. Such transitions were in fact observed in the spectrum following the $^{27}Al(n,\gamma)^{28}Al$ reaction[53].

In the same way that the total transition density may be obtained using this approach, the transition density of primary, secondary, etc. gamma rays may be calculated. The average intensity per gamma ray of the primary, secondary, transitions follows also.

The number of transitions in a cascade may also be of interest. For example, a 2-fold coincidence experiment is insensitive to single transitions, a 3-fold coincidence

Primary, Secondary, etc. Spectra

FIG A3·1·1

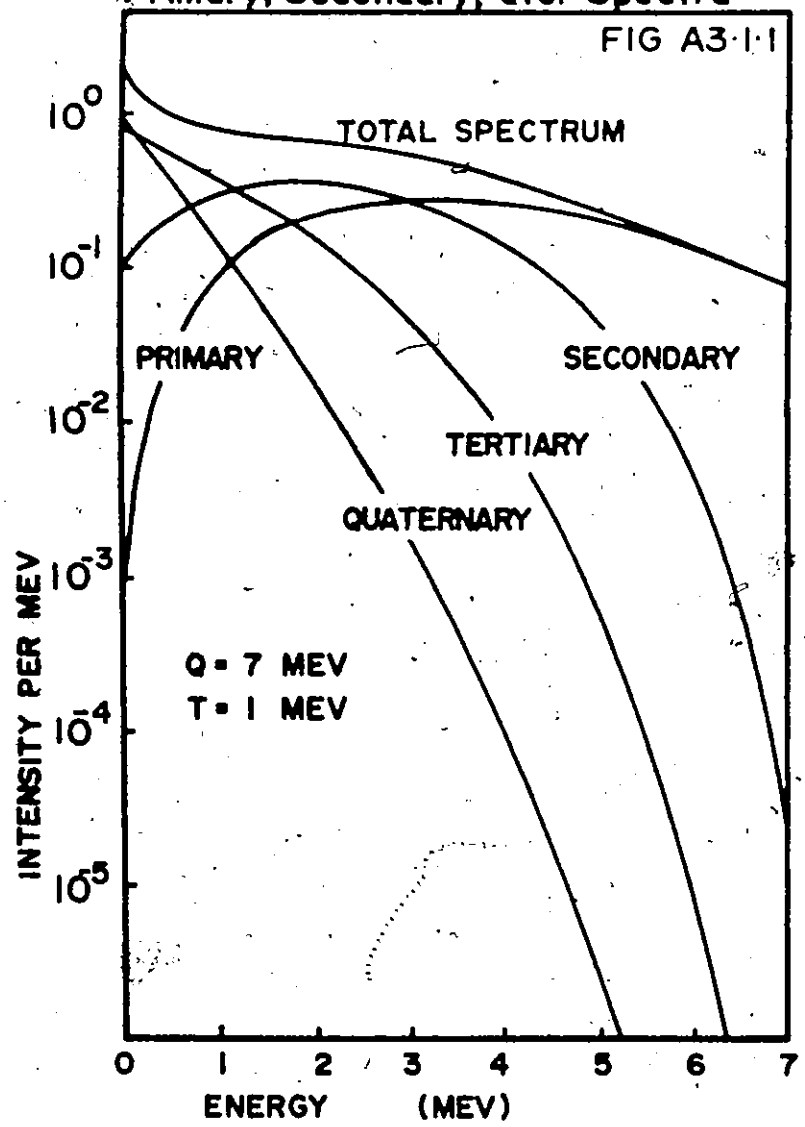

Primary, Secondary, etc. Peak Density

FIG A3·1·2

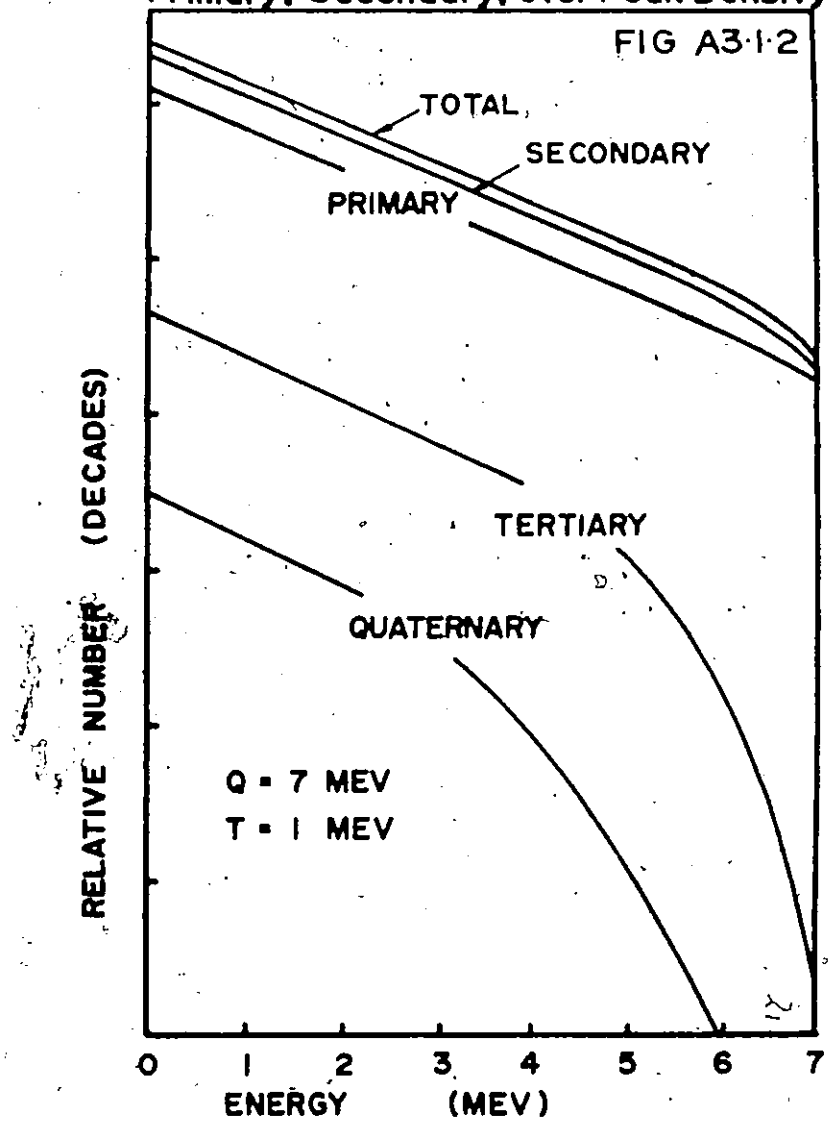

experiment is insensitive to 2 step cascades, etc. Such information may also be useful in the fitting of transitions into decay schemes.

The sequential nature of the calculation offers no simple a priori method of determining the number of gamma rays of a cascade. We construct all possible cascades of the desired number of transitions. A simple algorithm was developed in order to assure that all possible combinations were included in the calculation.

In the matrix

$$A = \begin{pmatrix} 0 & a_{12} & a_{13} & a_{14} & a_{15} \\ & 0 & a_{23} & a_{24} & a_{25} \\ & & 0 & a_{34} & a_{35} \\ - & 0 & - & 0 & a_{45} \\ & & & & 0 \end{pmatrix}$$

We consider the element subscripts to be labels of the energy bins in which the levels are situated. Each element therefore can represent an intensity of a gamma transition, and all possible transitions between bins are represented. The upper right hand element connects the capture and ground states.

In the special case of the 5 bins we write the square of a 5×5 matrix.

$$[A]^2 = \begin{pmatrix} 0 & 0 & a_{12}a_{13} & a_{12}a_{24}+a_{13}a_{34} & a_{12}a_{25}+a_{13}a_{35}+a_{14}a_{45} \\ 0 & 0 & 0 & a_{23}a_{34} & a_{23}a_{35}+a_{24}a_{45} \\ 0 & 0 & 0 & 0 & a_{34}a_{45} \\ 0 & 0 & 0 & 0 & 0 \\ 0 & 0 & 0 & 0 & 0 \end{pmatrix}$$

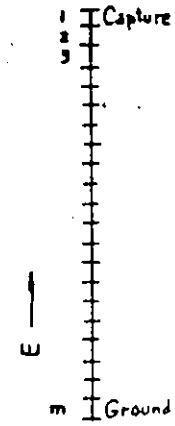

It may be seen that the elements of this matrix represent all possible 2 step transitions between all possible bins. Similarly the nth power of matrix A gives all the n step cascades between all the bins. Therefore all possible n step cascades between the capture and ground states are listed as the indices of the upper right hand side element in the matrix A raised to the nth power.

It should be kept in mind that <u>these</u> results are bin dependent. This is obvious when a purely continuous density is considered - there will be an infinite number of transitions in each cascade before the ground state is reached. That it is reached in fewer steps is a consequence of the digitization of the density, and a consideration of only transitions between bins. The calculation indicated by Fig. A3.2 will be quantitatively correct if the bin width near the ground state is of the order of the level spacing near the ground state. It is for this reason that two bin sizes are illustrated.

In all other calculations the effect of the bins is negligible. As the number of bins increases, the intensity contributed by these cascades to the multiplicity of the spectrum approaches zero.

SPECTRA OF 2, 3, and 4 STEP CASCADES

FIG A3·2

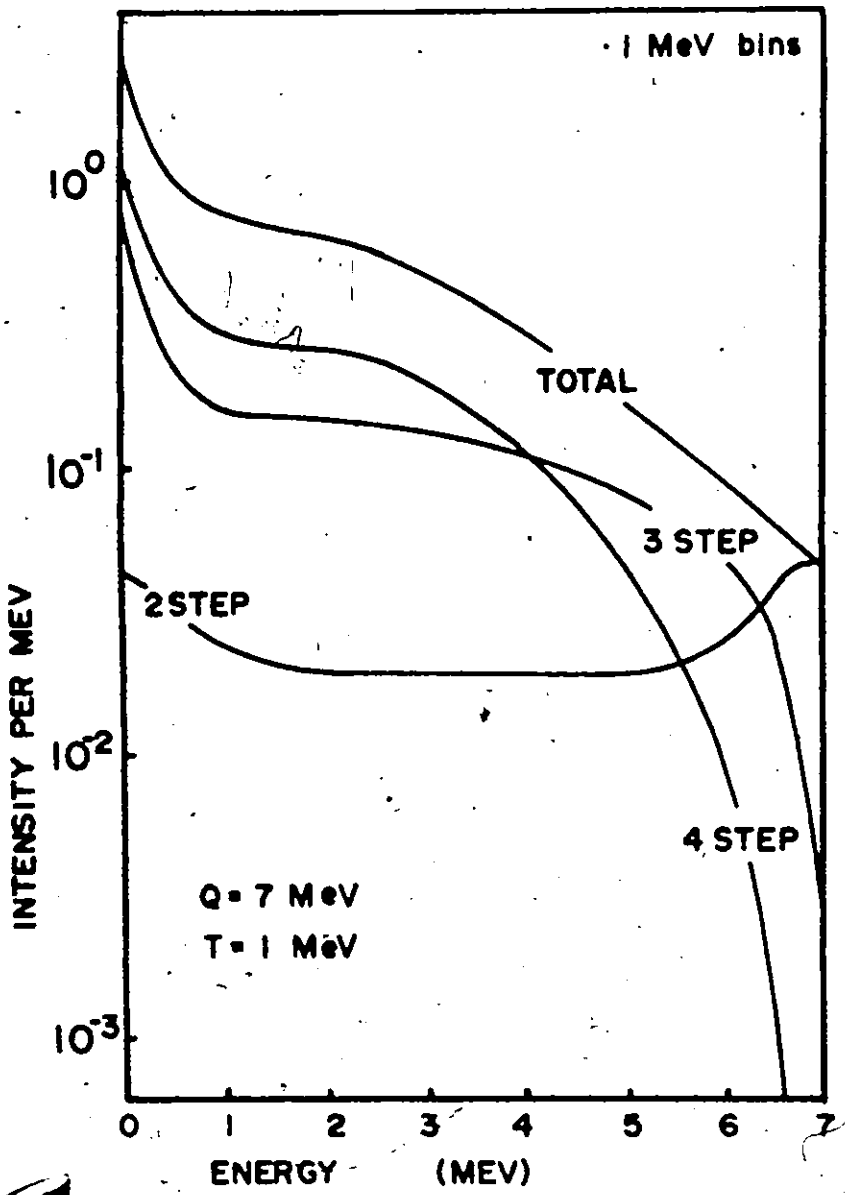

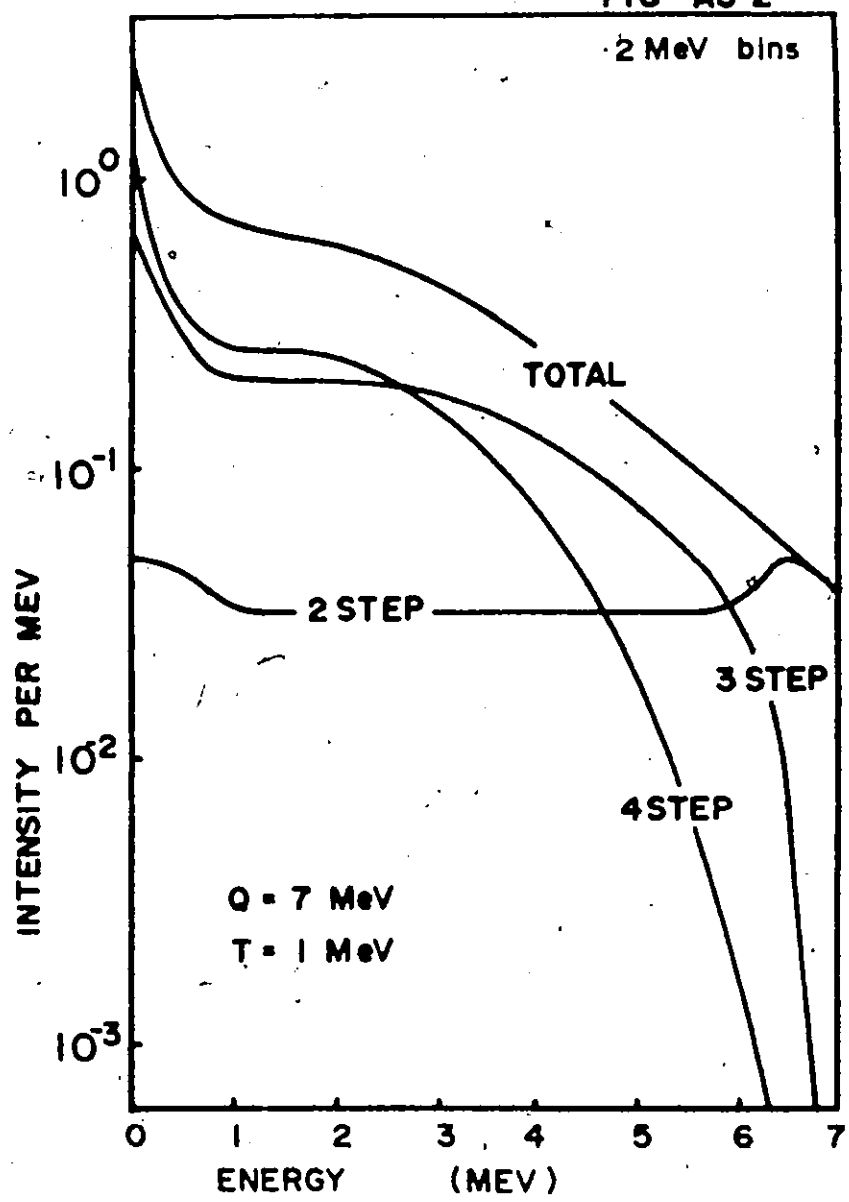

APPENDIX 4

SPECTRAL DATA

In this section we present first tabulations of observed transitions, followed by plots of the observed spectra. We have chosen to order the data according to mass number. The energy scale has been shifted by 1.022 MeV, so that the second escape peaks are labeled with the full energy of the gamma transition involved. The tabulations were obtained from the spectral data by a judicious method of subjectively evaluating correlations in the contents of neighbouring and near neighbouring channel locations. The statistical error in the determination of peak centroids approaches zero. However it is estimated that in favourable cases an error in locating the centroid position of approximately .1 channel, corresponding to a relative energy uncertainty of .2 keV, was introduced by the subjective nature of the judgement. This estimate is based on a careful study of the technique involving the centroid determination of peaks in computer generated spectra.

The foregoing method was not adopted until several non subjective methods had been considered. These involved computer fits of functions using various techniques. Gaussian distributions of varying width and linear components were attempted using both linear and non-linear fitting techniques.

Rejection of these methods was based on poor convergence, a disproportionate amount of computer effort required, difficulty in obtaining initial values of some parameters of the fitted function and failure or difficulty with closely spaced features.

As noted in Chapter 7, relative intensity calibration is via the ^{15}N spectrum, and absolute intensities were obtained by adjusting the spectral multiplicity to that predicted by the model calculations of Chapter 4.

The spectral data is followed by a pictorial representation of the result of the calculation described in Chapter 5. Five plots are presented for each spectrum. The graphs are actually histograms showing the sums of data in 10 channels of the spectrum. From the top of the page, we show

(a) the system background appropriate for the experiment,
(b) the 'raw' result of the experiment,
(c) the result of the experiment corrected for background ,
(d) the spectrum corrected for random addition, and
(e) the final result, comprised of only the second escape peak contributions to the system response.

Finally, for each spectrum where the statistical description of the spectrum was deemed reasonable (error discussions in Chapter 6), we include the result of the analysis. Histograms indicating the average number of counts per peak, the transition density, the cumulative number of transitions, and the cumulative (integral) of the total corrected intensity are presented.

***** C 13 ***** TABLE A4.1

	ENERGY (KEV)	INTENSITY (PH/CAP)
1	4946.2	6.27E-01
2	3694.5	3.54E-01

INTENSITY CALIBRATION VIA RASMUSSEN (29)

C 13 . GAMMA RAY PAIR SPECTRUM FIG A4·1·1

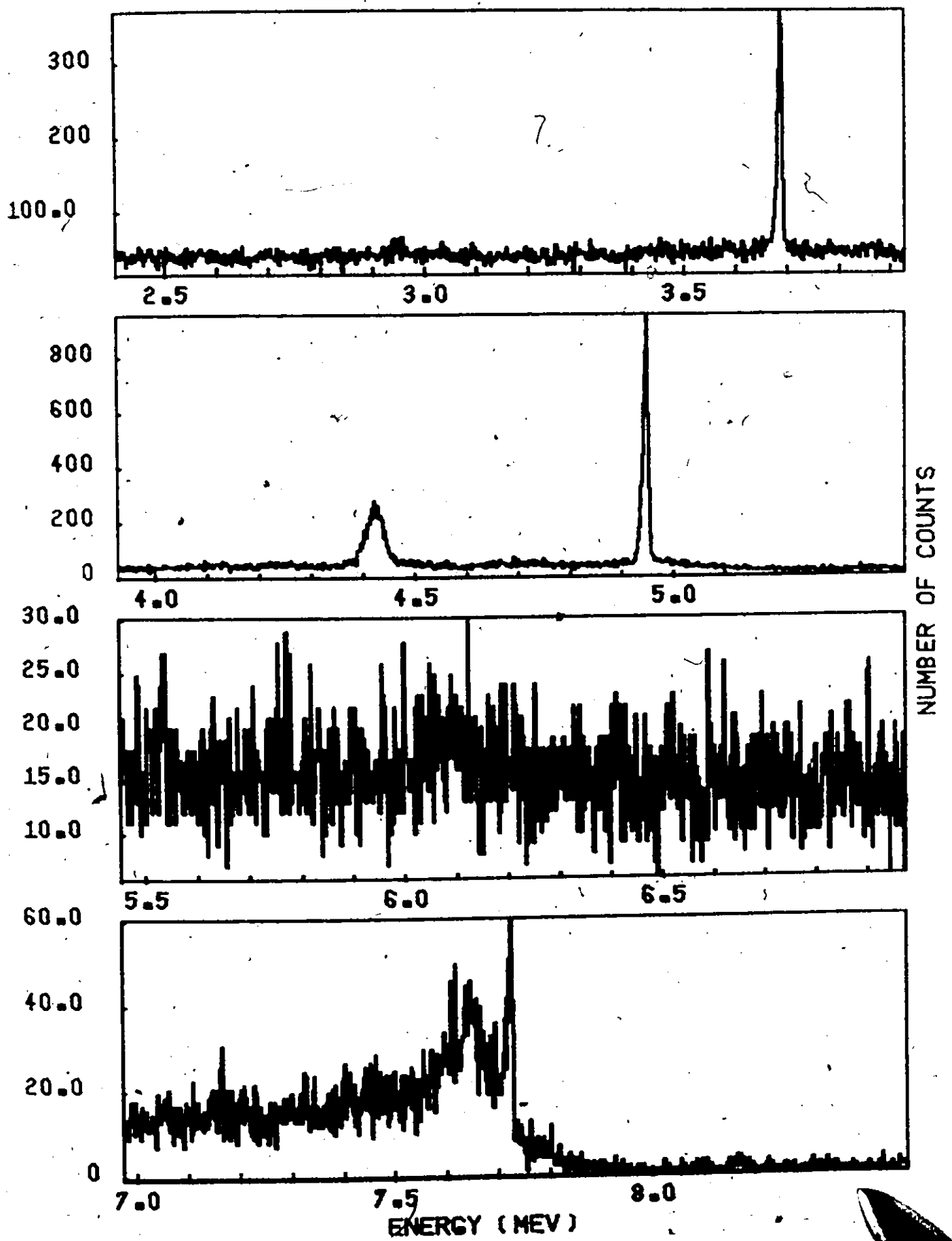

***** N 15 *****

	ENERGY (KEV)	INTENSITY (PH/CAP)
1	8310.9	4.09E-02
2	7298.0	1.05E-01
3	6322.1	1.69E-01
4	5562.2	1.09E-01
5	5534.2	1.96E-01
6	5298.0	2.00E-01
7	5269.2	2.93E-01
8	4508.8	2.04E-01
9	3677.9	1.97E-01
10	3532.6	1.12E-01
11	2519.9	8.12E-02

INTENSITY CALIBRATION VIA MARION (46)

***** MARION

	ENERGY (KEV)	INTENSITY (PH/CAP)
1	8310.3	4.40E-02
2	7298.7	1.00E-01
3	6322.1	1.88E-01
4	5562.0	1.03E-01
5	5533.0	1.88E-01
6	5297.4	2.14E-01
7	5268.5	3.06E-01
8	4508.8	1.66E-01
9	3677.7	1.59E-01
10	3532.1	9.90E-02
11	2519.9	6.10E-02

N 15 GAMMA RAY PAIR SPECTRUM FIG A4·2·1

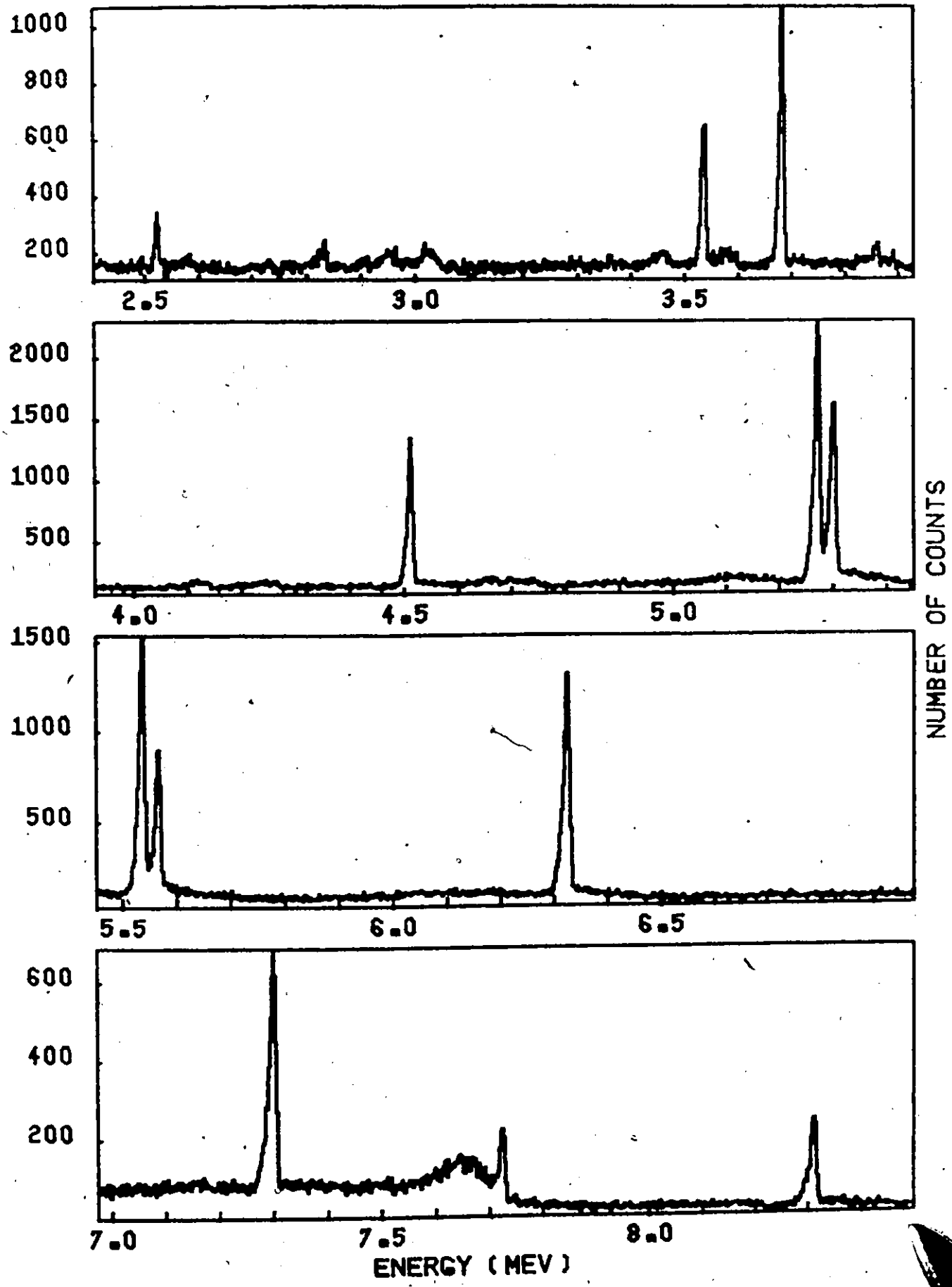

N 15 RESPONSE STRIPPING FIG A4·2·2

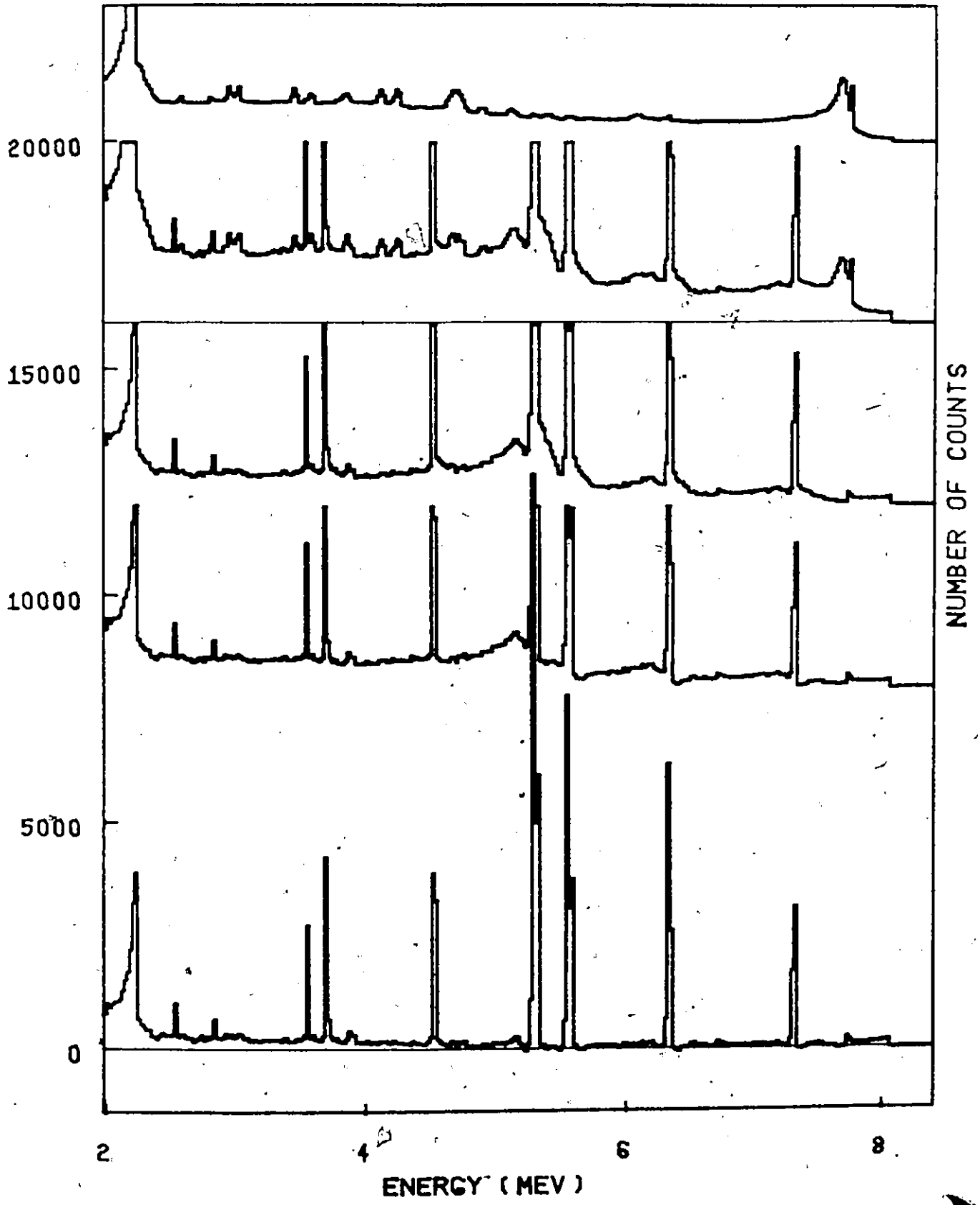

***** AL 28 ***** TABLE A4.3

	ENERGY (KEV)	INTENSITY (PH/CAP)		ENERGY (KEV)	INTENSITY (PH/CAP)		ENERGY (KEV)	INTENSITY (PH/CAP)		ENERGY (KEV)	INTENSITY (PH/CAP)
1	7725.3	3.02E-01	41	5523.9	7.37E-04	81	4185.4	7.09E-04	121	2988.4	5.84E-03
2	7695.5	3.99E-02	42	5452.7	2.22E-03	82	4169.7	1.43E-03	122	2976.4	3.92E-03
3	7341.9	5.75E-04	43	5444.3	1.11E-03	83	4133.8	8.74E-02	123	2960.4	1.18E-01
4	7269.9	4.38E-04	44	5427.3	1.48E-03	84	4101.3	7.29E-04	124	2922.3	3.03E-03
5	7238.8	7.40E-04	45	5411.2	2.24E-02	85	4069.6	1.47E-03	125	2894.2	1.03E-03
6	7176.3	1.38E-03	46	5377.6	1.12E-03	86	4055.0	2.22E-03	126	2887.5	3.10E-03
7	7135.4	5.14E-04	47	5344.5	1.87E-04	87	4016.2	9.01E-03	127	2878.2	2.08E-03
8	6937.4	1.26E-03	48	5302.7	5.24E-03	88	4003.6	1.51E-03	128	2863.8	1.05E-03
9	6894.0	3.12E-04	49	5269.9	9.40E-04	89	3950.6	7.67E-04	129	2821.7	4.53E-02
10	6861.9	1.87E-03	50	5238.9	2.83E-03	90	3935.8	4.63E-03	130	2754.5	7.00E-04
11	6822.5	5.41E-04	51	5211.0	2.84E-04	91	3902.4	4.68E-03	131	2731.9	7.11E-03
12	6801.3	3.08E-04	52	5203.2	2.84E-04	92	3890.5	2.35E-03	132	2710.0	7.58E-03
13	6752.4	7.68E-04	53	5176.5	8.56E-04	93	3875.9	3.39E-02	133	2691.9	7.32E-04
14	6747.4	4.60E-04	54	5134.8	3.35E-02	94	3849.5	3.90E-02	134	2656.7	2.25E-03
15	6723.7	9.95E-04	55	5104.2	4.61E-03	95	3824.3	7.28E-03	135	2626.3	1.54E-02
16	6710.3	9.40E-03	56	5069.3	1.73E-03	96	3789.8	1.06E-02	136	2590.5	4.74E-02
17	6619.9	4.30E-03	57	5032.7	2.91E-04	97	3754.0	9.35E-04	137	2578.1	2.43E-02
18	6590.9	1.65E-03	58	5005.6	5.84E-04	98	3723.3	9.46E-04	138	2566.0	2.02E-03
19	6459.6	2.32E-04	59	4997.1	8.78E-04	99	3709.2	6.18E-03	139	2549.7	2.45E-03
20	6440.0	6.85E-03	60	4985.0	1.17E-03	100	3678.1	3.85E-03	140	2535.3	8.27E-04
21	6398.8	5.85E-05	61	4903.8	3.44E-02	101	3659.6	9.70E-04	141	2502.5	1.70E-03
22	6350.1	1.04E-03	62	4869.3	5.43E-04	102	3639.8	9.77E-04	142	2485.7	2.16E-03
23	6315.6	2.11E-02	63	4764.7	1.17E-02	103	3624.0	9.84E-04	143	2451.5	4.00E-03
24	6253.8	2.29E-04	64	4755.6	6.70E-03	104	3591.6	6.08E-02	144	2419.9	1.37E-03
25	6197.5	7.08E-03	65	4734.6	6.63E-02	105	3561.1	1.21E-02	145	2381.0	1.70E-03
26	6100.9	2.76E-02	66	4691.2	5.40E-02	106	3541.7	5.10E-04	146	2347.0	1.75E-03
27	6018.4	2.05E-03	67	4660.6	3.09E-02	107	3480.7	2.16E-03	147	2299.0	1.84E-03
28	5988.9	2.28E-04	68	4620.7	2.90E-03	108	3465.4	9.15E-02	148	2282.8	4.78E-02
29	5968.9	2.91E-04	69	4596.7	1.17E-03	109	3392.5	7.75E-03	149	2271.6	1.99E-02
30	5923.4	4.83E-04	70	4576.1	4.10E-03	110	3347.3	6.33E-03	150	2255.5	4.83E-03
31	5879.7	3.88E-04	71	4512.7	1.33E-03	111	3303.4	1.45E-02	151	2171.4	3.20E-03
32	5859.8	1.60E-03	72	4485.9	6.69E-04	112	3265.5	6.58E-03	152	2139.0	2.12E-02
33	5829.5	1.45E-04	73	4427.7	1.16E-02	113	3207.9	1.69E-03	153	2130.7	4.50E-03
34	5797.1	1.50E-03	74	4397.6	6.86E-04	114	3192.0	8.53E-04	154	2108.5	2.67E-02
35	5765.8	4.07E-03	75	4378.2	5.52E-03	115	3142.6	1.75E-03			
36	5709.7	5.82E-03	76	4331.8	7.00E-04	116	3128.9	2.70E-03			
37	5649.4	9.74E-05	77	4280.4	2.13E-03	117	3074.7	9.25E-04			
38	5610.8	1.84E-04	78	4260.1	8.51E-02	118	3068.6	9.29E-04			
39	5585.7	1.17E-02	79	4240.5	1.44E-03	119	3034.1	1.03E-01			
40	5532.4	1.84E-04	80	4215.8	7.25E-04	120	3002.1	1.06E-02			

INTENSITY CALIBRATION VIA ISHAQ ET AL. (53)

AL 28 GAMMA RAY PAIR SPECTRUM FIG A4·3·1

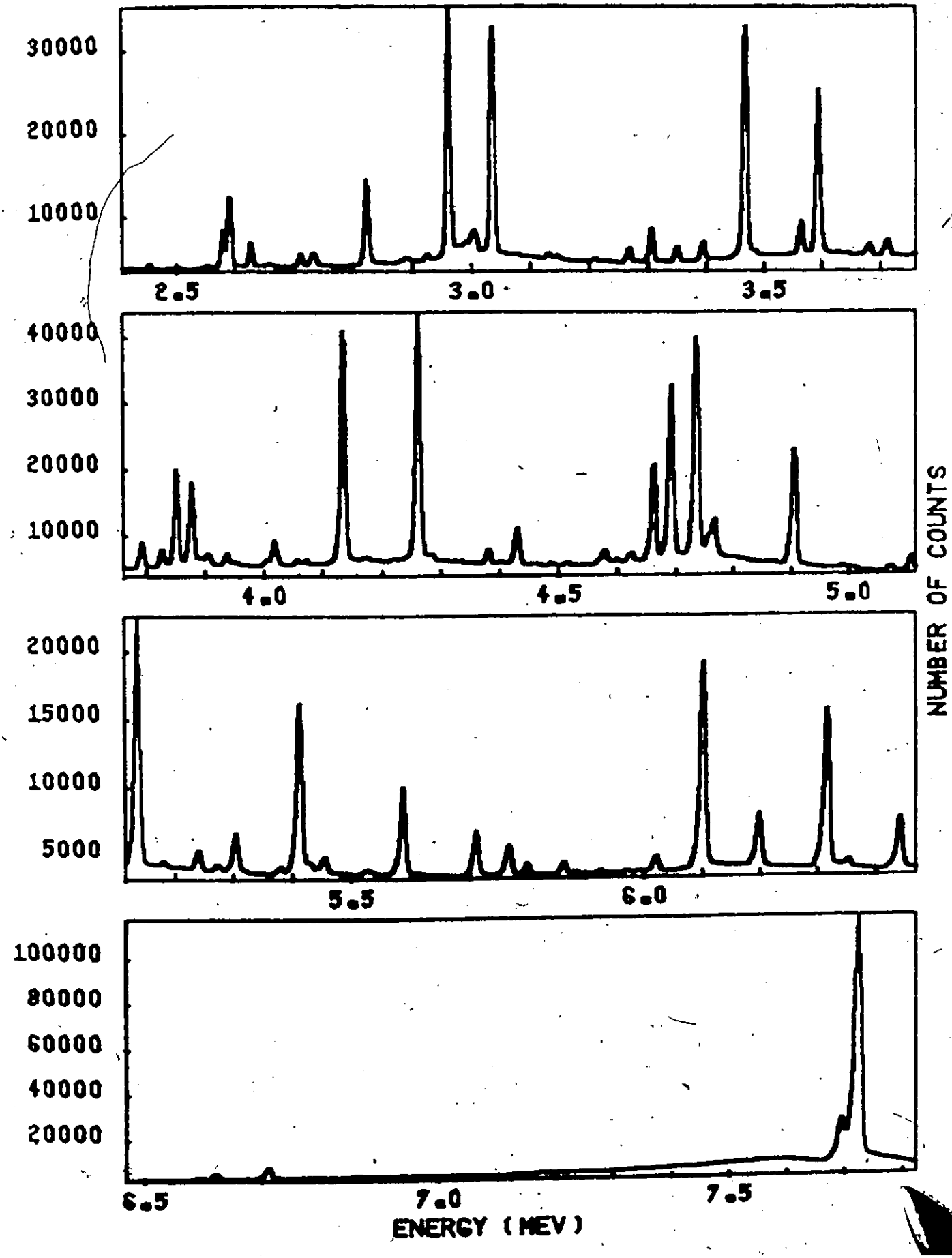

AL 28 RESPONSE STRIPPING FIG A4·3·2

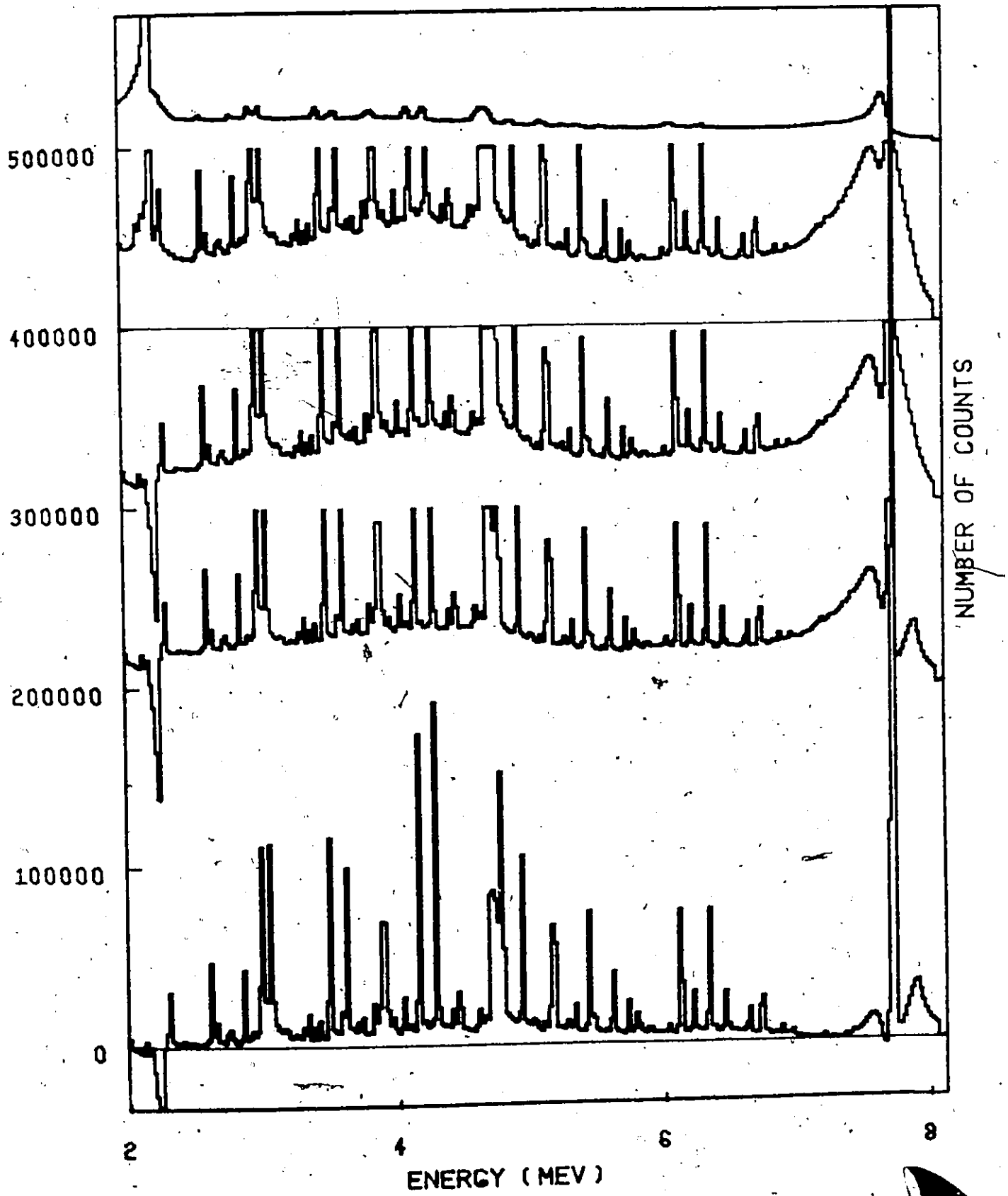

AL 28 STATISTICAL DATA FIG A4·3·3

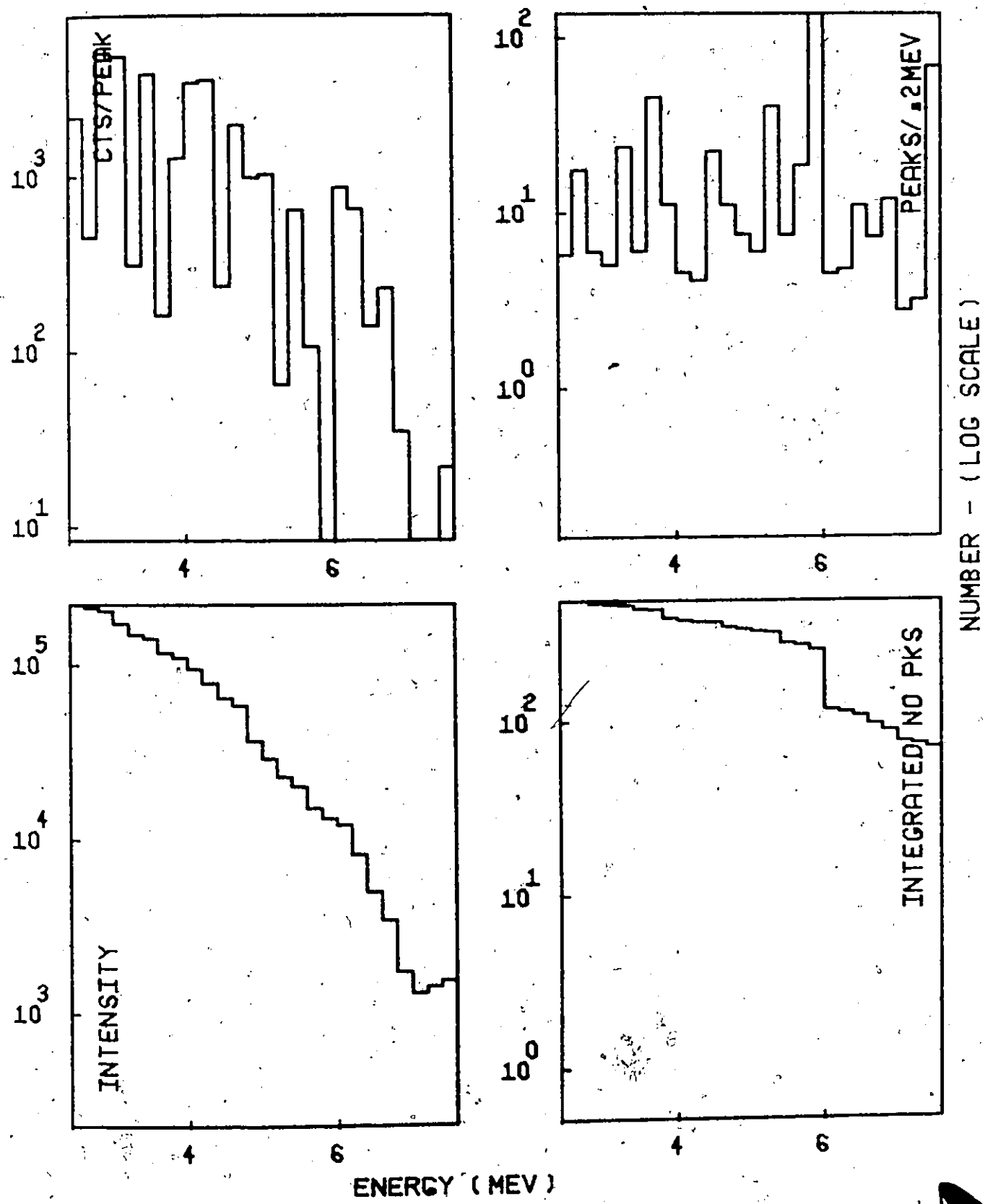

TABLE A4.4

***** SI 29 *****

	ENERGY (KEV)	INTENSITY (PH/CAP)
1	8472.6	2.33E-02
2	7199.0	6.76E-02
3	6744.2	9.62E-03
4	6389.4	1.12E-01
5	5272.8	4.02E-03
6	5106.5	3.53E-02
7	4934.9	7.17E-01
8	3954.5	3.39E-02
9	3864.4	1.32E-02
10	3683.7	2.19E-02
11	3661.3	5.89E-02
12	3539.8	9.21E-01
13	2780.8	1.89E-02
14	2424.9	3.63E-02
15	2092.6	2.37E-01

INTENSITY CALIBRATION VIA RASMUSSEN (29)

SI 29 GAMMA RAY PAIR SPECTRUM FIG A4·4·1

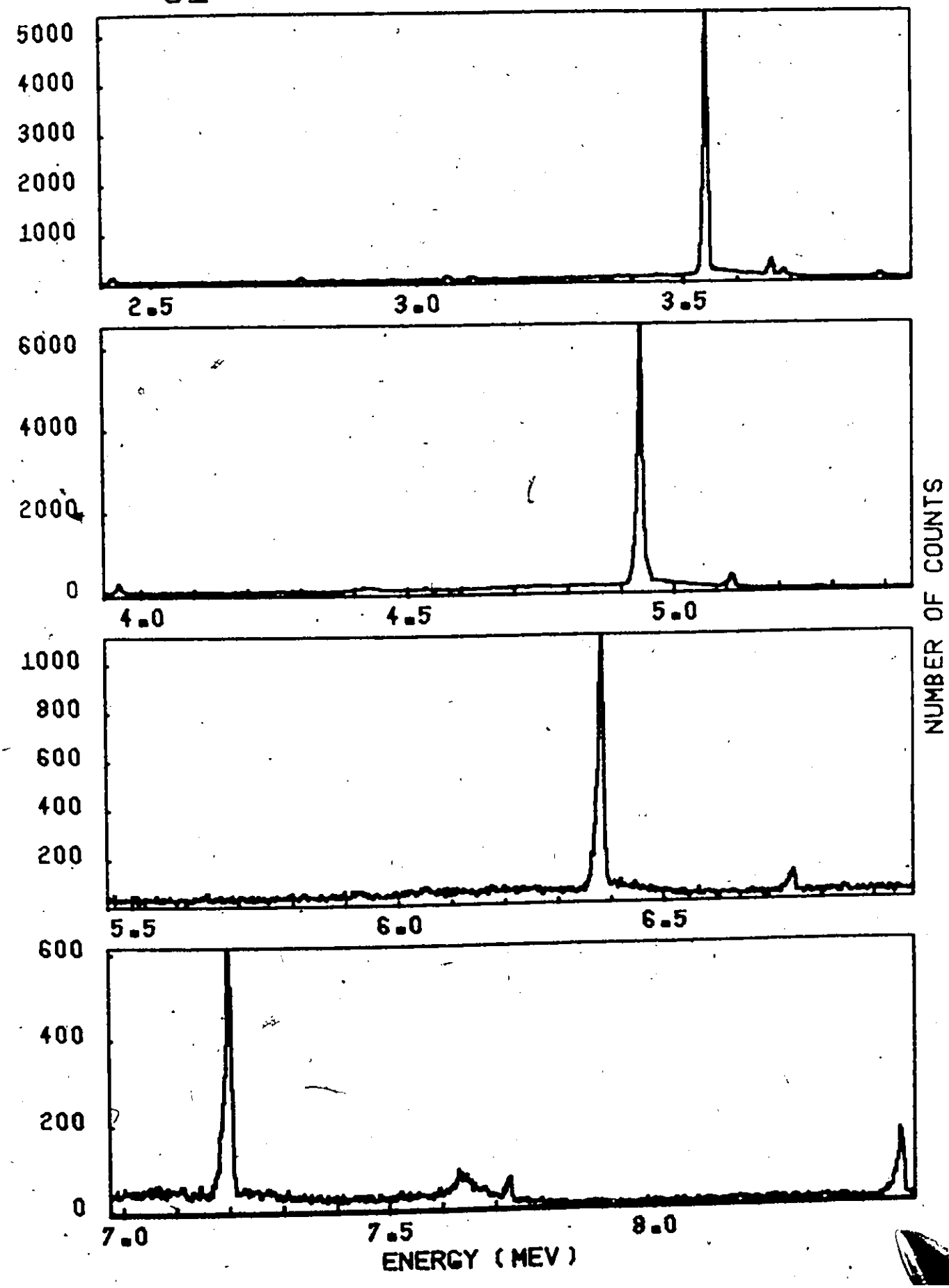

SI 29 RESPONSE STRIPPING FIG A4·4·2

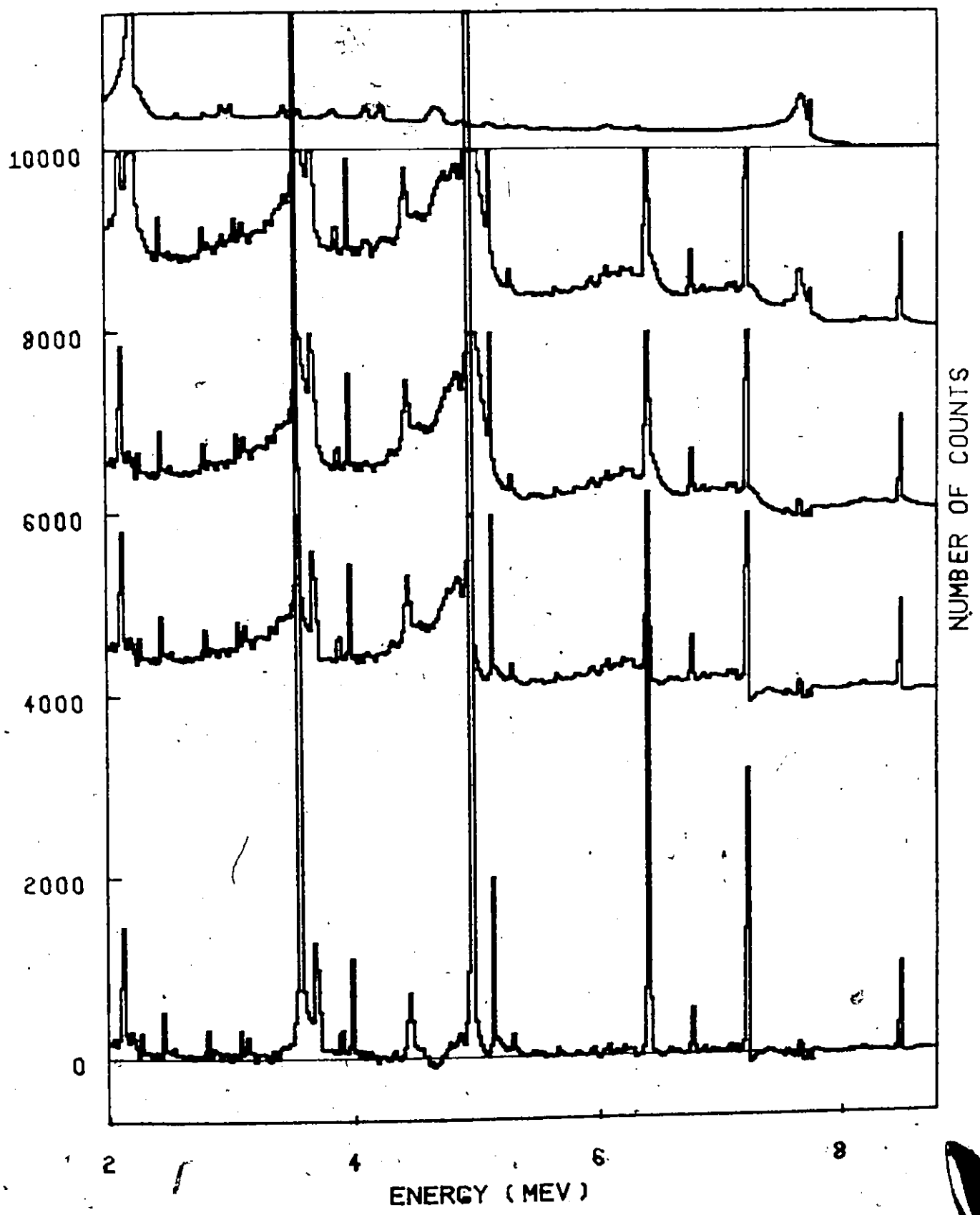

***** AR 41 ***** TABLE A4.5

	ENERGY (KEV)	INTENSITY (PH/CAP)
1	5581.5	1.18E-01
2	5182.3	2.14E-03
3	5135.9	1.08E-03
4	5064.1	4.89E-03
5	5013.8	1.64E-03
6	4980.1	1.65E-03
7	4945.3	6.17E-02
8	4907.0	1.12E-03
9	4744.5	5.89E-01
10	4690.9	2.47E-03
11	4421.8	1.29E-02
12	4259.5	1.80E-03
13	4102.7	5.12E-03
14	3700.8	1.04E-01
15	3684.1	3.00E-02
16	3452.0	2.22E-02
17	3365.9	4.54E-02
18	3264.0	2.83E-03
19	3150.6	4.10E-02
20	3089.1	1.36E-02
21	2865.9	2.02E-03
22	2842.9	9.57E-03
23	2811.2	6.35E-02
24	2781.2	1.99E-02
25	2772.2	8.45E-02
26	2614.4	3.07E-02
27	2516.3	3.19E-02
28	2490.0	1.21E-02
29	2432.5	8.98E-03
30	2131.3	3.94E-02

INTENSITY CALIBRATION VIA LYCKLAMA ET AL. (70)

AR 41 GAMMA RAY PAIR SPECTRUM FIG A4·5·1

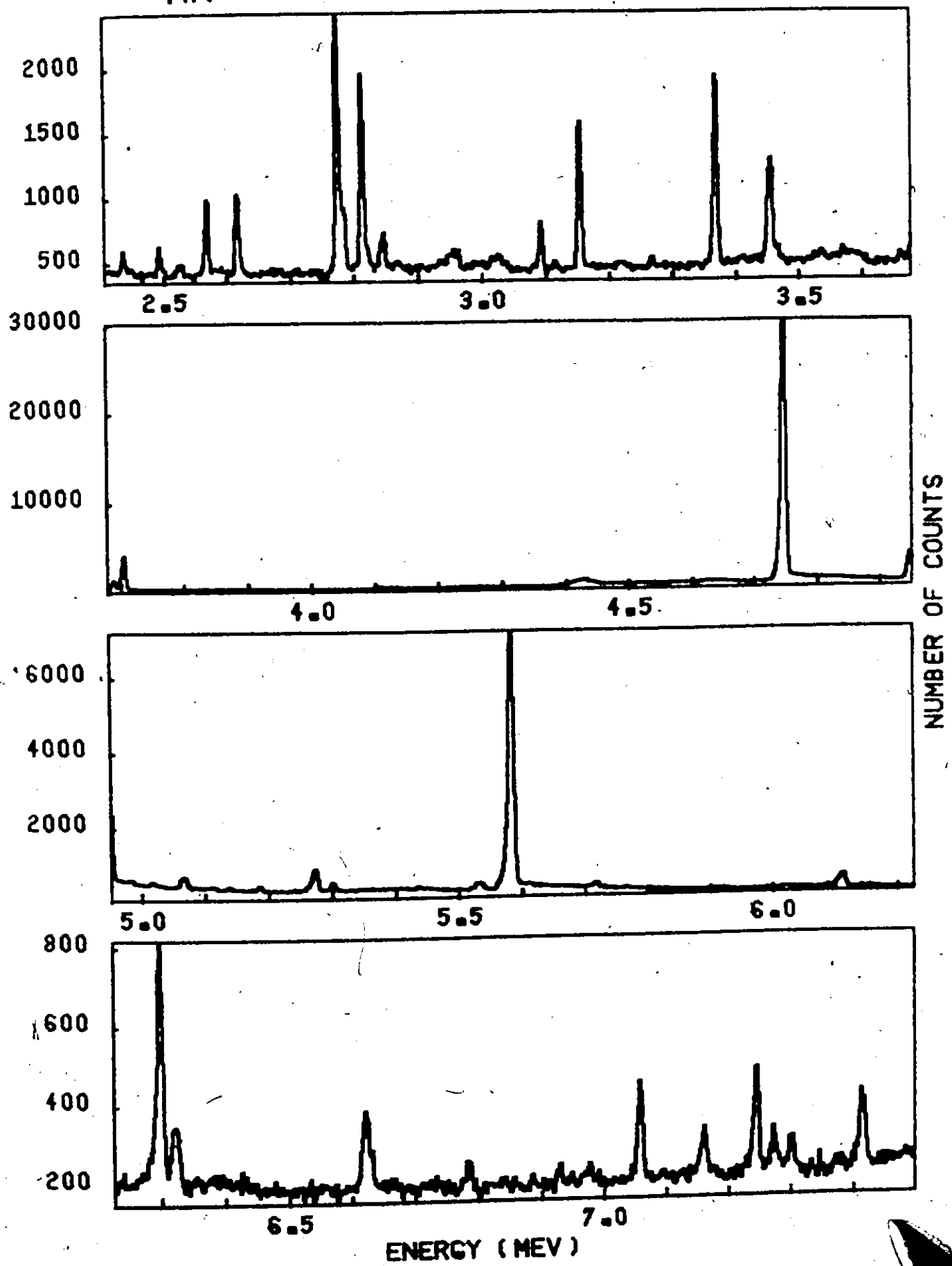

AR 41 RESPONSE STRIPPING FIG A4·5·2

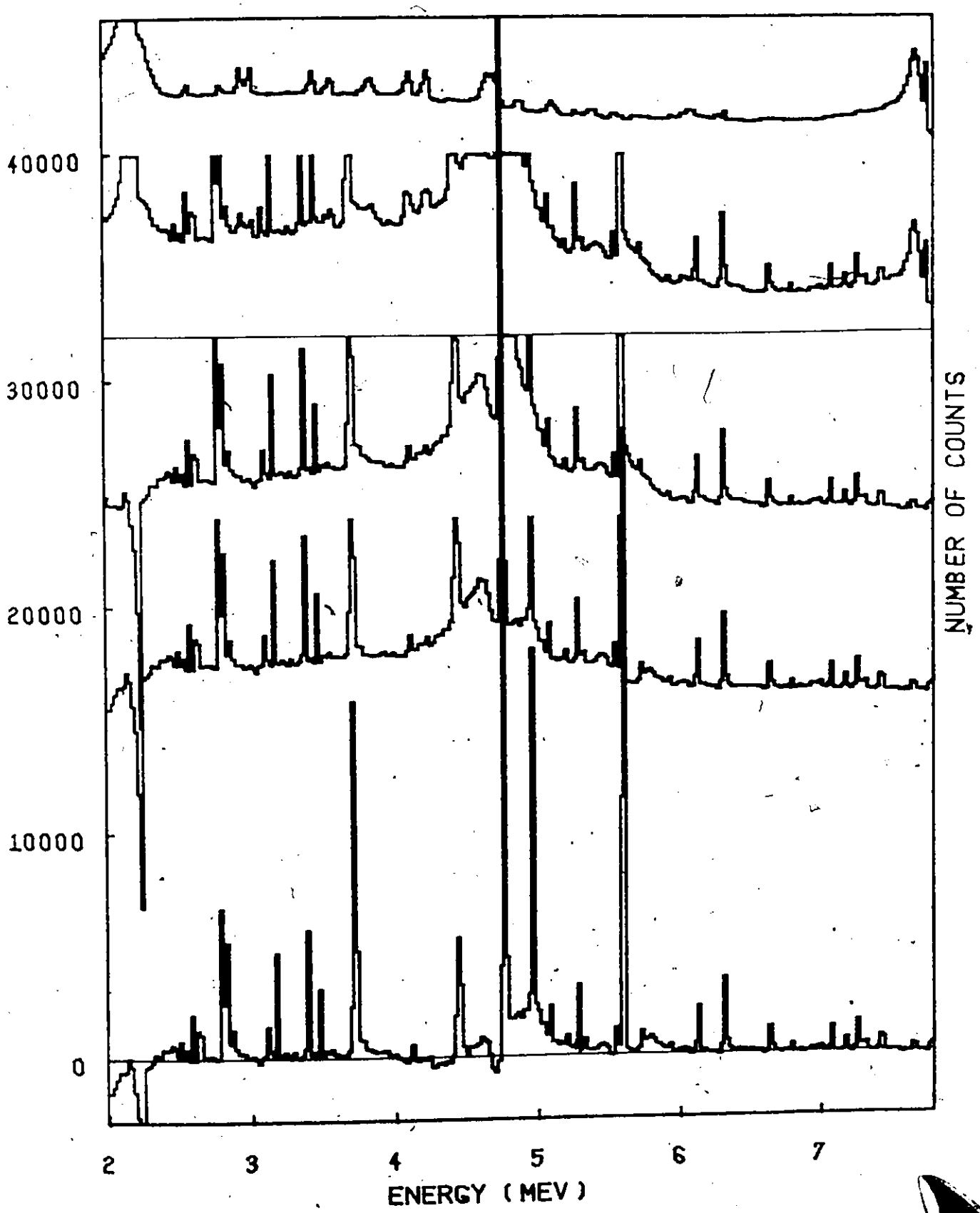

	ENERGY (KEV)	INTENSITY (PH/CAP)		ENERGY (KEV)	INTENSITY (PH/CAP)		ENERGY (KEV)	INTENSITY (PH/CAP)		ENERGY (KEV)	INTENSITY (PH/CAP)
1	8764.7	5.27E-03	41	6117.7	1.45E-03	81	5211.9	4.51E-03	121	4424.5	2.84E-03
2	8621.8	1.53E-03	42	6099.8	3.03E-03	82	5204.0	1.50E-03	122	4410.2	1.95E-03
3	8536.3	3.02E-02	43	6065.5	2.37E-03	83	5165.1	5.50E-03	123	4404.2	1.09E-03
4	8474.3	4.49E-03	44	6056.6	1.01E-02	84	5154.6	2.92E-03	124	4379.0	3.64E-03
5	8319.3	1.20E-02	45	6048.3	6.70E-03	85	5142.3	1.84E-03	125	4356.2	1.50E-03
6	8178.3	5.87E-02	46	5979.1	2.36E-03	86	5130.6	3.47E-03	126	4329.2	1.90E-03
7	8135.7	1.58E-02	47	5928.7	1.18E-03	87	5108.0	1.30E-03	127	4315.9	2.44E-03
8	7927.4	3.24E-03	48	5899.4	1.56E-02	88	5086.6	3.82E-03	128	4294.5	2.41E-03
9	7793.9	2.41E-04	49	5871.6	1.44E-03	89	5055.0	1.75E-03	129	4270.5	1.88E-03
10	7674.0	2.25E-03	50	5883.9	1.05E-03	90	5041.9	9.87E-04	130	4261.4	1.19E-03
11	7638.1	1.40E-02	51	5822.0	1.12E-03	91	4995.7	6.43E-03	131	4237.0	5.75E-03
12	7491.5	2.64E-03	52	5806.7	1.40E-03	92	4977.2	1.84E-02	132	4224.1	2.11E-03
13	7441.5	1.33E-03	53	5796.2	1.01E-03	93	4947.5	4.28E-03	133	4204.8	5.32E-04
14	7415.4	4.42E-04	54	5783.9	3.24E-03	94	4921.1	3.19E-03	134	4173.7	6.14E-03
15	7367.4	6.57E-04	55	5760.9	3.92E-04	95	4893.3	4.50E-03	135	4155.8	3.09E-03
16	7334.1	1.53E-03	56	5745.5	6.60E-03	96	4886.2	6.28E-03	136	4137.3	1.24E-03
17	7235.0	3.22E-03	57	5732.6	2.35E-03	97	4876.5	1.94E-03	137	4125.6	6.23E-04
18	7121.0	1.26E-02	58	5722.9	5.60E-04	98	4857.0	6.49E-04	138	4111.7	2.51E-03
19	7053.7	1.98E-03	59	5705.4	6.72E-04	99	4824.5	3.27E-03	139	4093.9	9.45E-04
20	6997.6	8.53E-04	60	5680.6	1.79E-03	100	4818.1	1.97E-03	140	4085.7	1.34E-03
21	6962.5	1.41E-03	61	5667.9	4.88E-03	101	4806.6	3.29E-04	141	4077.4	1.27E-03
22	6875.8	4.47E-03	62	5654.4	6.73E-04	102	4745.5	1.67E-03	142	4061.3	8.84E-03
23	6841.2	3.34E-02	63	5626.1	6.23E-03	103	4737.0	6.69E-04	143	4042.1	2.08E-03
24	6718.2	9.33E-03	64	5586.0	3.99E-03	104	4722.5	6.55E-03	144	4022.2	3.47E-03
25	6692.1	5.47E-04	65	5571.3	2.36E-03	105	4713.0	2.86E-03	145	4007.7	3.24E-03
26	6677.4	5.47E-04	66	5557.8	2.54E-03	106	4696.5	1.18E-03	146	4002.0	3.25E-03
27	6644.1	5.99E-03	67	5532.5	3.05E-03	107	4682.6	4.58E-03	147	3974.2	2.46E-03
28	6558.5	1.45E-02	68	5522.1	7.90E-04	108	4674.1	1.70E-03	148	3952.2	2.48E-04
29	6545.6	3.14E-03	69	5501.7	2.26E-03	109	4658.6	1.71E-03	149	3933.5	1.25E-03
30	6508.9	2.78E-03	70	5484.1	5.49E-03	110	4645.7	5.14E-04	150	3926.4	1.42E-03
31	6459.3	3.81E-03	71	5448.8	6.58E-03	111	4629.8	2.75E-03	151	3904.9	5.88E-04
32	6433.2	3.46E-04	72	5417.8	2.10E-04	112	4619.7	4.88E-03	152	3888.1	1.27E-03
33	6366.1	3.79E-03	73	5380.9	2.64E-03	113	4600.5	2.48E-03	153	3878.7	5.09E-03
34	6351.5	1.74E-02	74	5365.5	2.85E-03	114	4564.8	5.91E-04	154	3866.6	2.47E-03
35	6319.7	2.01E-02	75	5347.8	3.60E-03	115	4552.9	5.02E-04	155	3853.5	1.45E-03
36	6304.1	8.75E-03	76	5338.1	7.63E-03	116	4536.6	2.06E-03	156	3841.0	1.20E-03
37	6239.4	6.84E-04	77	5319.2	2.02E-03	117	4527.5	2.94E-03	157	3823.2	2.42E-03
38	6204.3	2.64E-03	78	5288.1	4.47E-03	118	4500.5	5.23E-03	158	3815.2	2.00E-03
39	6194.8	4.09E-03	79	5269.2	1.29E-02	119	4465.6	3.60E-03	159	3800.1	4.87E-03
40	6172.4	1.50E-02	80	5227.4	1.82E-03	120	4443.5	2.73E-03	160	3791.6	3.77E-03

	ENERGY (KEV)	INTENSITY (PH/CAP)		ENERGY (KEV)	INTENSITY (PH/CAP)		ENERGY (KEV)	INTENSITY (PH/CAP)
161	3769.4	2.38E-04	201	3156.6	2.24E-03	241	2509.1	3.24E-03
162	3750.9	1.26E-03	202	3139.9	1.02E-03	242	2501.2	6.13E-03
163	3734.6	1.50E-03	203	3126.0	1.71E-03	243	2477.7	5.87E-03
164	3721.0	2.66E-03	204	3118.1	2.98E-03	244	2443.4	3.03E-03
165	3712.8	2.73E-03	205	3105.6	3.11E-03	245	2417.0	2.07E-03
166	3695.3	7.33E-04	206	3090.7	2.32E-03	246	2410.8	5.61E-03
167	3683.4	2.64E-03	207	3084.3	4.20E-03	247	2406.4	7.31E-03
168	3668.6	2.65E-03	208	3050.4	4.40E-03	248	2373.9	4.10E-03
169	3656.6	1.67E-03	209	3031.5	3.72E-03	249	2362.1	3.71E-03
170	3638.2	3.12E-03	210	3012.7	1.24E-02	250	2352.0	2.64E-03
171	3623.9	6.91E-03	211	2993.8	5.16E-03	251	2340.9	2.23E-03
172	3608.6	1.45E-03	212	2964.8	2.08E-03	252	2329.6	4.28E-03
173	3597.5	3.62E-03	213	2951.7	4.39E-03	253	2317.7	1.60E-03
174	3572.7	8.35E-04	214	2930.1	1.11E-03	254	2289.9	2.11E-03
175	3557.4	1.68E-03	215	2901.5	3.19E-03	255	2277.9	1.43E-03
176	3543.7	6.50E-04	216	2887.2	1.87E-03	256	2268.4	9.62E-04
177	3528.2	9.81E-04	217	2871.1	4.09E-03	257	2244.0	4.45E-03
178	3518.7	8.54E-04	218	2864.5	3.37E-03	258	2130.0	3.06E-03
179	3505.0	1.39E-03	219	2852.6	3.29E-03	259	2112.3	1.03E-02
180	3498.8	1.92E-03	220	2836.3	2.47E-03	260	2106.7	7.41E-03
181	3493.3	1.06E-03	221	2815.7	3.37E-03	261	2079.5	2.57E-03
182	3478.8	1.40E-03	222	2798.6	5.28E-03	262	2074.0	2.01E-03
183	3459.5	6.74E-03	223	2791.7	2.65E-03	263	2059.3	2.64E-03
184	3444.2	2.24E-03	224	2773.8	1.34E-03	264	2020.3	2.18E-03
185	3432.5	1.91E-03	225	2753.3	2.49E-03	265	2005.2	1.28E-02
186	3416.9	2.88E-03	226	2720.2	4.06E-03			
187	3397.0	3.69E-03	227	2715.4	3.84E-03			
188	3378.9	1.11E-03	228	2694.8	6.26E-03			
189	3360.1	3.05E-03	229	2678.7	1.43E-03			
190	3352.3	4.38E-03	230	2665.8	4.83E-03			
191	3340.6	1.74E-03	231	2635.4	1.48E-02			
192	3327.5	3.40E-03	232	2612.0	6.28E-04			
193	3312.0	3.12E-03	233	2601.2	1.88E-03			
194	3279.5	3.27E-03	234	2584.8	2.86E-03			
195	3266.4	8.28E-03	235	2579.8	2.69E-03			
196	3247.5	1.50E-03	236	2569.5	2.17E-03			
197	3218.3	2.39E-03	237	2552.0	2.75E-03			
198	3205.0	2.30E-03	238	2549.0	2.39E-03			
199	3193.9	2.64E-03	239	2535.3	1.12E-03			
200	3165.5	1.56E-03	240	2530.1	1.31E-03			

SC 46 GAMMA RAY PAIR SPECTRUM FIG A4·6·1

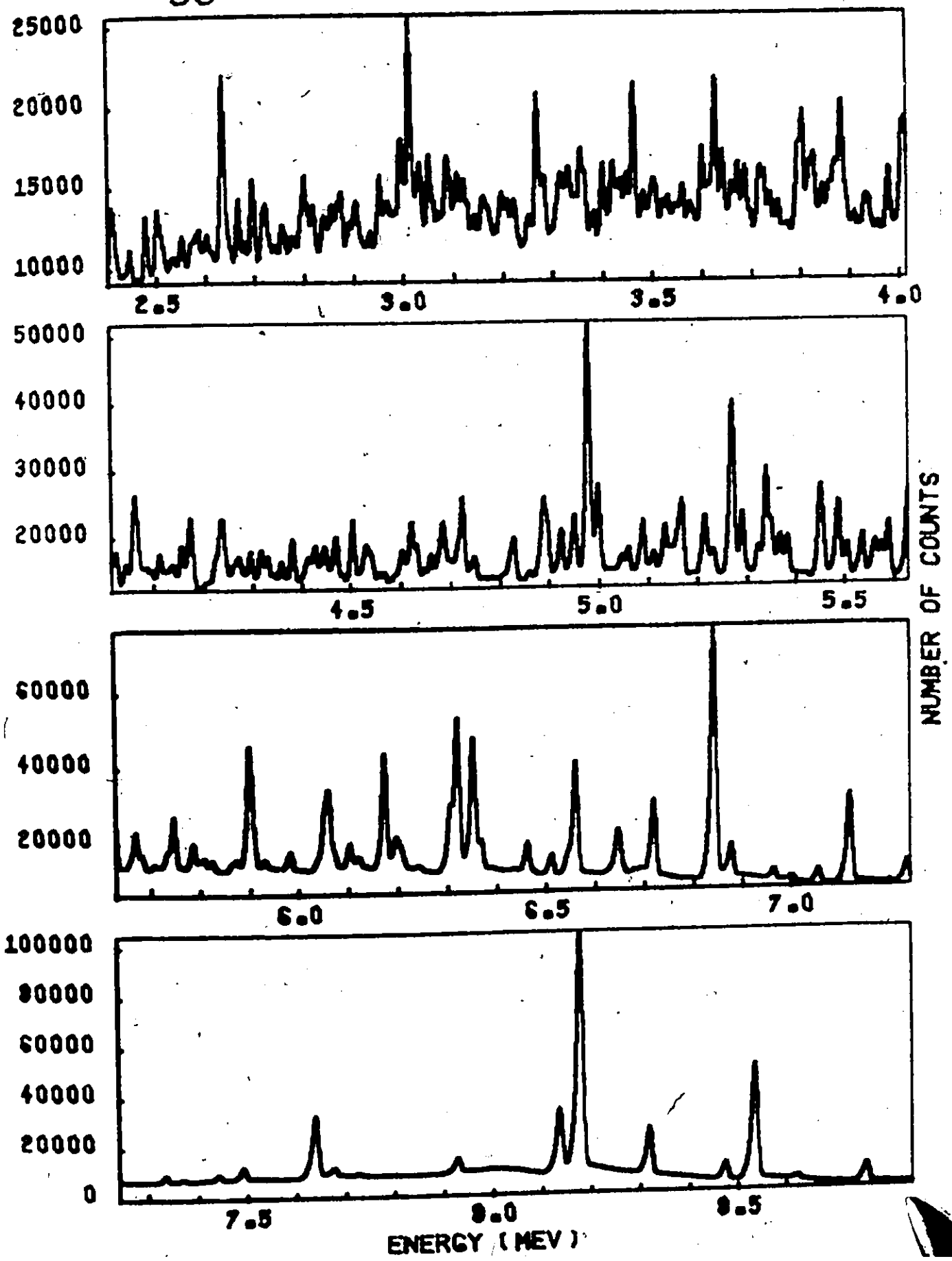

SC 46 RESPONSE STRIPPING FIG A4·6·2

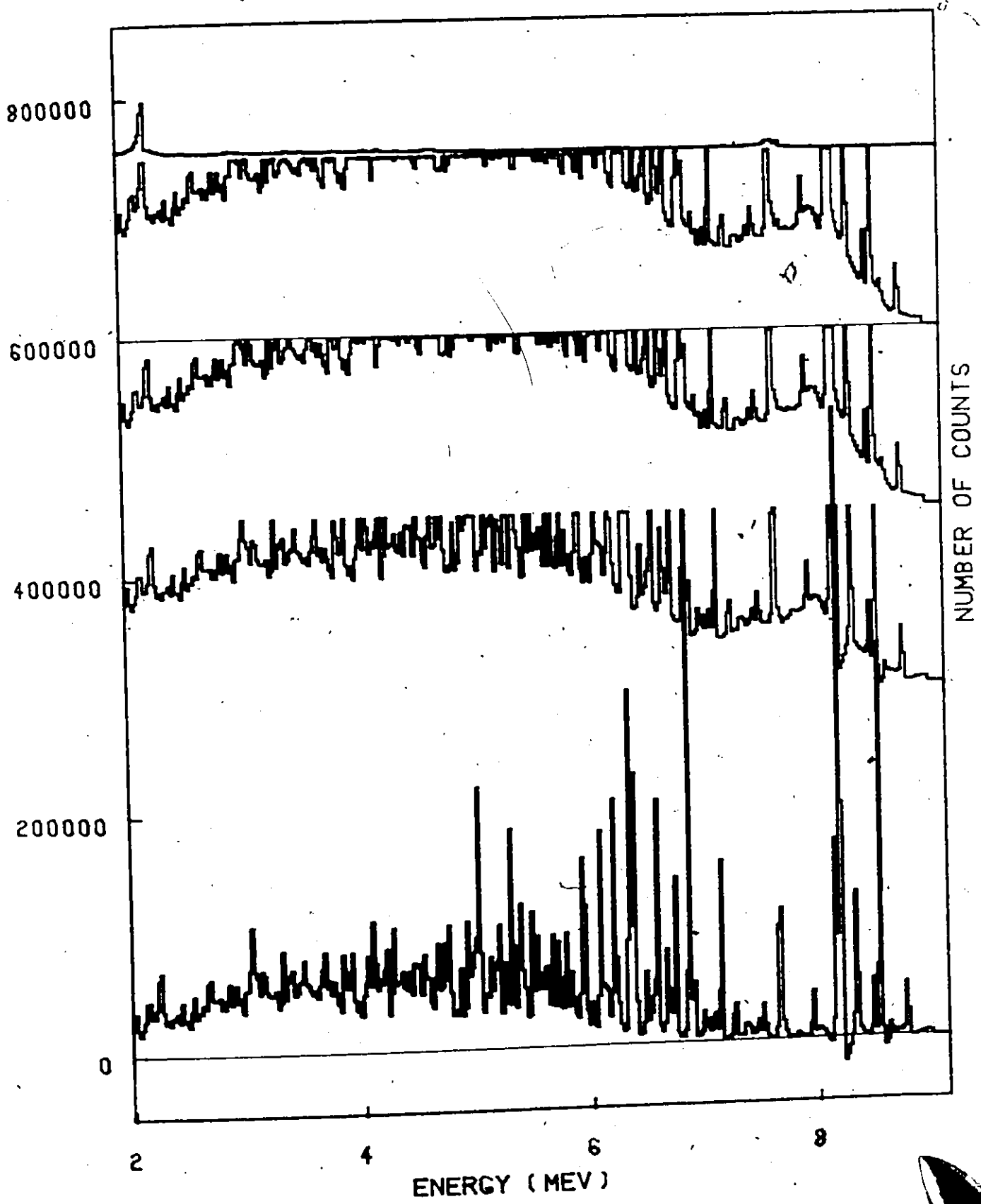

SC 46 STATISTICAL DATA FIG A4·6·3

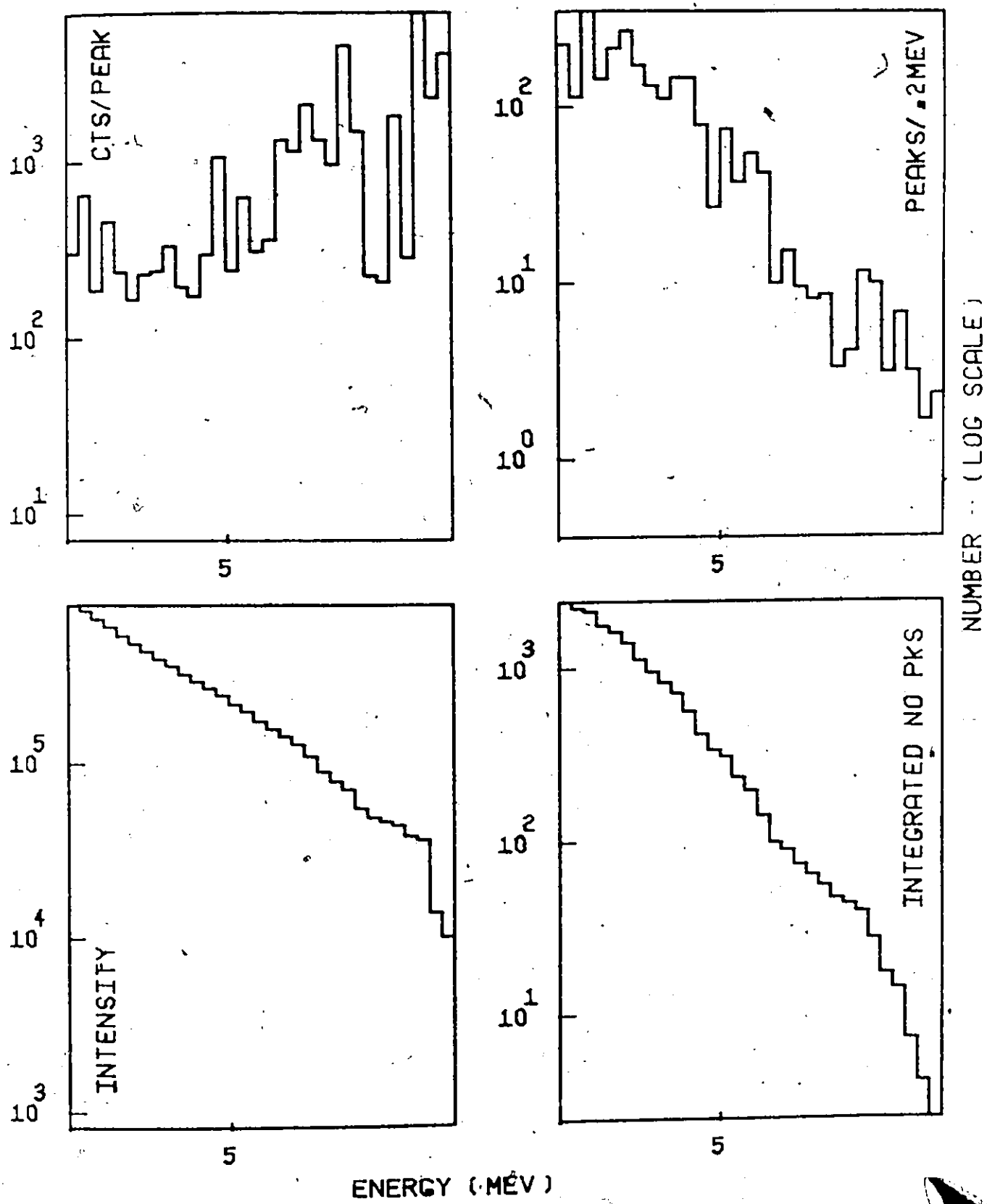

***** MN 56 ***** TABLE A4.7

	ENERGY (KEV)	INTENSITY (PH/CAP)		ENERGY (KEV)	INTENSITY (PH/CAP)		ENERGY (KEV)	INTENSITY (PH/CAP)		ENERGY (KEV)	INTENSITY (PH/CAP)
1	7270.3	3.35E-02	41	5245.3	1.69E-03	81	4415.4	1.96E-03	121	3873.0	1.33E-03
2	7243.8	1.23E-01	42	5199.1	8.46E-03	82	4398.7	1.40E-03	122	3857.8	5.98E-03
3	7159.7	5.96E-02	43	5181.6	3.79E-02	83	4381.0	5.37E-03	123	3846.0	1.34E-03
4	7057.8	1.10E-01	44	5129.5	1.51E-03	84	4364.5	1.23E-04	124	3837.0	8.09E-04
5	6928.7	2.34E-02	45	5111.7	1.91E-02	85	4348.0	3.09E-03	125	3820.4	5.79E-03
6	6783.3	3.42E-02	46	5102.0	3.53E-03	86	4330.4	5.88E-04	126	3815.0	1.07E-02
7	6624.9	1.19E-03	47	5068.3	2.73E-02	87	4324.1	1.43E-03	127	3798.7	4.45E-04
8	6619.6	1.52E-03	48	5035.5	1.02E-02	88	4319.5	1.09E-03	128	3783.6	3.24E-03
9	6553.8	1.91E-03	49	5015.0	6.12E-02	89	4298.5	3.39E-04	129	3772.8	1.23E-03
10	6429.1	7.29E-03	50	4982.9	5.14E-04	90	4268.5	6.92E-03	130	3752.3	4.29E-03
11	6318.1	1.28E-04	51	4969.8	3.61E-03	91	4251.7	2.06E-03	131	3738.4	2.28E-04
12	6103.9	2.00E-02	52	4949.4	2.02E-02	92	4230.6	3.63E-03	132	3723.2	3.41E-04
13	6030.6	5.20E-03	53	4935.2	3.64E-03	93	4223.5	7.27E-03	133	3716.2	3.42E-04
14	6019.2	6.72E-04	54	4907.9	6.80E-03	94	4199.2	1.66E-03	134	3697.0	1.15E-03
15	5976.6	1.84E-03	55	4875.2	7.18E-03	95	4191.6	3.50E-04	135	3685.9	1.36E-02
16	5920.5	8.22E-03	56	4854.1	7.03E-04	96	4187.2	5.24E-04	136	3669.8	1.52E-03
17	5905.6	1.03E-03	57	4841.0	6.34E-03	97	4173.9	3.52E-04	137	3658.7	3.50E-04
18	5846.0	2.95E-04	58	4829.7	1.25E-02	98	4131.9	6.48E-04	138	3642.3	6.13E-03
19	5794.8	1.46E-04	59	4816.7	7.10E-04	99	4127.7	4.90E-04	139	3626.8	6.76E-03
20	5760.9	1.74E-02	60	4798.1	7.13E-04	100	4110.4	3.51E-03	140	3605.6	5.97E-04
21	5733.9	1.46E-04	61	4793.9	9.51E-04	101	4103.7	3.85E-03	141	3601.5	9.61E-04
22	5714.5	1.33E-03	62	4768.8	4.77E-04	102	4088.5	3.31E-04	142	3588.5	7.25E-04
23	5707.0	4.42E-04	63	4764.1	2.39E-04	103	4084.5	4.12E-04	143	3580.6	4.35E-03
24	5678.6	2.96E-04	64	4751.7	2.39E-04	104	4076.0	1.66E-04	144	3573.9	2.42E-03
25	5637.5	2.96E-04	65	4739.4	7.24E-04	105	4068.3	1.66E-04	145	3559.4	9.78E-04
26	5625.3	2.22E-04	66	4725.4	2.76E-02	106	4051.5	1.33E-03	146	3553.9	2.69E-03
27	5601.8	4.44E-04	67	4709.0	7.30E-04	107	4048.1	9.19E-04	147	3549.2	2.70E-03
28	5563.9	2.75E-04	68	4690.0	1.00E-02	108	4035.8	1.59E-03	148	3527.6	1.98E-03
29	5543.1	1.85E-03	69	4670.6	7.37E-04	109	4029.8	1.68E-03	149	3524.7	1.48E-03
30	5527.4	6.72E-02	70	4643.9	8.40E-03	110	4024.5	1.01E-03	150	3498.9	5.38E-03
31	5493.5	2.76E-04	71	4636.7	2.23E-03	111	4007.2	5.10E-04	151	3484.4	1.13E-03
32	5485.5	5.52E-04	72	4618.5	9.96E-04	112	4001.1	5.94E-04	152	3479.3	1.01E-03
33	5464.7	2.76E-04	73	4603.3	2.49E-04	113	3979.4	3.76E-03	153	3458.9	4.03E-04
34	5437.0	1.27E-02	74	4588.7	4.26E-03	114	3971.6	2.31E-03	154	3451.6	4.04E-04
35	5432.9	1.33E-02	75	4567.2	1.94E-02	115	3961.7	6.02E-04	155	3437.4	8.19E-04
36	5404.5	3.89E-03	76	4550.6	6.84E-03	116	3955.0	6.03E-04	156	3430.8	1.64E-03
37	5313.6	8.39E-04	77	4473.1	9.65E-04	117	3927.1	4.35E-03	157	3418.1	1.92E-03
38	5298.3	5.60E-04	78	4469.8	5.65E-04	118	3901.7	2.62E-04	158	3409.1	3.17E-02
39	5290.3	5.60E-04	79	4446.0	7.70E-03	119	3897.0	9.69E-04	159	3399.6	3.87E-03
40	5254.3	1.24E-02	80	4423.7	5.72E-04	120	3883.7	1.50E-03	160	3387.8	1.95E-03

***** MN 56 ***** TABLE A4.7

	ENERGY (KEV)	INTENSITY (PH/CAP)		ENERGY (KEV)	INTENSITY (PH/CAP)		ENERGY (KEV)	INTENSITY (PH/CAP)
161	3363.5	8.47E-04	201	2937.6	6.52E-04	241	2437.8	4.44E-03
162	3345.9	5.39E-03	202	2926.9	4.15E-03	242	2428.6	1.83E-03
163	3337.4	1.14E-03	203	2922.8	3.39E-03	243	2405.7	2.90E-03
164	3316.9	8.65E-04	204	2898.7	1.81E-03	244	2396.4	2.26E-03
165	3301.4	1.74E-03	205	2893.7	1.03E-03	245	2372.1	2.32E-03
166	3293.8	1.16E-03	206	2885.6	4.89E-04	246	2368.4	3.87E-03
167	3298.2	1.17E-03	207	2872.4	1.72E-03	247	2342.6	3.18E-03
168	3271.8	3.23E-03	208	2864.4	4.13E-03	248	2338.4	5.59E-03
169	3266.8	5.01E-03	209	2857.9	2.54E-03	249	2331.2	1.53E-02
170	3259.9	1.77E-03	210	2842.1	8.10E-04	250	2320.2	2.44E-03
171	3247.3	8.95E-04	211	2832.9	3.91E-03	251	2310.0	1.64E-03
172	3242.5	8.97E-04	212	2817.4	1.21E-03	252	2294.8	9.19E-03
173	3236.8	4.47E-04	213	2806.6	1.21E-03	253	2286.2	1.68E-03
174	3231.6	3.03E-04	214	2802.2	1.02E-03	254	2261.0	2.60E-03
175	3222.4	1.52E-04	215	2790.0	6.51E-04	255	2254.8	1.74E-03
176	3213.7	6.05E-04	216	2779.5	1.76E-03	256	2241.8	1.77E-03
177	3203.9	3.34E-03	217	2769.2	9.16E-04	257	2211.3	1.29E-02
178	3195.6	1.07E-03	218	2764.1	1.12E-03	258	2205.3	7.40E-03
179	3191.5	7.66E-04	219	2740.3	7.15E-04	259	2191.9	2.82E-03
180	3172.5	1.70E-03	220	2729.4	1.03E-03	260	2183.1	3.81E-03
181	3159.6	1.09E-03	221	2721.6	8.78E-04	261	2176.6	8.63E-03
182	3144.4	2.51E-03	222	2708.4	3.16E-03	262	2159.1	1.96E-03
183	3135.6	2.52E-03	223	2696.4	3.10E-03	263	2147.3	3.99E-03
184	3124.7	1.90E-03	224	2677.7	7.86E-03	264	2138.5	3.02E-03
185	3116.1	2.23E-03	225	2658.5	7.38E-03	265	2122.5	4.12E-03
186	3098.1	3.24E-04	226	2644.1	8.48E-04	266	2090.4	7.54E-03
187	3089.3	3.26E-04	227	2622.7	5.78E-03	267	2063.2	1.12E-02
188	3076.6	3.28E-04	228	2610.6	4.27E-03	268	2044.7	1.02E-01
189	3072.7	3.29E-04	229	2598.6	3.69E-03	269	2023.9	8.79E-03
190	3061.9	1.54E-03	230	2594.5	4.93E-03	270	2016.5	2.67E-02
191	3058.2	1.26E-03	231	2582.0	3.03E-03			
192	3047.5	3.70E-03	232	2561.4	1.90E-03			
193	3034.1	1.39E-03	233	2557.9	1.82E-03			
194	3021.7	2.92E-03	234	2545.7	5.46E-04			
195	3003.4	6.36E-03	235	2534.6	2.40E-03			
196	2991.4	1.14E-03	236	2515.0	3.29E-03			
197	2976.4	2.53E-03	237	2508.5	3.40E-03			
198	2970.2	5.08E-03	238	2471.3	3.33E-03			
199	2960.7	4.24E-03	239	2451.9	2.19E-03			
200	2953.8	2.80E-03	240	2443.1	2.10E-03			

MN 56 GAMMA RAY PAIR SPECTRUM FIG A4·7·1

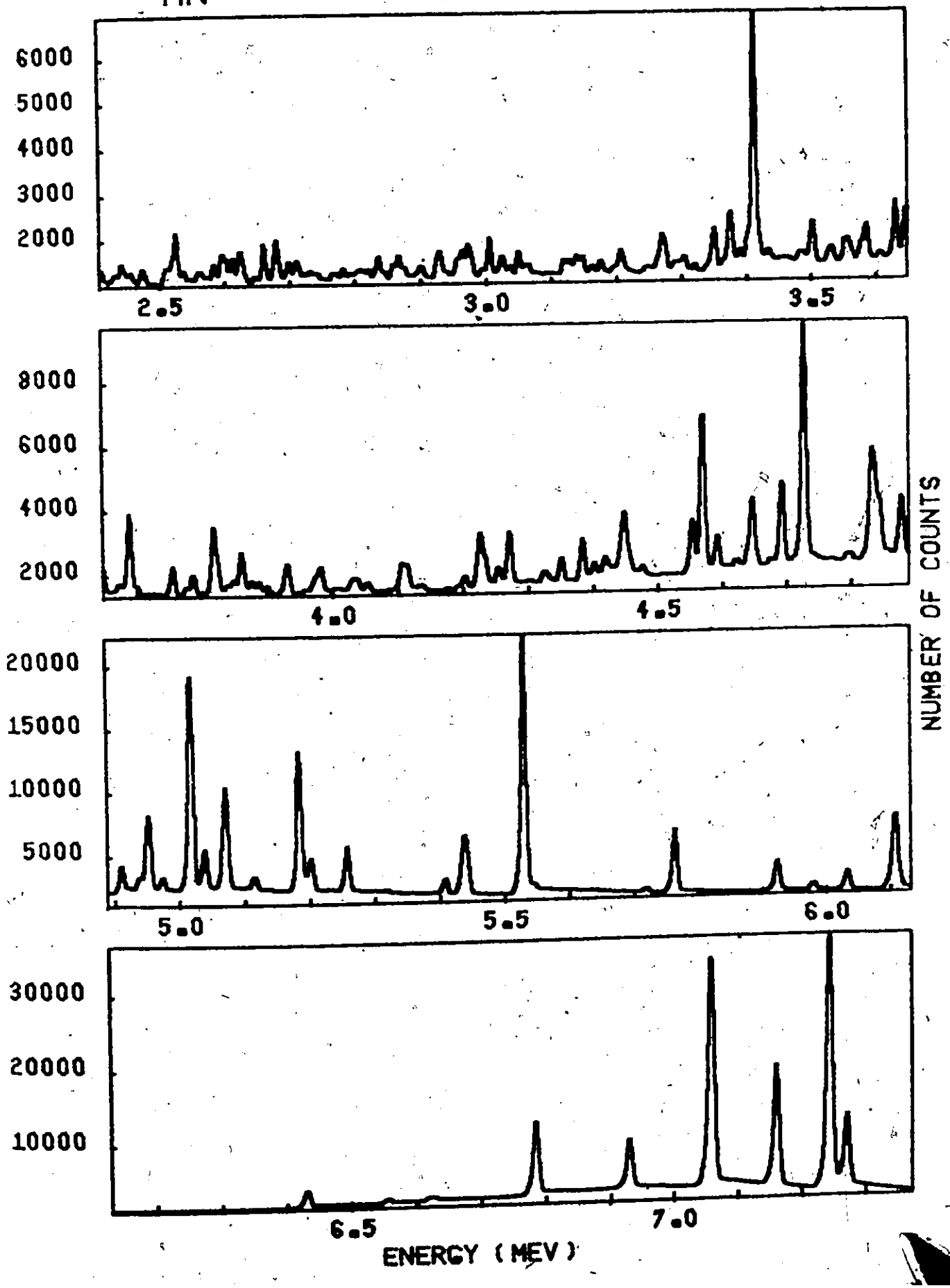

MN 56 RESPONSE STRIPPING FIG A4·7·2

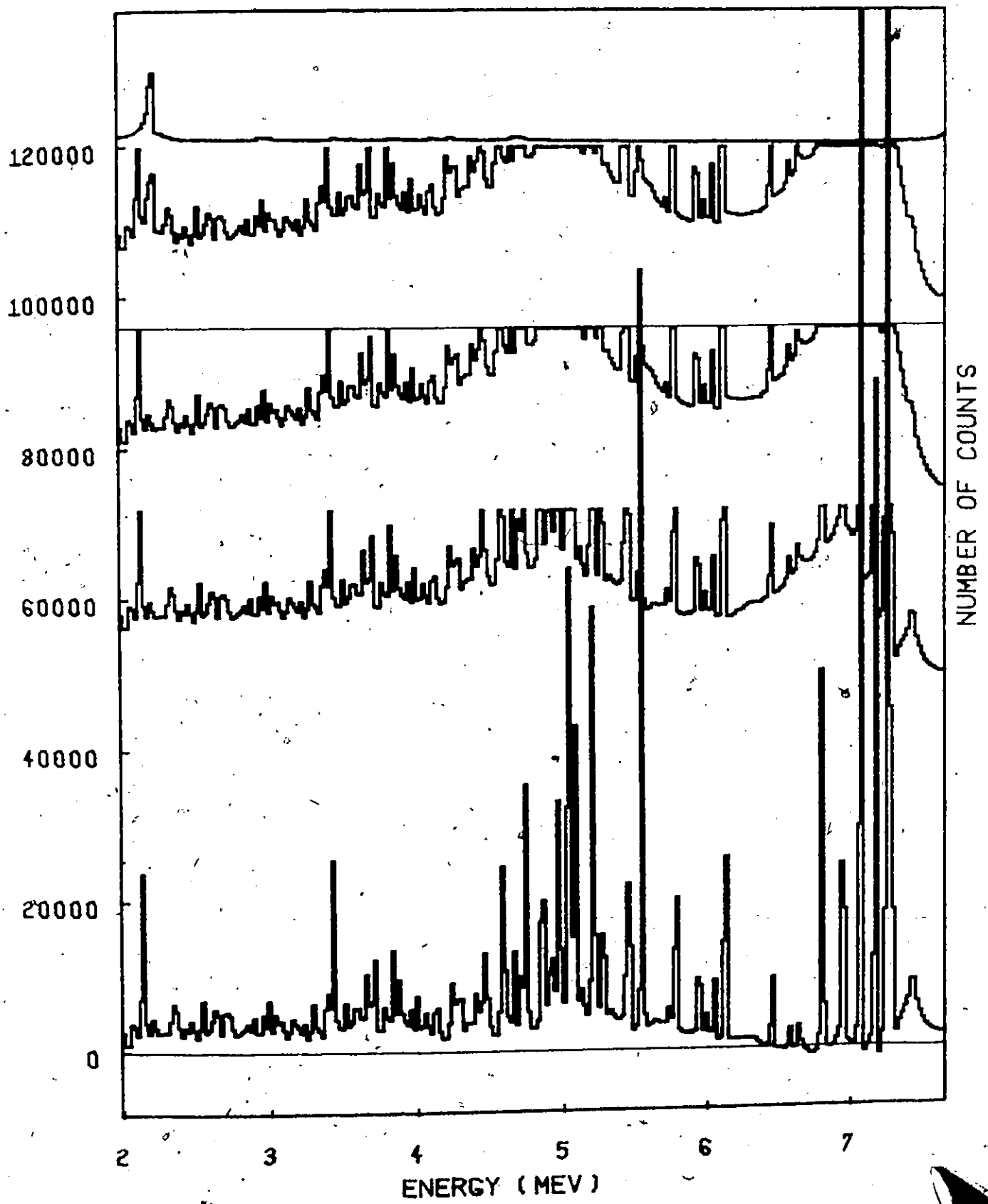

MN 56 STATISTICAL DATA FIG A4·7·3

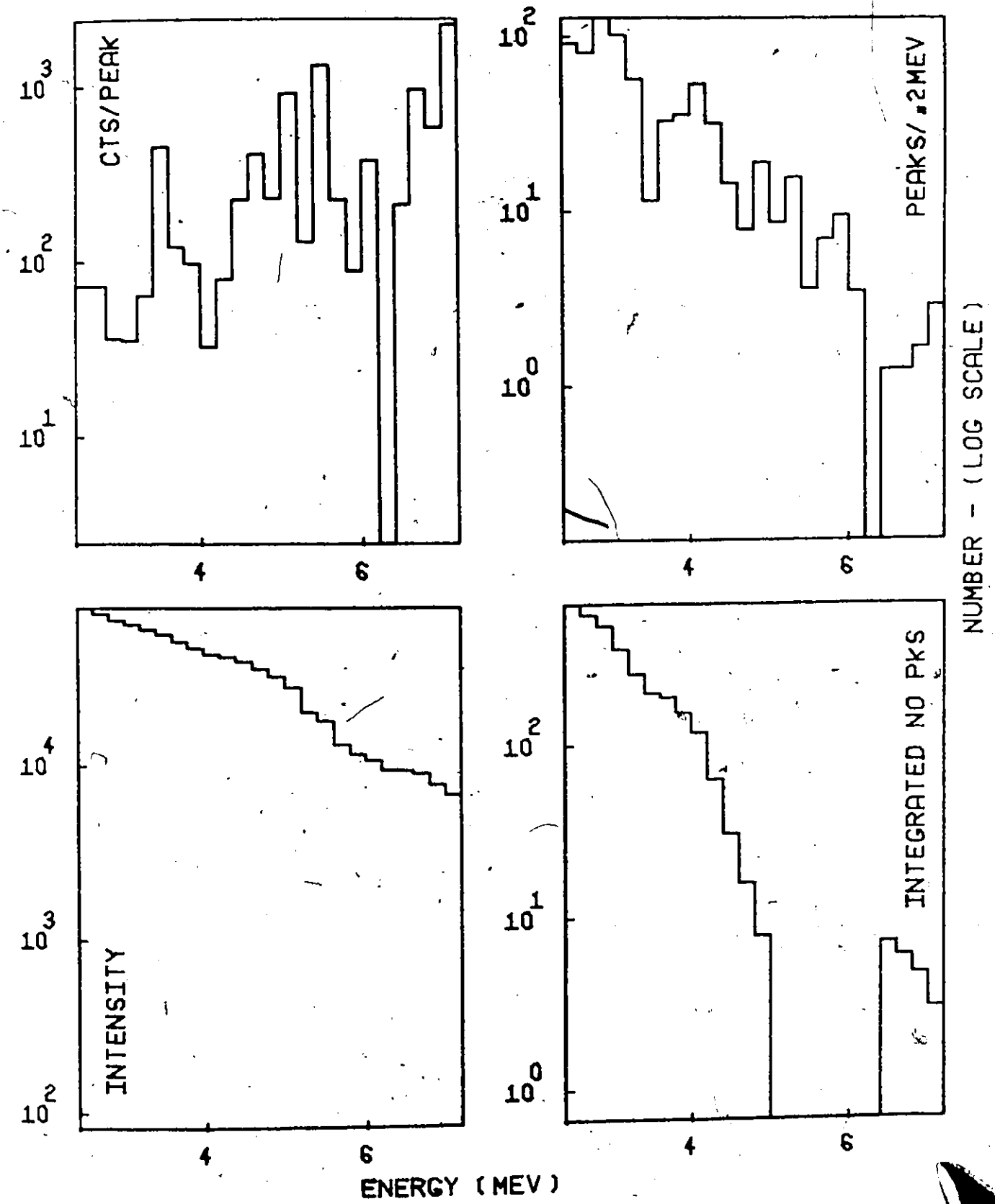

***** CO 60 ***** TABLE A4.8

	ENERGY (KEV)	INTENSITY (PH/CAP)		ENERGY (KEV)	INTENSITY (PH/CAP)		ENERGY (KEV)	INTENSITY (PH/CAP)		ENERGY (KEV)	INTENSITY (PH/CAP)
1	7492.0	2.27E-02	41	5144.4	5.58E-04	81	4377.5	3.45E-03	121	3744.4	1.69E-03
2	7433.1	1.70E-03	42	5128.8	4.10E-03	82	4372.9	2.57E-03	122	3732.6	2.26E-04
3	7214.3	2.93E-02	43	5095.5	1.87E-04	83	4351.6	2.78E-03	123	3726.6	4.53E-04
4	7207.0	1.39E-02	44	5071.7	2.63E-03	84	4338.3	8.24E-04	124	3703.5	2.97E-03
5	7055.5	1.33E-02	45	5041.7	1.89E-03	85	4330.1	2.73E-03	125	3694.7	2.40E-03
6	6995.0	2.16E-02	46	5004.1	6.07E-03	86	4313.6	1.28E-03	126	3685.7	3.45E-03
7	6948.3	5.31E-03	47	4964.2	1.72E-03	87	4302.2	1.67E-03	127	3678.8	3.69E-03
8	6876.4	6.42E-02	48	4946.2	5.19E-03	88	4290.0	1.03E-03	128	3666.5	2.55E-03
9	6705.3	5.83E-02	49	4923.1	7.74E-03	89	4276.6	1.87E-03	129	3651.8	9.32E-04
10	6485.8	4.78E-02	50	4907.0	1.42E-02	90	4255.1	1.17E-03	130	3640.3	4.68E-04
11	6340.3	3.95E-04	51	4894.7	5.84E-03	91	4250.5	7.81E-04	131	3629.6	3.53E-04
12	6317.4	1.97E-04	52	4886.4	6.83E-03	92	4241.8	2.61E-04	132	3621.1	2.12E-03
13	6292.6	5.37E-03	53	4871.2	1.18E-03	93	4209.6	7.98E-03	133	3613.2	3.79E-03
14	6275.5	6.26E-03	54	4837.0	1.02E-03	94	4156.5	4.15E-03	134	3604.9	4.75E-04
15	6257.7	4.47E-04	55	4827.3	2.41E-04	95	4152.4	2.90E-03	135	3594.5	5.96E-04
16	6149.1	3.56E-03	56	4817.7	1.81E-04	96	4129.8	2.29E-03	136	3588.5	1.67E-03
17	6110.3	4.45E-03	57	4800.4	5.46E-04	97	4113.9	1.35E-03	137	3577.2	1.80E-03
18	6040.2	3.99E-03	58	4783.0	1.04E-03	98	4103.5	7.97E-04	138	3563.8	1.81E-03
19	5975.7	5.32E-02	59	4774.3	1.83E-04	99	4076.9	1.45E-03	139	3546.0	2.43E-04
20	5925.4	1.40E-02	60	4759.7	1.84E-04	100	4032.4	7.10E-03	140	3534.4	3.67E-04
21	5852.1	2.37E-03	61	4732.0	2.53E-03	101	4028.0	8.42E-03	141	3528.9	4.90E-04
22	5742.5	1.66E-02	62	4720.9	1.73E-03	102	4020.1	2.62E-03	142	3511.4	7.40E-04
23	5704.2	3.80E-03	63	4707.3	3.42E-03	103	3995.1	1.57E-03	143	3505.3	9.90E-04
24	5660.4	5.71E-02	64	4667.0	2.32E-03	104	3978.5	1.75E-03	144	3493.3	1.37E-03
25	5638.9	8.09E-03	65	4647.1	2.27E-03	105	3967.7	6.51E-03	145	3481.3	1.50E-03
26	5614.7	8.58E-03	66	4624.9	3.05E-03	106	3957.8	3.35E-04	146	3467.5	2.64E-03
27	5603.1	9.53E-03	67	4607.9	7.72E-03	107	3930.8	8.54E-03	147	3455.0	2.23E-03
28	5568.3	6.37E-04	68	4591.7	1.67E-03	108	3904.6	1.45E-03	148	3449.0	1.12E-03
29	5531.2	2.13E-04	69	4573.2	5.15E-04	109	3899.4	3.08E-03	149	3431.0	3.56E-04
30	5511.1	4.12E-03	70	4566.5	4.52E-04	110	3876.7	1.72E-04	150	3418.1	4.17E-04
31	5446.5	7.13E-04	71	4547.9	3.70E-03	111	3871.6	3.45E-04	151	3403.7	9.60E-04
32	5410.3	2.86E-04	72	4529.2	1.83E-03	112	3842.5	3.58E-03	152	3392.0	4.22E-04
33	5370.4	4.02E-03	73	4511.8	1.31E-04	113	3833.8	1.05E-03	153	3381.6	6.49E-03
34	5359.3	3.66E-03	74	4497.8	3.63E-04	114	3824.7	2.46E-03	154	3365.2	1.83E-04
35	5308.8	1.01E-03	75	4484.1	9.11E-04	115	3817.1	2.82E-03	155	3350.2	7.38E-04
36	5271.1	8.83E-03	76	4470.5	1.65E-03	116	3795.6	1.21E-03	156	3336.5	2.97E-03
37	5215.0	2.58E-03	77	4445.6	6.76E-04	117	3781.4	3.32E-04	157	3321.3	7.48E-04
38	5182.5	2.22E-02	78	4427.6	4.32E-04	118	3769.5	7.79E-04	158	3301.7	1.45E-03
39	5169.1	2.60E-03	79	4416.1	9.29E-04	119	3758.9	1.23E-03	159	3285.0	3.30E-03
40	5151.8	9.29E-04	80	4397.1	2.87E-03	120	3750.4	1.31E-02	160	3249.9	1.74E-03

***** CO 60 *****

	ENERGY (KEV)	INTENSITY (PH/CAP)		ENERGY (KEV)	INTENSITY (PH/CAP)		ENERGY (KEV)	INTENSITY (PH/CAP)
161	3240.4	1.82E-03	201	2780.2	2.03E-03	241	2101.1	2.42E-03
162	3217.8	4.79E-03	202	2769.9	1.26E-03	242	2087.9	1.06E-03
163	3202.5	9.91E-04	203	2761.5	1.23E-03	243	2076.6	3.23E-03
164	3195.6	3.12E-03	204	2741.7	3.04E-03	244	2064.1	2.56E-03
165	3187.3	5.99E-04	205	2729.6	2.87E-03	245	2058.3	1.84E-03
166	3175.1	2.68E-04	206	2723.0	7.79E-04	246	2034.9	9.36E-03
167	3160.3	8.78E-04	207	2716.9	1.25E-03			
168	3154.9	8.12E-04	208	2693.8	2.43E-03			
169	3129.8	1.58E-03	209	2682.0	8.83E-04			
170	3124.5	1.93E-03	210	2662.8	1.14E-03			
171	3118.9	6.90E-04	211	2641.4	6.21E-04			
172	3107.4	5.14E-04	212	2634.7	1.25E-03			
173	3099.0	2.87E-03	213	2616.7	1.35E-03			
174	3087.0	1.17E-03	214	2609.3	4.75E-03			
175	3065.5	1.02E-03	215	2591.2	1.63E-03			
176	3050.5	1.76E-03	216	2580.8	6.94E-04			
177	3037.1	3.68E-04	217	2571.3	4.50E-03			
178	3030.5	9.39E-04	218	2559.1	2.07E-03			
179	3022.1	9.10E-04	219	2552.4	1.02E-03			
180	3009.0	1.77E-03	220	2540.9	7.61E-04			
181	2997.2	2.77E-03	221	2528.8	3.94E-03			
182	2979.6	2.45E-03	222	2519.8	6.84E-04			
183	2963.0	1.08E-03	223	2503.0	1.62E-03			
184	2956.1	2.52E-03	224	2486.3	8.92E-04			
185	2949.4	2.81E-03	225	2473.2	8.54E-04			
186	2928.4	3.70E-03	226	2455.4	2.12E-03			
187	2917.3	7.17E-04	227	2443.4	6.34E-04			
188	2901.1	1.23E-03	228	2423.7	4.97E-04			
189	2894.1	7.27E-04	229	2400.6	1.07E-03			
190	2886.7	2.74E-03	230	2384.9	9.95E-04			
191	2867.4	1.59E-03	231	2361.5	1.27E-03			
192	2861.4	1.11E-03	232	2347.4	1.29E-03			
193	2850.0	2.99E-04	233	2340.7	1.56E-03			
194	2838.0	1.58E-03	234	2321.1	2.92E-03			
195	2826.5	5.31E-04	235	2310.4	2.42E-03			
196	2822.8	6.47E-04	236	2298.5	1.36E-03			
197	2811.0	1.19E-03	237	2282.7	4.70E-03			
198	2804.0	1.73E-03	238	2265.1	5.64E-04			
199	2793.4	1.75E-03	239	2251.8	1.43E-03			
200	2787.4	1.32E-03	240	2243.0	1.45E-03			

CO 60 GAMMA RAY PAIR SPECTRUM FIG A4·8·1

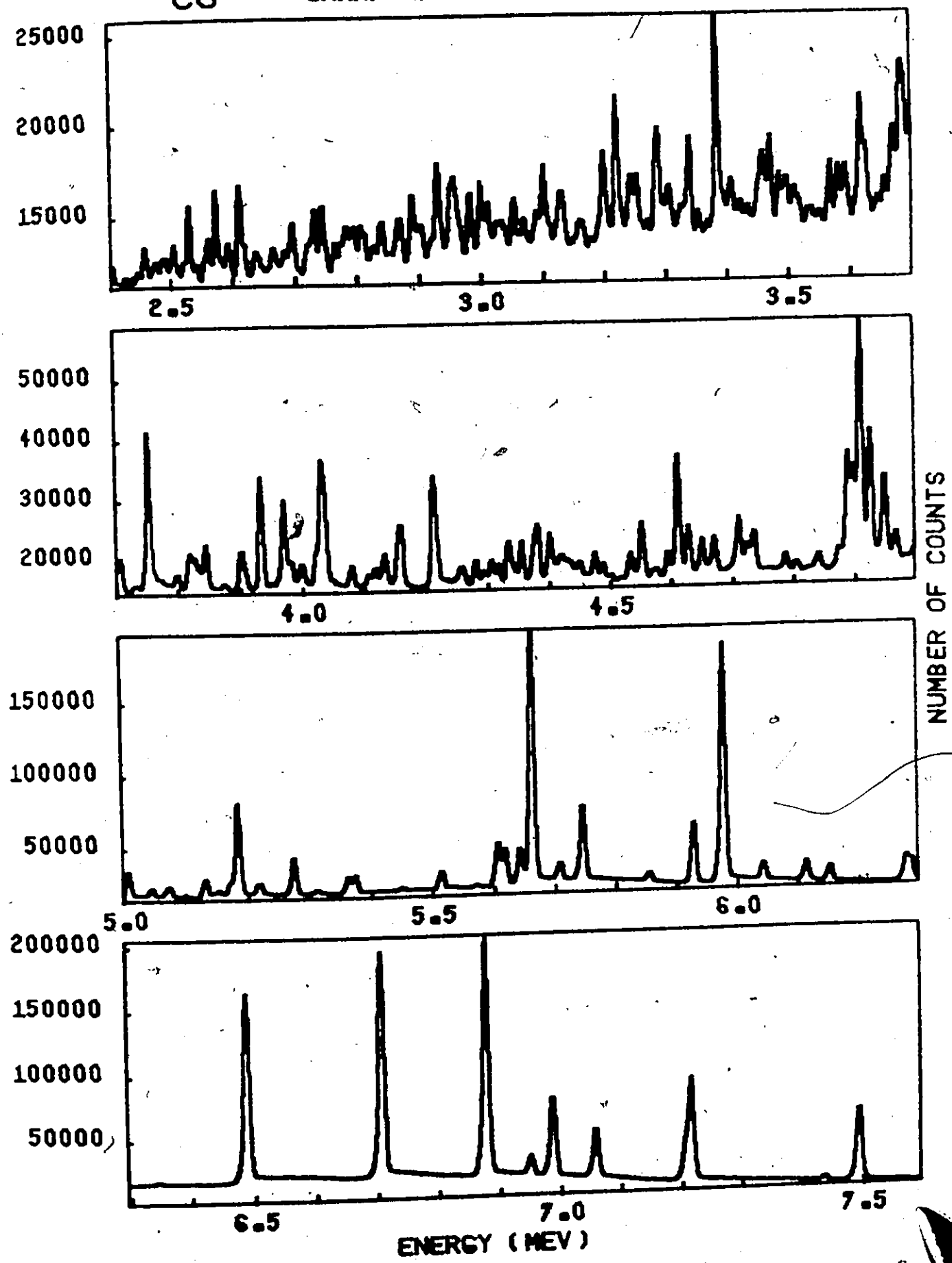

CO 60 RESPONSE STRIPPING FIG A4·8·2

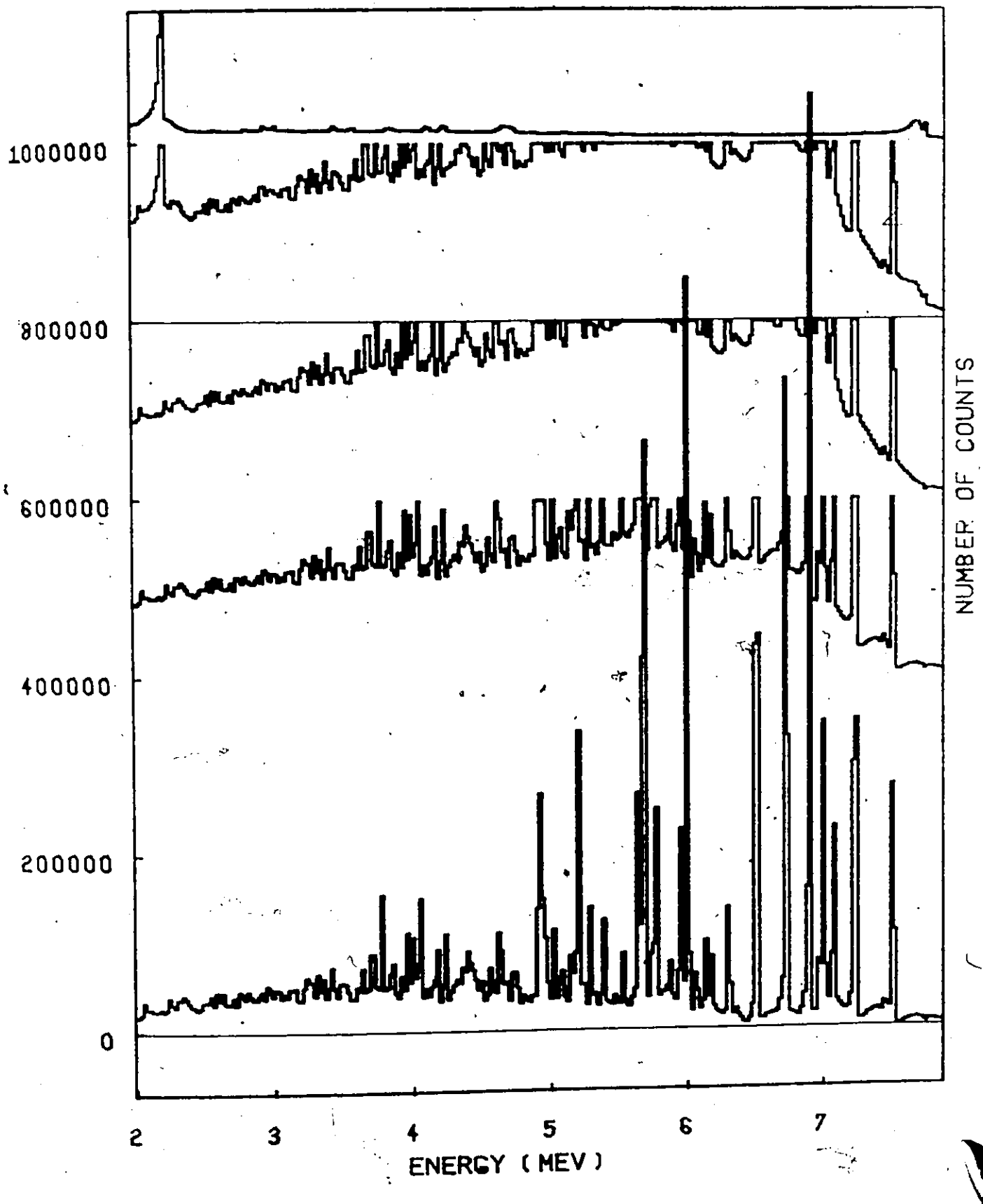

CO-60 STATISTICAL DATA FIG A4·8·3

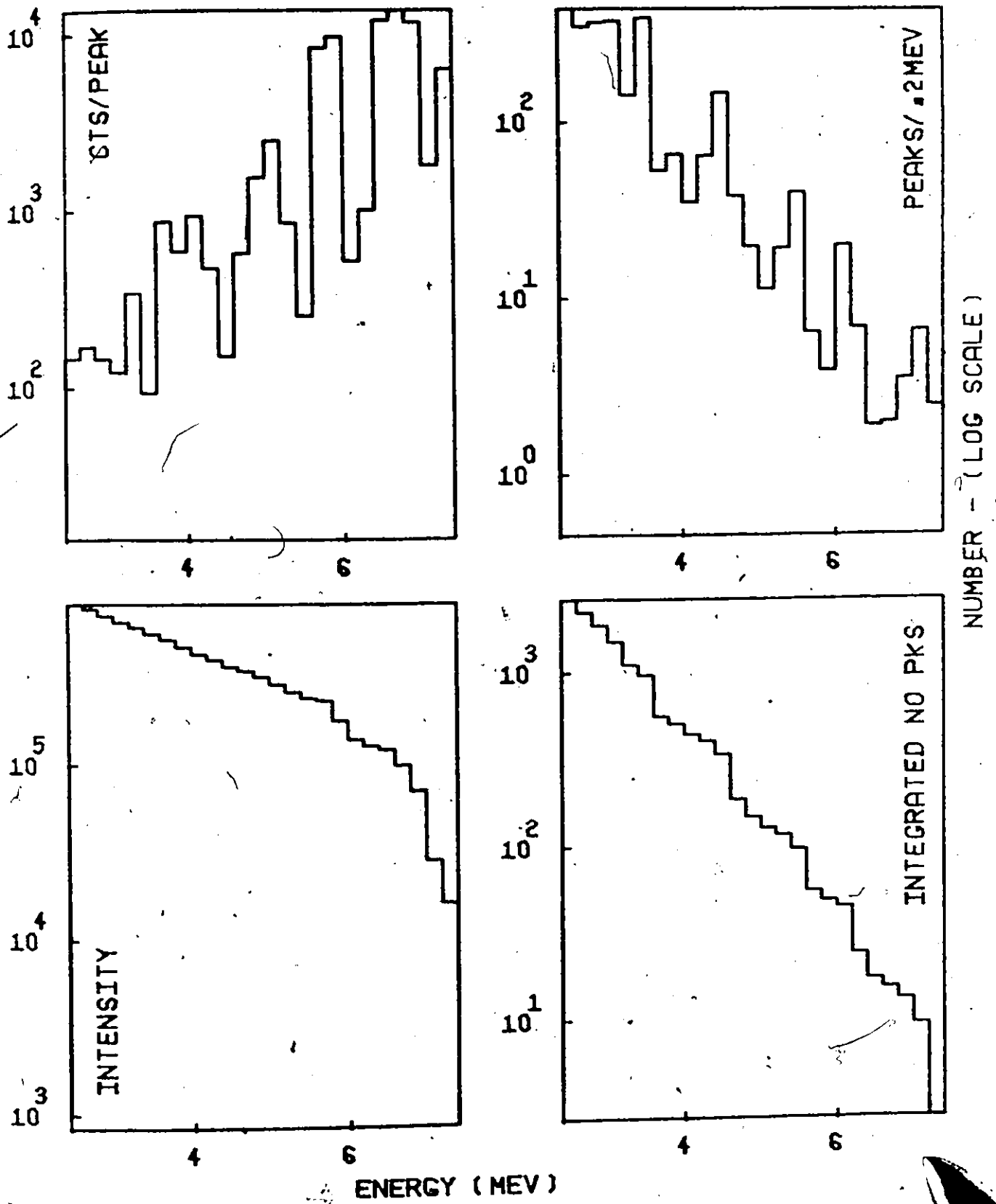

***** CU 64 ***** TABLE A4.9

	ENERGY (KEV)	INTENSITY (PH/CAP)		ENERGY (KEV)	INTENSITY (PH/CAP)		ENERGY (KEV)	INTENSITY (PH/CAP)		ENERGY (KEV)	INTENSITY (PH/CAP)
1	7915.2	3.32E-01	41	5584.1	1.08E-03	81	4658.5	8.80E-03	121	4019.8	1.41E-03
2	7755.6	1.59E-02	42	5554.6	2.84E-03	82	4645.0	4.53E-04	122	3994.9	5.10E-04
3	7636.3	1.64E-01	43	5527.2	1.66E-03	83	4638.0	2.25E-04	123	3981.0	1.61E-03
4	7570.6	1.65E-02	44	5518.0	6.62E-04	84	4617.2	4.57E-04	124	3976.7	9.55E-04
5	7412.7	7.64E-04	45	5508.4	3.33E-04	85	4610.6	1.29E-03	125	3969.8	2.93E-04
6	7305.3	9.18E-02	46	5492.3	3.34E-04	86	4603.4	6.49E-03	126	3959.1	4.44E-04
7	7251.2	4.27E-02	47	5449.5	1.62E-03	87	4581.7	5.35E-04	127	3938.3	4.48E-04
8	7175.0	2.67E-02	48	5440.8	3.35E-04	88	4572.9	1.23E-03	128	3923.4	4.18E-03
9	7036.1	3.73E-03	49	5417.5	1.97E-02	89	4563.3	3.55E-03	129	3917.5	5.01E-03
10	7020.1	8.93E-04	50	5408.6	7.02E-03	90	4528.3	6.24E-04	130	3907.6	8.26E-04
11	6986.8	3.61E-02	51	5377.4	4.90E-04	91	4518.0	1.33E-03	131	3884.1	1.81E-03
12	6672.7	2.00E-02	52	5321.6	3.29E-04	92	4503.4	6.67E-03	132	3863.8	5.34E-04
13	6615.9	1.19E-02	53	5298.8	3.30E-04	93	4498.6	6.29E-03	133	3845.2	6.45E-03
14	6593.6	6.43E-03	54	5279.8	2.48E-03	94	4475.7	5.70E-03	134	3829.9	3.08E-04
15	6474.6	1.96E-03	55	5258.2	1.11E-02	95	4449.5	3.03E-03	135	3818.9	1.09E-03
16	6415.1	1.52E-03	56	5242.4	9.96E-04	96	4442.8	6.55E-03	136	3803.4	1.09E-03
17	6392.5	1.43E-02	57	5218.7	3.33E-04	97	4422.7	6.19E-03	137	3790.1	2.36E-04
18	6362.8	1.05E-03	58	5188.0	8.34E-03	98	4405.8	5.98E-03	138	3783.5	7.87E-04
19	6319.2	3.51E-03	59	5183.7	5.84E-03	99	4391.7	2.67E-03	139	3776.6	2.75E-03
20	6307.5	2.12E-03	60	5151.3	3.02E-03	100	4382.5	1.05E-03	140	3758.2	7.94E-04
21	6230.2	1.21E-03	61	5139.2	2.68E-03	101	4354.6	4.23E-04	141	3752.7	3.33E-03
22	6164.7	1.68E-03	62	5084.8	3.38E-03	102	4320.3	1.64E-02	142	3729.6	5.62E-04
23	6133.9	2.08E-03	63	5078.4	6.78E-04	103	4312.8	7.30E-03	143	3719.5	1.05E-03
24	6109.4	1.93E-03	64	5058.3	3.13E-04	104	4298.2	2.44E-03	144	3713.6	1.21E-03
25	6101.2	7.40E-04	65	5020.8	3.60E-03	105	4286.8	4.61E-03	145	3684.3	9.78E-03
26	6061.5	6.52E-03	66	5008.7	4.71E-04	106	4277.4	8.66E-04	146	3667.8	9.83E-04
27	6054.6	1.48E-03	67	4982.9	2.37E-03	107	4271.7	4.34E-04	147	3659.0	8.93E-04
28	6009.2	1.78E-02	68	4945.0	1.91E-02	108	4259.4	7.24E-04	148	3651.8	1.10E-03
29	5996.2	2.07E-03	69	4901.8	9.67E-04	109	4247.3	7.27E-04	149	3628.3	1.87E-03
30	5894.4	4.42E-04	70	4882.4	4.86E-04	110	4234.5	8.78E-04	150	3617.1	3.76E-03
31	5864.4	1.48E-03	71	4847.5	1.14E-03	111	4217.1	7.34E-04	151	3591.0	7.74E-03
32	5852.1	4.42E-04	72	4831.0	8.22E-04	112	4204.7	3.84E-03	152	3580.8	9.91E-04
33	5769.9	5.63E-03	73	4804.0	1.32E-03	113	4192.9	4.45E-04	153	3575.8	3.54E-04
34	5728.1	5.64E-04	74	4791.3	1.16E-03	114	4168.2	8.96E-04	154	3560.9	4.96E-04
35	5714.7	5.85E-04	75	4780.8	3.32E-03	115	4165.6	8.97E-04	155	3553.5	9.32E-04
36	5707.6	3.76E-04	76	4764.5	3.35E-04	116	4144.4	2.41E-03	156	3541.5	7.18E-04
37	5696.8	1.88E-04	77	4732.5	2.02E-03	117	4133.2	2.27E-03	157	3531.6	7.92E-04
38	5634.7	4.47E-03	78	4723.9	6.73E-04	118	4090.2	1.69E-03	158	3522.0	2.10E-03
39	5613.7	5.32E-03	79	4709.3	8.14E-04	119	4050.5	2.33E-03	159	3510.8	1.60E-03
40	5599.8	1.51E-03	80	4691.2	8.18E-04	120	4033.8	1.40E-03	160	3503.0	4.37E-04

TABLE A4.9

***** CU 64 *****

	ENERGY (KEV)	INTENSITY (PH/CAP)		ENERGY (KEV)	INTENSITY (PH/CAP)		ENERGY (KEV)	INTENSITY (PH/CAP)
161	3492.5	1.62E-03	201	2875.2	5.74E-04	241	2331.1	8.26E-04
162	3473.6	2.52E-03	202	2864.0	1.15E-03	242	2292.0	2.22E-03
163	3456.4	7.45E-04	203	2856.9	1.11E-03			
164	3442.0	1.65E-03	204	2839.1	1.16E-03			
165	3434.9	1.76E-03	205	2832.4	1.55E-03			
166	3414.1	1.28E-03	206	2823.7	1.31E-03			
167	[illegible]	2.31E-03	207	2812.1	1.19E-03			
168	3367.0	8.52E-04	208	2799.0	1.20E-03			
169	3342.8	9.38E-04	209	2774.6	2.22E-03			
170	3332.1	6.34E-04	210	2770.4	1.44E-03			
171	3316.3	4.21E-03	211	2754.7	7.93E-04			
172	3306.6	9.54E-04	212	2741.8	9.84E-04			
173	3283.4	8.15E-04	213	2733.4	3.05E-03			
174	3280.2	1.71E-03	214	2724.5	2.21E-03			
175	3265.0	1.65E-03	215	2699.1	1.38E-03			
176	3257.1	3.56E-03	216	2691.8	1.29E-03			
177	3252.7	2.22E-03	217	2674.2	7.49E-04			
178	3246.5	7.97E-04	218	2657.9	1.85E-03			
179	3233.7	1.01E-03	219	2615.6	4.86E-04			
180	3216.4	8.09E-04	220	2606.5	2.07E-03			
181	3196.2	8.51E-04	221	2598.0	6.49E-04			
182	3188.0	9.29E-04	222	2583.4	7.54E-04			
183	3176.3	1.29E-03	223	2573.1	2.65E-03			
184	3153.9	3.56E-03	224	2559.3	1.24E-03			
185	3141.3	2.31E-03	225	2551.3	1.16E-03			
186	3136.5	2.21E-03	226	2535.3	1.86E-03			
187	3109.1	1.60E-03	227	2512.4	2.79E-03			
188	3080.8	1.25E-03	228	2496.4	9.29E-03			
189	3052.4	2.96E-03	229	2474.3	1.13E-03			
190	3024.0	2.11E-03	230	2466.0	1.76E-03			
191	3019.0	2.31E-03	231	2448.6	1.05E-03			
192	2995.5	2.70E-03	232	2433.8	6.36E-04			
193	2978.1	1.28E-03	233	2421.7	7.55E-04			
194	2959.4	9.69E-04	234	2414.8	9.72E-04			
195	2949.7	2.20E-03	235	2403.4	8.82E-04			
196	2944.7	1.19E-03	236	2389.8	8.94E-04			
197	2932.8	3.74E-03	237	2384.2	2.02E-03			
198	2906.5	9.22E-04	238	2366.5	1.37E-03			
199	2899.4	7.61E-04	239	2361.0	1.14E-03			
200	2883.6	8.96E-04	240	2338.2	1.88E-03			

CU 64 GAMMA RAY PAIR SPECTRUM FIG A4·9·1

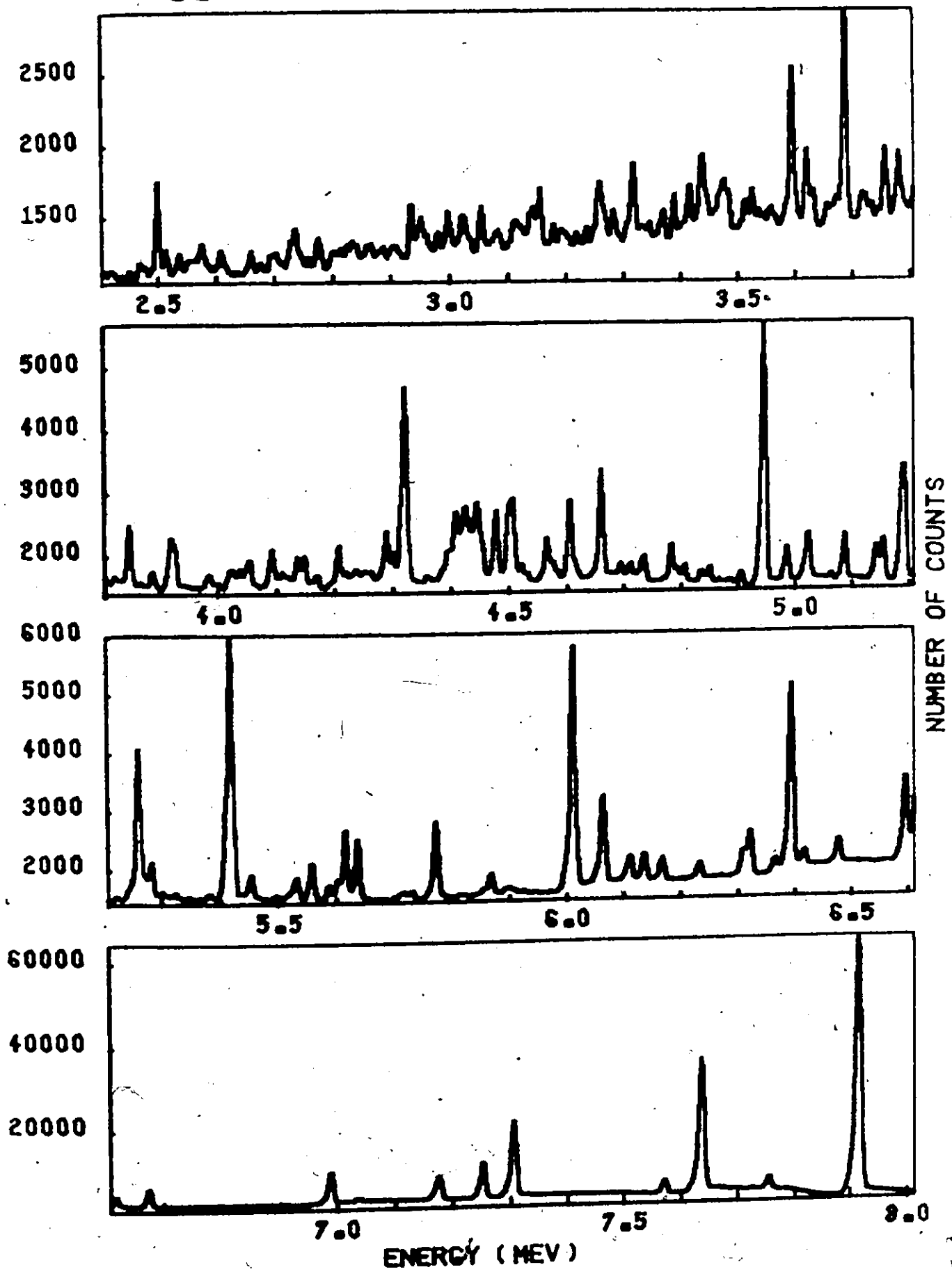

CU 64 RESPONSE STRIPPING FIG A4·9·2

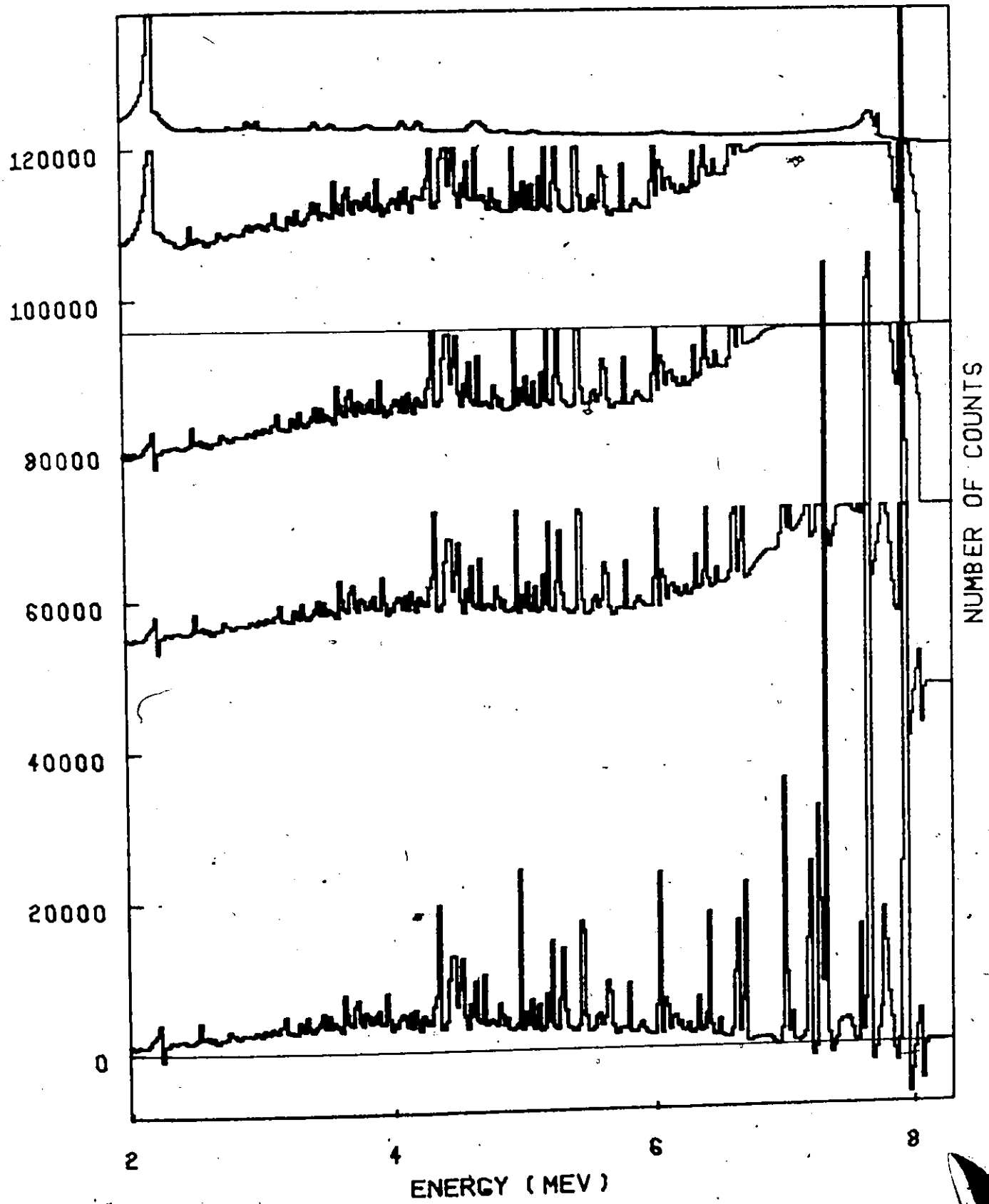

CU 64 STATISTICAL DATA FIG A4·9·3

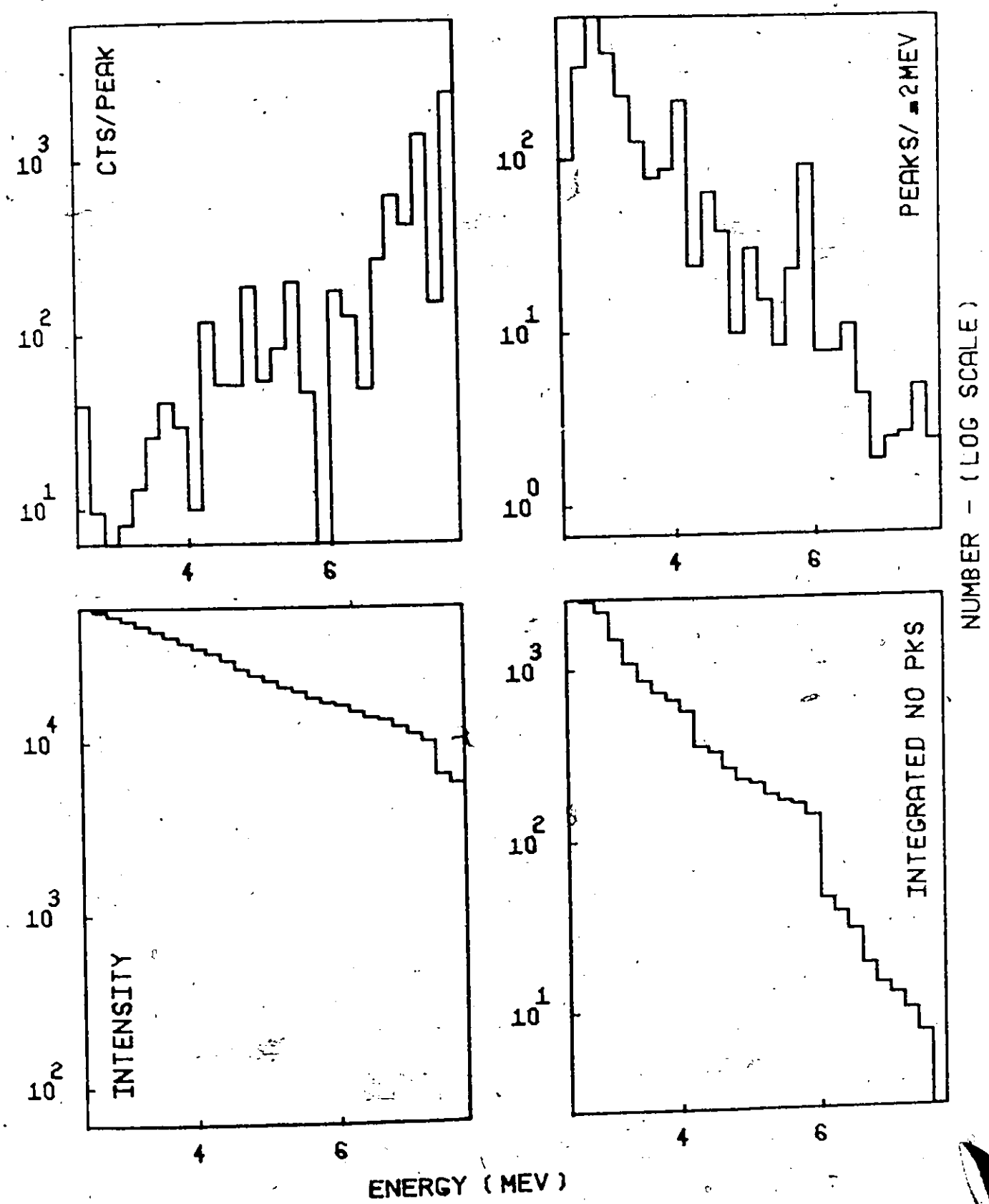

	ENERGY (KEV)	INTENSITY (PH/CAP)		ENERGY (KEV)	INTENSITY (PH/CAP)		ENERGY (KEV)	INTENSITY (PH/CAP)		ENERGY (KEV)	INTENSITY (PH/CAP)
1	7327.7	1.58E-04	41	6098.3	1.57E-03	81	5491.2	4.31E-04	121	4844.9	1.66E-03
2	7283.6	4.28E-03	42	6083.7	2.24E-04	82	5467.4	1.26E-03	122	4828.5	1.32E-03
3	7241.3	2.65E-03	43	6070.6	1.69E-04	83	5452.9	8.79E-04	123	4812.2	5.29E-04
4	7208.2	6.98E-04	44	6059.2	3.42E-03	84	5442.7	1.08E-03	124	4798.4	2.66E-04
5	7162.8	7.31E-04	45	6026.9	2.95E-03	85	5416.8	3.96E-03	125	4783.3	4.76E-03
6	7124.0	1.93E-04	46	6014.0	9.26E-04	86	5397.7	9.16E-04	126	4762.8	1.04E-03
7	7063.5	6.13E-03	47	6004.7	5.05E-04	87	5374.8	3.13E-03	127	4752.2	3.46E-04
8	7020.2	1.60E-02	48	5985.5	1.46E-03	88	5363.9	1.05E-03	128	4733.7	1.67E-03
9	6976.2	1.89E-03	49	5976.8	1.07E-03	89	5345.6	4.09E-04	129	4723.4	4.65E-04
10	6926.2	7.31E-03	50	5972.2	1.04E-03	90	5325.4	2.73E-04	130	4693.1	1.27E-03
11	6881.8	7.46E-04	51	5942.5	4.21E-04	91	5302.5	1.68E-03	131	4660.4	1.02E-03
12	6857.9	5.57E-04	52	5934.7	3.64E-04	92	5294.6	9.59E-04	132	4648.8	1.73E-03
13	6810.5	2.14E-02	53	5926.9	3.92E-04	93	5284.8	7.19E-04	133	4617.7	1.08E-03
14	6783.4	1.78E-03	54	5905.8	2.52E-04	94	5269.8	2.75E-04	134	4596.5	3.61E-04
15	6718.3	3.20E-04	55	5883.6	1.99E-03	95	5246.2	3.10E-04	135	4587.3	4.34E-04
16	6691.2	9.59E-04	56	5869.8	3.00E-03	96	5234.3	3.45E-04	136	4567.3	1.14E-03
17	6660.1	7.97E-04	57	5855.4	1.07E-03	97	5205.5	7.61E-04	137	4543.5	9.03E-04
18	6585.3	2.85E-03	58	5850.6	5.88E-04	98	5196.8	4.50E-04	138	4529.6	5.64E-04
19	6541.3	1.89E-03	59	5834.1	6.16E-04	99	5178.8	7.63E-04	139	4512.8	1.06E-03
20	6533.5	1.26E-03	60	5815.9	7.00E-04	100	5156.6	1.91E-03	140	4501.6	2.62E-03
21	6465.0	1.13E-03	61	5805.2	3.36E-04	101	5149.9	1.88E-03	141	4483.8	8.44E-04
22	6419.3	2.56E-03	62	5785.7	2.39E-03	102	5132.4	2.44E-04	142	4466.1	7.23E-04
23	6403.6	3.18E-03	63	5777.6	1.87E-03	103	5119.4	9.90E-04	143	4459.7	5.75E-04
24	6392.2	4.43E-03	64	5757.2	1.90E-03	104	5104.9	3.32E-04	144	4433.9	8.97E-04
25	6369.6	1.31E-03	65	5723.7	3.61E-04	105	5094.1	7.48E-04	145	4426.7	2.18E-03
26	6359.3	8.71E-04	66	5694.7	2.43E-03	106	5081.8	3.95E-03	146	4422.7	7.65E-04
27	6343.1	1.56E-03	67	5689.2	3.05E-03	107	5067.6	1.75E-03	147	4413.7	1.13E-03
28	6314.8	1.55E-03	68	5675.8	3.87E-03	108	5036.8	4.19E-04	148	4403.5	9.73E-04
29	6304.7	3.66E-03	69	5663.6	2.73E-03	109	5023.2	1.01E-03	149	4390.9	6.81E-04
30	6295.1	7.51E-03	70	5653.4	8.21E-04	110	5013.1	7.57E-04	150	4372.2	8.68E-04
31	6265.5	3.10E-04	71	5646.2	4.60E-04	111	4996.1	2.49E-03	151	4367.6	9.60E-04
32	6230.1	1.67E-03	72	5627.9	8.55E-04	112	4991.5	1.90E-03	152	4346.6	1.75E-03
33	6223.5	1.79E-03	73	5614.5	7.90E-04	113	4979.8	1.02E-03	153	4327.6	1.11E-03
34	6202.3	1.85E-03	74	5580.0	2.37E-03	114	4959.7	2.64E-03	154	4318.4	9.75E-04
35	6198.4	2.04E-03	75	5568.1	1.39E-03	115	4945.1	4.91E-03	155	4311.4	6.51E-04
36	6178.8	9.25E-04	76	5558.1	5.28E-04	116	4933.1	1.07E-03	156	4305.2	5.36E-04
37	6171.5	4.32E-04	77	5542.3	9.58E-04	117	4916.3	1.16E-03	157	4285.5	5.16E-04
38	6142.5	1.68E-03	78	5529.5	4.30E-04	118	4893.0	6.92E-04	158	4271.9	9.88E-04
39	6127.9	2.25E-04	79	5509.0	8.60E-04	119	4888.2	6.93E-04	159	4259.2	6.38E-04
40	6117.5	6.18E-04	80	5498.0	7.28E-04	120	4878.2	8.68E-04	160	4247.6	1.14E-03

***** AS 76 ***** TABLE A4.10

	ENERGY (KEV)	INTENSITY (PH/CAP)
161	4236.1	5.47E-04
162	4201.9	3.85E-04
163	4173.9	1.07E-03
164	4158.8	1.54E-03
165	4152.9	8.55E-04
166	4135.1	4.42E-04
167	4120.1	2.97E-04
168	4092.8	6.03E-04
169	4084.0	8.11E-04
170	4071.7	6.68E-04
171	4037.6	3.93E-04
172	4015.9	5.33E-04
173	4002.5	2.36E-04
174	3979.1	2.38E-04
175	3963.4	6.68E-04
176	3934.6	9.68E-04
177	3916.2	8.32E-04
178	3901.0	1.13E-03
179	3885.5	6.74E-04

AS 76 GAMMA RAY PAIR SPECTRUM FIG A4·10·1

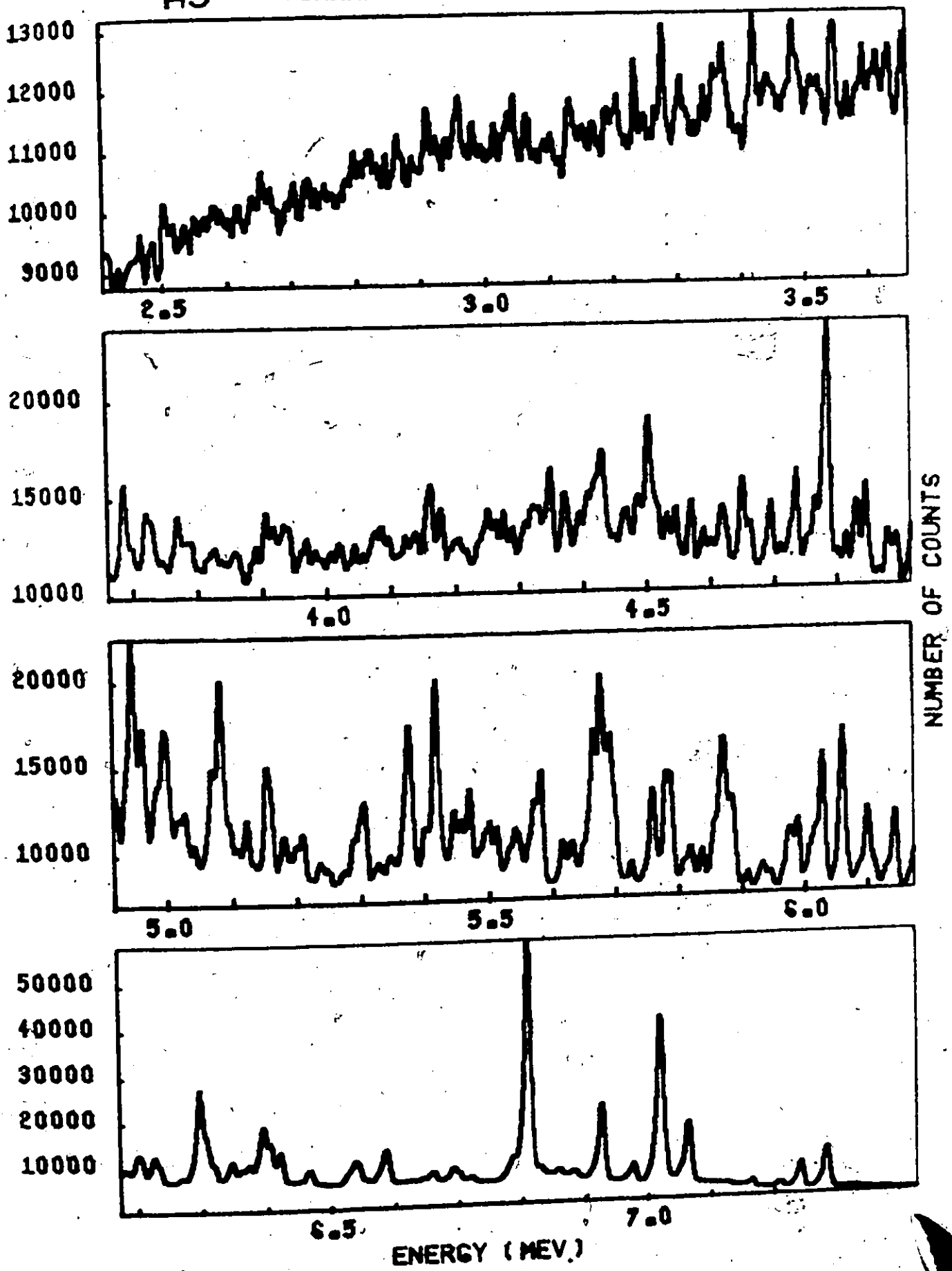

AS 76 RESPONSE STRIPPING FIG A4·10·2

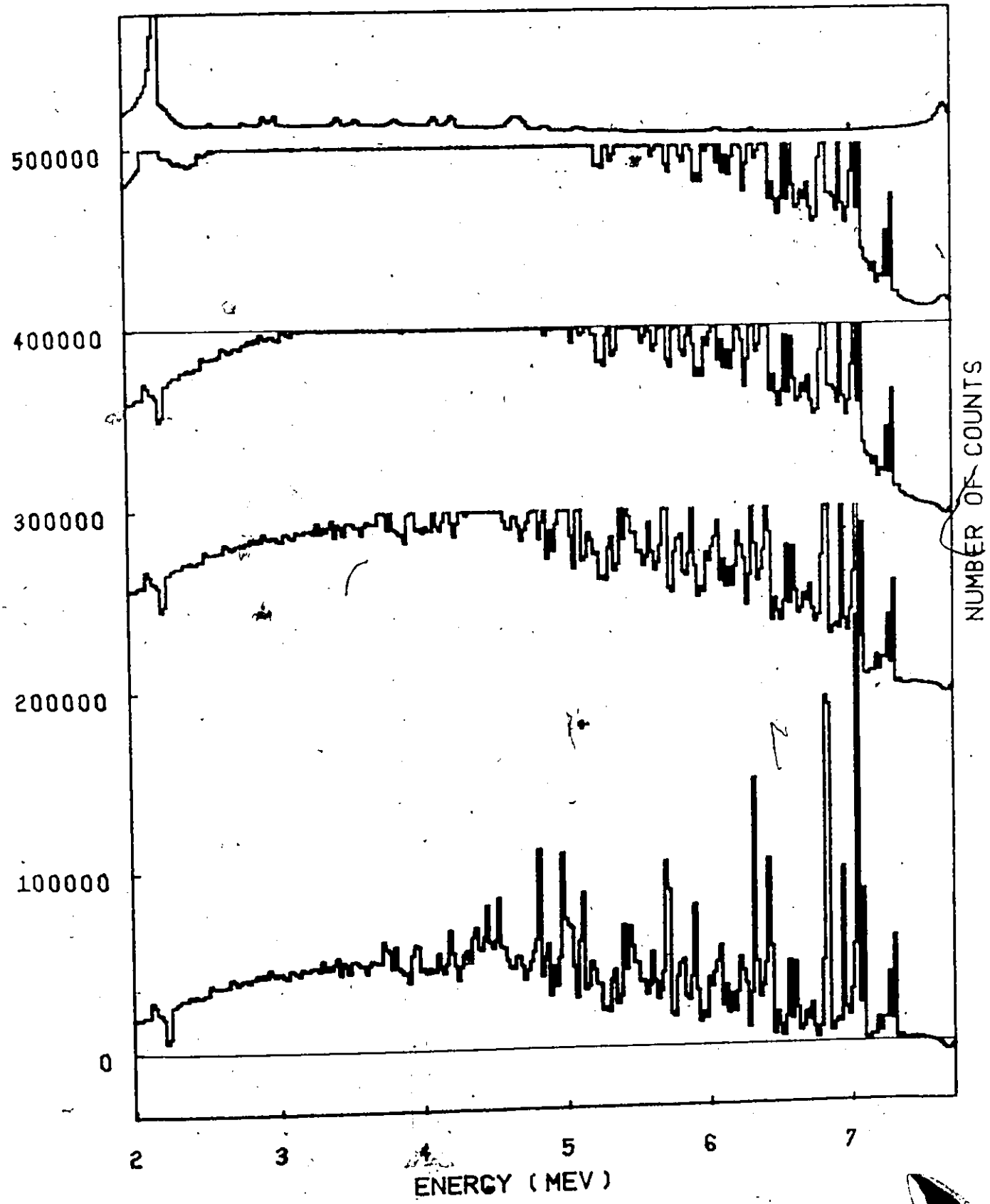

AS 76 STATISTICAL DATA FIG A4·10·3

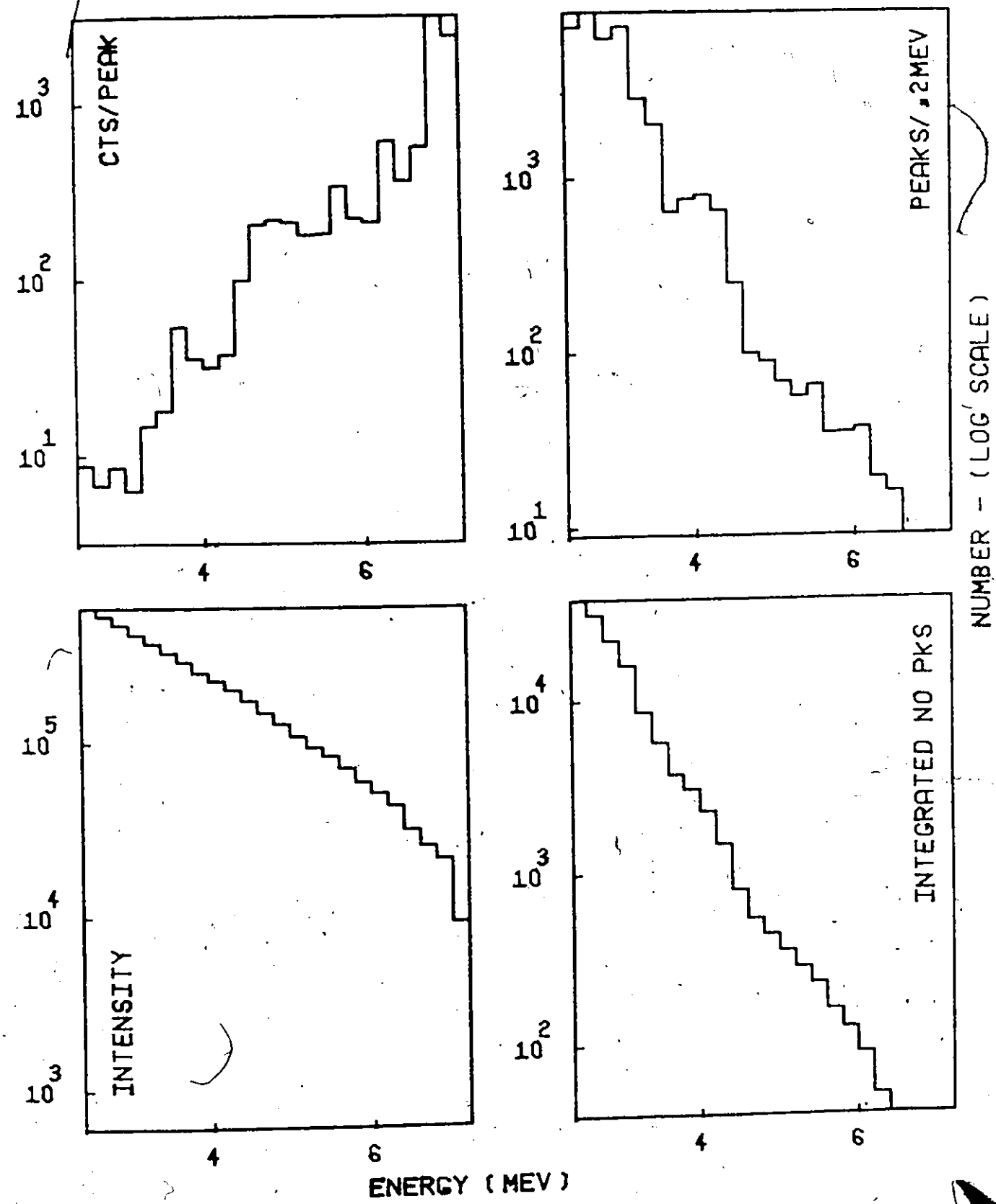

***** PH 104 ***** TABLE A4.11

	ENERGY (KEV)	INTENSITY (PH/CAP)		ENERGY (KEV)	INTENSITY (PH/CAP)		ENERGY (KEV)	INTENSITY (PH/CAP)		ENERGY (KEV)	INTENSITY (PH/CAP)
1	6998.3	6.19E-04	41	5766.9	1.31E-04	81	5126.4	1.59E-04	121	4543.5	1.46E-03
2	6946.9	1.02E-04	42	5759.3	4.38E-04	82	5108.5	1.07E-03	122	4521.1	2.85E-04
3	6900.1	2.12E-05	43	5740.9	1.77E-04	83	5096.0	6.40E-04	123	4515.8	6.73E-04
4	6815.8	6.31E-05	44	5711.3	6.33E-04	84	5082.8	2.14E-04	124	4508.2	1.35E-03
5	6784.9	1.76E-03	45	5695.7	5.07E-04	85	5072.9	4.28E-04	125	4484.6	1.83E-03
6	6730.5	2.87E-05	46	5674.2	8.88E-04	86	5062.0	3.22E-04	126	4470.5	5.99E-04
7	6707.9	1.43E-05	47	5661.2	1.52E-04	87	5051.9	2.69E-04	127	4462.9	1.66E-04
8	6626.4	4.25E-05	48	5637.5	1.78E-04	88	5022.4	1.07E-03	128	4449.5	1.52E-03
9	6613.8	2.55E-04	49	5616.8	1.37E-03	89	5006.2	1.13E-03	129	4430.1	2.93E-04
10	6516.9	4.21E-05	50	5605.0	9.41E-04	90	4973.4	7.51E-04	130	4423.7	7.12E-04
11	6483.3	8.40E-05	51	5589.5	4.33E-04	91	4968.2	4.55E-04	131	4417.9	4.83E-04
12	6476.1	8.39E-05	52	5548.2	1.33E-03	92	4959.1	3.15E-04	132	4402.4	8.22E-04
13	6462.1	2.80E-05	53	5522.9	2.81E-03	93	4945.5	1.85E-03	133	4398.9	6.96E-04
14	6420.5	1.57E-03	54	5509.7	8.69E-04	94	4926.1	1.02E-03	134	4381.6	1.91E-03
15	6353.7	1.77E-03	55	5496.8	4.35E-04	95	4916.4	2.02E-03	135	4374.2	3.83E-04
16	6343.0	1.76E-04	56	5474.4	7.17E-04	96	4903.3	1.03E-03	136	4363.9	4.69E-04
17	6316.5	5.87E-05	57	5464.9	1.18E-03	97	4894.3	3.56E-04	137	4360.0	6.62E-04
18	6302.3	7.33E-04	58	5460.5	8.97E-04	98	4861.5	1.04E-03	138	4347.5	2.78E-04
19	6290.2	5.86E-05	59	5453.9	2.56E-04	99	4851.3	1.01E-03	139	4338.0	2.79E-04
20	6268.4	1.17E-04	60	5434.7	1.10E-03	100	4835.9	1.81E-03	140	4327.2	1.17E-03
21	6210.4	3.18E-03	61	5424.1	7.20E-04	101	4826.7	5.43E-04	141	4306.8	1.51E-03
22	6193.6	6.13E-04	62	5413.9	6.69E-04	102	4813.1	4.72E-04	142	4291.6	6.94E-04
23	6171.7	2.89E-03	63	5399.2	2.58E-04	103	4804.5	4.55E-04	143	4273.6	8.87E-04
24	6135.7	1.46E-04	64	5392.2	2.58E-04	104	4779.1	6.42E-04	144	4259.1	1.18E-03
25	6109.0	1.31E-03	65	5363.2	3.63E-04	105	4769.4	5.88E-04	145	4250.8	1.03E-03
26	6082.5	2.41E-03	66	5347.1	6.23E-03	106	4751.7	7.20E-04	146	4239.2	8.82E-04
27	6070.0	2.63E-04	67	5324.4	8.32E-04	107	4745.2	9.80E-04	147	4221.2	1.24E-03
28	6046.2	3.28E-03	68	5312.2	4.69E-04	108	4728.3	1.71E-03	148	4202.0	2.53E-04
29	5990.0	4.81E-04	69	5299.7	3.13E-04	109	4712.0	5.22E-04	149	4188.9	8.36E-04
30	5965.8	1.31E-04	70	5290.5	1.04E-04	110	4694.9	1.50E-03	150	4173.6	7.95E-04
31	5948.7	3.06E-04	71	5266.7	4.55E-03	111	4669.7	1.31E-03	151	4164.9	1.26E-03
32	5930.7	2.62E-04	72	5255.0	8.90E-04	112	4663.2	4.51E-04	152	4149.4	7.86E-04
33	5916.6	5.29E-03	73	5238.3	9.44E-04	113	4650.1	4.72E-04	153	4136.0	1.43E-03
34	5906.3	5.68E-04	74	5221.0	7.88E-04	114	4633.7	2.31E-03	154	4122.2	8.69E-04
35	5881.1	5.24E-04	75	5204.9	2.26E-03	115	4617.6	3.37E-04	155	4110.1	1.04E-03
36	5869.8	1.31E-04	76	5182.7	3.17E-04	116	4603.9	1.10E-03	156	4099.3	1.08E-03
37	5848.8	8.74E-05	77	5173.8	3.70E-04	117	4599.8	1.20E-03	157	4084.1	4.94E-04
38	5836.4	3.50E-04	78	5154.4	2.54E-03	118	4582.3	6.61E-04	158	4065.6	2.80E-04
39	5813.0	1.44E-03	79	5147.0	3.71E-04	119	4567.7	2.82E-04	159	4059.4	5.45E-04
40	5798.0	2.23E-03	80	5135.5	5.84E-04	120	4547.2	1.52E-03	160	4049.7	5.78E-04

***** RH 104 ***** TABLE A4.11

	ENERGY (KEV)	INTENSITY (PH/CAP)
161	4023.8	1.69E-03
162	4014.3	8.38E-04
163	4002.1	7.78E-04
164	3990.3	4.47E-04
165	3969.3	1.35E-03
166	3948.7	1.04E-03
167	3932.4	7.23E-04
168	3914.4	6.24E-04
169	3902.8	5.22E-04
170	3889.0	6.29E-04
171	3871.0	7.54E-05
172	3859.4	1.38E-03
173	3849.7	8.97E-04
174	3837.5	2.59E-04
175	3823.4	8.44E-04
176	3815.8	8.62E-04
177	3799.4	5.42E-04
178	3792.2	5.74E-04
179	3780.0	2.81E-04
180	3765.7	5.96E-04
181	3750.8	9.46E-04
182	3725.9	7.64E-04
183	3710.9	7.84E-04
184	3695.9	4.35E-04
185	3684.4	1.44E-03
186	3669.8	6.02E-04
187	3659.4	8.98E-04
188	3642.8	1.76E-03

RH 104 GAMMA RAY PAIR SPECTRUM FIG A4·11·1

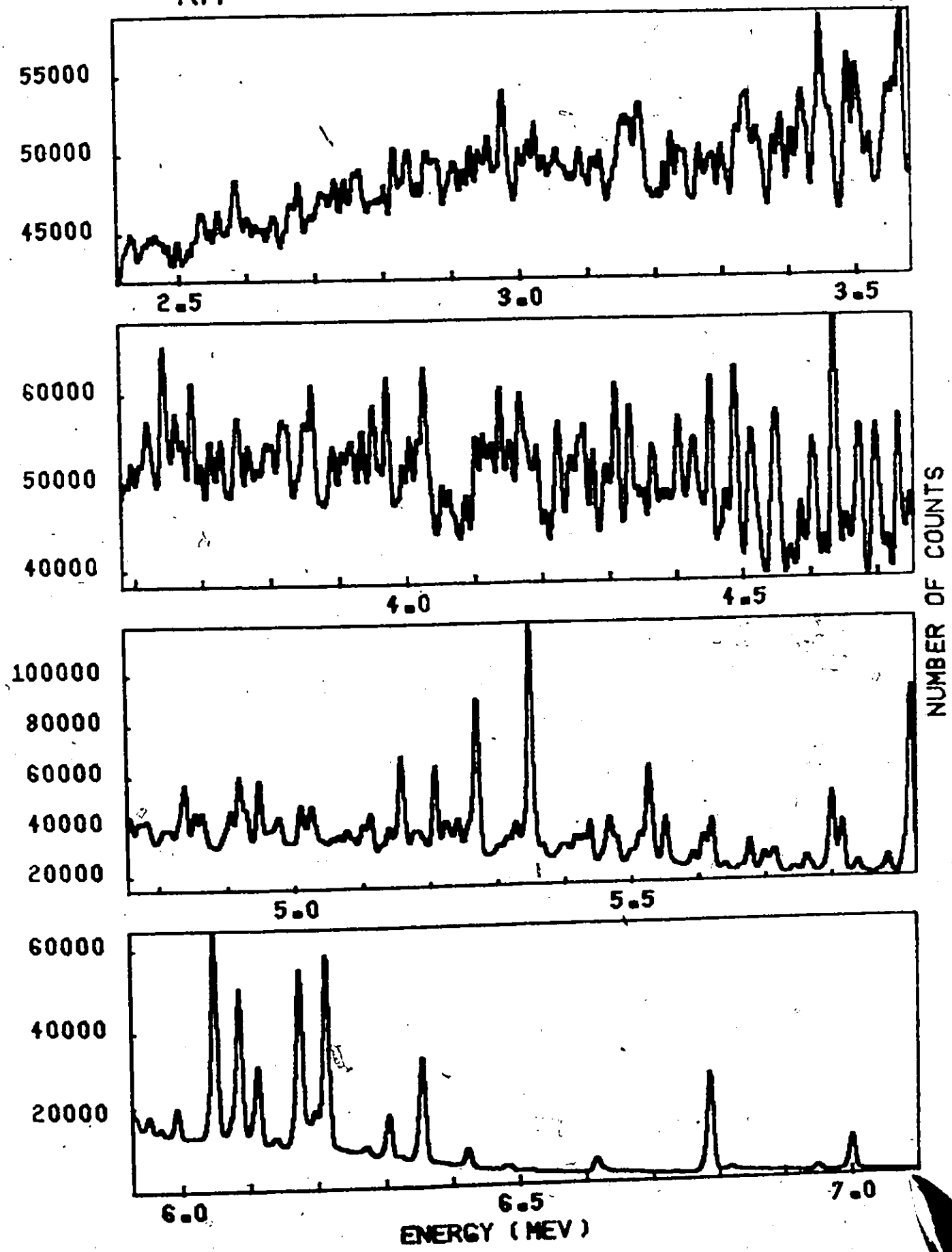

RH 104 RESPONSE STRIPPING FIG A4·11·2

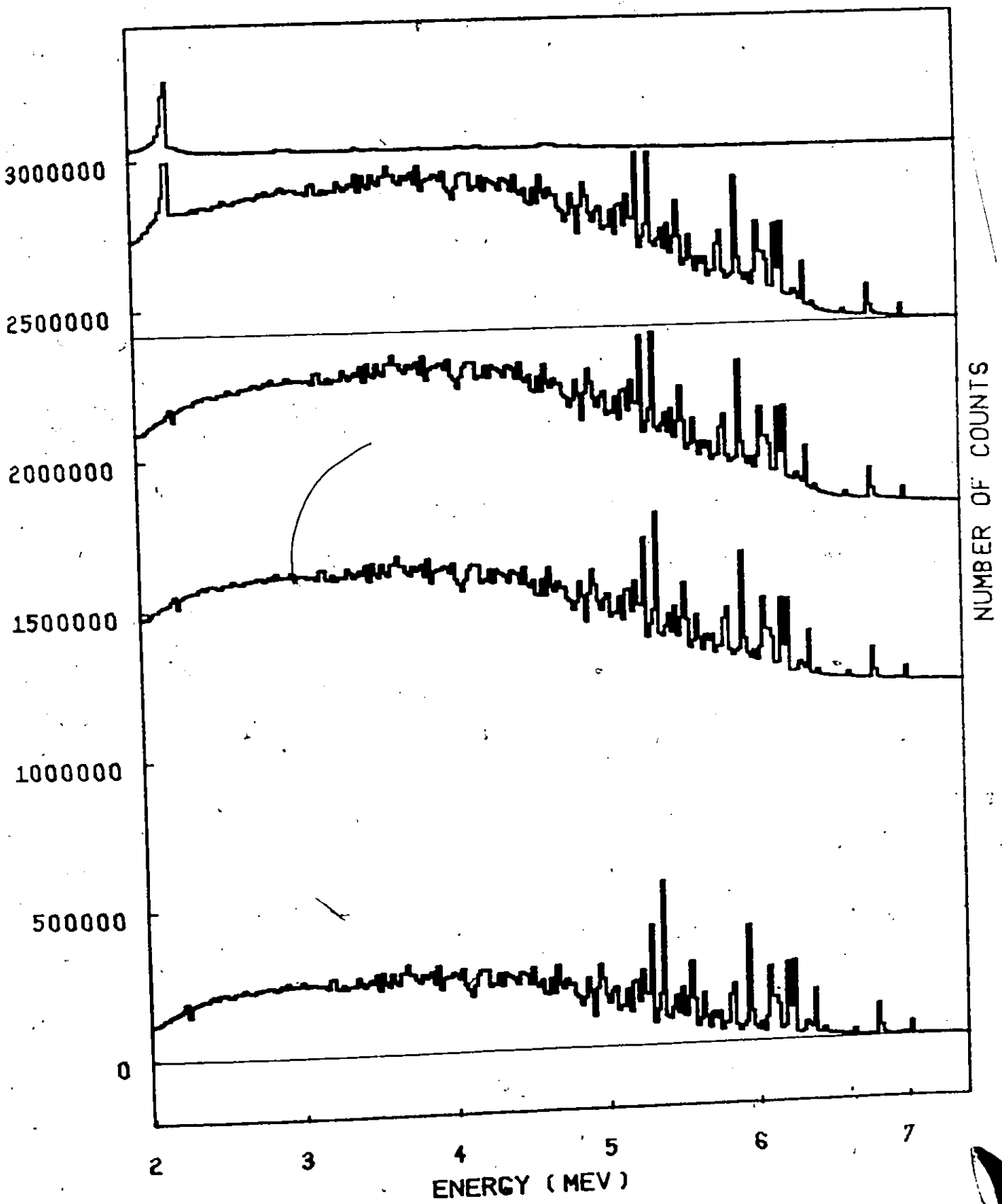

RH 104 STATISTICAL DATA FIG A4·11·3

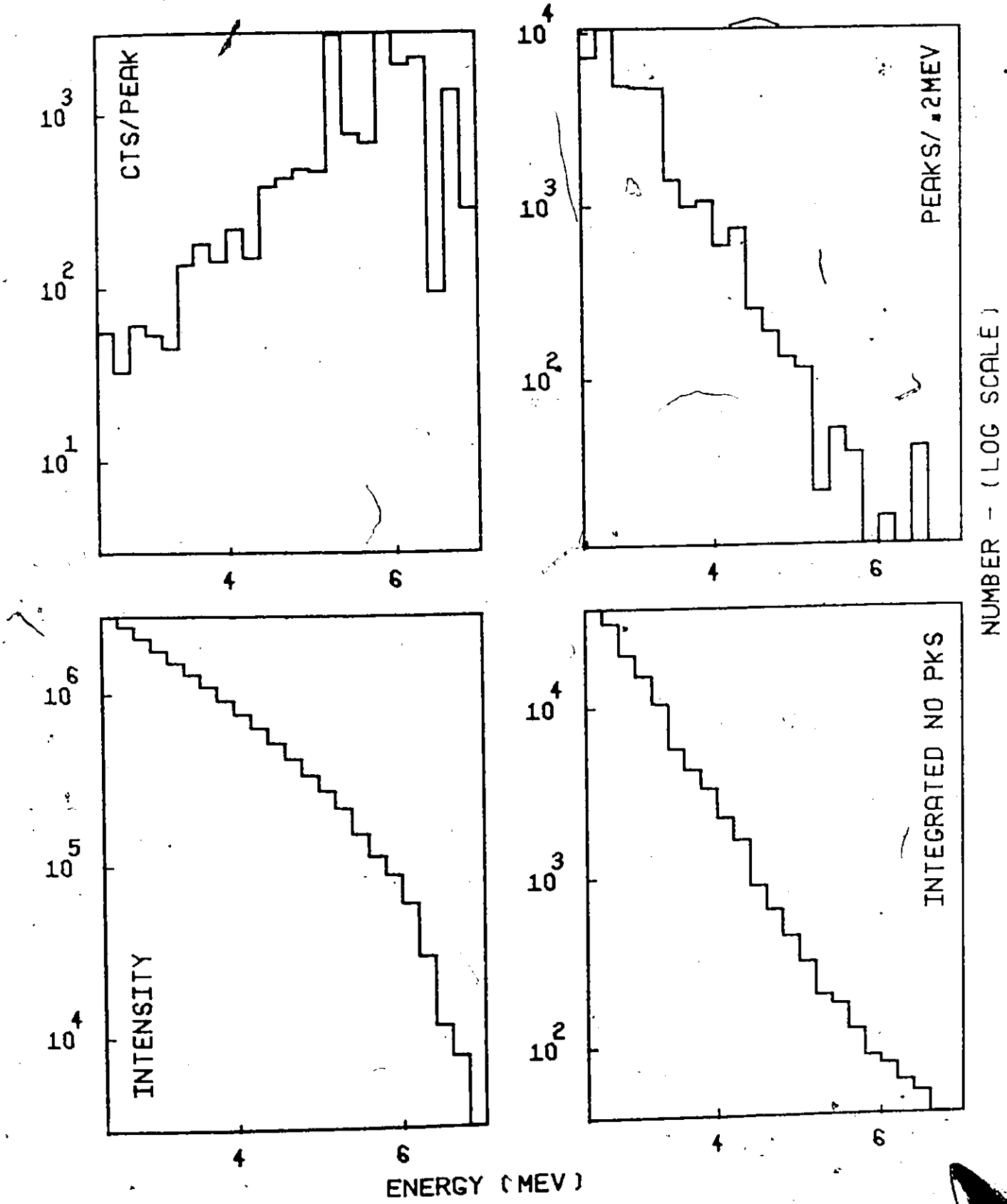

***** AG 110 ***** TABLE A4.12

	ENERGY (KEV)	INTENSITY (PH/CAP)		ENERGY (KEV)	INTENSITY (PH/CAP)		ENERGY (KEV)	INTENSITY (PH/CAP)		ENERGY (KEV)	INTENSITY (PH/CAP)
1	6806.6	1.55E-04	41	5643.6	1.33E-03	81	4946.2	3.00E-03	121	4368.9	1.47E-03
2	6702.7	2.32E-05	42	5634.5	1.21E-03	82	4932.1	1.49E-03	122	4345.8	7.39E-04
3	6607.9	2.78E-04	43	5615.2	1.91E-03	83	4922.0	8.85E-04	123	4335.9	4.88E-04
4	6569.3	3.41E-04	44	5580.3	2.55E-03	84	4884.7	4.75E-04	124	4310.9	1.33E-03
5	6539.7	2.53E-03	45	5554.5	8.13E-04	85	4879.5	3.91E-04	125	4299.4	4.93E-04
6	6446.3	6.33E-04	46	5540.6	1.16E-03	86	4862.4	1.49E-03	126	4287.5	8.43E-04
7	6425.9	4.85E-04	47	5520.2	2.21E-03	87	4851.9	9.28E-04	127	4280.5	5.69E-04
8	6380.9	2.94E-04	48	5515.8	2.85E-03	88	4834.9	3.96E-04	128	4252.6	7.79E-04
9	6370.4	8.40E-05	49	5506.7	9.89E-04	89	4818.6	8.23E-04	129	4229.7	8.96E-04
10	6309.1	2.09E-04	50	5485.5	1.16E-04	90	4811.8	1.51E-03	130	4216.8	6.00E-04
11	6293.8	6.28E-05	51	5468.4	7.00E-04	91	4804.1	7.40E-04	131	4188.8	5.67E-04
12	6280.9	5.85E-04	52	5458.9	3.50E-04	92	4793.2	4.86E-04	132	4173.6	1.68E-04
13	6267.4	8.14E-04	53	5439.9	1.75E-04	93	4773.5	5.17E-04	133	4155.9	6.24E-04
14	6258.3	4.59E-04	54	5430.9	6.43E-04	94	4759.3	1.35E-03	134	4141.2	1.10E-03
15	6251.4	2.09E-04	55	5423.6	1.23E-03	95	4744.2	2.31E-04	135	4125.1	4.77E-04
16	6215.7	9.99E-05	56	5418.0	6.57E-04	96	4727.7	6.39E-04	136	4107.5	3.08E-04
17	6192.1	4.49E-04	57	5387.7	1.72E-03	97	4720.2	1.05E-03	137	4101.1	3.43E-04
18	6174.2	2.00E-04	58	5359.3	1.60E-03	98	4712.6	5.54E-04	138	4079.3	9.85E-04
19	6152.0	9.97E-05	59	5326.2	5.68E-04	99	4695.4	9.08E-04	139	4065.0	6.42E-04
20	6143.5	4.98E-05	60	5319.2	4.02E-04	100	4689.2	8.21E-04	140	4053.3	1.13E-03
21	6108.2	6.47E-04	61	5292.2	3.32E-04	101	4681.5	9.70E-04	141	4050.5	1.40E-03
22	6101.4	1.04E-03	62	5280.5	8.79E-04	102	4675.7	8.54E-04	142	4047.9	1.22E-03
23	6081.8	5.97E-04	63	5272.2	6.18E-04	103	4653.9	5.04E-04	143	4041.7	1.49E-03
24	6075.8	2.98E-04	64	5250.2	4.05E-04	104	4623.5	1.94E-03	144	4037.2	1.31E-03
25	6057.2	5.67E-03	65	5241.6	2.74E-03	105	4584.8	4.04E-04	145	4015.7	3.71E-04
26	6035.2	8.44E-04	66	5226.2	1.72E-03	106	4578.1	5.73E-04	146	3995.3	1.16E-03
27	6022.1	2.28E-03	67	5207.1	2.80E-03	107	4566.7	5.24E-04	147	3987.0	6.24E-04
28	5995.3	1.14E-03	68	5200.2	1.56E-03	108	4550.7	8.15E-04	148	3979.8	3.04E-04
29	5987.8	1.14E-03	69	5156.9	1.13E-03	109	4528.2	1.45E-03	149	3970.7	5.38E-05
30	5952.9	2.48E-04	70	5146.8	4.83E-04	110	4519.1	1.49E-03	150	3954.2	8.30E-04
31	5925.7	7.42E-05	71	5138.3	3.86E-04	111	4507.0	6.53E-04	151	3946.9	1.07E-03
32	5910.6	3.97E-04	72	5113.1	2.67E-03	112	4492.5	2.94E-04	152	3936.5	7.08E-04
33	5896.5	8.93E-04	73	5092.4	2.26E-03	113	4477.2	1.22E-04	153	3921.4	1.06E-03
34	5851.3	1.99E-04	74	5079.7	1.83E-03	114	4460.2	5.23E-04	154	3915.9	6.03E-04
35	5812.4	2.48E-03	75	5055.3	1.95E-03	115	4445.7	6.65E-04	155	3903.8	5.32E-04
36	5794.4	5.01E-03	76	5035.5	3.92E-04	116	4429.4	5.27E-04	156	3892.1	8.11E-04
37	5773.1	1.84E-03	77	5001.8	9.76E-04	117	4418.7	3.88E-04	157	3885.5	3.70E-04
38	5741.0	8.65E-04	78	4997.2	7.87E-04	118	4399.6	3.55E-04	158	3871.4	4.27E-04
39	5709.7	2.19E-03	79	4975.6	3.00E-04	119	4393.7	7.46E-04	159	3866.1	4.83E-04
40	5701.5	7.04E-03	80	4964.6	4.65E-04	120	4381.6	3.39E-04	160	3847.4	4.12E-04

***** AG 110 ***** TABLE A4.12

	ENERGY (KEV)	INTENSITY (PH/CAP)		ENERGY (KEV)	INTENSITY (PH/CAP)
161	3839.7	1.35E-03	201	3289.1	2.05E-04
162	3823.4	8.31E-04	202	3276.8	8.60E-04
163	3797.4	5.41E-04	203	3264.7	2.63E-04
164	3791.2	4.96E-04	204	3251.2	9.37E-04
165	3782.1	4.20E-04	205	3237.5	3.11E-04
166	3775.1	4.21E-04	206	3228.9	2.90E-04
167	3757.7	1.73E-04	207	3212.8	4.72E-04
168	3747.9	2.68E-04	208	3208.3	4.28E-04
169	3739.4	1.58E-04	209	3185.0	4.45E-04
170	3726.3	1.27E-04	210	3174.1	4.70E-04
171	3718.2	2.71E-04	211	3137.2	2.80E-04
172	3697.5	9.32E-04	212	3132.6	3.87E-04
173	3685.8	1.82E-03	213	3125.3	4.59E-04
174	3664.5	4.23E-04	214	3105.0	4.40E-04
175	3658.4	2.94E-04	215	3096.3	4.30E-04
176	3643.7	7.38E-04	216	3078.2	7.24E-04
177	3623.1	3.80E-04	217	3064.9	3.77E-04
178	3615.9	4.32E-04	218	3058.7	2.07E-04
179	3593.5	1.14E-03	219	3048.2	3.19E-04
180	3589.1	5.57E-04	220	3033.9	3.84E-04
181	3583.3	7.23E-04	221	3021.6	2.49E-04
182	3564.9	6.10E-04	222	3010.3	2.38E-04
183	3558.5	1.19E-03	223	3004.1	3.45E-04
184	3543.6	4.62E-04	224	2988.0	3.16E-04
185	3529.5	4.47E-04	225	2948.9	4.25E-04
186	3506.3	6.77E-04	226	2886.5	4.62E-04
187	3487.8	1.58E-04	227	2865.9	6.38E-04
188	3459.6	4.61E-04	228	2808.9	6.29E-04
189	3451.7	9.24E-04	229	2773.7	3.61E-04
190	3444.8	6.96E-04	230	2665.7	3.90E-04
191	3432.2	8.25E-04	231	2586.6	3.21E-04
192	3415.2	3.25E-04	232	2533.8	5.57E-04
193	3407.8	6.78E-04	233	2523.5	4.50E-04
194	3398.7	6.59E-04	234	2492.1	4.62E-04
195	3392.3	6.81E-04	235	2476.8	3.52E-04
196	3368.1	3.75E-04	236	2049.3	1.05E-03
197	3363.7	3.76E-04			
198	3335.7	1.59E-04			
199	3326.8	2.44E-04			
200	3318.7	5.47E-04			

AG 110 GAMMA RAY PAIR SPECTRUM FIG A4·12·1

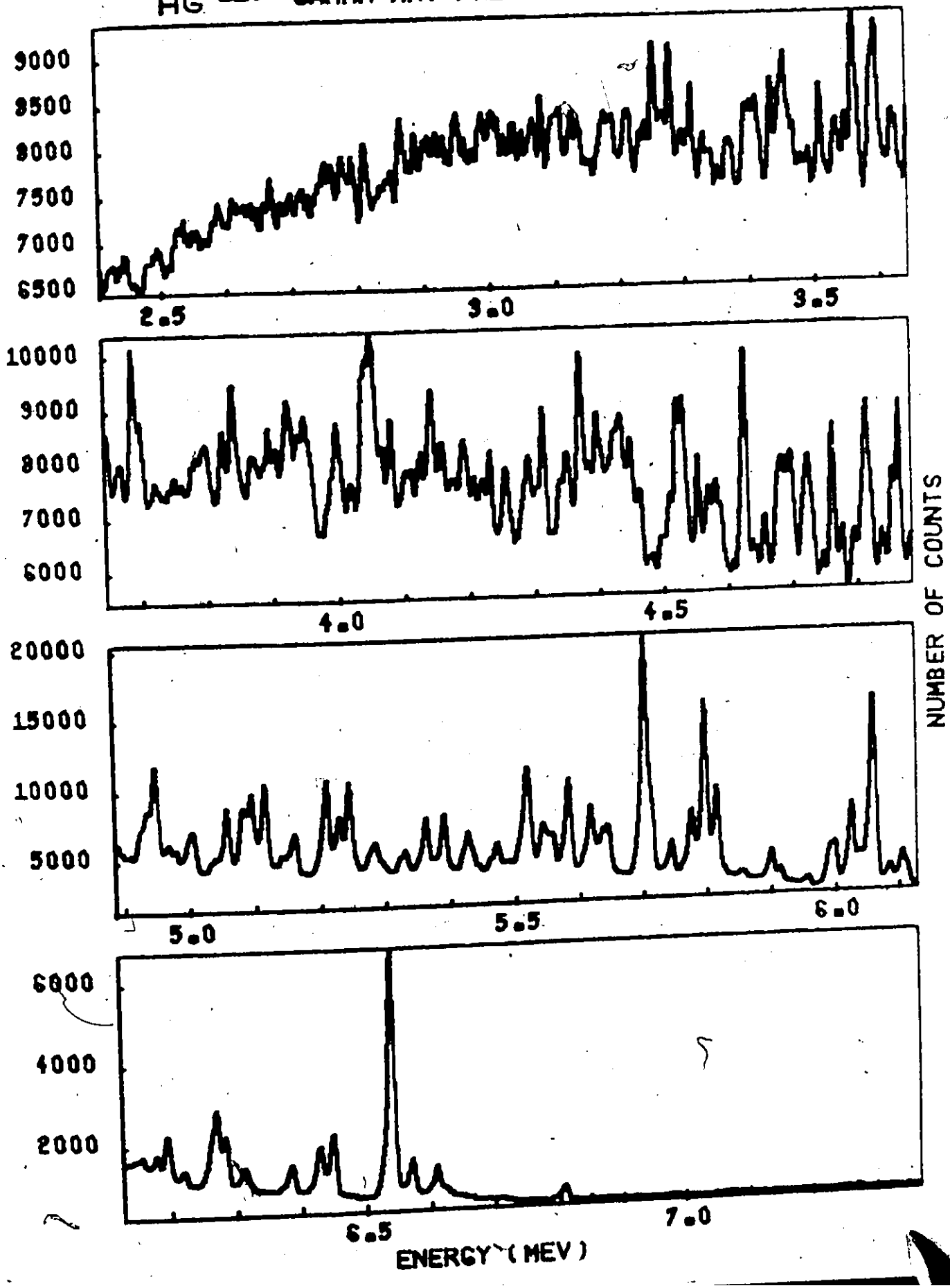

AG 110 RESPONSE STRIPPING FIG A4·12·2

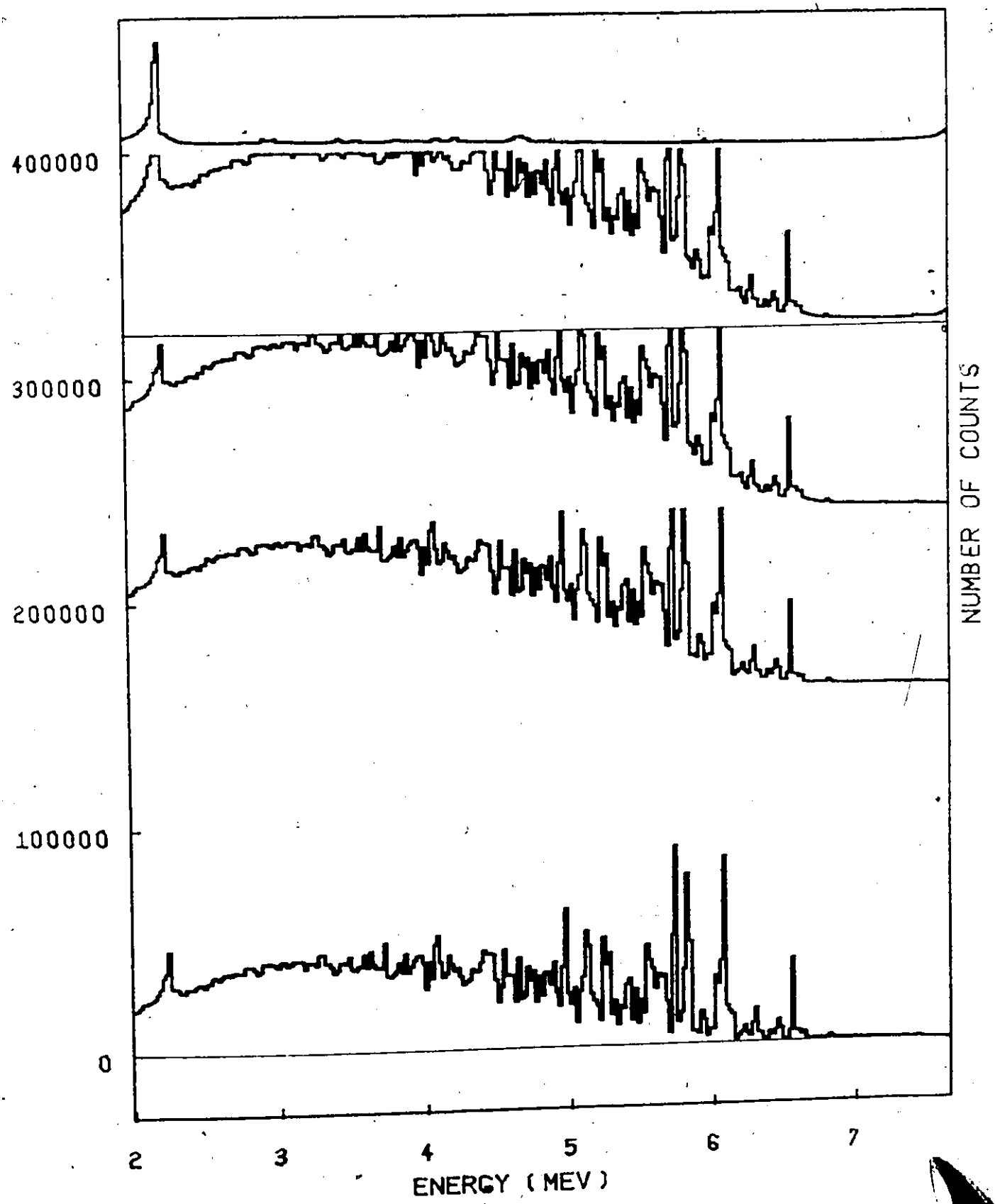

AG 110 STATISTICAL DATA FIG A4·12·3

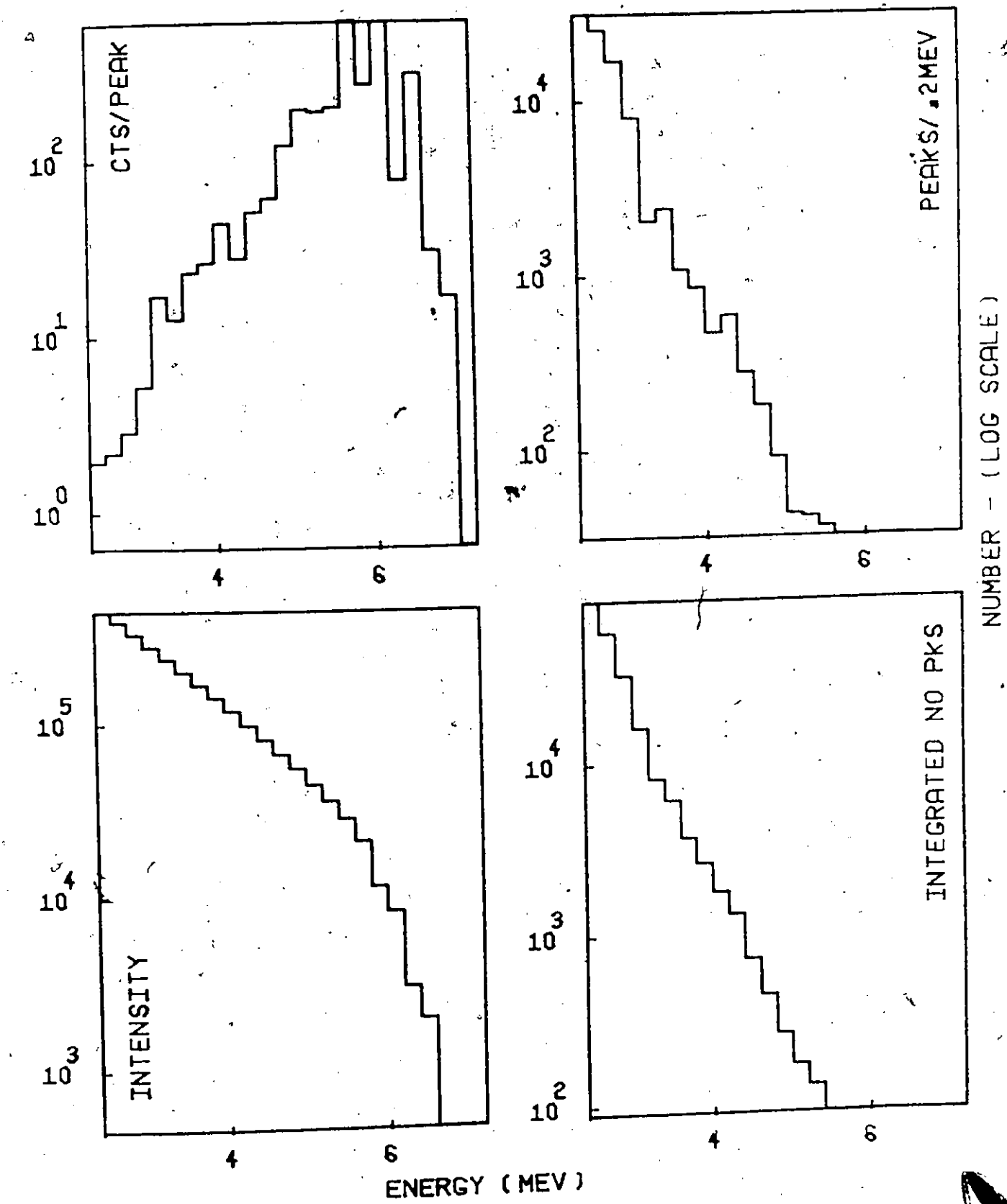

***** IN 116 ***** TABLE A4.13

	ENERGY (KEV)	INTENSITY (PH/CAP)		ENERGY (KEV)	INTENSITY (PH/CAP)		ENERGY (KEV)	INTENSITY (PH/CAP)		ENERGY (KEV)	INTENSITY (PH/CAP)
1	6560.8	6.28E-05	41	5191.6	2.38E-04	81	4536.1	3.56E-04	121	3840.7	1.54E-04
2	6469.0	1.95E-05	42	5172.9	2.06E-03	82	4519.4	2.64E-04	122	3811.1	3.51E-04
3	6410.3	4.47E-04	43	5140.9	2.37E-03	83	4478.5	2.20E-04	123	3792.9	7.52E-04
4	6324.7	3.03E-04	44	5119.2	5.11E-04	84	4473.0	2.36E-04	124	3774.3	9.27E-04
5	6275.9	3.24E-05	45	5103.7	3.49E-03	85	4462.1	2.53E-04	125	3745.5	6.41E-04
6	6228.9	2.59E-04	46	5081.9	3.62E-04	86	4442.2	1.17E-03	126	3740.7	4.07E-04
7	6135.5	3.09E-04	47	5049.0	2.43E-04	87	4431.9	6.21E-04	127	3720.9	2.21E-04
8	6126.6	7.25E-05	48	5033.3	6.69E-04	88	4426.0	1.05E-03	128	3699.4	3.98E-04
9	6110.4	1.02E-04	49	5015.2	3.66E-04	89	4421.4	1.04E-03	129	3684.9	1.79E-03
10	6101.4	5.37E-05	50	5006.3	1.25E-03	90	4409.7	6.41E-04	130	3661.7	1.94E-04
11	6048.3	2.28E-04	51	4986.9	2.15E-04	91	4401.7	4.01E-04	131	3635.3	4.24E-04
12	5993.7	8.82E-05	52	4969.8	2.09E-03	92	4387.3	2.90E-04	132	3619.3	6.40E-04
13	5891.6	4.31E-03	53	4958.8	8.65E-04	93	4372.1	6.48E-04	133	3612.5	9.38E-04
14	5834.5	2.50E-04	54	4945.8	2.45E-03	94	4352.8	1.14E-04	134	3593.5	5.31E-04
15	5812.1	3.57E-04	55	4926.8	2.49E-04	95	4323.8	1.31E-03	135	3572.7	1.84E-04
16	5776.1	3.21E-04	56	4912.7	1.16E-03	96	4310.3	8.75E-04	136	3546.9	5.75E-04
17	5769.7	7.50E-04	57	4898.1	2.65E-04	97	4262.1	5.19E-04	137	3540.7	4.07E-04
18	5753.5	2.86E-04	58	4877.5	2.97E-04	98	4246.3	3.53E-04	138	3515.5	2.74E-04
19	5731.8	2.60E-04	59	4870.0	1.55E-03	99	4226.2	1.54E-03	139	3507.1	2.93E-04
20	5712.8	1.43E-04	60	4849.4	5.99E-04	100	4204.7	3.41E-04	140	3497.7	3.11E-04
21	5704.1	7.15E-05	61	4823.6	6.98E-04	101	4197.5	3.16E-04	141	3480.3	3.75E-04
22	5664.1	7.16E-05	62	4809.0	9.55E-04	102	4180.7	1.57E-04	142	3457.9	3.13E-04
23	5618.0	7.48E-05	63	4775.4	1.86E-03	103	4152.9	2.11E-04	143	3448.8	7.32E-04
24	5580.3	6.20E-04	64	4768.0	9.82E-04	104	4136.2	4.57E-04	144	3440.3	5.44E-04
25	5572.4	4.66E-04	65	4744.1	1.13E-03	105	4120.7	6.40E-04	145	3428.5	5.47E-04
26	5526.5	2.64E-04	66	4737.6	4.05E-04	106	4112.9	5.78E-04	146	3419.1	2.99E-04
27	5499.0	8.10E-04	67	4724.8	3.26E-04	107	4087.3	5.07E-04	147	3404.7	2.72E-04
28	5491.7	4.68E-04	68	4708.6	1.31E-04	108	4074.5	1.09E-03	148	3399.9	3.98E-04
29	5443.1	1.88E-04	69	4701.1	9.50E-04	109	4059.9	5.33E-04	149	3383.0	4.70E-04
30	5410.7	1.29E-03	70	4683.5	4.44E-04	110	4044.3	8.43E-04	150	3374.3	7.57E-04
31	5385.5	1.41E-04	71	4677.6	6.59E-04	111	4024.2	2.64E-04	151	3353.0	1.21E-03
32	5358.6	1.07E-03	72	4665.2	5.29E-04	112	4013.4	4.09E-04	152	3348.7	6.96E-04
33	5347.8	9.77E-04	73	4653.6	1.03E-03	113	4006.8	4.77E-04	153	3332.8	7.02E-04
34	5333.7	1.75E-03	74	4624.3	4.51E-04	114	3988.3	4.46E-04	154	3325.8	5.33E-04
35	5319.3	6.79E-04	75	4615.0	4.69E-04	115	3978.3	7.50E-04	155	3309.5	1.32E-04
36	5296.4	2.69E-04	76	4599.0	8.75E-04	116	3949.4	5.65E-04	156	3294.4	2.25E-04
37	5289.1	1.43E-04	77	4591.0	9.45E-04	117	3927.7	1.14E-03	157	3282.1	3.18E-04
38	5267.9	1.27E-04	78	4581.2	1.29E-03	118	3897.5	2.76E-04	158	3266.1	2.59E-04
39	5246.6	7.10E-04	79	4557.4	4.77E-04	119	3876.3	9.51E-04	159	3255.1	3.23E-04
40	5212.1	8.91E-05	80	4550.5	1.71E-04	120	3859.8	1.87E-04	160	3242.5	2.83E-04

	ENERGY (KEV)	INTENSITY (PH/CAP)
161	3224.5	2.11E-04
162	3197.9	2.68E-04
163	3177.8	2.71E-04
164	3160.9	4.04E-04
165	3152.2	2.96E-04
166	3126.4	5.46E-04
167	3116.5	6.49E-04
168	3106.2	3.29E-04
169	3098.9	3.18E-04
170	3081.3	5.08E-04
171	3060.7	3.31E-04
172	3052.3	3.12E-04
173	3036.5	2.53E-04
174	3029.7	4.13E-04
175	3015.7	4.02E-04
176	2994.2	3.86E-04
177	2986.2	5.43E-04
178	2962.0	1.93E-04
179	2947.6	3.24E-04
180	2934.0	2.91E-04
181	2928.8	4.16E-04
182	2908.2	3.47E-04
183	2892.9	5.07E-04
184	2881.4	2.93E-04
185	2864.8	3.03E-04
186	2846.4	3.61E-04
187	2823.4	2.96E-04
188	2817.0	2.97E-04
189	2810.6	3.93E-04
190	2799.5	2.38E-04
191	2784.3	3.12E-04
192	2755.6	3.35E-04
193	2734.4	2.29E-04
194	2726.8	2.99E-04
195	2702.4	1.82E-04
196	2681.6	2.38E-04
197	2666.9	2.49E-04
198	2602.2	3.00E-04
199	2596.4	5.26E-04
200	2592.5	4.75E-04
201	2572.4	2.88E-04
202	2528.0	3.28E-04
203	2486.0	2.89E-04
204	2407.5	2.59E-04
205	2336.3	5.56E-04
206	2316.2	2.84E-04

IN 116 GAMMA RAY PAIR SPECTRUM FIG A4·13·1

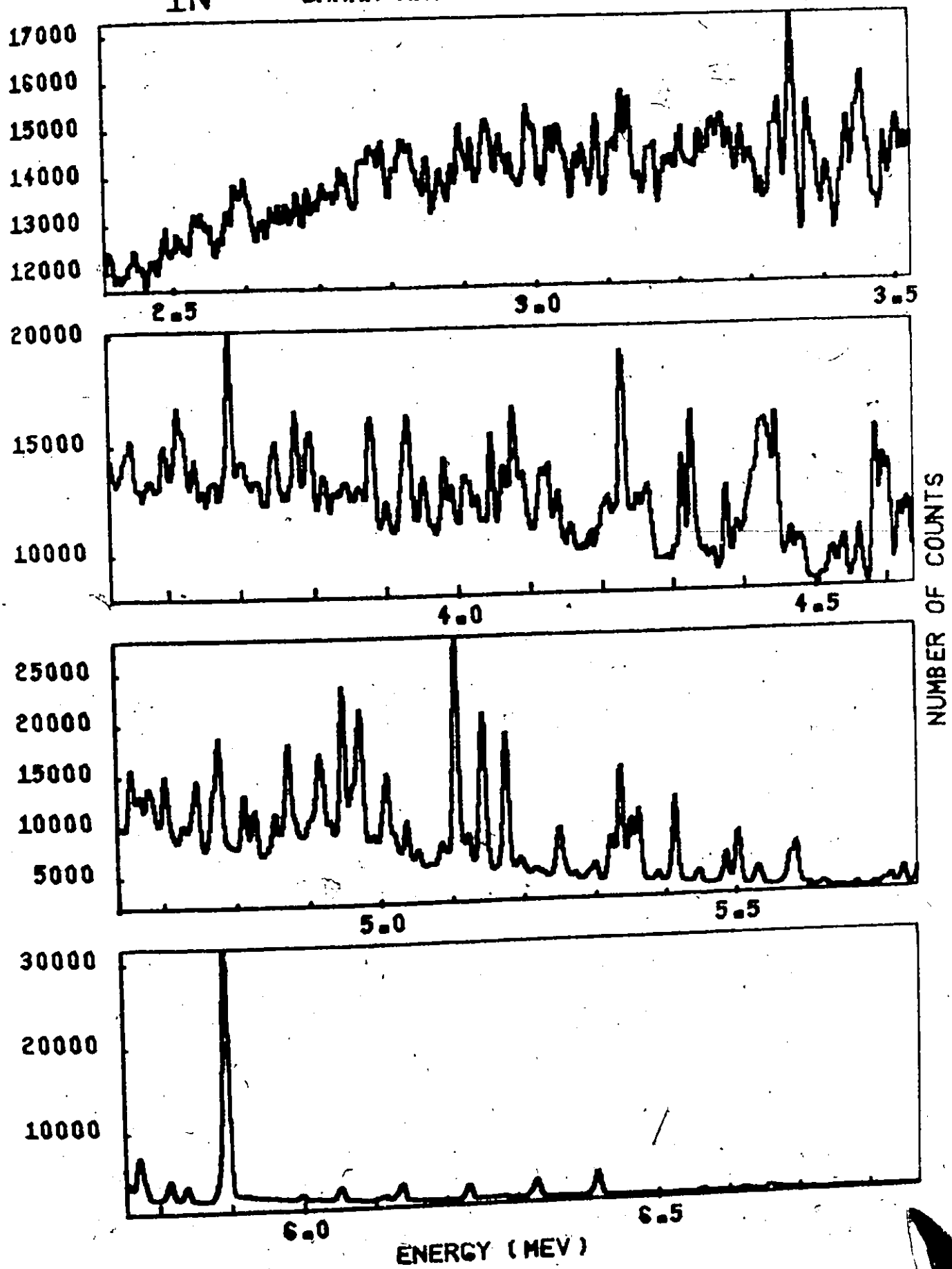

IN 116 RESPONSE STRIPPING FIG A4·13·2

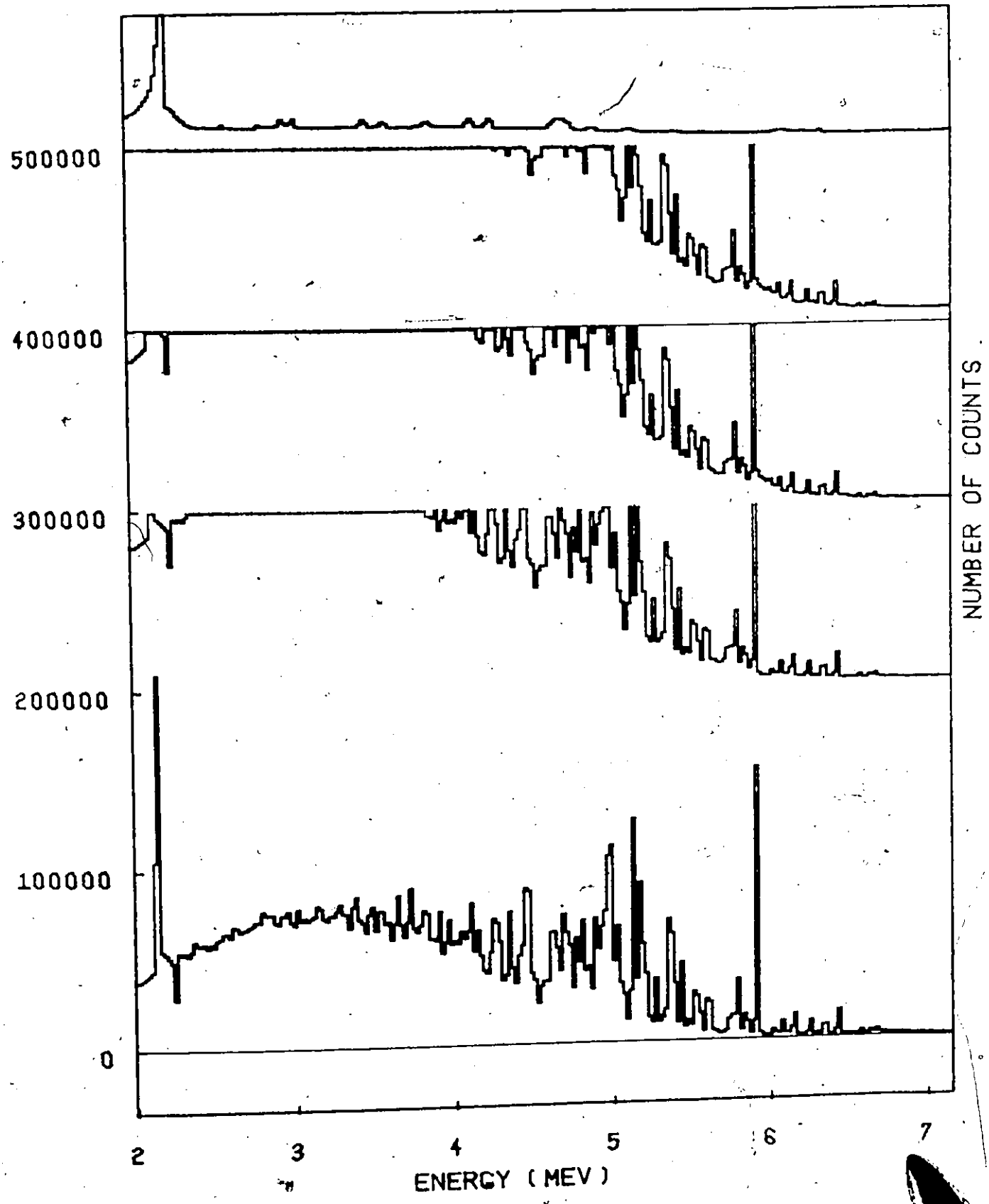

IN 116 STATISTICAL DATA FIG A4·13·3

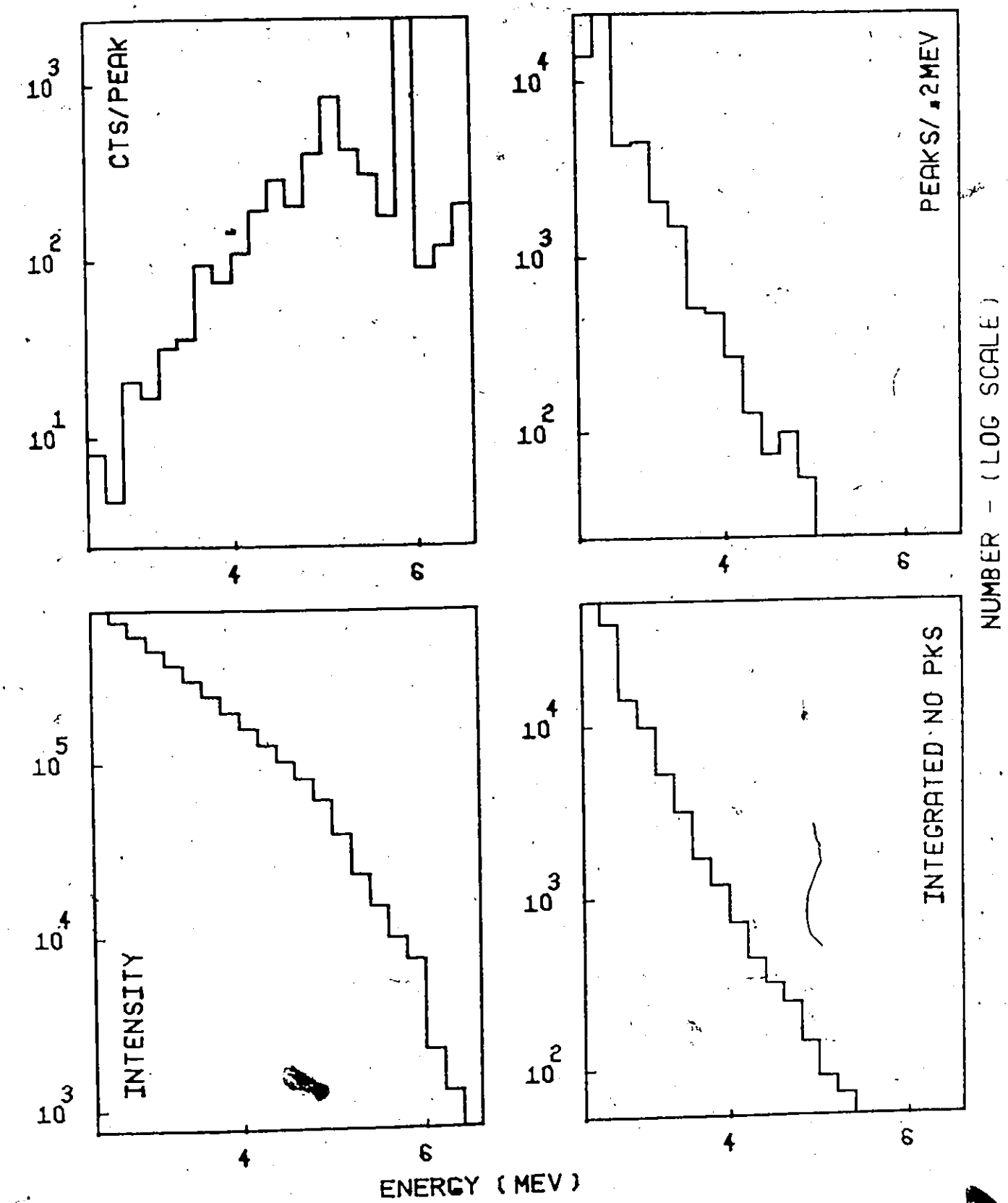

TABLE A4.14

***** CS 134 *****

	ENERGY (KEV)	INTENSITY (PH/CAP)		ENERGY (KEV)	INTENSITY (PH/CAP)		ENERGY (KEV)	INTENSITY (PH/CAP)		ENERGY (KEV)	INTENSITY (PH/CAP)
1	6890.4	2.54E-04	41	5720.5	6.01E-04	81	5047.0	3.41E-04	121	4521.1	4.05E-04
2	6890.0	2.43E-04	42	5709.2	1.13E-04	82	5047.3	4.53E-04	122	4511.9	3.67E-04
3	6830.7	4.32E-04	43	5674.9	1.50E-04	83	5032.8	3.28E-04	123	4497.1	5.13E-04
4	6713.8	1.35E-03	44	5653.9	1.88E-04	84	5021.7	2.73E-03	124	4481.4	2.91E-04
5	6696.5	2.96E-03	45	5637.0	3.16E-03	85	5014.8	2.45E-03	125	4471.4	7.02E-04
6	6655.7	2.73E-04	46	5625.7	1.81E-03	86	5007.6	1.06E-03	126	4447.7	6.67E-04
7	6619.5	2.22E-04	47	5615.6	6.79E-04	87	4982.9	3.31E-04	127	4443.7	7.21E-04
8	6512.5	4.65E-04	48	5599.5	7.55E-05	88	4967.9	1.28E-03	128	4425.8	6.57E-04
9	6438.3	9.94E-04	49	5570.1	3.14E-03	89	4960.3	5.63E-04	129	4416.1	6.46E-04
10	6407.0	6.20E-05	50	5531.8	2.27E-04	90	4945.5	1.85E-03	130	4406.1	4.59E-04
11	6386.9	4.33E-04	51	5519.1	1.52E-04	91	4933.1	1.00E-03	131	4397.6	1.35E-04
12	6371.6	1.95E-04	52	5505.3	4.29E-03	92	4924.0	1.55E-03	132	4385.1	2.85E-04
13	6319.1	7.40E-04	53	5493.6	3.30E-03	93	4897.3	9.36E-04	133	4378.7	5.44E-04
14	6307.6	5.54E-04	54	5473.5	6.46E-04	94	4892.4	5.99E-04	134	4375.4	5.17E-04
15	6266.9	9.22E-05	55	5467.3	1.90E-04	95	4879.3	2.61E-04	135	4354.2	2.88E-04
16	6246.2	3.38E-04	56	5447.6	6.85E-04	96	4860.2	1.84E-04	136	4340.8	5.96E-04
17	6198.7	4.29E-04	57	5436.5	1.26E-03	97	4853.2	3.68E-04	137	4321.1	3.46E-04
18	6188.3	1.96E-03	58	5411.4	1.14E-04	98	4836.6	3.69E-04	138	4316.1	4.06E-04
19	6174.7	3.43E-03	59	5398.5	2.76E-04	99	4828.3	7.67E-04	139	4302.0	8.74E-04
20	6165.5	7.04E-04	60	5376.8	3.33E-03	100	4818.8	4.51E-04	140	4274.5	2.32E-04
21	6149.4	3.67E-04	61	5326.7	2.48E-04	101	4810.0	5.05E-04	141	4263.9	3.60E-04
22	6137.8	6.42E-04	62	5314.7	9.09E-04	102	4800.3	1.60E-04	142	4256.1	4.66E-04
23	6109.2	1.53E-04	63	5270.0	1.83E-03	103	4788.4	3.47E-04	143	4252.1	4.82E-04
24	6088.2	7.58E-05	64	5263.3	1.16E-03	104	4781.7	5.08E-04	144	4237.3	7.94E-04
25	6067.9	1.26E-04	65	5253.1	4.66E-03	105	4771.3	7.24E-04	145	4223.7	6.22E-04
26	6050.9	3.05E-03	66	5223.6	1.54E-03	106	4754.2	1.29E-03	146	4206.6	8.40E-05
27	5975.7	1.16E-03	67	5205.8	7.94E-04	107	4727.9	2.17E-04	147	4198.1	4.59E-04
28	5958.4	2.77E-04	68	5201.5	5.02E-04	108	4719.4	9.79E-04	148	4181.9	5.00E-04
29	5949.2	6.80E-04	69	5187.6	1.26E-04	109	4699.7	1.91E-04	149	4176.7	4.78E-04
30	5941.1	2.27E-04	70	5177.0	8.39E-05	110	4687.3	6.58E-04	150	4173.6	4.63E-04
31	5914.1	6.80E-04	71	5161.0	5.04E-04	111	4687.5	5.74E-04	151	4162.5	3.79E-04
32	5898.8	1.86E-03	72	5151.2	5.05E-04	112	4667.7	1.13E-03	152	4149.9	2.02E-04
33	5887.1	2.52E-04	73	5135.9	5.06E-04	113	4657.3	1.13E-03	153	4137.4	5.23E-04
34	5857.6	4.28E-04	74	5130.2	5.06E-04	114	4649.0	1.06E-03	154	4131.1	5.24E-04
35	5848.3	1.76E-04	75	5113.5	2.96E-04	115	4621.5	7.87E-04	155	4114.1	4.64E-04
36	5802.0	1.41E-03	76	5102.2	2.12E-04	116	4604.4	8.93E-05	156	4106.5	5.28E-04
37	5790.7	2.14E-03	77	5082.6	4.67E-04	117	4588.5	1.23E-03	157	4087.7	1.35E-04
38	6303.9	2.04E-04	78	5075.2	4.25E-04	118	4578.3	7.58E-04	158	4070.4	6.22E-04
39	5748.0	1.46E-03	79	5064.4	5.11E-04	119	4564.0	9.16E-04	159	4066.3	4.79E-04
40	5728.4	1.24E-03	80	5057.9	3.41E-04	120	4541.6	1.32E-03	160	4038.6	3.22E-04

***** CS 134 *****

	ENERGY (KEV)	INTENSITY (PH/CAP)
161	4032.8	2.18E-04
162	4019.0	3.49E-04
163	4015.3	4.22E-04
164	4011.1	3.42E-04
165	4004.6	3.18E-04
166	3991.9	2.95E-04
167	3974.6	8.23E-04
168	3952.7	7.53E-04
169	3937.4	8.43E-04
170	3924.0	6.16E-04
171	3919.6	5.59E-04
172	3900.7	9.71E-05
173	3881.1	2.05E-04
174	3871.2	6.48E-04
175	3849.9	4.94E-04
176	3844.1	3.67E-04
177	3832.1	2.99E-04
178	3809.1	5.52E-04
179	3801.2	5.23E-04
180	3797.0	3.02E-04
181	3776.2	8.13E-05
182	3762.2	2.04E-04
183	3752.7	7.18E-04
184	3747.1	4.42E-04
185	3737.7	5.36E-04
186	3725.9	1.04E-04
187	3716.4	1.14E-04
188	3695.7	3.77E-04
189	3684.1	8.21E-04
190	3670.5	5.29E-04
191	3654.1	2.02E-04
192	3650.0	1.92E-04
193	3642.8	2.35E-04
194	3625.9	1.47E-04
195	3615.5	5.45E-04
196	3599.4	1.06E-03
197	3581.6	4.72E-04
198	3578.4	4.15E-04
199	3567.5	1.85E-04
200	3557.6	3.49E-04
201	3548.5	1.52E-04
202	3534.2	1.64E-04
203	3529.1	4.00E-04
204	3510.7	1.30E-04
205	3498.2	3.58E-04

CS 134 GAMMA RAY PAIR SPECTRUM FIG. A4-14-1

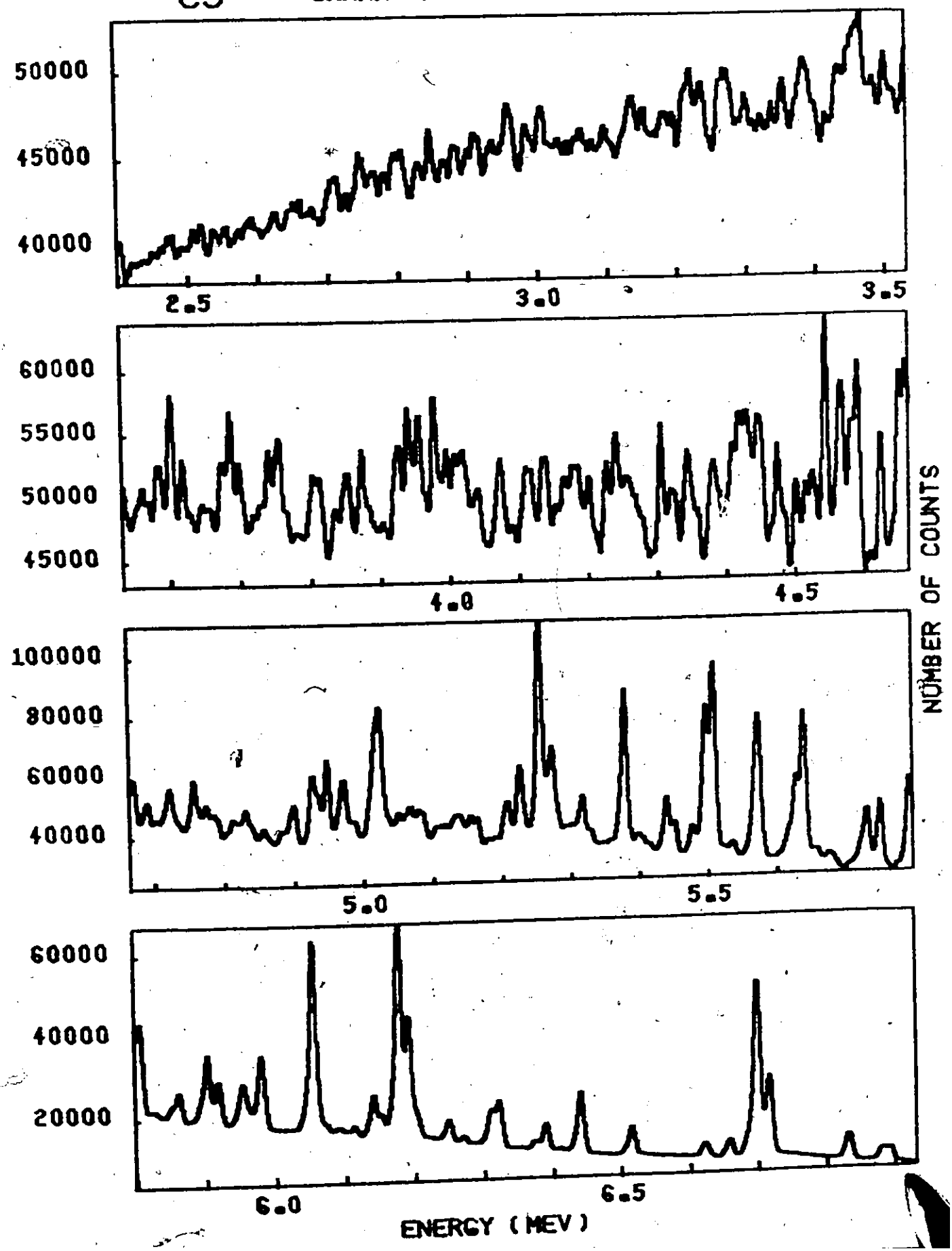

CS 134 RESPONSE STRIPPING FIG A4·14·2

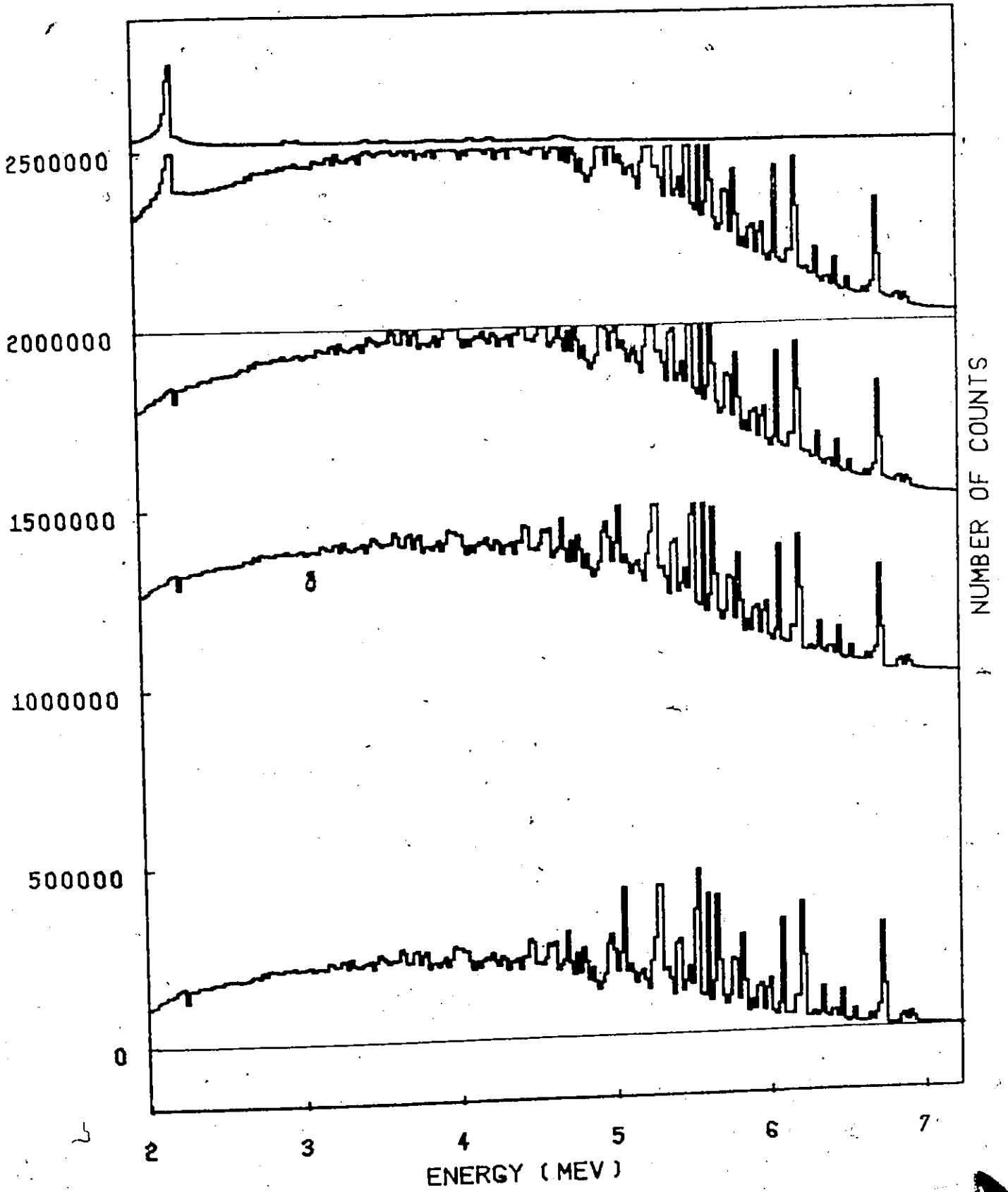

CS 134 STATISTICAL DATA FIG A4·14·3

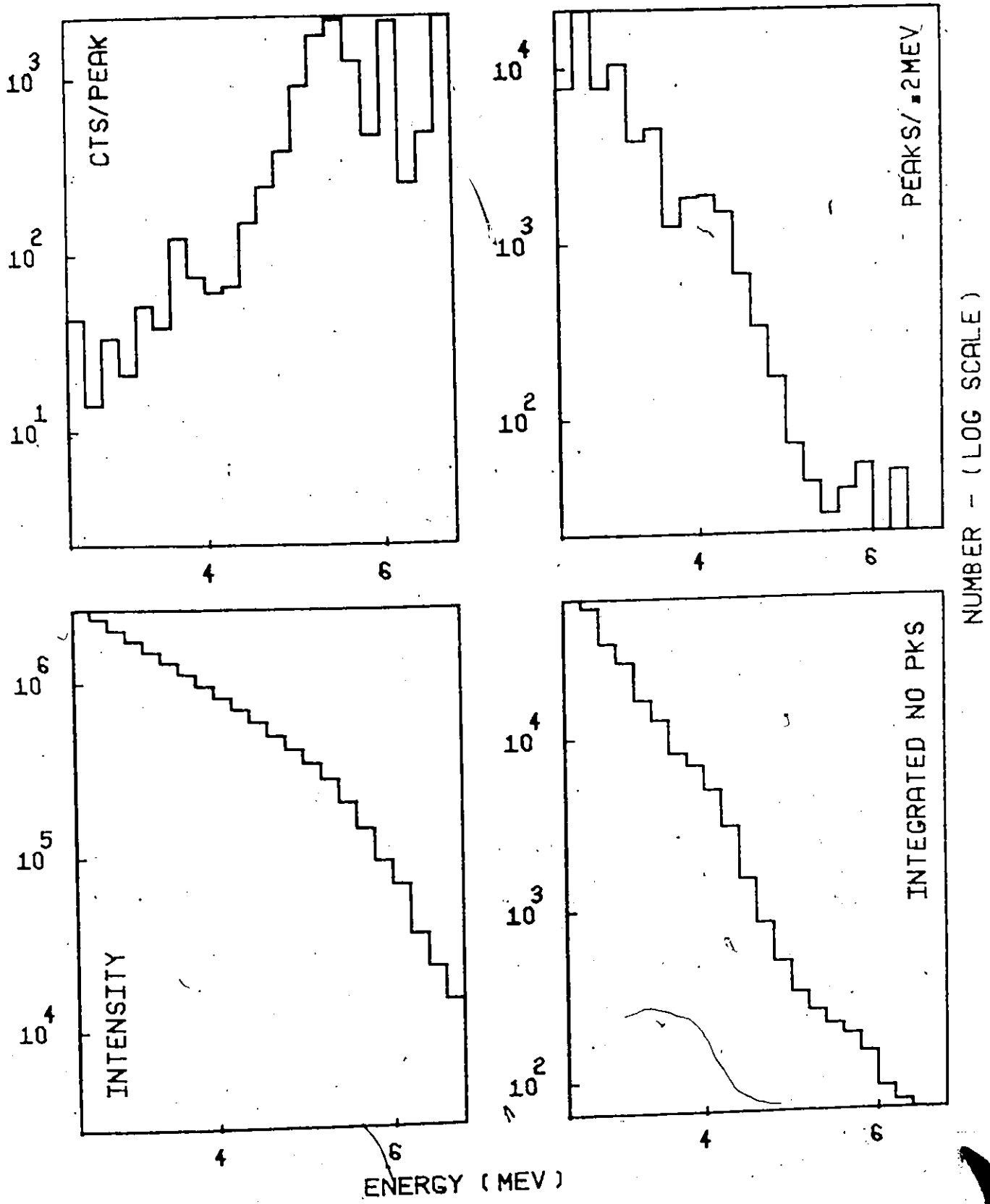

	ENERGY (KEV)	INTENSITY (PH/CAP)
1	6179.6	2.69E-04
2	6120.9	1.63E-03
3	6080.8	2.25E-03
4	6033.8	9.34E-04
5	6005.8	8.58E-04
6	5969.9	4.29E-04
7	5911.2	8.71E-03
8	5858.0	1.93E-03
9	5801.7	2.86E-04
10	5754.3	1.43E-04
11	5711.0	1.57E-03
12	5646.3	1.15E-03
13	5602.9	1.69E-03
14	5495.0	1.27E-03
15	5425.5	1.90E-04
16	5384.8	7.37E-04
17	5354.9	2.36E-03
18	5317.8	6.22E-04
19	5306.9	6.95E-04
20	5278.7	2.40E-03
21	5257.3	1.40E-03
22	5247.1	8.68E-04
23	5226.9	2.41E-04
24	5206.8	1.02E-03
25	5177.5	2.18E-03
26	5159.5	8.12E-04
27	5140.4	3.47E-03
28	5111.2	9.04E-04
29	5082.4	1.08E-03
30	5078.3	1.60E-03
31	5029.4	3.48E-03
32	5008.8	3.76E-03
33	4998.1	1.01E-03
34	4992.8	1.14E-03
35	4946.5	5.05E-03
36	4938.9	3.64E-03
37	4916.3	8.93E-04
38	4872.1	1.13E-03
39	4862.7	4.21E-03
40	4856.2	2.22E-03
41	4827.8	5.48E-04
42	4806.4	3.24E-04
43	4794.9	3.75E-04
44	4775.2	2.89E-03
45	4744.2	7.35E-04
46	4723.6	4.33E-04
47	4705.5	5.38E-04
48	4694.0	9.24E-04
49	4684.5	3.60E-04
50	4664.7	6.98E-04
51	4658.1	4.14E-04
52	4635.3	1.38E-03
53	4615.0	6.03E-04
54	4609.1	5.25E-04
55	4592.4	7.12E-04
56	4574.7	5.04E-04
57	4546.0	6.15E-04
58	4534.6	8.85E-04
59	4508.4	1.19E-03
60	4500.3	6.23E-04
61	4459.6	1.15E-03

RE 186 GAMMA RAY PAIR SPECTRUM FIG A4·15·1

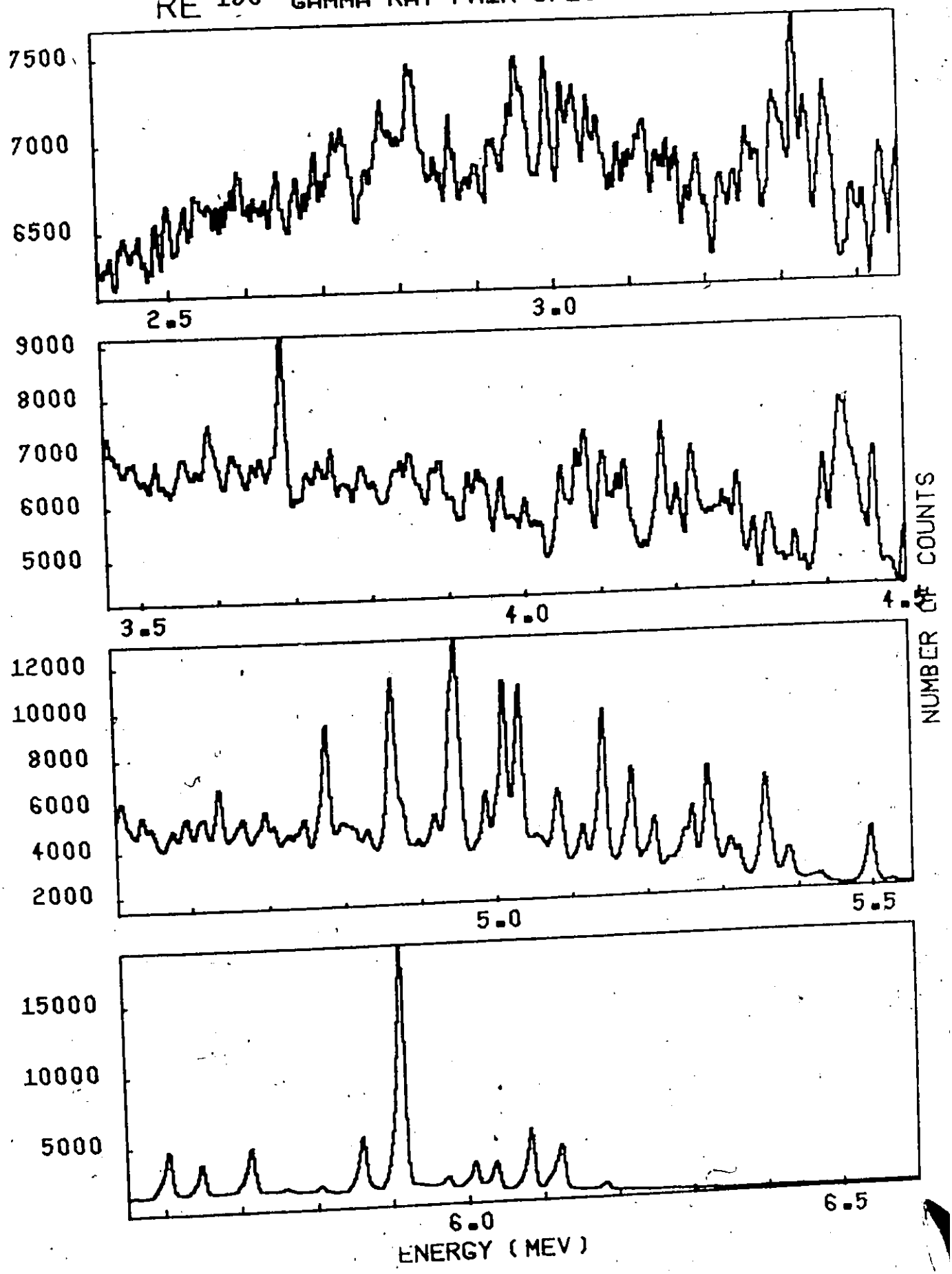

RE 186 RESPONSE STRIPPING FIG A4·15·2

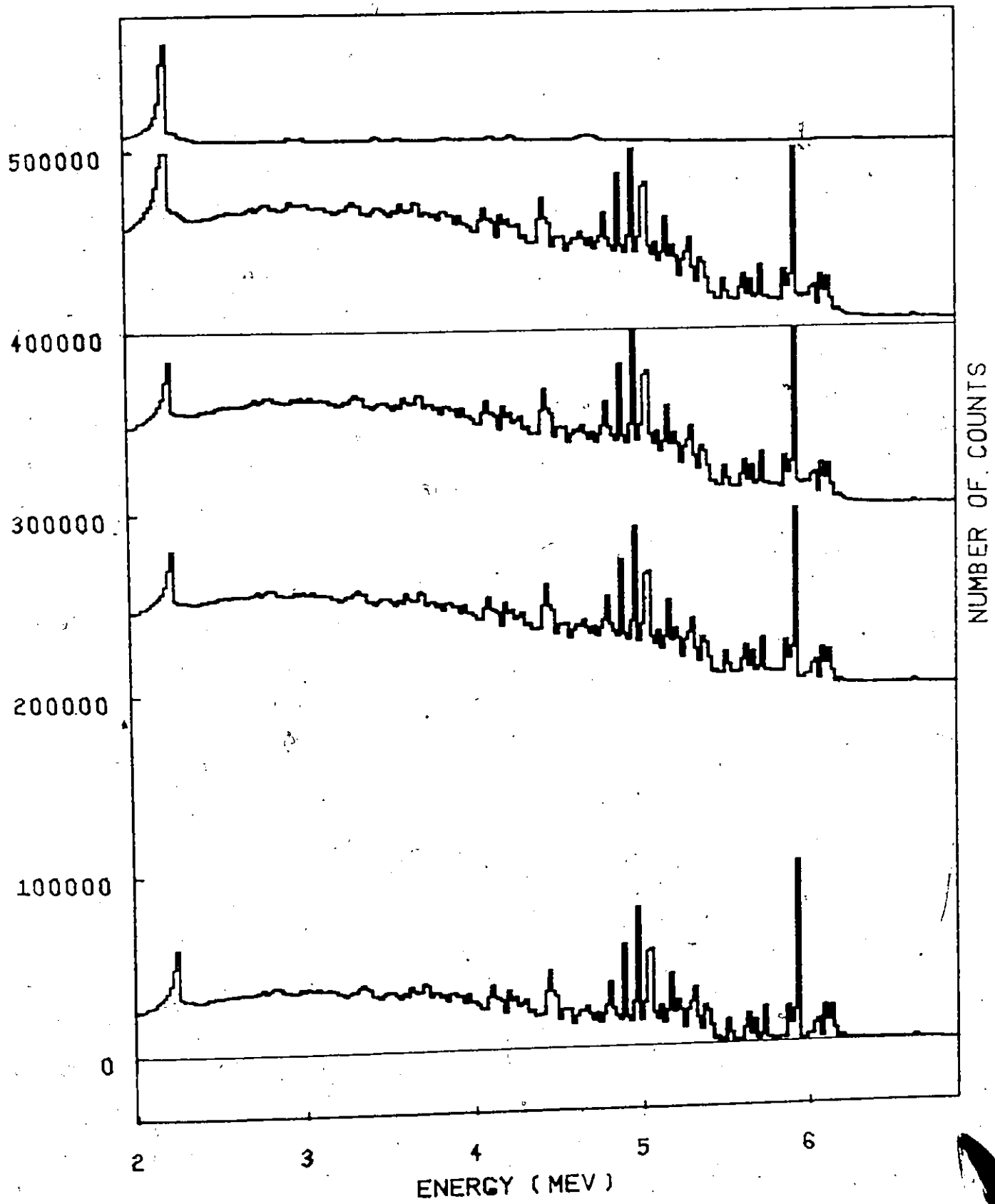

RE 186 STATISTICAL DATA FIG A4·15·3

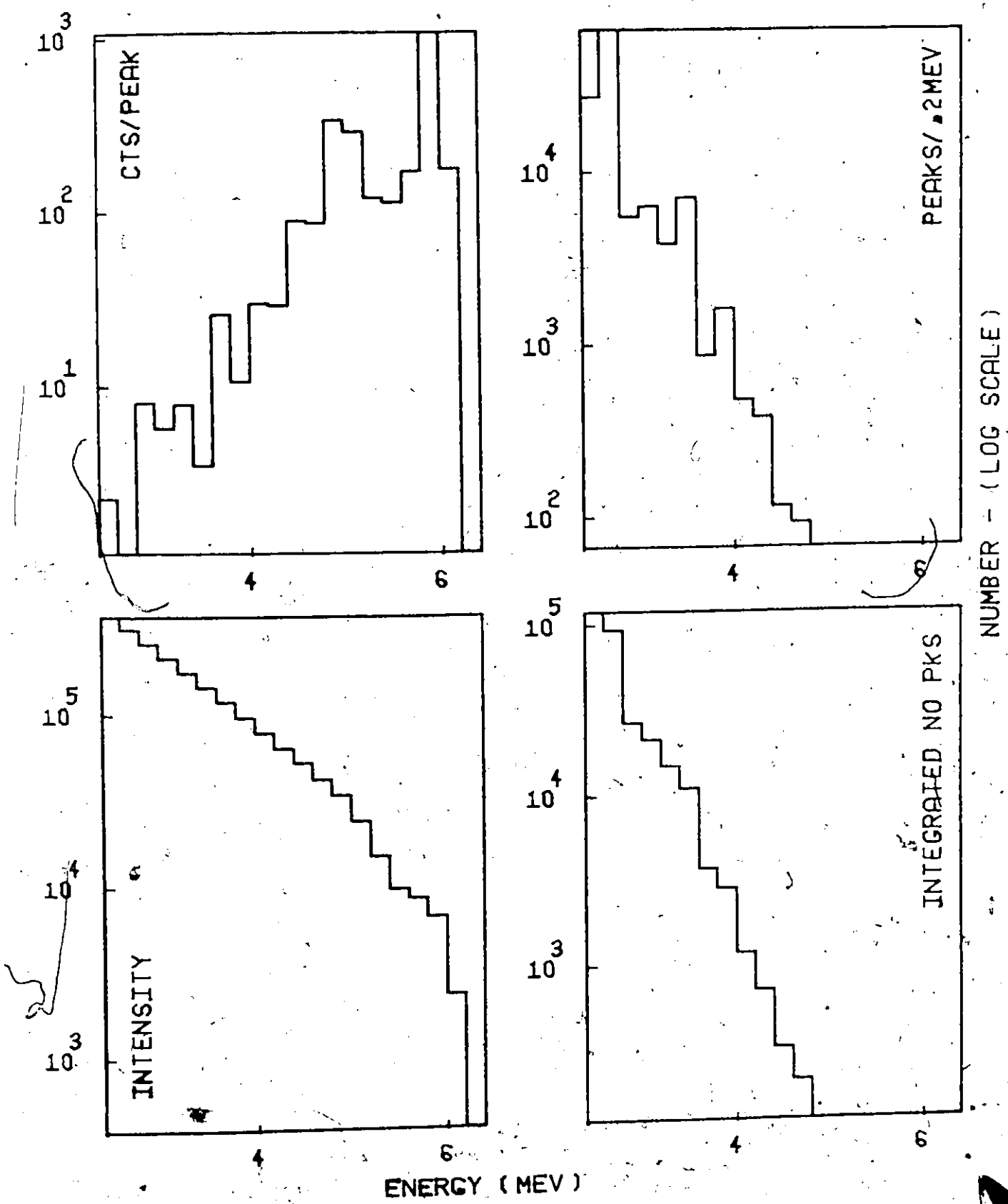

***** AU 198 ***** TABLE A4.16

	ENERGY (KEV)	INTENSITY (PH/CAP)		ENERGY (KEV)	INTENSITY (PH/CAP)		ENERGY (KEV)	INTENSITY (PH/CAP)		ENERGY (KEV)	INTENSITY (PH/CAP)
1	6510.9	1.01E-02	41	5347.7	1.52E-03	81	4690.9	1.09E-03	121	4242.7	1.40E-03
2	6456.0	1.44E-02	42	5321.4	4.34E-04	82	4675.9	4.27E-04	122	4233.9	1.09E-03
3	6318.1	2.18E-02	43	5308.3	3.26E-03	83	4656.3	1.23E-03	123	4225.4	1.00E-03
4	6275.0	8.26E-03	44	5279.9	3.92E-03	84	4645.5	2.21E-03	124	4220.7	3.14E-04
5	6251.0	3.60E-02	45	5226.3	4.16E-03	85	4637.4	2.71E-03	125	4213.8	2.20E-04
6	6163.9	1.64E-03	46	5219.4	3.29E-03	86	4614.6	1.49E-03	126	4208.9	5.04E-04
7	6147.7	7.47E-03	47	5206.1	1.32E-03	87	4603.5	1.99E-03	127	4188.9	3.04E-03
8	6105.5	4.82E-03	48	5174.7	2.87E-03	88	4600.5	1.74E-03	128	4171.3	9.24E-04
9	6057.6	8.34E-04	49	5149.0	5.09E-03	89	4588.2	6.06E-03	129	4163.3	4.79E-04
10	6015.4	6.66E-04	50	5142.1	4.20E-03	90	4574.9	4.76E-03	130	4156.8	7.04E-04
11	6000.4	3.50E-04	51	5116.5	1.55E-03	91	4544.9	4.68E-03	131	4148.3	8.98E-04
12	5982.3	9.78E-03	52	5103.2	1.00E-02	92	4528.2	2.16E-03	132	4133.9	1.19E-03
13	5961.6	1.25E-04	53	5086.3	4.64E-03	93	4510.7	2.94E-03	133	4122.8	1.91E-03
14	5940.4	3.95E-03	54	5081.5	3.57E-03	94	4506.1	2.94E-03	134	4109.5	9.42E-04
15	5879.0	2.91E-03	55	5058.4	3.58E-04	95	4497.1	6.40E-04	135	4089.8	6.54E-04
16	5838.6	1.98E-03	56	5041.1	2.33E-03	96	4480.5	1.09E-03	136	4074.3	1.54E-03
17	5808.4	2.50E-03	57	5036.2	2.14E-03	97	4461.8	1.81E-03	137	4063.7	5.94E-04
18	5787.7	4.16E-04	58	5025.4	9.34E-04	98	4455.7	1.75E-03	138	4058.0	2.64E-04
19	5784.5	6.25E-04	59	5007.6	9.75E-04	99	4442.6	2.47E-03	139	4043.2	3.98E-04
20	5766.4	5.31E-03	60	4999.3	4.30E-03	100	4435.9	2.87E-03	140	4038.1	5.82E-04
21	5723.3	3.48E-03	61	4975.7	1.57E-03	101	4432.9	2.81E-03	141	4026.5	1.84E-03
22	5710.2	1.21E-02	62	4958.4	8.48E-03	102	4423.2	3.53E-03	142	4009.0	2.65E-03
23	5676.7	1.74E-03	63	4945.3	9.50E-03	103	4418.3	2.69E-03	143	4001.6	1.31E-03
24	5643.0	8.98E-04	64	4932.6	2.18E-03	104	4411.0	1.21E-03	144	3989.4	6.40E-04
25	5619.8	2.75E-03	65	4905.6	4.00E-03	105	4408.6	1.18E-03	145	3983.8	1.20E-03
26	5594.1	4.50E-03	66	4900.0	4.20E-03	106	4403.6	1.25E-03	146	3967.0	1.17E-03
27	5580.1	3.00E-04	67	4888.5	3.21E-03	107	4398.9	1.71E-03	147	3942.0	1.18E-03
28	5558.8	2.50E-04	68	4866.1	3.43E-03	108	4388.6	3.97E-04	148	3934.4	9.19E-04
29	5554.7	2.20E-04	69	4853.2	3.44E-03	109	4373.6	1.59E-03	149	3924.3	1.14E-03
30	5539.7	1.50E-03	70	4831.1	1.43E-03	110	4365.5	2.13E-03	150	3908.8	6.62E-04
31	5524.5	8.03E-03	71	4824.4	8.16E-04	111	4359.2	8.67E-04	151	3898.4	5.54E-04
32	5513.6	1.51E-03	72	4800.6	8.82E-03	112	4351.4	2.67E-04	152	3892.2	5.55E-04
33	5493.6	4.52E-03	73	4786.8	1.96E-03	113	4338.7	2.00E-03	153	3882.3	2.23E-04
34	5473.9	2.01E-03	74	4784.0	1.65E-03	114	4322.5	2.58E-03	154	3865.6	4.48E-04
35	5462.8	2.01E-03	75	4768.8	1.86E-03	115	4306.2	7.94E-04	155	3856.1	1.17E-03
36	5419.7	1.21E-03	76	4765.8	1.86E-03	116	4300.6	8.57E-04	156	3846.4	4.51E-04
37	5396.4	1.72E-03	77	4753.5	6.23E-04	117	4279.6	3.63E-03	157	3841.4	1.31E-03
38	5388.3	1.73E-03	78	4739.0	1.04E-03	118	4266.9	7.73E-04	158	3834.7	4.99E-04
39	5365.5	1.62E-03	79	4733.9	2.71E-03	119	4259.8	7.13E-04	159	3824.7	1.09E-03
40	5354.7	3.57E-03	80	4728.8	1.67E-03	120	4249.4	1.49E-03	160	3809.7	1.46E-03

	ENERGY (KEV)	INTENSITY (PH/CAP)
161	3799.1	1.10E-03
162	3795.6	3.68E-04
163	3787.1	9.69E-04
164	3776.2	4.17E-04
165	3770.5	6.04E-04
166	3763.6	5.12E-04
167	3757.6	3.73E-04
168	3750.1	4.21E-04
169	3737.0	1.13E-03
170	3730.8	5.66E-04
171	3716.4	8.30E-04
172	3716.8	1.62E-03
173	3692.9	8.37E-04
174	3684.3	5.76E-03
175	3661.7	6.88E-04
176	3653.4	6.32E-04
177	3639.3	7.94E-04
178	3630.3	1.04E-03

AU 198 GAMMA RAY PAIR SPECTRUM FIG A4·16·1

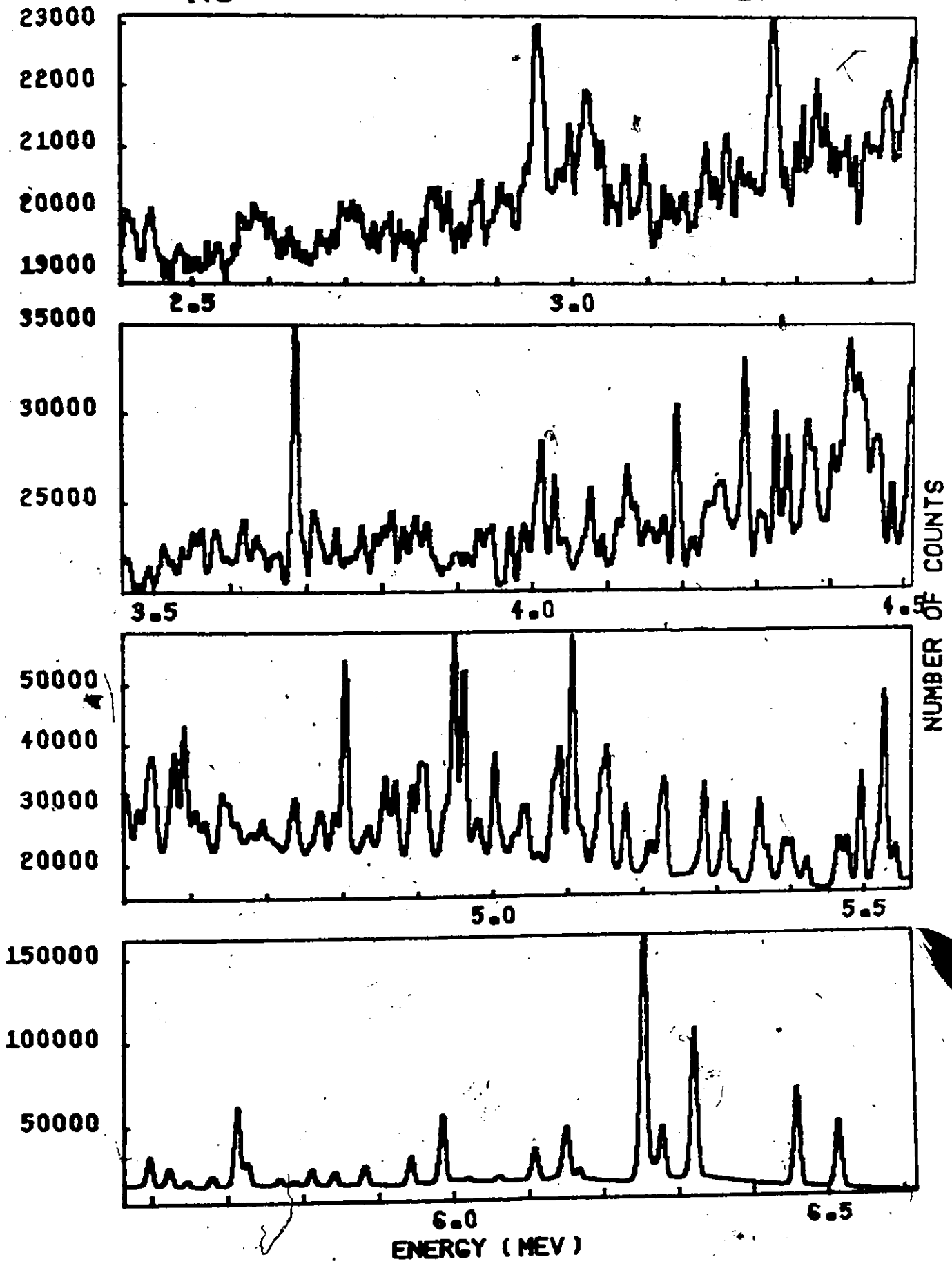

AU 198 RESPONSE STRIPPING FIG A4·16·2

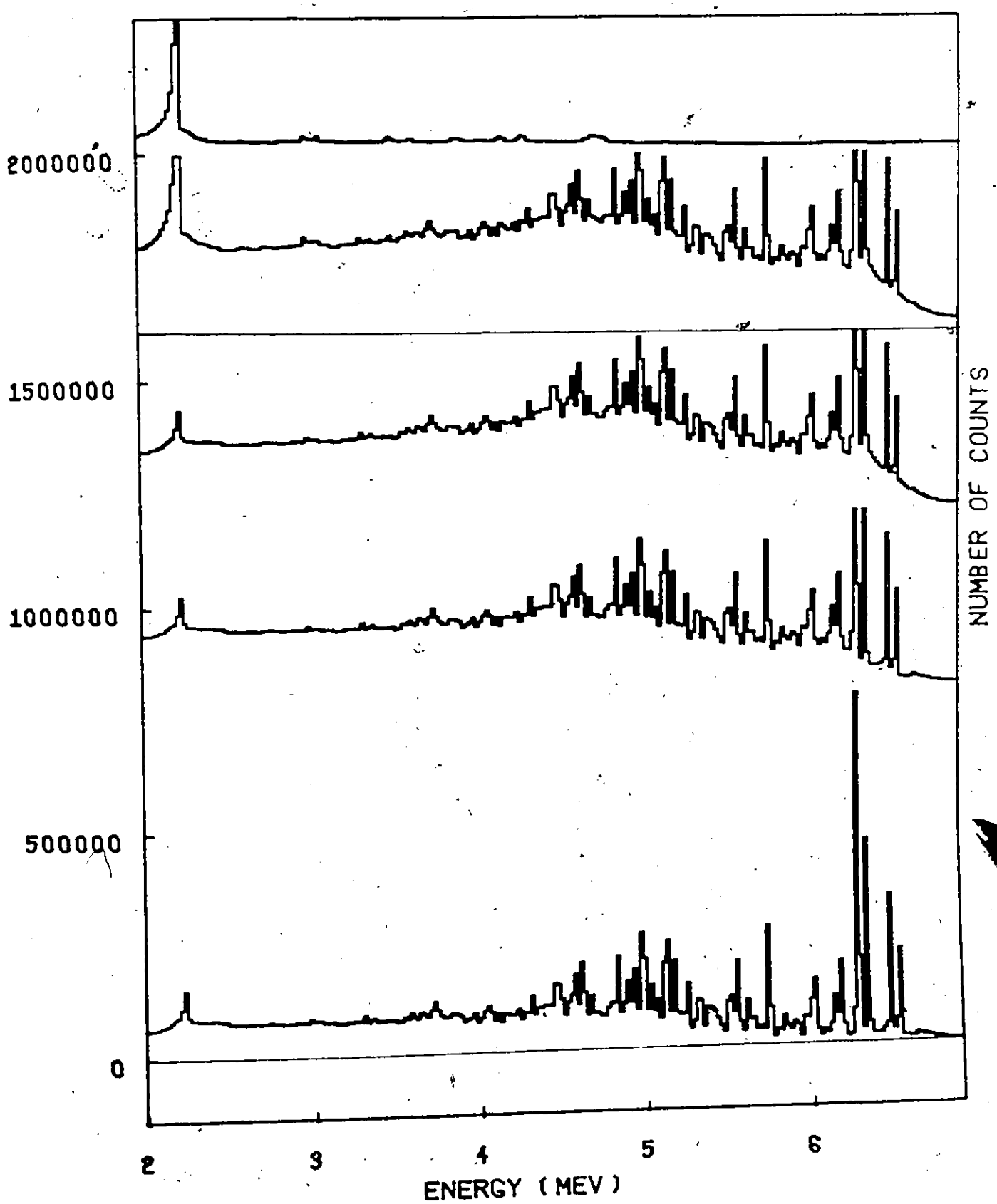

AU 198 STATISTICAL DATA FIG A4·16·3

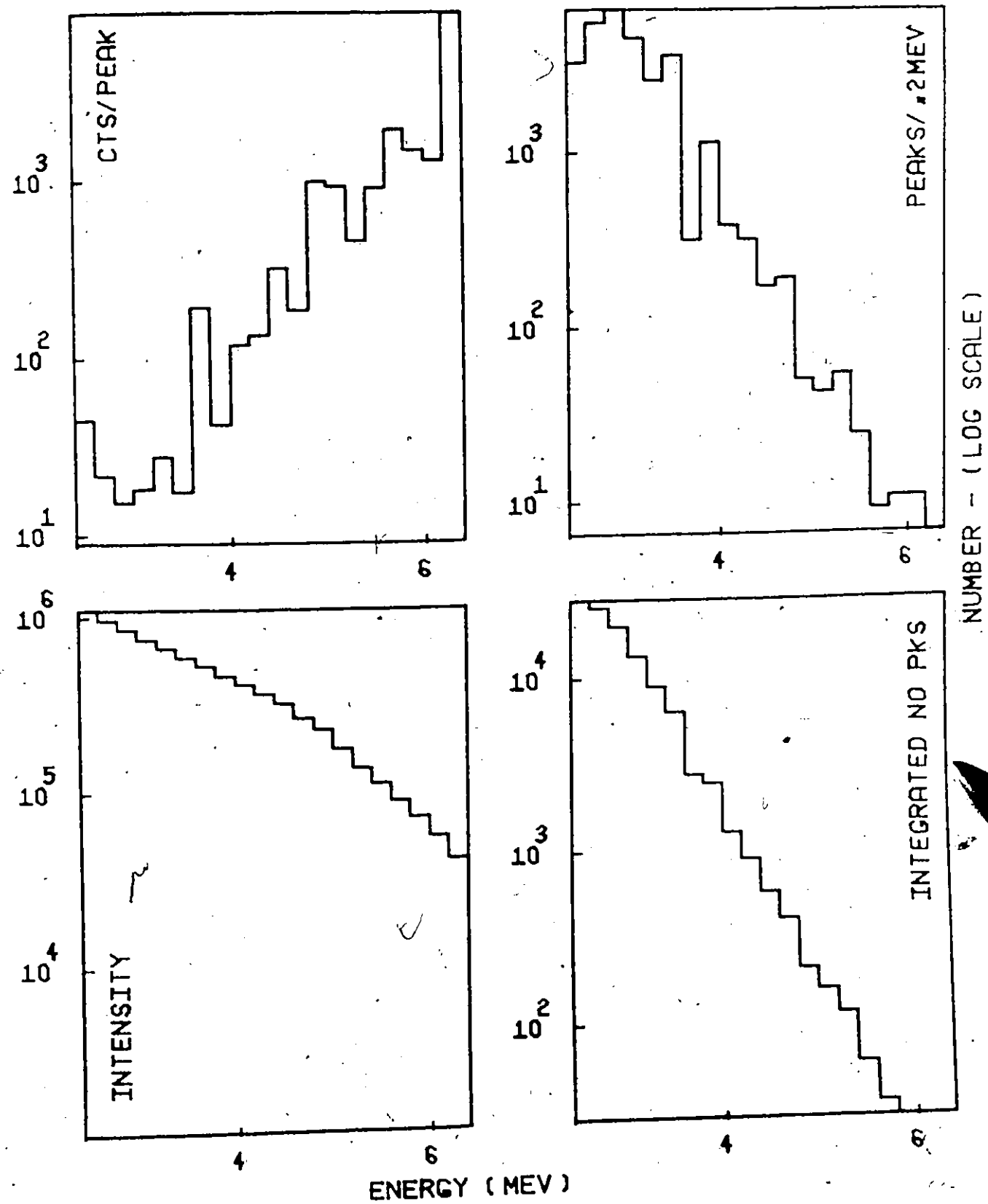

TABLE A4.17

***** TL 204 *****

	ENERGY (KEV)	INTENSITY (PH/CAP)		ENERGY (KEV)	INTENSITY (PH/CAP)		ENERGY (KEV)	INTENSITY (PH/CAP)		ENERGY (KEV)	INTENSITY (PH/CAP)
1	6655.7	1.40E-03	41	4715.8	2.52E-03	81	3786.0	1.18E-04	121	2947.9	2.38E-04
2	6515.7	1.87E-02	42	4706.9	9.04E-03	82	3762.1	2.52E-04	122	2938.6	1.30E-04
3	6355.4	3.05E-04	43	4688.9	1.52E-02	83	3699.1	2.04E-04	123	2926.6	1.63E-04
4	6337.1	3.20E-03	44	4662.5	1.06E-03	84	3684.5	1.46E-03	124	2906.5	2.77E-04
5	6237.1	6.09E-04	45	4609.3	1.67E-03	85	3671.6	1.51E-04	125	2863.9	1.88E-04
6	6223.4	1.04E-02	46	4602.3	4.31E-03	86	3656.5	1.52E-04	126	2844.3	1.24E-04
7	6198.7	1.83E-03	47	4571.1	3.13E-03	87	3651.4	1.93E-04	127	2815.9	1.04E-04
8	6183.6	1.14E-02	48	4542.1	4.91E-03	88	3598.3	1.70E-04	128	2806.9	2.21E-04
9	6167.5	2.47E-02	49	4520.2	2.94E-04	89	3576.7	1.13E-04	129	2779.4	1.73E-04
10	6120.1	2.83E-03	50	4496.9	6.69E-03	90	3563.7	2.45E-04	130	2751.8	7.87E-05
11	6026.4	3.43E-03	51	4466.2	2.98E-04	91	3539.2	2.42E-04	131	2714.3	1.88E-04
12	5918.6	1.21E-02	52	4448.8	4.20E-04	92	3467.9	5.41E-04	132	2697.3	1.37E-04
13	5891.5	1.13E-03	53	4440.0	1.14E-03	93	3451.0	1.32E-04	133	2665.2	9.96E-05
14	5868.4	1.13E-03	54	4404.5	1.40E-03	94	3440.4	1.20E-04	134	2638.1	2.40E-04
15	5854.2	7.54E-04	55	4392.8	5.49E-04	95	3428.0	4.40E-05	135	2633.5	2.18E-04
16	5749.8	3.77E-04	56	4380.4	7.96E-04	96	3415.5	1.21E-04	136	2621.5	1.71E-04
17	5642.7	4.39E-02	57	4344.8	6.06E-03	97	3410.2	2.04E-04	137	2573.4	1.85E-04
18	5604.4	3.84E-02	58	4310.8	3.12E-03	98	3386.8	2.19E-04	138	2557.8	2.14E-04
19	5534.3	1.78E-02	59	4287.7	7.55E-04	99	3377.5	2.71E-04	139	2515.6	1.33E-04
20	5522.4	3.18E-03	60	4261.4	3.75E-04	100	3356.4	6.51E-05	140	2497.4	2.25E-04
21	5504.5	1.59E-03	61	4226.6	6.83E-03	101	3302.1	2.35E-04	141	2458.6	1.39E-04
22	5452.0	9.91E-03	62	4197.5	5.23E-03	102	3287.9	4.39E-04	142	2428.6	1.90E-04
23	5405.3	1.86E-02	63	4160.9	6.45E-04	103	3260.5	1.85E-04	143	2397.3	1.47E-04
24	5299.5	6.48E-04	64	4127.8	2.61E-04	104	3255.8	1.51E-04	144	2346.4	1.55E-04
25	5281.2	2.85E-02	65	4116.1	2.49E-03	105	3233.2	4.24E-04	145	2328.5	1.58E-04
26	5262.8	1.13E-02	66	4102.3	9.21E-04	106	3211.3	2.34E-04	146	2319.5	9.57E-04
27	5240.2	2.67E-03	67	4078.2	1.13E-03	107	3207.4	3.19E-04	147	2289.6	1.65E-04
28	5181.5	2.04E-02	68	4069.0	4.65E-04	108	3183.3	5.60E-05	148	2129.5	5.45E-04
29	5172.3	2.92E-03	69	4035.9	4.03E-04	109	3159.4	6.84E-05	149	2112.3	8.81E-04
30	5155.1	8.99E-04	70	4017.4	1.42E-03	110	3143.8	1.50E-04	150	2084.2	7.49E-04
31	5143.8	6.76E-04	71	4009.1	1.15E-03	111	3129.2	3.49E-04	151	2063.0	2.57E-04
32	5129.1	6.77E-03	72	3973.8	4.81E-04	112	3117.5	4.21E-04	152	2027.5	2.72E-04
33	5015.7	8.48E-03	73	3957.3	2.76E-04	113	3095.7	1.07E-04	153	2013.4	1.39E-03
34	4982.4	3.00E-03	74	3942.9	1.53E-03	114	3068.6	2.28E-04			
35	4945.0	4.75E-03	75	3907.6	4.02E-04	115	3039.1	2.69E-04			
36	4914.8	2.33E-02	76	3902.1	1.76E-04	116	3028.0	1.54E-04			
37	4868.4	4.03E-03	77	3879.1	7.59E-05	117	3011.1	4.09E-04			
38	4841.6	6.09E-03	78	3865.6	2.56E-04	118	2998.8	1.44E-04			
39	4806.3	2.05E-03	79	3826.9	1.30E-04	119	2975.9	1.14E-04			
40	4753.6	1.99E-02	80	3793.7	1.31E-04	120	2958.8	1.73E-04			

TL 204 GAMMA RAY PAIR SPECTRUM FIG A4-17-1

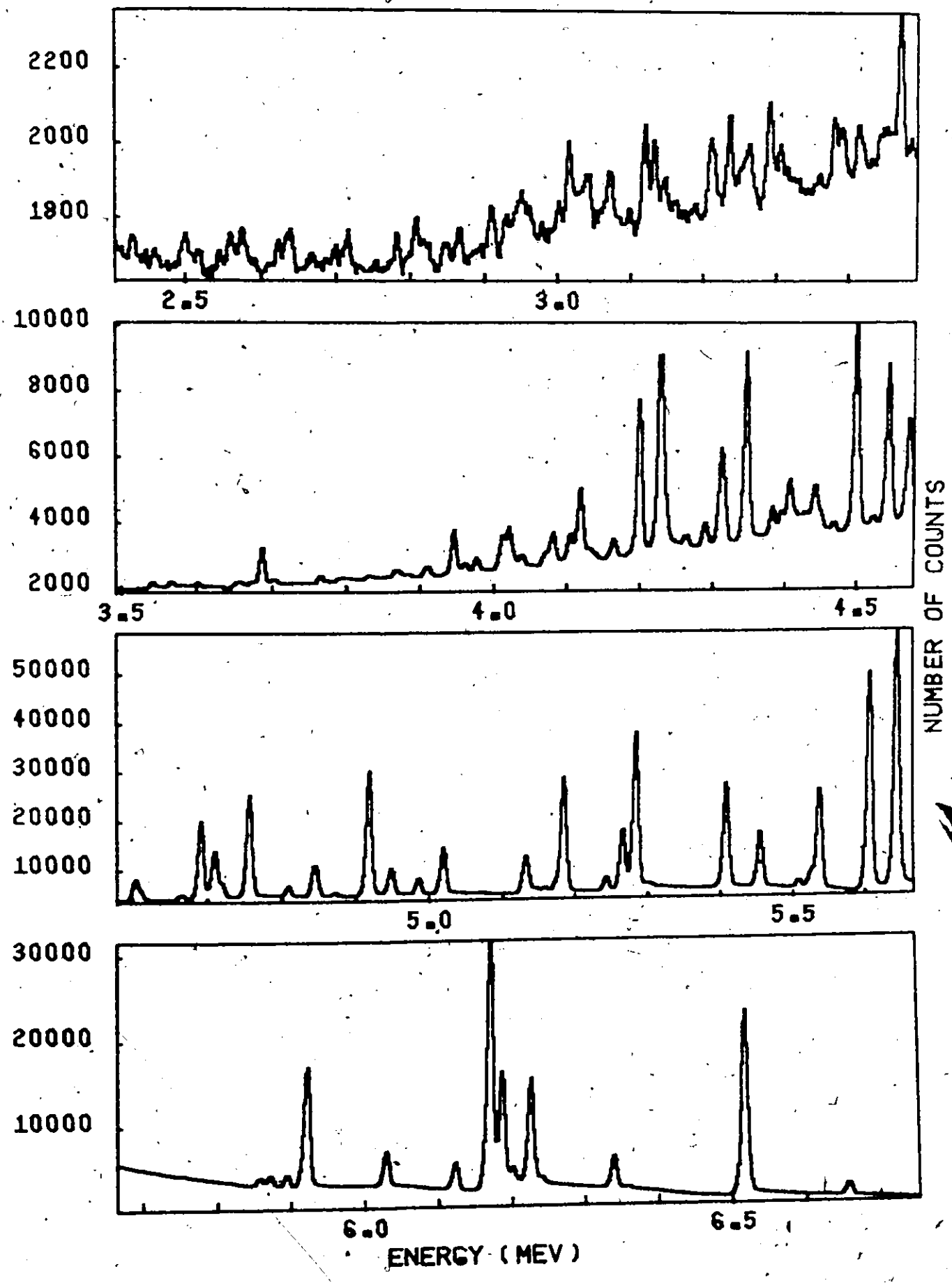

TL 204 RESPONSE STRIPPING FIG A4·17·2

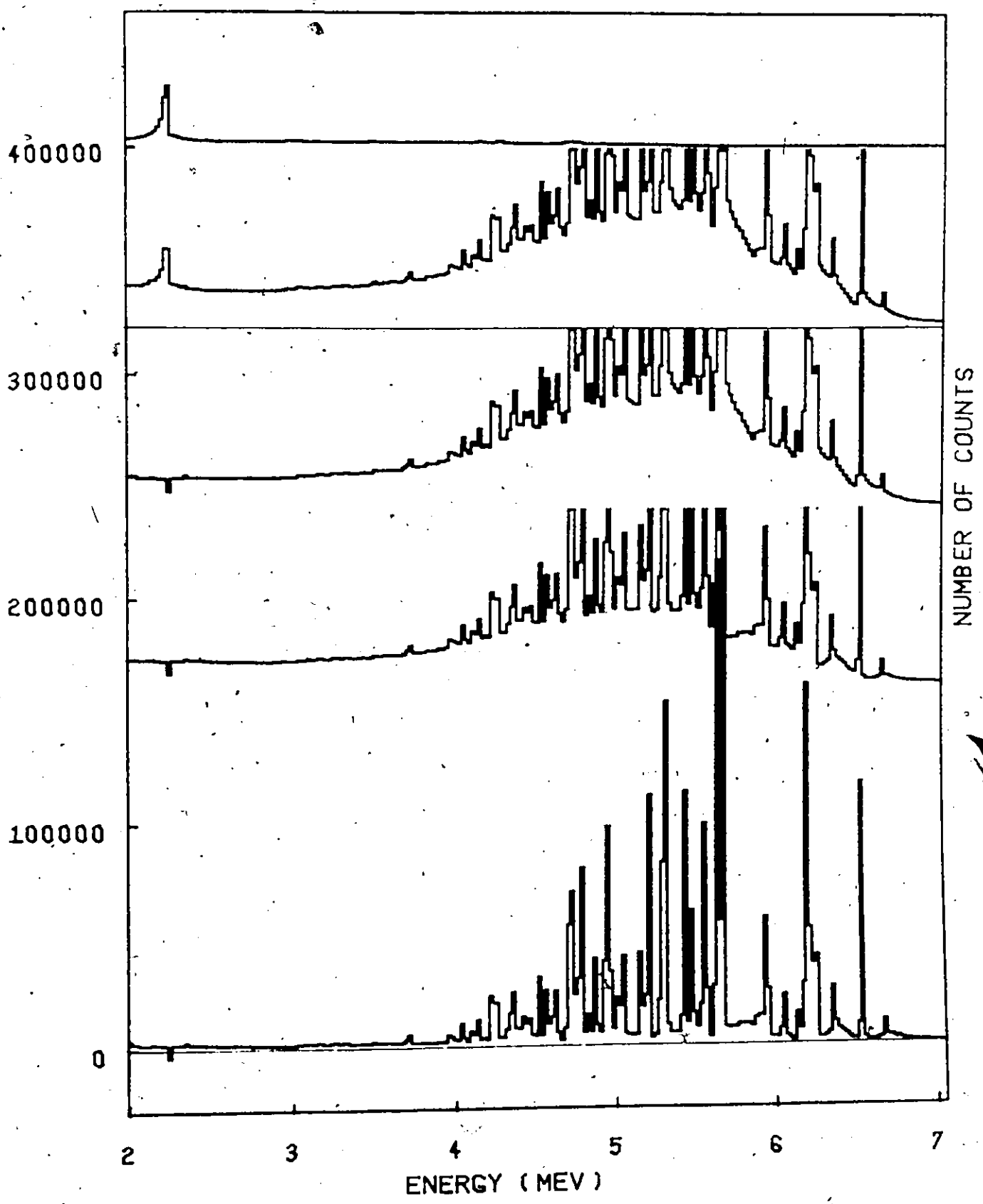

TL 204 STATISTICAL DATA FIG A4·17·3

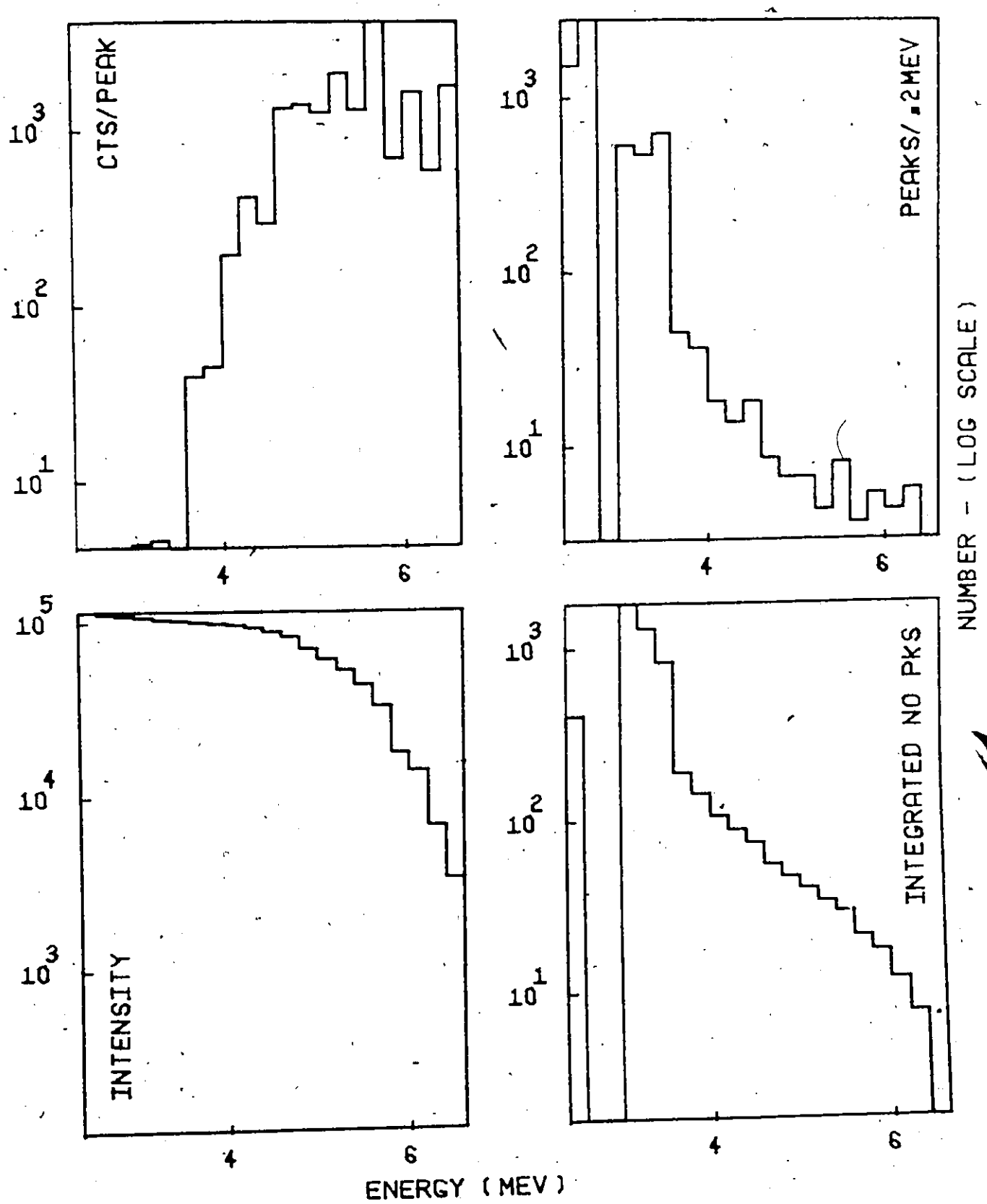

BIBLIOGRAPHY

1. K. Siegbahn, Alpha-, Beta-, and Gamma-ray Spectroscopy, edited by K. Siegbahn, North-Holland Publishing Co., Amsterdam (1965).

2. D. D. Slavinskas, T. J. Kennett, and W. V. Prestwich, Nucl. Instr. and Meth. 37, 36 (1965).

3. J. M. Blatt and V. F. Weisskopf, Theoretical Nuclear Physics, John Wiley and Sons, New York (1952).

4. M. A. Preston, Physics of the Nucleus, Addison-Wesley Publishing Co. (1963).

5. D. J. Hughes, Neutron Cross Sections, Pergamon Press, New York (1957).

6. M. G. Mayer, Phys. Rev. 78, 16 (1950).

7. I. N. Sneddon, Special Functions of Mathematical Physics and Chemistry, Interscience Publishers Inc., New York (1961).

8. D. D. Slavinskas, Ph.D. Thesis, McMaster University (1967).

9. E. Segrè, Nuclei and Particles, W. A. Benjamin Inc., New York (1964) Chapter 6.

10. D. Alburger, ibid. 1, chapter XII.

11. T. Ericson, Adv. Phys. 9, 425 (1960).

12. H. Bethe, Phys. Rev. 50, 332 (1936).
H. Bethe, Rev. Mod. Phys. 9, 69 (1937).

13. N. Bohr, Nature, Lond., 137, 344 (1936).

14. A. Gilbert and A.G. W. Cameron, Can. J. Phys. 43, 1446 (1965).

15. C. Bloch, Phys. Rev. 93, 1094 (1954).

16. A.G.W. Cameron, (Proc. of the 2nd.U.N. Conf. on the Peaceful Uses of Atomic Energy, United Nations, Geneva, 1958), Vol. 15, p. 425.

17. T. D. Newton, Can. J. Phys. 34, 804 (1965).

18. T. Ericson, Nucl. Phys. 8, 265 (1958).

19. A. Bohr, B. Mottelson and D. Pines, Phys. Rev. 110, 936 (1958).

20. H. K. Vonach, R. Vandenbosch, and J. R. Huizenga, Nucl. Phys. 60, 70 (1964).

21. R. L. Wine, Statistics for Scientists and Engineers, Prentice-Hall Inc., N.J. (1964), Chapter 6.

22. A. Paulsen, Zeitschrift fur Phyzik, 205, 226 (1967).

23. J. D. Jackson, Classical Electrodynamics, Wiley, New York (1962).

24. Ibid. 3, chapter XII.

25. S. A. Moszkowski, ibid 1, chapter XV.

26. C. E. Porter and R. G. Thomas, Phys. Rev. 104, 483 (1956).

27. B. B. Kinsey, G. A. Bartholomew, and W. H. Walker, Phys. Rev. 78, 481 (1950);
B. B. Kinsey, G. A. Bartholomew, Can. J. Phys. 31, 537 (1953);
_____, Can. J. Phys. 31, 1051 (1953).

28. G. A. Bartholomew, A. Doveika, K. M. Eastwood, and S. Monaro; and L. V. Groshev, A. M. Demidov, V. I. Pelekhov, and L. L. Sokolovski, Nuclear Data A3, 367 (1967); Nuclear Data A5, 1 (1968); Nuclear Data A5, 243 (1969).

29. N. C. Rasmussen, Y. Hukai, T. Inouye, and V.J. Orphan, MITNE-85 (1969).

30. M. A. Lone, E. D. Earle, and G. A. Bartholomew, Nucl. Phys. 156, 113 (1970).

31. L. M. Bollinger and G. E. Thomas, Phys. Rev. 2C, 1951 (1970).

32. H. Baba, Nucl. Phys. A159, 625 (1970).

33. L. B. Hughes, Ph.D. Thesis, McMaster University (1967).

34. C. O. Muelhause, Phys. Rev. 79, 277 (1950).

35. J. E. Draper and T. E. Springer, Nucl. Phys. 16, 27 (1960).

36. R.R. Johnson and N. M. Hintz, Phys. Rev. 153, 1169 (1966).

37. K. J. Yost, Nuclear Sci. Engng., 32, 62 (1968).

38. I. Bergqvist and N. Starfelt, Nucl. Phys. 39, 353 (1962).

39. D. G. Sarantites, Nucl. Phys. A93, 576 (1967).

40. M. Hillman and J. R. Grover, Phys. Rev. 185, 1303 (1969).

41. D. Sperber and J. W. Mandler, Nucl. Phys. A113, 689 (1968).

42. E. S. Troubetzkoy, Phys. Rev. 122, 212 (1961).

43. J.R. Huizenga and R. Vandenbosch, Phys. Rev. 120, 1305 (1960).

44. H. K.Vonach, R. Vandenbosch, and J. R. Huizenga, Nucl. Phys. 60, 70 (1964).

45. T. von Egidy, Neutron Capture Gamma-Ray Spectroscopy, (Proceedings of the International Symposium on Neutron Capture Gamma-Ray Spectroscopy, Studsvik, 1969) p. 541.

46. J. B. Marion, Nucl. Data A4, 301 (1968).

47. L. Nichol, A. Lopez, A. Robertson, W.V. Prestwich and T. J. Kennett, Nucl. Instr. and Meth., 81, 263 (1970).

48. D. Halliday, Introductory Nuclear Physics, John Wiley and Sons, New York (1950).

49. H. J. Fiedler, L.B. Hughes, T. J. Kennett, W. V. Prestwich, and B. J. Wall, Nucl. Instr. and Meth. 40, 229 (1966).

50. L. Nichol, A. H. Colenbrander and T. J. Kennett, Can. J. Phys. 47, 953 (1969).

51. M. Strauss, private communication.

52. G. E. Thomas D. E. Batchley and L. M. Bollinder, Nucl. Instr. and Meth. 56, 325 (1967).

53. A.F.M. Ishaq, A. H. Colenbrander, and T. J. Kennett, Accepted for publication in Can. J. Phys.

54. R. L. Chase, Nuclear Pulse Spectroscopy, McGraw-Hill Book Co., Inc., New York (1961) Chapter 1.

55. V. Fano, Phys. Rev. 72, 26 (1947).

56. H. M. Mann, Bull. Am. Phys. Soc. 11, 127 (1966).

57. Ibid 54, Chapter 9.

58. R. van Lieshout, A. H. Wapstra, R. A. Ricci and R. K. Girgis, ibid 1, Chapter VIII.

59. Ibid. 21, Chapter 3.

60. P. P. Zachar, M. Eng. Thesis, McMaster University (1972).

61. G. M. Barrow, Physical Chemistry, McGraw-Hill, New York, (1961) Chapter 2.

62. J. DeJuren and H. Rosenwasser, Phys. Rev. 93, 831 (1954).

63. C. M. Lederer, J. M. Hollander, I. Perlman, Table of Isotopes, Wiley and Sons, New York (1968).

64. Ibid. 63, p. 186.

65. G. A. Bartholomew, Ibid. 45, p. 553.

66. H. Eves, Elementary Matrix Theory, Allyn and Bacon Inc., Boston (1966).

67. E. P. Wigner, (Proc. Conf. on Neutron Physics by Time-of-flight, Gatlinburg, 1956) p. 59.

68. J. E. Lynn, The Theory of Neutron Resonance Reactions, Clarendon Press, Oxford, (1968) p. 180.

69. J. B. Garg, W. W. Havens, and J. Rainwater, Phys. Rev. 136, B177 (1964).

70. H. Lycklama, N. P. Archer and T. J. Kennett, Nuclear Physics, A100, 33 (1967).